For Reference

NOT TO BE TAKEN FROM THIS ROOM

THE UNIVERSITY OF ALBERTA

AN INITIAL ASSESSMENT OF THE REPRESENTATIVENESS AND ACCURACY OF ALBERTA HAILPAD DATA

by

© LUBOMIR WOJTIW

A THESIS
SUBMITTED TO THE FACULTY OF GRADUATE STUDIES AND RESEARCH
IN PARTIAL FULFILMENT OF THE REQUIREMENTS FOR THE DEGREE
OF MASTER OF SCIENCE
IN
METEOROLOGY

DEPARTMENT OF GEOGRAPHY

EDMONTON, ALBERTA
FALL, 1977

DEDICATED TO

my loving wife, Marie, without whose support this would not have been possible

ABSTRACT

In this dissertation five simulation techniques ((1) sampling without replacement from the observed distribution of impact energy densities; (2) sampling with replacement from the observed distribution; (3) sampling from an idealized two-parameter gamma distribution; (4) stratified sampling from the observed distribution of impact energy densities; and (5) spatial sampling from a contoured pattern of the observed impact energy density field) are presented and applied using the Monte Carlo method in an attempt to simulate the sort of sampling a hailpad network would produce. Data from the 29 July 1974 hailswath is used to illustrate the approach for each of these five techniques. An estimate of the errors involved in the mean impact energy densities for the hailpad observations is also included using the first four techniques. Data from five hailswaths that occurred in central Alberta during the three years 1974 to 1976 are used in the analysis.

The collection and calculation of the impact energy densities from the hailpad data are also described. Graphs of the probability density function of the sample means, the probability distribution function of the sample means, and the standard deviation of the sample means as a function of the sample size are given for each simulation technique outlined above.

The results show that the probability density function of the sample means approximates the Gaussian form (in most cases) for sample sizes greater than about 15. The results further show that the variation of the standard deviation as a function of the sample size is proportional to $k^{-1/2}$ for non-stratified sampling, stratified sampling, and sampling from the fitted two-parameter gamma distribution. These results show good agreement with the predictions of the central-limit theorem.

To test how adequately the two-parameter gamma distribution fitted the original data, the Chi-square test was used. The results for the five hailswaths show that this distribution gives a reasonable fit for the impact energy densities.

Which technique best simulates the sort of sampling which hailpads do in a hailswath, depends on the nature of the hailswath itself. Sampling with replacement (non-stratified), is probably best applicable to hailswaths where the impact energy density distribution in any small subsection of the hailswath is essentially the same as that in the entire hailswath. Sampling from a fitted two-parameter gamma distribution is probably best applicable to severe hailswaths where a large range of impact energy densities is observed. Stratified sampling can be used as a simulation technique for hailswaths where the impact energy densities are continuous in space. In deciding which technique best simulates the hailswath it is necessary to consider the

auto-correlation function for the impact energy densities.

Using the Monte Carlo method, the results indicate that in order to commit a 10 percent error between the average of the sample means and the the mean of the sample means. 90 hailpads are required in a 1000 km^2 area (or 1 hailpad per 11.1 km^2) for non-stratified sampling and 200 hailpads per 1000 km^2 area (1 hailpad per 5.0 km^2) are needed for the fitted two-parameter gamma distribution. An improvement in the sampling density is observed for stratified sampling, where for a 10 percent error between the estimates, 10 hailpads are needed in a 1000 km^2 area (1 hailpad per 100 km^2). The major conclusion of this dissertation is that the present dense network (with 1 observation per 5.7 km^2) of hailpads is sufficient in density to produce an error of less than 10 percent in the impact energy density. The precipitation network (of 1 observation per 70 km^2) is, on the other hand, insufficent in density at this error level (for sampling from the fitted two-parameter gamma distribution and for non-stratified sampling). Assuming a 100 percent response in the hailpad observations for the area affected by the swath, the minimum error in the impact energy density with the present precipitation network would be at least 18 percent.

ACKNOWLEDGEMENTS

The author acknowledges with gratitude his indebtedness to Dr. E.P.Lozowski for suggesting the problem explored in this dissertation as a thesis topic and for his advice and criticism throughout the period during which this extensive research was carried out.

My sincere thanks are also extended to the staff of the Atmospheric Sciences Division of the Research Council of Alberta for their co-operation in completing this work. In particular to Drs. B.L. Barge and R.G. Humphries for their enthusiasm; to Misses M. Wong and M. Cyncar for their assistance in revisions; and to Mr. G. Lunn for reading some of the drafts.

I wish to express my thanks to the Alberta Weather Modification Board for providing part of the funds to carry out the computing on the University of Alberta Computer and for the financial support of the networks from which the data was collected, and to the Department of Geography for providing additional funds to carry out some of the computing in this dissertation. Thanks also are due Redberger for running the computer programs on the DEC PDP-9 computer, and to Drs. K.D. Hage and R.T. Hardin for reading the final drafts, and serving on the examining committee.

TABLE OF CONTENTS

CHAPTER PAGE

DEDICATION iv

ABSTRACT v

ACKNOWLEDGEMENTS viii

TABLE OF CONTENTS ix

LIST OF TABLES xi

LIST OF FIGURES xii

I. INTRODUCTION 1

1.1 Background 1

1.2 Purpose of Study 5

1.3 Precipitation Patterns-Hailfall 6

1.4 Precipitation Patterns-Rainfall 10

II. DATA COLLECTION AND REDUCTION 22

2.1 Observations 22

2.2 Analysis of the Hailpads 26

2.3 Calculation of the Impact Energy Density 28

III. THE MONTE CARLO METHOD 35

3.1 Introduction 35

3.2 Sampling Techniques 40

IV. APPLICATION OF THE MONTE CARLO METHOD TO HAILPAD DATA 43

4.1 Sampling Without Replacement 45

4.2 Sampling With Replacement 52

4.3 Sampling From a Fitted Two-parameter Gamma Distribution 56

4.4 Stratified Sampling 61

4.5 Spatial Sampling 65

V. RESULTS FOR OTHER STORMS 75

5.1 Introduction 75

5.2 Comparison of the Sampling Techniques 78

5.2.1 Probability Density Function 80

5.2.2 Probability Distribution Function 81

5.2.3 Standard Deviation of the Sample Means as a Function of the Sample Size 81

5.2.4 Mean Difference Between Estimates for a Sampling Normalized per 1000 km^2 84

VI. CONCLUSIONS 87

TABLE OF SYMBOLS 92

BIBLIOGRAPHY 93

APPENDIX I. FORTRAN IV COMPUTER PROGRAMS 107

APPENDIX II. HAILSWATHS USED IN THE ANALYSIS 131

APPENDIX III. GRAPHS OF PERCENTAGE FREQUENCY OF OCCURRENCE OF IMPACT ENERGY DENSITY 138

APPENDIX IV. GRAPHS OF CUMULATIVE FREQUENCY OF IMPACT ENERGY DENSITY 143

APPENDIX V. GRAPHS OF SAMPLING WITH REPLACEMENT 148

APPENDIX VI. GRAPHS OF SAMPLING WITHOUT REPLACEMENT 165

APPENDIX VII. GRAPHS OF SAMPLING FROM A FITTED GAMMA DISTRIBUTION 182

APPENDIX VIII. GRAPHS FOR STRATIFIED SAMPLING 199

LIST OF TABLES

Table Description Page

1.1 Estimates of the Error of (or Uncertainty of) Areal Mean Rainfall for a Given Number of Gauges 12

5.1 Summary of Hailswaths Analyzed 77

5.2 Summary of the Chi-Square Test for the Hailswaths Analyzed 79

5.3 Summary of the Variation of the Standard Deviation of the Sample Means as a Function of the Sample Size for the Four Techniques 82

LIST OF FIGURES

Figure Page

1.1 Map showing area of the Alberta Hail Project 4

1.2 Diagram showing hailstreaks and hailswaths in a 10-hour period on 21 April 1967 in Illinois 9

1.3 Diagram showing the number of measurable stones from 3 April 1974 storm 11

1.4 Diagram showing results of estimating required distances between gauges as a function of the 2-year-24-hour and 2-year-1-hour rainfall 13

1.5 Graph showing sampling error relations on 1036 km^2 15

1.6 Diagram showing Type 1 and Type 2 errors in Eddy's model 17

1.7 Graph showing difference between estimates of hourly sub-catchment rainfall related to raingauge density 19

2.1 Map showing networks in the Alberta Hail Project 23

2.2 Diagram showing location of hailpad stations in the dense network 24

2.3 A picture of hailpad stand 25

2.4 A picture of a pad sander used to eliminate coarseness in the styrofoam 27

2.5 A picture of an uninked hailpad and the same pad after inking 28

2.6 Hailpad overlay used in analysis 29

2.7 Graph showing conversion from dent diameter (on hailpad) to hail diameter 30

3.1 Distribution of 40,000 random numbers drawn from subroutine GGU3 for the expanded interval $[0,100]$ 38

4.1 The hailfall and hailpad locations for the 29 July 1974 hailswath 44

4.2 The percentage frequency of occurrence of impact energy density values for 29 July 1974 hailswath 46

4.3 The cumulative frequency of impact energy density for 29 July 1974 hailswath 47

4.4 The probability density function of the sample means for 29 July 1974 hailswath (sampling without replacement) 49

4.5 Isopleths of the probability distribution function of the sample means for 29 July 1974 hailswath (sampling without replacement) 50

4.6 The standard deviation of the sample means as a function of the sample size (sampling without replacement) 51

4.7 The probability density function of the sample means for 29 July 1974 hailswath (sampling with replacement) 53

4.8 Isopleths of the probability distribution function of the sample means for 29 July 1974 hailswath (sampling with replacement) 54

4.9 The standard deviation of the sample means as a function of the sample number (sampling with replacement) 55

4.10 Density function for the gamma distribution 57

4.11 The probability density function of the sample means for the 29 July 1974 hailswath (sampling from a two-parameter gamma distribution) 60

4.12 Isopleths of the probability distribution function of the sample means for 29 July 1974 hailswath (sampling from a two-parameter gamma distribution) 61

4.13 The standard deviation of sample means as a function of the sample size (sampling from a two-parameter gamma distribution) 62

4.14 The probability density function of the sample means for 29 July 1974 hailswath (stratified sampling) 63

4.15 The probability distribution function of the sample means for 29 July 1974 hailswath (stratified sampling) 65

4.16 The probability distribution function of the

sample means for the 29 July 1974 hailswath (stratified sampling) 66

4.17 The probability distributin function of the sample means for 29 July 1974 hailswath (stratified sampling) 67

4.18 The standard deviation of the sample means as a function of the sample size (stratified sampling) 68

4.19 The contoured values for the 34 impact energy densities for the 29 July 1974 hailswath 70

4.20 The probability density function (spatial sampling) 71

4.21 The standard deviation of the sample means as a function of the sample size (spatial sampling) 72

5.1 The mean difference (in percent) between estimates for sample density in a 1000 km² area (sampling with replacements) 83

5.2 The mean difference (in percent) between estimates for a sample density of 1000 km² (sampling from a two-parameter gamma distribution) 85

5.3 The mean difference (in percent) between estimates for a sample density of 1000 km² (stratified sampling) 86

CHAPTER 1

INTRODUCTION

1.1 Background

Hail has been reported in central Alberta during the last 20 years on an average of 60.2 days [1] each year between 15 May and 15 September (Wojtiw,1977). Although hail damage on many of these days is of no consequence, claims for hail damage in the same period are received by the Alberta Hail and Crop Insurance Corporation on an average of 50 days each season throughout Alberta, with the majority of these hail days occurring in central Alberta (Summers and Wojtiw,1971). The total annual loss to agriculture from hail is now estimated to average between 50 and 60 million dollars each year (Wojtiw,1975b). Concern over such heavy agricultural losses and an enthusiastic meteorological research interest in severe storms led to the creation in 1974 of a hail suppression and hail research program called the Alberta Hail Project(AHP). The program, supported by the Government of Alberta, is under the auspices of the Alberta Weather Modification Board(AWMB) with participation by the Alberta

---

[1] The standard deviation is 9.1 days, while the median value is 58 days.

Research Council(ARC), the Atmospheric Environment Service of Environment Canada(AES), and the Universities of Alberta and McGill. This program was created from the Alberta Hail Studies(1956-1973) program(ALHAS), and the research programs in existence in 1973 were continued in the AHP program. The ALHAS program was directed by the Alberta Research Council with financial and scientific contributions supplied by the Atmospheric Environment Service of Environment Canada, the National Research Council of Canada and the Stormy Weather Group of McGill University.

The AWMB was formed in March 1973 by the Legislative Assembly of Alberta, in response to the report of the Special Legislative Committee on Crop Insurance and Weather Modification (Stromberg,1972). The Board was established under the Alberta Department of Agriculture with a five year mandate to administer hail suppression and hail research programs. A truncated circle containing 47,900 km² (Figure 1.1), centered on the meteorological radar site at the Red Deer Industrial Airport was designated as the project boundary. The circular area was divided into a northern and a southern part with a buffer zone between. Each zone has different cloud seeding criteria and rules (Deibert and Renick,1975; Deibert,1976; Deibert,1977).

The Alberta Hail Project collects various data (radar and rawinsonde measurements, hailpads, hailcards, among others) to further increase knowledge of hailstorms and to evaluate the success of the hail suppression technique. Of

the ground measurements collected, hailpad data (see Chapter 2 for details) are considered to be the prime source of objective hailfall data, and they are to be used in the evaluation of the hail suppression hypothesis. The hailpad data to be used in the evaluation come from a network with an average spacing of one hailpad per 70 km^2. Before the data can be used in any evaluation scheme, it is desirable to know if there are sufficient hailpads in the network to measure adequately the hailfall and what degree of error is associated with the hailpad values. The answer depends on what is meant by "adequately". If, for instance, it is desirable to compare areal energy density patterns on the ground (from the hailpads) with radar echoes aloft, the spatial resolution of the hailpad network should be as good as that of the radar. The radar [2] echoes aloft are recorded by a 10 cm radar with a resolution of 1.6 km^2 at a range of 50 km, while the areal energy density of the hailswath is estimated using data from a network with an average spacing of one hailpad per 70 km^2. Since the average spacing of the two sets of measurements differs by at least an order of magnitude, they are not readily comparable. If, on the other hand, it is desirable to obtain an accurate estimate of the mean areal energy density of the hailswath, the required

---

[2] Characteristics of the S-band radar: frequency=2.880 GHz; pulse repetition frequency=480 s^{-1} ; pulse duration=1.75 μs; beam width=1.15° (all planes); antenna rotation rate=8 RPM; and elevation program-spiral scan of 1 per revolution to 8° or to 20°.

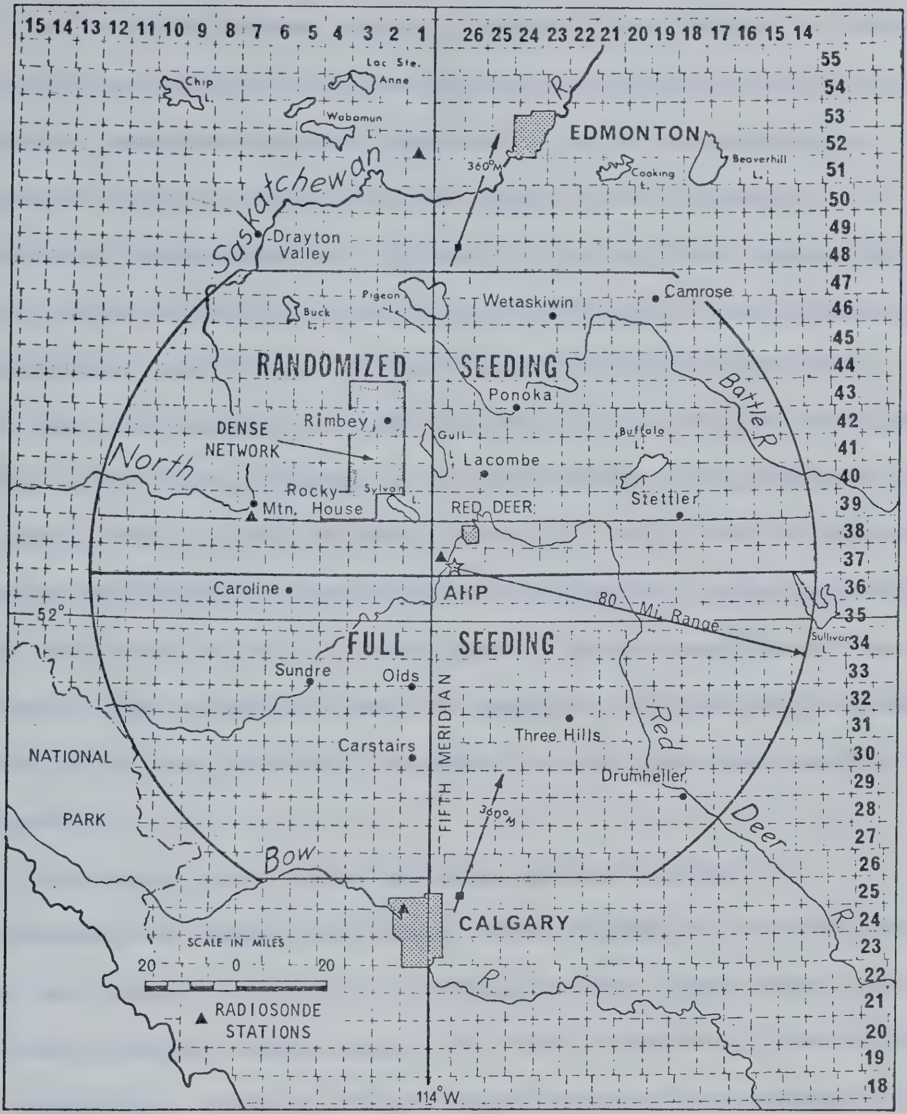

Figure 1.1 Map showing area of the Alberta Hail Project

network density can be specified in terms of the inaccuracy that one is prepared to tolerate.

1.2 Purpose of Study

It is this latter aspect, namely, the desire to obtain an accurate estimate of the mean areal energy density of the hailswath and the density required, to do this which is addressed in this dissertation. Here five different simulation techniques are presented and applied using the Monte Carlo method (discussed in Chapter 3). The purpose is to estimate the errors involved in determining the mean areal energy density of the hailswath from hailpad records with a given areal density. The collection and reduction of the data used in this dissertation are described in Chapter 2 while in Chapter 4 the five techniques are examined using data from the 29 July 1974 hailswath as an example of the approach. The results from the analysis of five hailstorms (1974-1975) are given in Chapter 5, with the conclusions in Chapter 6.

This work is a first effort, as far as can be determined, in using the Monte Carlo method to examine the sampling density problem for hailpad data. The technique is not new; similar ideas have been used elsewhere, for example in theoretical work on radar signal statistics (Marshall and Hitschfeld,1953; Smith,1964); comparison of rainfall measurements on the ground with radar signals (Collier,et.al.,1975), and with hail crop damage data (Morgan and Towery,1974). To assist in obtaining a finer scale picture of the areal energy density distribution than is permitted by the large scale network, data from a dense

network (see Figure 2.2) have been collected during the years 1974 and 1975. The average spacing in this network is one hailpad per 5.7 km².

The problem of assessing the accuracy of hailfall networks has received some attention in the United States and in Alberta, Canada. A brief summary of this work, including a discussion of the hailfall phenomenon, is given in Section 1.3. Hailfalls are believed by various authors (Changnon, 1968b; Morgan and Towery, 1974), to vary more in space and time than do rainfalls. Due to this variability, assessing the accuracy of a network is a more difficult problem for hailfall than for rainfall; thus, the limited efforts in this area of research to date. Considerable effort has been devoted to the problem of assessing the accuracy of measurements obtained using raingauge networks. A review of the literature on this subject is included in Section 1.4 in order to give an idea of the type of behaviour which may be expected for hailfall.

1.3 Precipitation Patterns - Hailfall

Extensive research programs into the climatology of hail in Alberta [3], Colorado [4], and Illinois [5] have been

---

[3] (Douglas and Hitschfeld, 1959; Longley and Thompson, 1965; Paul, 1967; Summers and Wojtiw, 1971; Wojtiw, 1975)

[4] (Schleusener, 1963; Renne and Sinclair, 1968; Beckwith, 1960; Swinbank, 1971; Schickedanz and Changnon, 1970, 1971)

[5] (Huff and Changnon, 1959; Huff, 1960, 1961; Changnon, 1962, 1967, 1969a, 1971)

pursued continuously since the late 1950's, and they have produced much of the total climatic information about hail available in the world. These hail studies have yielded extensive, largely unsummarized, information relevant to the time and space variations of hail.

One of the first programs to aim at eventual hail suppression efforts was begun during the late 1950's in Colorado (Schleusener and Jennings,1960). With it, the hailpad (see Chapter 2) as a hail sensor was introduced to obtain quantitative measurements of hail size distribution and number concentration. In the 1960's more hail networks, also composed of hailpad sensors, were instituted in western South Dakota (Koscielski,1967), western North Dakota (Schleusener, et al.,1965), and Nebraska (Musil and Dennis,1968). More densely spaced networks, largely utilizing rain/hail separators and raingauges, were installed in central Illinois in 1967 (Changnon,1969a) and in north-eastern Colorado in 1969 (Swinbank,1971) to provide the basic data for the evaluation of suppression experiments.

In the analysis of 17 years of volunteer reports of hailfall, Summers and Wojtiw (1971) found that hailswaths which caused damage to crops in Alberta were most frequently from 3 to 8 km wide, with some severe storms producing swaths with crop damage 30 km wide. A hailswath has been defined as a precipitation pattern observed on the surface, resulting from convective activity from which hail was

reported (Wojtiw,1975a). Wojtiw used six hail reports from the same storm system as a minimum criterion to define a hailswath. Areas of 3 to 10 km² where rain without hail can exist, have been observed in the hailswaths of some severe storms (Pell,1969). Within many hailswaths, Changnon, et.al. (1967), using very dense instrumented networks in Illinois, identified a hail entity called a "hailstreak", and defined this as "the surface outline of a single volume of hail produced in a storm". Figure 1.2 (Changnon,1968d) shows an example of hailstreaks (small enclosed areas) in two major hailswaths (the two large strips extending across the figure) indicating that the two large storms which traversed this 57,000 km² area of Illinois, produced semi-continuously several separate volumes of hail. Also shown in the figure are many other hailstreaks which are associated with other systems which crossed the region in the 10-hour period. The region between the hailstreaks and the envelope of the hailfall pattern are undefined by the author, but probably consist of areas of hail or rain used in defining the envelope of the hailfall pattern. The hailstreaks shown in Figure 1.2 were drawn using data from a dense network of hailpads (one hailpad per 7 km²), supplemented with insurance loss and field survey data. From observations of 434 hailstreaks in central Illinois and around the St.Louis area in 1967-1968, Changnon (1970) computed that "their median area was 10.5 km² (ranging from 2.3 to 2040.9 km²), with an average width of 2.8 km and an average length of

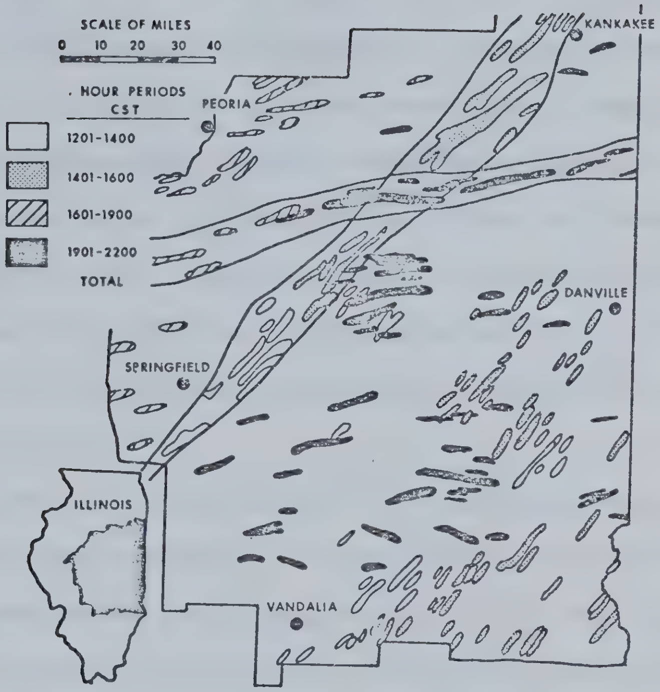

Figure 1.2 Diagram showing hailstreaks and hailswaths in a 10-hour period on 21 April 1967 in a region of Illinois. Hailstreaks are the small enclosed patches; hailswaths are large strips that traverse the map. (after Changnon,1968d)

15.3 km". Further time-space analysis of hailstreaks led to the definition and study of "hail areas" (Changnon,1968c),that is, the surface outline of the hailstreak at any given instant. Admirat (1972) has applied the term "hail core" to the concentrated high-loss (severe damage) segment of the hailstreak.

An even finer areal study of hailfall patterns (Morgan

and Towery,1974) was undertaken using very dense networks (hailpads spaced 10 to 100 m apart) over 0.3 to 3 km² areas. Networks of this type in Colorado and Illinois sensed only segments of a hailstreak which crossed the networks, but they provided extremely detailed information on the structure of streaks. Figure 1.3 shows the hailstone number density pattern for a hailstreak that crossed a 1.6 by 1 km network with 120 hailpads, and it depicts the considerable variability in the frequency of stone occurrence (values from 1076 to 3767 m^{-2})[6].

In Alberta, limited efforts in assessing the sampling density have been conducted (Strong,1974). This dissertation is a continuation of that work, and is a serious first effort to determine the necessary sampling density for hailpad data.

1.4 Precipitation Patterns - Rainfall

In this section, a review is given of the literature on network measurements of rainfall, as the results may provide an idea of what can be expected for hailfall. For rainfall, a number of studies have addressed themselves to problems of the relationship between the network density (number of observations per unit area) and the representativeness of the mean value of the rainfall from a particular event for a

---

[6] Values on Figure 1.3 are given in units per ft², the conversion is 100 ft^{-2}=1076 m^{-2}.

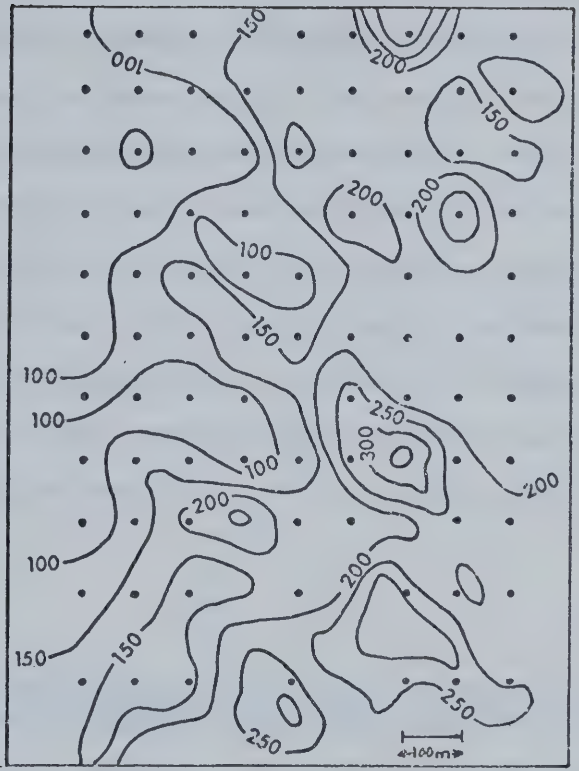

Figure 1.3 Diagram showing the number of measurable stones from 3 April 1974 storm (after Morgan and Towery, 1974)

given area. The required density of a network for rainfall is determined mainly by the variability of the precipitation events and the measurement objectives. Generally long-duration and large-area precipitation is much less variable than short-duration and small-area precipitation; therefore, the density requirements for the latter case are much higher. For example, it was found for the 2927 km² (208 mi²)

Chickasha watershed that at the 5 percent significance level, 10 gauges were as good as 158 in assessing mean-daily areal rainfall. However, for other objectives such as sampling peak storm-rainfall, the reduced network of 10 gauges was of questionable value (Nicks,1965).

Neff (1965), using network density of one recording gauge for each of the 241 km² of area in the Reynolds Creek basin, found that as the gauge density is decreased, the accuracy of estimating the areal mean is likewise decreased. The estimates Neff obtained had the 95 percent confidence limits given in Table 1.1. These results show that the 95 percent confidence limits in the mean areal rainfall are inversely proportional to $N^{.61}$, where N is the number of raingauges.

Table 1.1 Estimates of the Error of (or Uncertainty of) Areal Mean Rainfall for a Given Number of Gauges

No. of Gauges	95% Confidence Limits
90	± 2.0 cm
30	± 3.6 cm
10	± 6.9 cm
4	±13.2 cm

Numerous empirical studies of dense networks have been made in order to determine the number of raingauges necessary to estimate areal rainfall amounts with a specific accuracy. From one such study of 15 networks in the United

States, Hershfield (1965) adopted an inter-gauge correlation coefficient of 0.9 as the criterion for raingauge spacing. His results are shown in Figure 1.4.

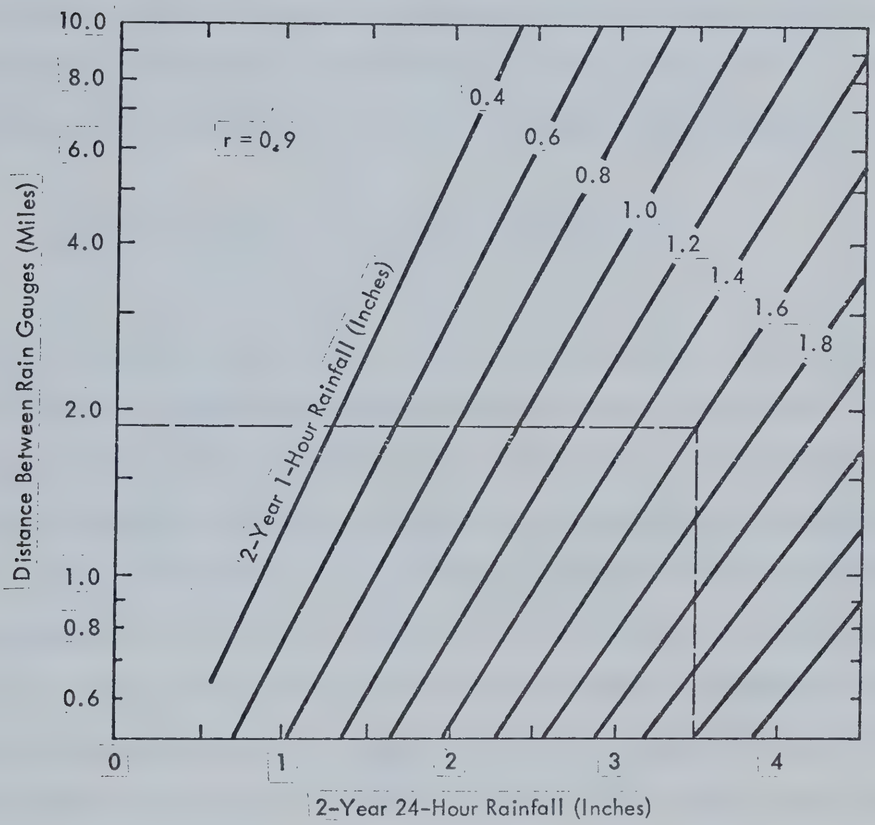

Figure 1.4 Diagram showing results of estimating required distances between gauges as a function of the 2-year-24 hour and 2-year-1-hour rainfall (Note 0.9 inter-gauge correlation coefficient) (after Hershfield, 1965)

Huff (1970), using data from two dense networks of raingauges in Illinois, obtained estimates of sampling errors in the measurement of areal mean precipitation on areas of 130 to 1295 km^2 for daily, monthly and seasonal precipitation. The storm sampling error was found to increase with increasing areal mean precipitation and to decrease with increasing sampling density (gauges per unit area) and increasing storm duration (Figure 1.5). In this figure the sampling errors were fitted using Equation 1.1.

$$\log E=-1.5069+0.65P+0.82G-0.22T-0.45A \qquad (1.1)$$

where A is the area (mi^2), E is the average sampling error in inches, P the areal mean precipitation in inches, G the gauge density in mi^2 per gauge, and T the storm duration in hours. Equation 1.1 was computed by combining all network data from the East Central Illinois Network (49 recording raingauges in 1036 km^2 (400 mi^2)) in the May to September period. Relatively large differences were frequently found in the sampling errors among storms of apparently similar characteristics (i.e. frontal storms, air mass storms, and low pressure center passages). Huff found that air mass storms require the greatest sampling density among synoptic storm types to maintain a given error level. In the warm season, rainshowers and thunderstorms were found to require nearly twice as many gauges as steady rain for a given measurement reliability. Also, the sampling density

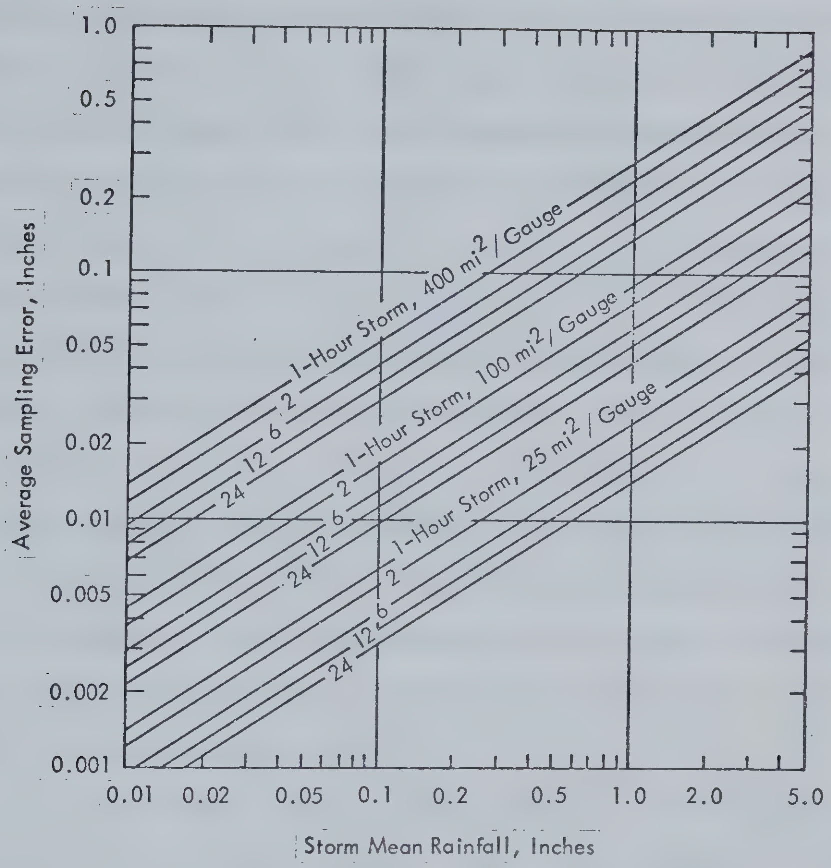

Figure 1.5 Graph showing sampling error relations on 1036 km^2 (after Huff,1970)

requirements for the May to September period were two to three times those needed in the October to April period.

A considerable difference in the magnitude of storm sampling errors during the May to September period was found between consecutive 5-year periods on the same network.

Analyses indicated that this difference resulted partially from a much higher number of air mass storms in one of the periods. Therefore, caution should be used when interpreting sampling error relations based upon observational periods of five years or less. Huff also concluded that sampling requirements for the measurement of monthly and seasonal rainfall are less stringent than those for individual storm precipitation. He found that for seasonal rainfall and a relatively sparse density of 518 km^2 per gauge, the average sampling error was less than 5 percent for the entire range of seasonal rainfalls. By way of contrast, for a 6 hour rainfall with a mean of 1.27 cm, the average error with the same network density was 14 percent. Huff mentions that his results apply to the establishment of raingauge networks in the Midwest United States and in other areas which have a similar precipitation climate.

In more recent studies, Eddy (1976), using rainfall observations from the Illinois State Water Survey at Goose Creek and the East Central Illinois networks, devised a model using optimal interpolation objective analysis in order to estimate the rainfall, the gauge density and the accumulation time. In this model, the á priori rainfall was modelled by fitting a gamma distribution function to the observed rainfall amounts from individual storms and to the composite data from a combination of storms. The Type 1 and

Type 2 errors [7] are graphically depicted in Figure 1.6. He

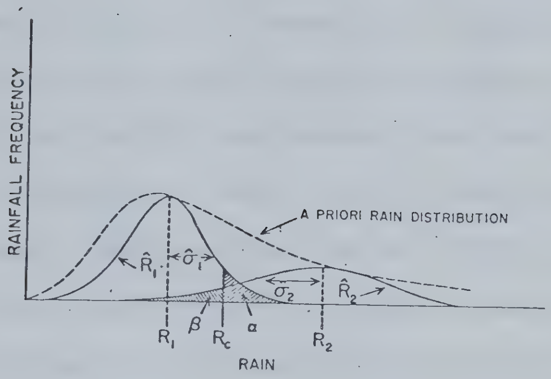

Figure 1.6 Distribution of two objective analysis sets about their respective true values with a priori true rainfall distribution superimposed. The Type 1 (α) and Type 2 (β) errors are indicated. (after Eddy,1976)

concludes that for a dense network (816 km^2 area) the optimal values [8] give an average density of 16.3 km^2 per gauge with an accumulation time of about 10 min while for a sparse network (25,900 km^2 area) one gauge per 104 km^2 will give the desired accuracy [9] if at least one hour of rain is

---

[7] "Given an acceptable objective analysis $\hat{R}$, one can say that it represents a random deviation from population R_2 if $\hat{R} > R_c$ and from R_1 if $\hat{R} < R_c$ with the following expectation of misclassification: The fraction of the time R_2 would be chosen (using $\hat{R} > R_c$), when R_1 was the truth, would be α (Type 1 error). The fraction of the time when R_1 would be chosen (using $\hat{R} < R_c$), when R_2 was the truth, would be β (Type 2 error)."

[8] Minimum rainfall of interest Rm=0.02 inches; Type 1 error (α =0.01), Type 2 error (β =0.10)

[9] Minimum rainfall of interest Rm=0.1 inches; Type 1 error (α =.1), Type 2 error (β =0.15)

collected by any gauge during a 24 hour period. The analyzed rain came from unstable summer showers and was observed using tipping bucket raingauges. Consequently, Eddy's numerical results apply to shower-type rainfall and should not be transferred to other locations without a careful consideration of whether the showers have the same statistical structure as that found in Eddy's data sample.

In another study, Collier, et.al. (1975) compared calibrated radar measurements of areal rainfall with rainfall measurements obtained solely with raingauge networks of various densities. In that study, the authors compared the accuracy of the two methods of measurement in hilly terrain over a period of one hour, using results obtained with a one degree beamwidth and a 5.6 cm wavelength radar. The comparisons were made over areas which varied in size from 20 to 100 km². The raingauge network was distributed over 1000 km² and consisted of 62 battery operated Plessey MM37 tipping bucket raingauges, incorporating a magnetic tape event recorder. Figure 1.7 shows the results of this study; that is, the accuracy of the investigations achieved by a calibrated radar [10] and by raingauge networks of various densities. The curved lines (solid indicate the calibrated radar, and hyphenated signify the raingauges) show the mean percentage differences from

---

[10] The radar calibration is performed with one or more rain gauges.

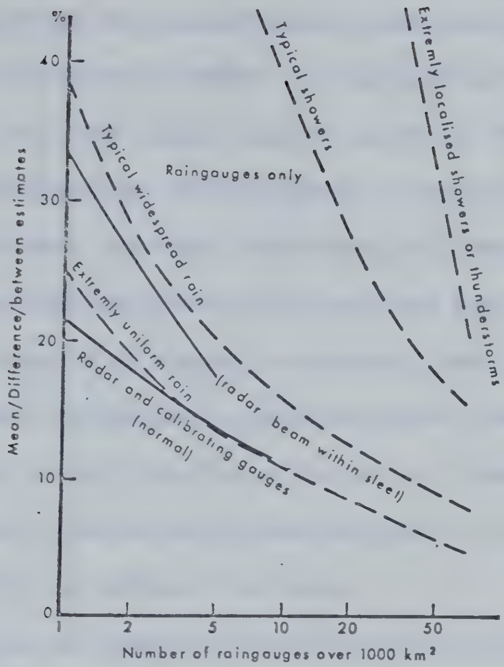

Figure 1.7 Graph showing difference between estimates of hourly sub-catchment rainfall related to raingauge density (after Collier,et.al.,1975)

the optimum estimates [11] of hourly sub-catchment [12] rainfall as measured by various numbers of raingauges distributed over the 1000 km² area, and the calibrated radar system. The results from the raingauge networks show a large difference in accuracy between days with showers and those with

---

[11] The observed radar echo intensity pattern was used to interpolate between the gauges so as to obtain a reliable estimate of rainfall features on a scale smaller than the gauge spacing. The resultant distribution of precipitation is called the optimum field, while the values in the field are the optimum estimates.

[12] one of 16 unequal segments of the 1000 km² area.

widespread rain. The accuracy which could be achieved by a radar calibrated by raingauges and incorporating a model (Harrold and Kitchingman,1975) to reduce the melting layer error is shown by the upper solid curve in Figure 1.7.

The solid lines on the diagram are the mean percentage differences between optimum estimates of hourly rainfall and radar estimates calibrated using various numbers of calibration sites. The higher accuracy line (lower solid line on diagram) indicates occasions when the radar beam is entirely within rain. The lower accuracy line (upper solid line on diagram) indicates occasions when a mixture of rain and snow (sleet) is within the beam.

The hyphenated lines on the diagram represent the mean percentage differences between optimum estimates of hourly rainfall and estimates using various numbers of raingauges without a radar. Upper lines show showery conditions, lower lines indicate widespread rain. The diagram (Figure 1.7) can be used for example to derive the number of raingauges required to measure rainfall with the same accuracy as a radar system calibrated with a specified number of raingauge sites. For example in typical showers a radar system calibrated using two raingauge sites gives the same accuracy as a raingauge network of about 50 raingauges over 1000 km^2.

In this chapter several research projects dealing with precipitation patterns have been summarized. The efforts made by various researchers to assess the relationship between hailfall and rainfall variability, and network

density have also been presented. The limited effort in resolving this problem for hailfall has been twofold: unavailability of quantitative data and the variability in space and time of hailfall. Much more work has been done on assessing the required network density for rainfall. Before introducing the approach for assessing the hailpad network density, a discussion of the collection and reduction of the hailpad data will be given, so that the reader may become familiar with the observations used.

CHAPTER 2

DATA COLLECTION AND REDUCTION

2.1 Observations

The primary source of objective hailfall data is the hailpad-a styrofoam pad of dimensions 30.5 cm x 30.5 cm x 2.5 cm. Hailpads were set out in two networks operated by the Alberta Hail Project during the summer months in central Alberta from 1974 to 1976.

The two networks and their locations are shown in Figure 2.1 and Figure 2.2. These are:

(1) a precipitation network of 500 stations over an area of 34,467 km^2 [1]

(2) a dense network of 162 stations over an area of 932 km^2 (embedded within the large precipitation network in the Rimbey district of Alberta).

By analysis of the pads, the hail size distribution, and the areal concentration of the hailstones for the duration of a hailstorm can be obtained. However, the pads do not give time-resolved information about the hailfall, which may be important for relating cloud seeding events to hailfall on the ground.

All stations (volunteer observers) in the two networks

---

[1] No stations are located on the western edge of the project area, hence the figure reported here is smaller than that given in Chapter 1.

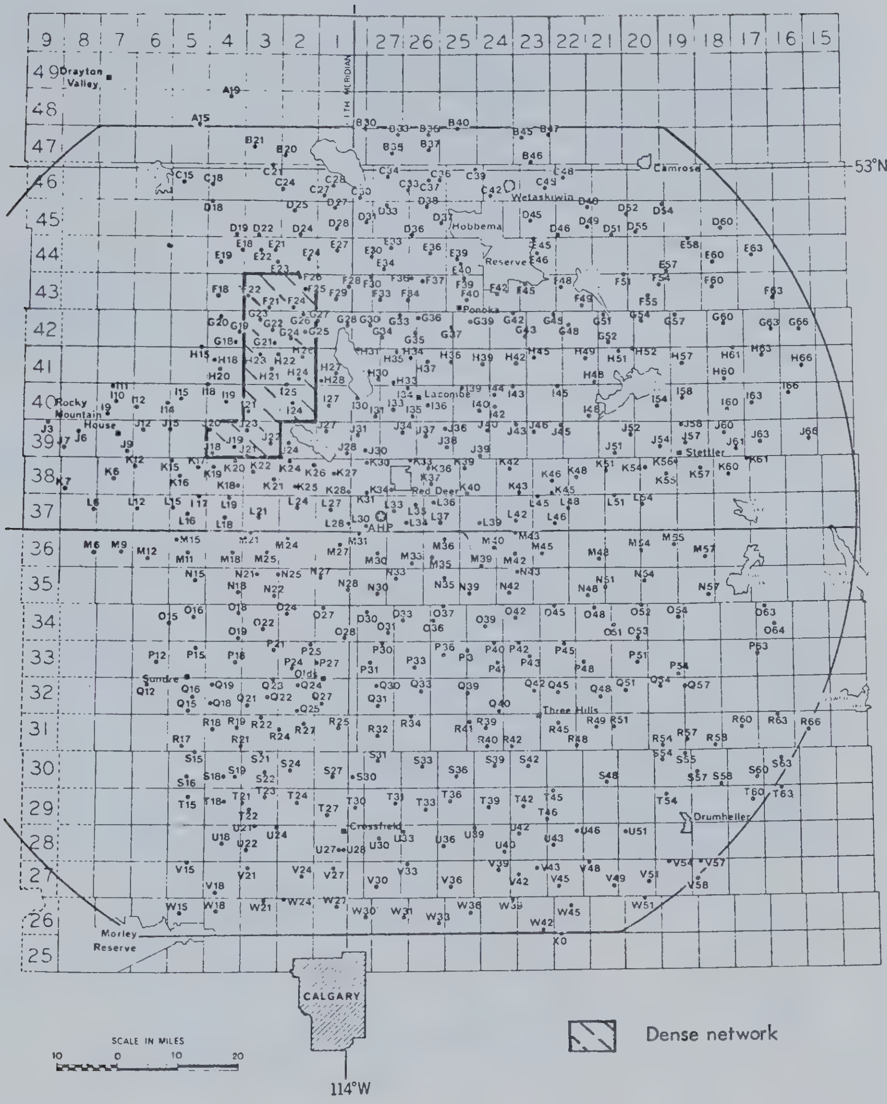

Figure 2.1 Map showing networks in the Alberta Hail Project

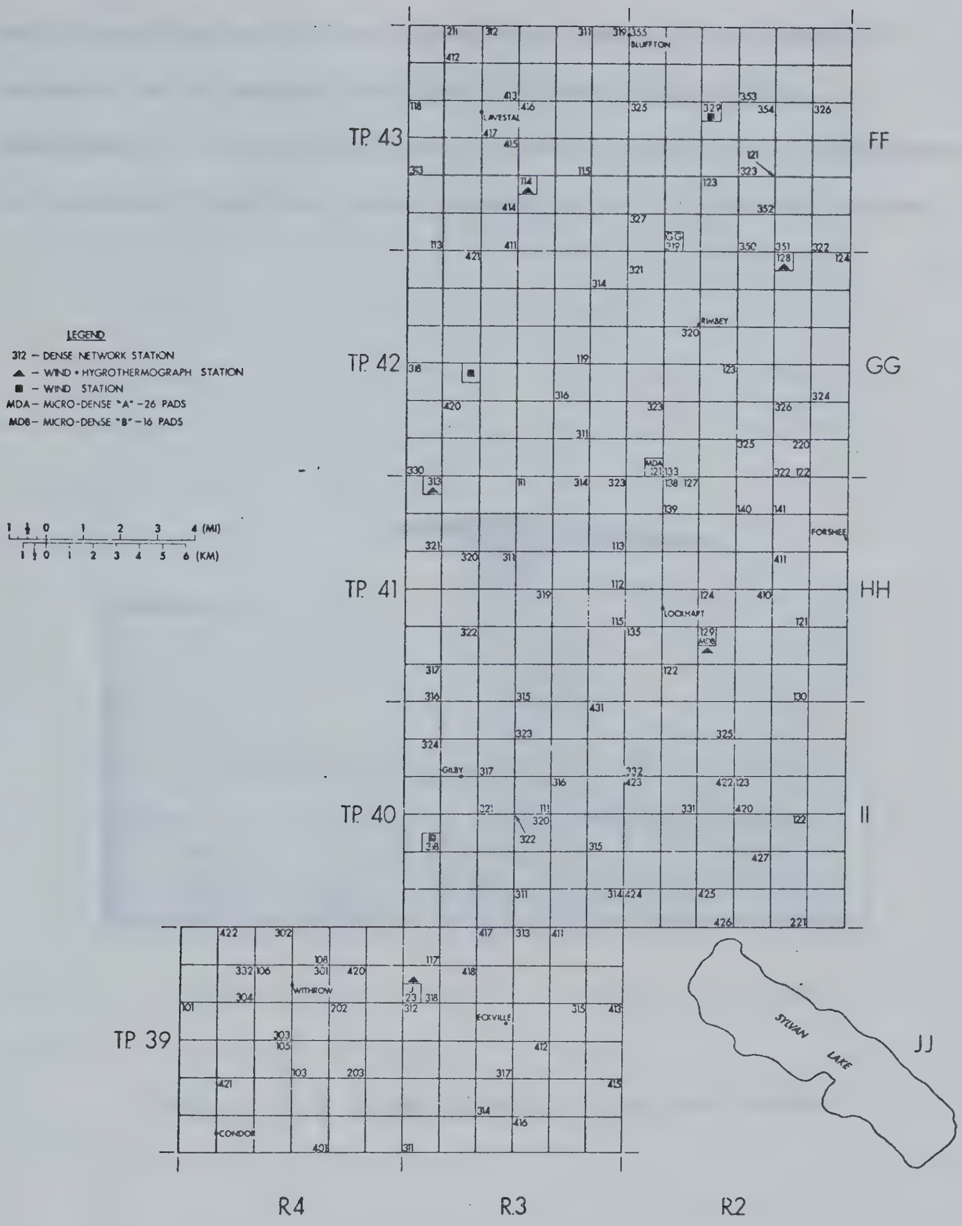

Figure 2.2 Diagram showing location of hailpad stations in the dense network (Stations are located in the quarter section where the numbers are printed)

were supplied with four styrofoam pads, a pad holder [2] mounted on a supporting stand [3] (see Figure 2.3), a raingauge [4] and appropriate forms to report the occurrence of hailfall and the total amount of daily precipitation.

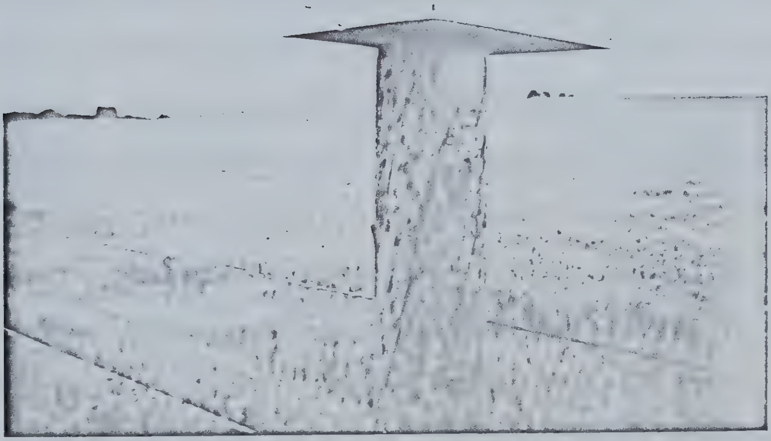

Figure 2.3 A picture of a hailpad stand

---

[2] A 30.5 cm x 30.5 cm x 2.5 cm plywood board with two narrow metal slits on two of the sides of the board to hold the hailpad in place.

[3] A 5.1 cm x 10.2 cm x 1.8 m two-by-four, or fence pole if available.

[4] A plastic wedge type manufactured by Edwards Manufacturing Co., Minnesota, U.S.A. called Tru-Check.

Each station operator was asked to change the pad immediately after the hailstorm or once per week, or if the pad became damaged in any way. Field tests in 1975 showed that the pad begins to deteriorate after 10 days in sunlight. Beyond ten days, the deterioration is rapid and the sizes of hail dents made thereafter are unreliable.

When they arrive from the manufacturer, the styrofoam pads are quite coarse. In order that the roughness is not mistaken for small hail dents, a pad sander (Figure 2.4) was developed in 1975 at the Alberta Research Council. The dented pads, returned from the field, were then inked with a print roller to provide contrast between the uninked hail dents and the inked undented background styrofoam. Figure 2.5 shows an example of an uninked and an inked pad. A quantitative measure of the number of hailstones in various size categories can be obtained from the hail dents. These measurements are used to calculate the impact energy per unit area (subsequently referred to as the _impact energy density_) (see Section 2.3).

2.2 Analysis of the Hailpads

The analysis of the pads for hail size distribution and concentration was carried out by hand. This involves the use of a transparent overlay (see Figure 2.6) with imprinted circles of diameters 0.25 cm to 2.54 cm at .25 cm intervals, and 2.54 cm to 5.08 cm at .63 cm intervals. The dent was estimated to the nearest .13 cm and placed in the

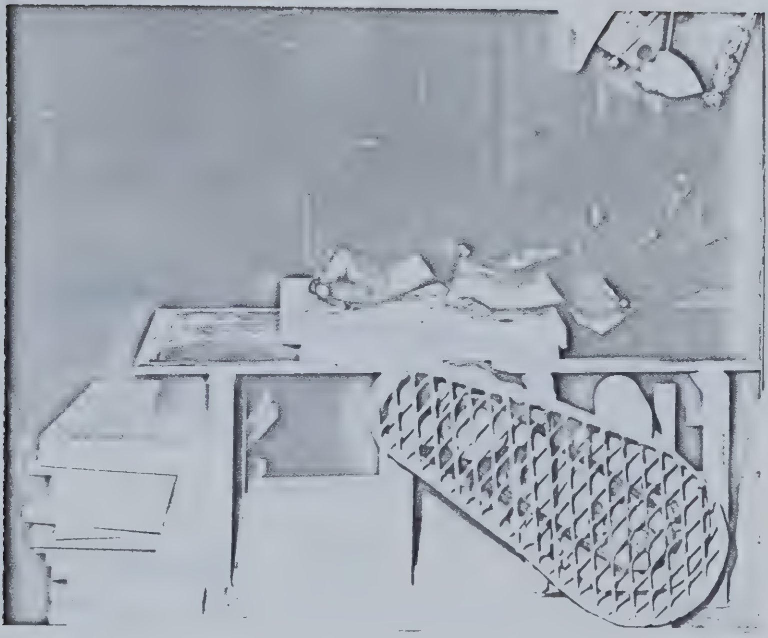

Figure 2.4 A picture of a pad sander used to eliminate coarseness in the styrofoam

appropriate size category. For example, if a dent was larger than .25 cm but smaller than .38 cm, it would be placed in the .25 cm category. This procedure gives rise to an underestimate of the sizes, and as a result an underestimate of the calculated impact energy density. The magnitude of the error in the impact energy density decreases as D^4. The maximum error in the impact energy density occurs if all the size categories are underestimated by one size category. In this case the error in the impact energy density is 80.2 percent for the .25 cm category and decreases proportionally as D^4 to an error of 17.7 percent in the 2.54 cm category.

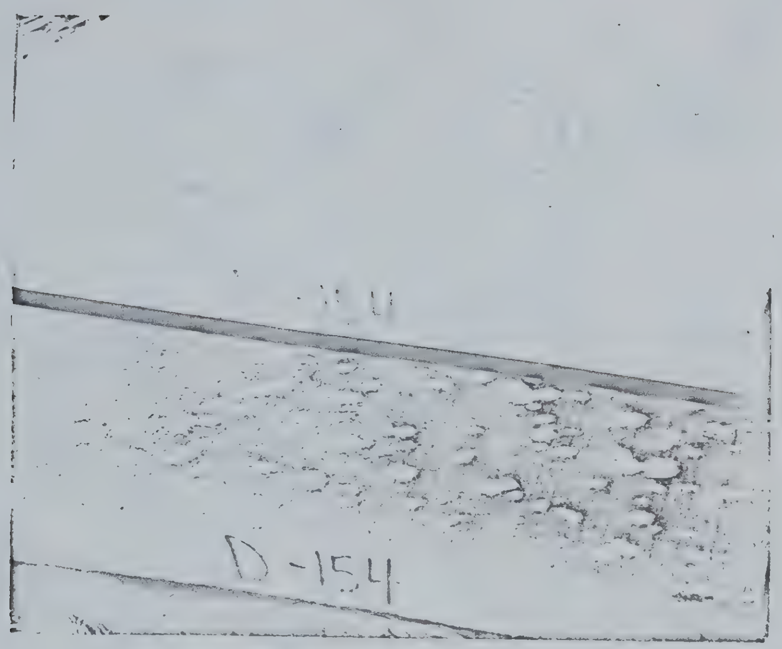

Figure 2.5 A picture of an uninked hailpad (above) and the same pad after inking (below)

For the 29 July 1974 hailswath the maximum error in the impact energy density, assuming that all the dent size categories are underestimated by one size category, is 36.9 percent.

The number of dents of each size category was recorded for each hailpad. In order to convert from dent sizes to hail sizes, the calibration curve shown in Figure 2.7 was used (Lozowski and Strong,1977).

2.3 Calculation of Impact Energy Density

The kinetic energy of a hailstone upon impact (impact

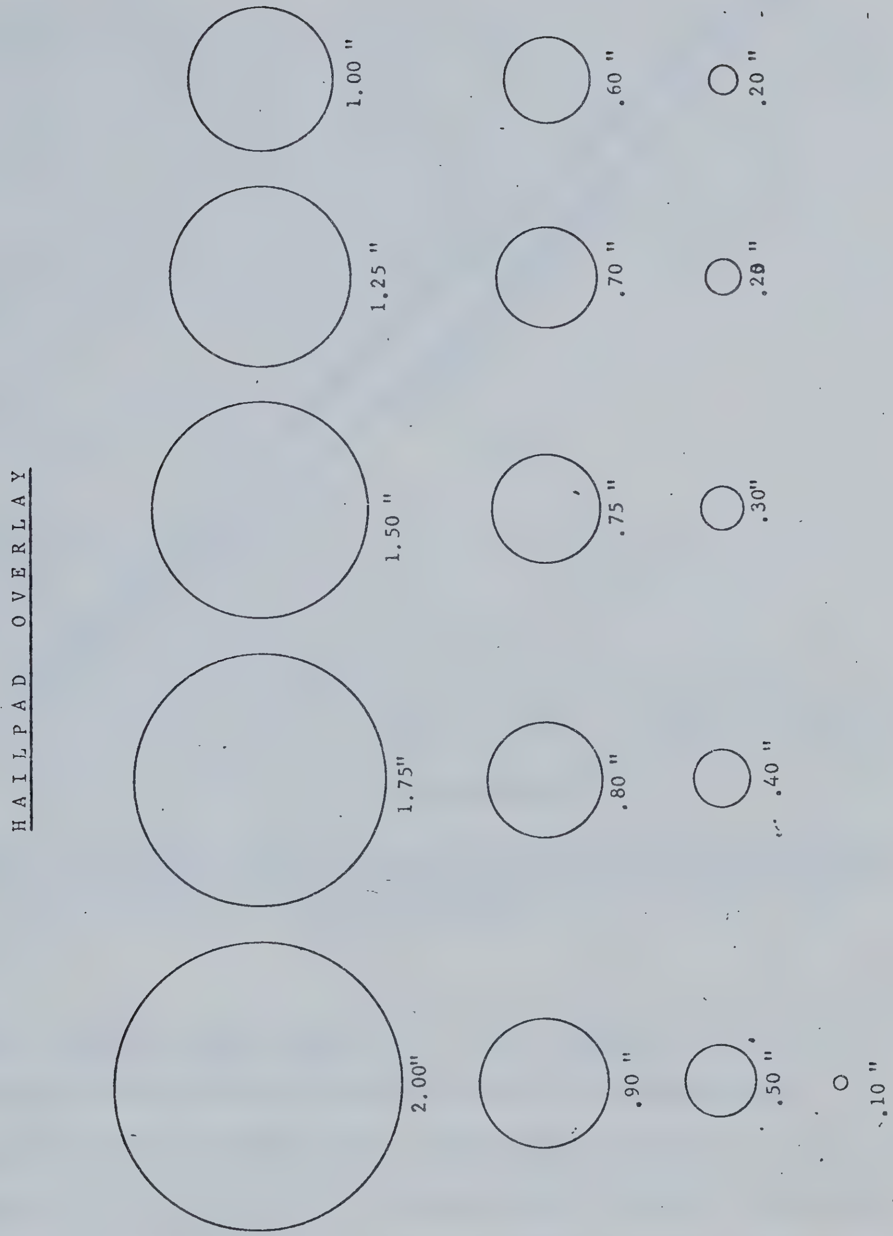

Figure 2.6 Hailpad overlay used in analysis

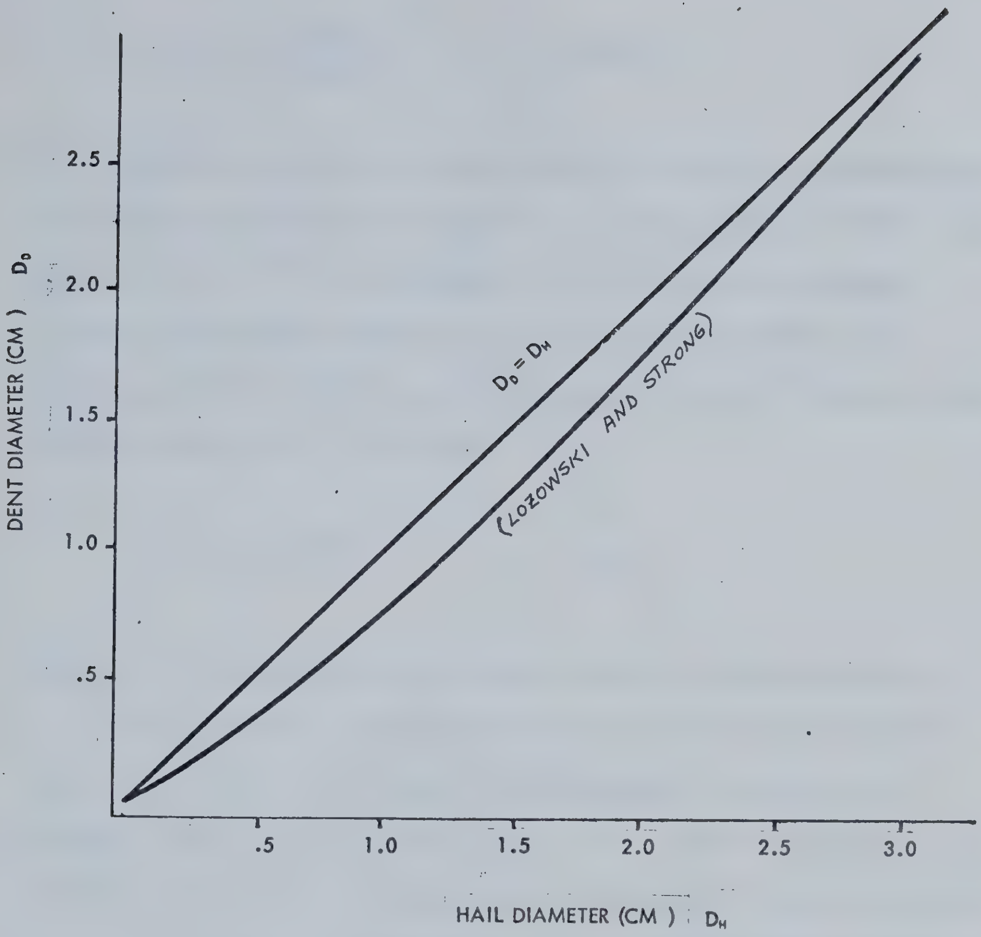

Figure 2.7 Graph showing conversion from dent diameter (on the hailpad) to hail diameter (after Lozowski and Strong, 1977)

energy), assuming no horizontal wind component, can be calculated from the hailpad data using the following formulae (Strong, 1974). For a spherical hailstone of mass m, diameter D, density ρ, and falling with terminal velocity V_T through air of density ρ_a, the equation of motion can be solved to yield:

$$V_T = \left(\frac{4 \rho g D}{3 \rho_a C_D} \right)^{1/2} \qquad (2.1)$$

The following parameters were found to be most appropriate for typical Alberta conditions (at a pressure of 890mb and a temperature of 22°C) (Strong,1974): drag coefficient C_D =0.60, hailstone density ρ =0.89 g cm^{-3}, surface air density ρ_a =1.05x $x10^{-3}$ gm cm^{-3} and g=981.3 cm s^{-2}. Using these values, Equation 2.1 becomes:

$$V_T = 13.6 \, D^{1/2} \qquad (2.2)$$

where V_T is in meters per second and D in centimeters.

This relation was confirmed by Lozowski and Beattie (1975), who used high-speed photography to measure the terminal velocity of hailstones up to 1 cm in diameter for several 1974 Alberta hailstorms. They found that the curve $V_T = 13.3 \, D^{1/2}$ was a reasonable fit to their measurements. The kinetic energy for a single stone on impact is therefore:

$$I_E = \left(\frac{\pi \rho^2 g}{9 \rho_a C_D} \right) D^4 \qquad (2.3)$$

Substituting the typical values for the various parameters into Equation 2.3 yields:

$$I_E = 4.307 \times 10^{-2} \, D^4 \qquad (2.4)$$

where I_E is in Joules and D in centimeters.

This equation gives the kinetic energy of a single hailstone. In order to calculate the total kinetic energy for the stones on the hailpad, for each of the size categories, an impact energy is determined for each category and these values are then summed. Equation 2.4 for the impact energy density on the hailpad then becomes:

$$I_{ET} = 4.636\times10^{-1}\sum_{i=1}^{P} A_i D_i^4 \quad (Jm^{-2}) \quad (2.5)$$

where D_i is the diameter, and A_i is the number of hailstones on the hailpad in the i th size category (for i=1,P where P is the number of size categories).

For a hailstone falling with velocity V_T, in a horizontal wind V_H and assuming that the horizontal velocity component of the hailstone equals the wind speed, the total impact energy becomes:

$$I_{ET} = 0.5m \left(V_T^2 + V_H^2\right) \qquad (2.6)$$

where $V_H = V_T \tan\theta$ and $m = \frac{\pi\rho D^3}{6}$ and where θ is the angle to the vertical at which the hailstone strikes the horizontal pad. The impact energy then is

$$I_{ET} = \left(\frac{\pi\rho^2 g}{9\rho_a C_D}\right) D^4 \sec^2\theta \qquad (2.7)$$

or upon substituting the typical values given previously into Equation 2.7, we obtain:

$$I_{ET} = 0.4636D^4(\sec^2\theta) \quad (\mathrm{J\ m^{-2}}) \qquad (2.8)$$

Equation 2.8 is the impact energy density for an individual hailstone falling with velocity V_T in a horizontal wind V_H. To obtain the total impact energy density for the hailpad, the value obtained in Equation 2.8 is summed over all hailstones and their angles of impact. Equation 2.9 is the equivalent counterpart to Equation 2.5 for a hailstone falling in a wind:

$$I_{ETH} = 4.636 \times 10^{-1} \sum_{i=1}^{P} A_i D_i^4 \sec^2\theta_i \qquad (2.9)$$

where D_i is the diameter, A_i is the number of hailstones in the i th size category (for i=1,P where P is the number of size categories).

The equations for a hailstone falling in a horizontal wind are given for completeness, since these have not yet been incorporated into the calculation of impact energy density from the hailpads. Hence the impact energy density values used in the following chapters will be values calculated assuming no horizontal wind component. The reason for this lack of implementation is that few hailpads have a wind measurement associated with them. Wind speed, however, is an important quantity. Strong winds can cause 30 percent more damage to crops than light to moderate winds (Wojtiw and Renick,1973). Morgan (1976) suggests that wind contributes to even greater crop damage but the magnitude of

the effect is not given. Hence this quantity should not be ignored in the evaluation of hail suppression. Using a hailcube, five hailpads joined to form a cube (minus the bottom hailpad), Morgan has been able to estimate the horizontal wind component from the hailpads (Vento and Morgan, 1976). These cubical units have not been used in Alberta in the networks but should be considered in setting up future networks. Hence the (vertical) impact energy values calculated by Equation 2.5 are used in the Monte Carlo method described in the next chapter.

CHAPTER 3

THE MONTE CARLO METHOD

3.1 Introduction

Hailpad measurements are a "random" sample of energy densities from a true distribution of energy densities which could be determined in principle only if the ground were completely covered with hailpads. From the point of view of comparing seeded and unseeded hailstorms, a true mean impact energy density for the hailswath is desired. Since the true mean impact energy density is not available in reality, a procedure like the Monte Carlo method is used to obtain an estimate of the uncertainty of the mean impact energy for the hailswath. This is done by averaging the hailpad observations, perhaps weighting them according to the area they represent, and estimating how the hailpad average differs from the true mean. In this dissertation a certain true distribution function is assumed (obtained from the hailpad observations) and the Monte Carlo method is used to simulate the "random" sampling. Thus for a given true mean value a distribution of observed means is obtained. This distribution of observed means could theoretically be obtained with a variety of hailpad networks of varying areal distribution and given density.

To illustrate the basics of this problem consider the following example (Panofsky and Brier, 1963). When a sample

of an apple pie is cut and tasted, it is possible to conclude that "This pie is good" or "This pie needs more sugar". Of course, neither of these statements is based on complete knowledge, since nothing is known about the pie as a whole, but only about the sample tasted. What we really mean, is, since the sample chosen tastes good, and since the other pieces probably taste the same (i.e. we are making the implicit assumption that the pie's properties are homogeneously distributed), it is reasonable to presume that the rest of the pie will taste good. Thus, from the characteristics of the small sample, inferences on the characteristics of the whole are drawn. Actually, one piece from the entire pie would be a very poor sample of the pie in the statistical sense, for the oven may have been slanted, and all the sugar may have drifted into the sample tested. As a result drawing conclusions about the whole pie would be incorrect. A better method would have been to collect a "random" sample by spooning a taste from various parts of the pie. In order that all of the sample pieces do not come from the same sector of the pie, it is better to choose a representative sample from each area. This is "stratified sampling"; that is, the pie is divided into M uniform sectors and k spoonfuls from each sector are chosen at random. These basic ideas can be applied in a similar fashion, using the Monte Carlo method, to impact energy density values calculated from hailpad data. Here sampling is carried out for impact energy density values on a

hailswath basis and not on a hail day basis where more than one hailswath may have occurred (i.e. one pie at a time and not many pies which may have been cooked on other stoves).

The method of simulating statistical trials (or sampling) using computational techniques and recording numerical characteristics obtained from these experiments is called the Monte Carlo method. The term "Monte Carlo" originated in 1942, at Los Alamos, in studies conducted by von Neumann, and it appeared in publication in the works of N. Metropolis and S. Ulam (1949) and Shrieder (1966). For impact energy density values the method is to select a random sample many times using computational techniques and to record the numerical results. The prime requirement of the Monte Carlo method is the availability of random numbers. These can be obtained on the computer by employing one of a number of subroutines which generate random numbers, based on arithmetical algorithms from the computer library. In this analysis the subroutine used to select the samples (i.e. to generate the random numbers) is GGU3 found in the *IMSLLIB library. The numbers obtained from this subroutine are uniformly distributed on the interval 0,1 . Figure 3.1 shows the distribution of 40,000 random numbers obtained from subroutine GGU3 for an expanded interval 0,100 in five unit steps. The results show that the number of values in each interval appears to be uniformly distributed with a mean of 2000 and a standard deviation of 33.9, with the lowest interval having a value of 1918 (4.1 percent

below the mean), while the largest interval has a value of 2066 (3.3 percent above the mean). The above subroutine is

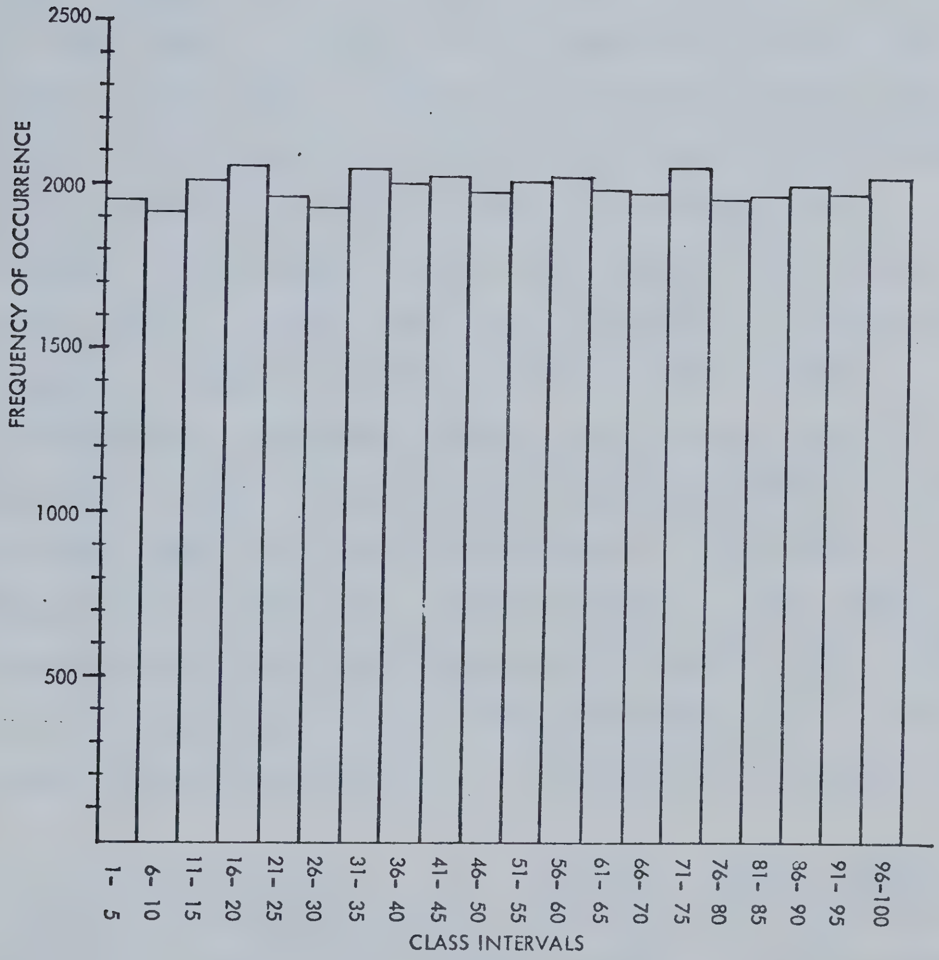

Figure 3.1 Distribution of 40,000 random numbers drawn from subroutine GGU3 for the expanded interval [0,100]

number of ways [1] of selecting the random numbers on the computer for use in the Monte Carlo method.

The Monte Carlo experiments for the hailpad data can give an estimate of the distribution of the possible average impact energy densities which may be observed with a network of given size. In theory, if the size of the network (i.e. number of stations in a fixed area) becomes infinite, the answer to how the distribution of the average impact energy densities should behave is given in the central-limit theorem of probability theory. This theorem (see Feller, 1950; pp191ff.) states that the distribution of the sum of k mutually independent random variables, with a common distribution, approaches a normal distribution as $k \longrightarrow \infty$. The mean is equal to that of the common distribution and the variance equal to k times the variance of the common distribution. Hence, for a random sample of impact energy density values the distribution of the mean of such a sample is expected to approach the normal distribution [2] as the sample number increases (i.e. as the number of stations in a

---

[1] Some of the others ways are: GGBIN-one binomial pseudo random deviate; GGBTA-Beta random deviate generator; GGCSS-generator of a chi-squared deviate; GGMEXP-generator of exponential deviates and GGPOSH-generator of Poisson random deviates, among others.

[2] A sample can be tested if it comes from a normal distribution if the z score (distribution of the standardized variable) of its statistic lies outside the range -1.96 to 1.96 for the region of significance at the 5 percent level. For the z score distribution the mean is 0 and the variance is 1.

fixed area increases). In practice with the hail energy density distributions, it is found that with *k* greater than 25, the distribution of the mean impact energy density shows some resemblance to the normal distribution.

3.2 Sampling Techniques

There are numerous ways of selecting a sample from a set of values. In this dissertation five techniques are given and described below. Some of these techniques represent more the sort of sampling which hailpads do, than others. However, all five will be considered at least briefly, so that an intercomparison can be made. The five techniques are:

a) The original data are picked at random _without replacement_, and various statistical parameters are calculated. Thus, the samples in a single draw are determined by the elements selected. In this technique the number of samples drawn is limited to the number of members in the data set or population, since the first cannot exceed the latter.

b) The original data is picked randomly _with replacement_. Here, it is possible to choose the same data value many times. This approach has the advantage over the one in (a) in that the sample number is no longer restricted to the number of members in the data set, but can be any size.

c) _A distribution is fitted_ to the original data and

random selection is carried out from the fitted distribution. This procedure allows the selection of many more random variables than the original data set. However, the results are only as reliable as the fit of the distribution to the original data.

d) Stratified Sampling: The cumulative distribution of impact energy density values from the original data is divided into M equal segments of probability values and a random selection of k values is made from each segment. If M=1, the technique is equivalent to technique (b). If, however, three segments (M=3) are used then one-third of the impact energy density values will come from the low band of values, another third from the intermediate values, while the last third will be drawn from the high band of values. This procedure guarantees that all the samples do not come from the same band of values, as is possible in procedure (b).

e) Spatial Sampling: In this technique a "true" spatial distribution is estimated by an interpolation, contouring, or an objective analysis method. This technique accounts for the fact that the impact energy density values are distributed in a two-dimensional space, as is the sampling network. Thus emphasis is placed on the spatial distribution of the impact energy densities. A random network (but with a certain average spacing and hence a fixed density) is imposed and a value from each network grid is randomly selected.

In Chapter 4 these five techniques for selecting impact energy density values are applied to the 29 July 1974 hailswath as an example of the procedure. The computer program for the first four techniques was developed in FORTRAN IV on the University of Alberta AMDAHL 470V/6 computer. It appears in Appendix I. The computer program used for the contouring technique in the fifth sampling approach was developed by R. Newton (1973) in a modified FORTRAN IV language on a DEC PDP-9 computer.

CHAPTER 4

APPLICATION OF THE MONTE CARLO METHOD TO HAILPAD DATA

In this chapter the Monte Carlo method is applied to the impact energy density values and the distribution of the means of k samples is determined. The method is used with the five techniques described in Chapter 3: sampling without replacement from the observed distribution of impact energy densities; sampling with replacement from the observed distribution; sampling from an idealized two-parameter gamma distribution; stratified sampling from the observed distribution of impact energy densities; and spatial sampling from a contoured pattern of the observed energy density field. The data from the 29 July 1974 storm are used to illustrate the techniques. This was a severe hail day on which 34 hailpads were returned in a hailswath area of 3183 km^2. The storm began west of Rocky Mountain House in the middle of the afternoon and moved south-east towards Three Hills. Figure 4.1 shows the precipitation reports [1] and the location of the hailpad observations for this hailswath. Golfball-size hail was reported by the volunteer observers south of Red Deer.

Figure 4.2 shows the distribution of the impact energy

---

[1] In Figure 4.1, the numbers indicate hail of different size categories: 1-shot; 2-pea; 3-grape; 4-walnut; 5-golfball; 6-greater than golfball; 0 is hail of unknown size; R denotes rain only and X no rain or hail.

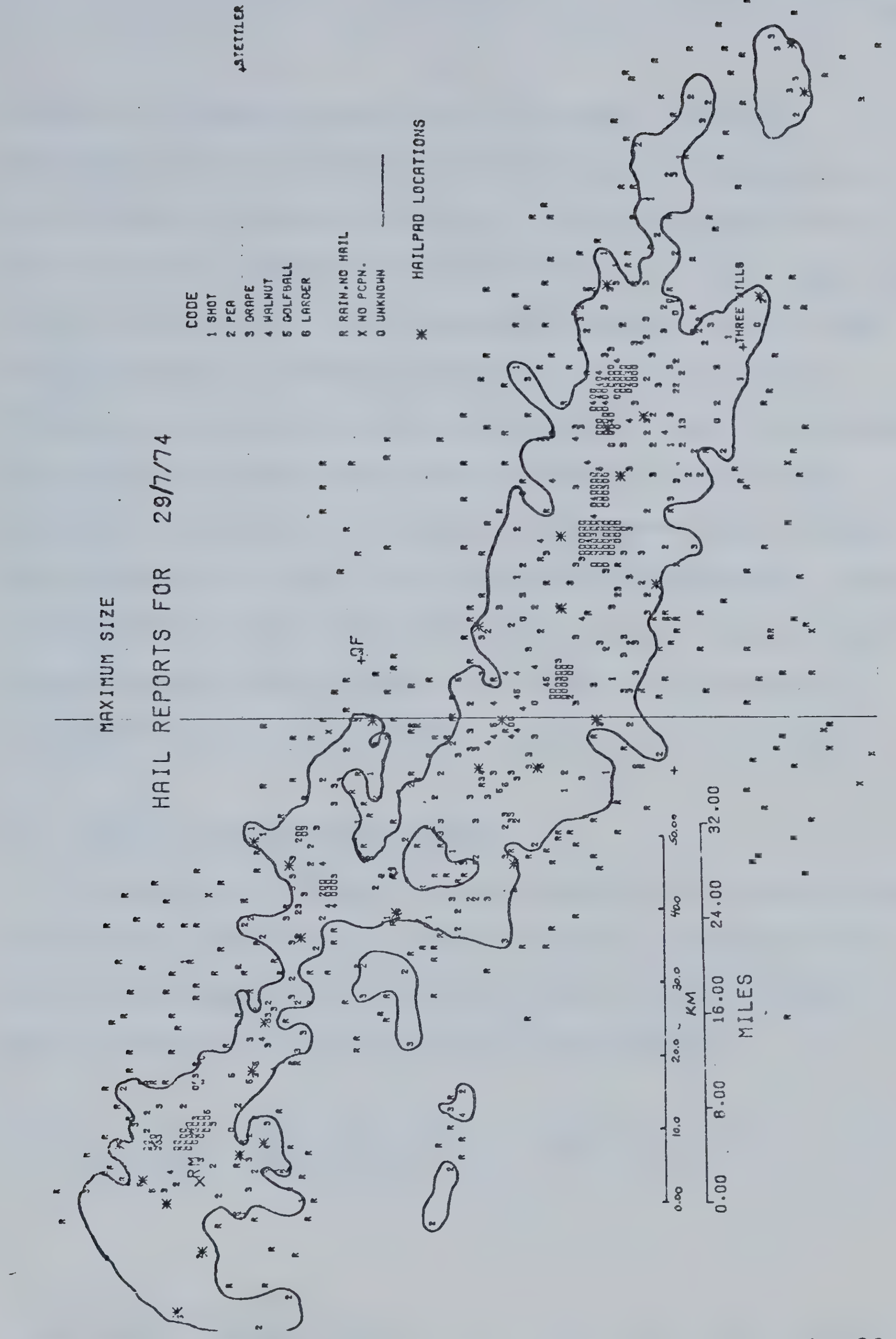

Figure 4.1 The hailfall and hailpad locations for the 29 July 1974 hailswath (The vertical line is the 5th Meridian. The numbers outside the hailswath resulted from other systems which occurred that day. The station symbols are: RM-Rocky Mtn. House; QF-Red Deer Mun. Airport)

density[2] calculated from the 34 hailpads for this hailswath. In this figure the impact energy density values are grouped in classes of 25 J m^{-2}. The population mean is 84.1 J m^{-2}, the standard deviation 120.6 J m^{-2}, the range from 0.5 to 546.8 J m^{-2}[3], and the median value 41.2 J m^{-2}. The curve through the triangles in Figure 4.2 is the best fitting two-parameter gamma distribution, which is discussed in Section 4.3. The cumulative frequency of the energy density is displayed in Figure 4.3 where the curve through the triangles is again the best fitting two-parameter gamma distribution. Other hailswaths were examined and the impact energy density distributions for these are presented in Appendix III while the results are discussed in Chapter 5.

4.1 Sampling Without Replacement

A sample of k impact energy densities is drawn randomly N times from the total number Z of impact energy densities for the hailswath. The standard deviation of the sample mean, denoted by s, is calculated according to:

$$s^2 = \frac{\sum_{i=1}^{N} \left(\bar{x}_i - \bar{\bar{x}}_i\right)^2}{N} \qquad (4.1)$$

---

[2] The impact energy densities for the 29 July 1974 hailswath are given in Appendix II.

[3] In three years of data (1974-1976) the hailpad impact energy density values ranged from 0.1 to 2332.6 J m^{-2}.

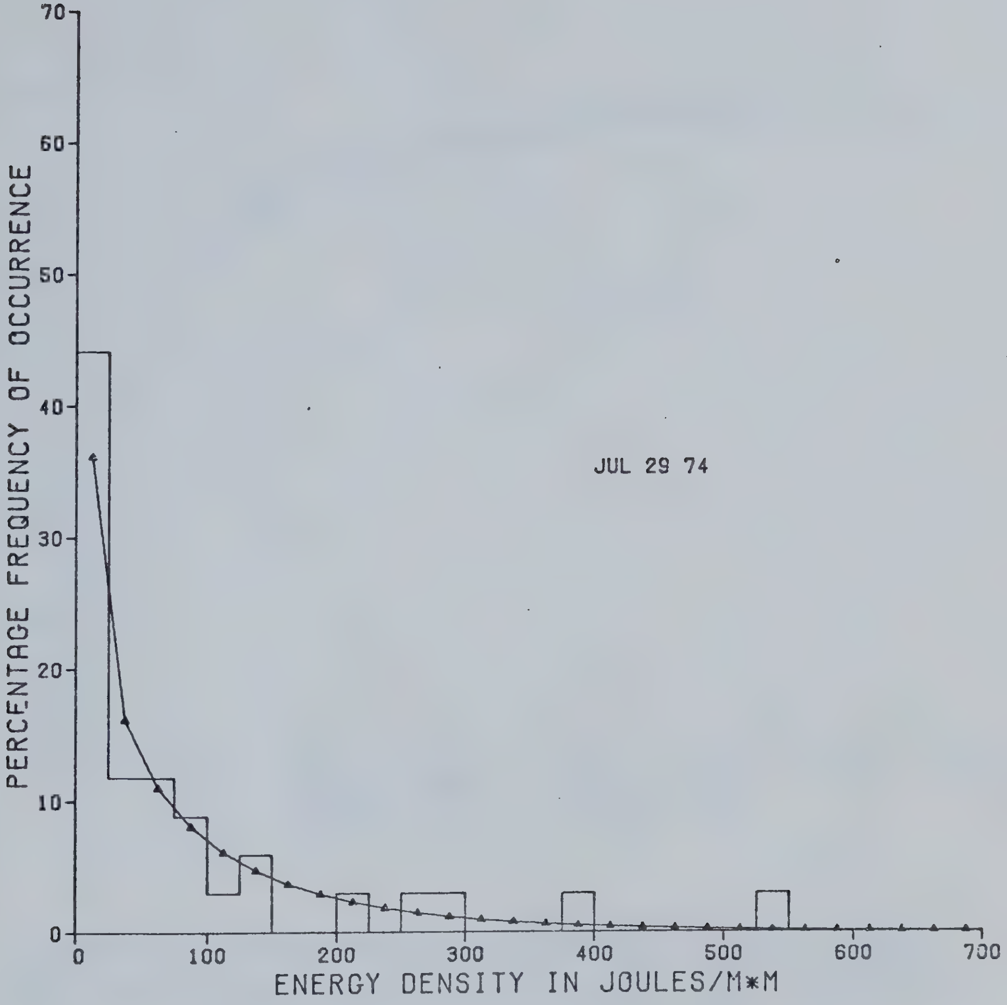

Figure 4.2 The percentage frequency of occurrence of impact energy density values for 29 July 1974 hailswath (The curve through the triangles is the best fitted two-parameter gamma distribution)

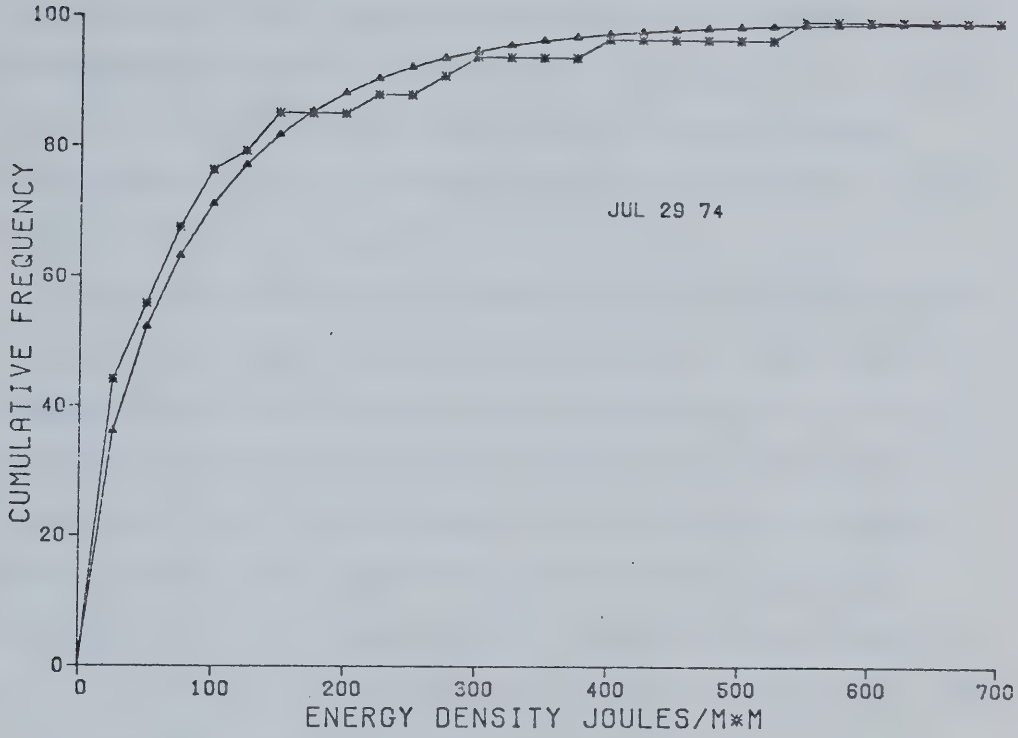

Figure 4.3 The cumulative frequency of impact energy density for 29 July 1974 hailswath (The "stars" represent the original data, while the "triangles" the best fitted two-parameter gamma distribution)

In Equation 4.1 the sample means are $\bar{x}_i$ (where i=1,N) * , while the mean of the sample means is given by $\bar{\bar{x}}_i$. The k samples are drawn at random and the distribution of the means

---

* N-1 is used in preference to N in the denominator of Equation 4.14.1 in order to obtain an unbiased estimator. The difference for the values of N used in this thesis is small.

of the samples is determined. Using $N \ll 1000$ might not give as reliable an estimate of the distribution of the means while $N \gg 1000$ would consume too much computer time, consequently $N=1000$ was chosen as a compromise. For the 29 July 1974 hailswath the total number of impact energy densities is $Z=34$. For sampling without replacement k (the sample size) was chosen as 5, 15 and 25.

For this hailswath the probability density functions [5] of the sample means are given in Figure 4.4. For $k=5$, the distribution of the sample means varies from 5 to 175 J m^{-2} with no clearly defined single maximum near the population mean of 84.1 J m^{-2}. The standard deviation of the sample means is 49.3 J m^{-2}. For $k=25$ the distribution becomes narrower, with the sample means ranging in value from 45 to 110 J m^{-2} (standard deviation of the means is 12.1 J m^{-2}), and it approaches a delta function as $k \rightarrow Z$.

An alternative way of displaying the above information is presented in Figure 4.5. Equi-probability isopleths of cumulative frequency of occurrence are drawn as a function of the sample size. Figure 4.5 depicts the probability distribution function. For $k=5$, 2.5 percent of the sample means are less than 20 J m^{-2} or greater than 195 J m^{-2}. This implies that with $k=5$ there is a 5 percent probability of

---

[5] The impact energy densities are grouped in 5 J m^{-2} intervals (e.g. 0.0-4.9; 5.0-9.9; and so on) in the graphs of the probability density function of the sample mean. The value plotted is in the middle of this class interval i.e. 2.5, 7.5 and so on.

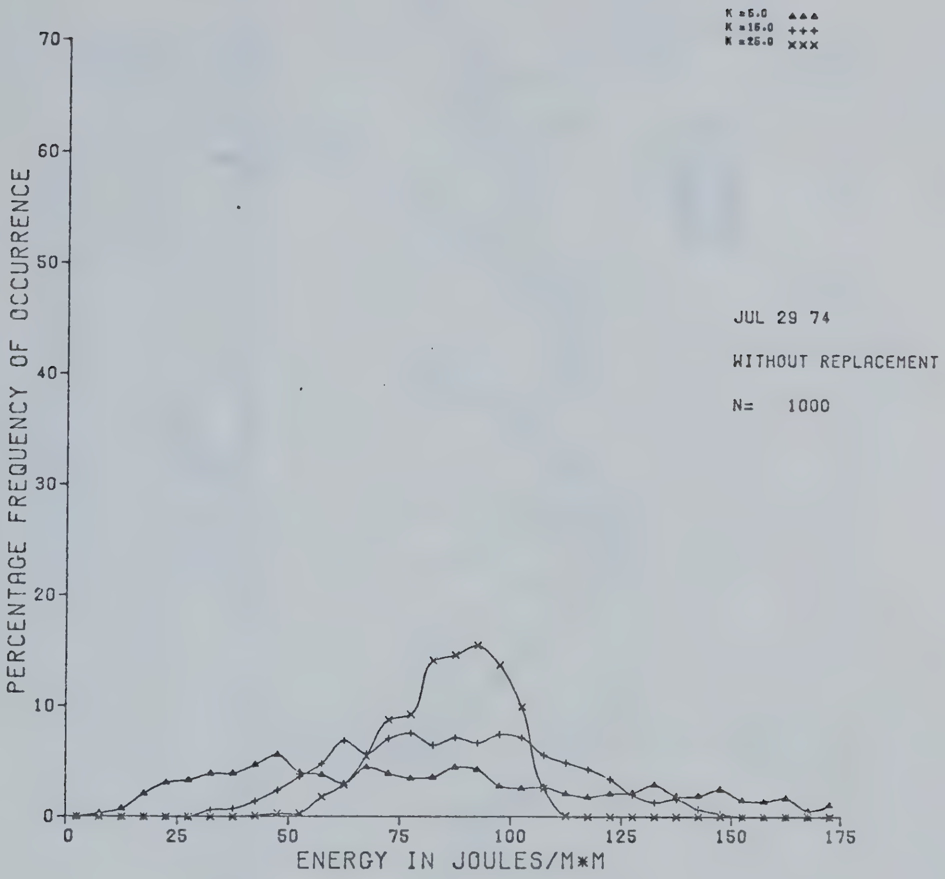

Figure 4.4 The probability density function of the sample means for 29 July 1974 hailswath (sampling without replacement)(Impact energy density values are grouped in 5 J m classes)

obtaining a sample mean which is at least 132 percent in error from the population mean. As the sample size increases towards the population size of 34 the equi-probability lines converge toward the population mean. Figure 4.6 displays the standard deviation of the sample means as a function of the

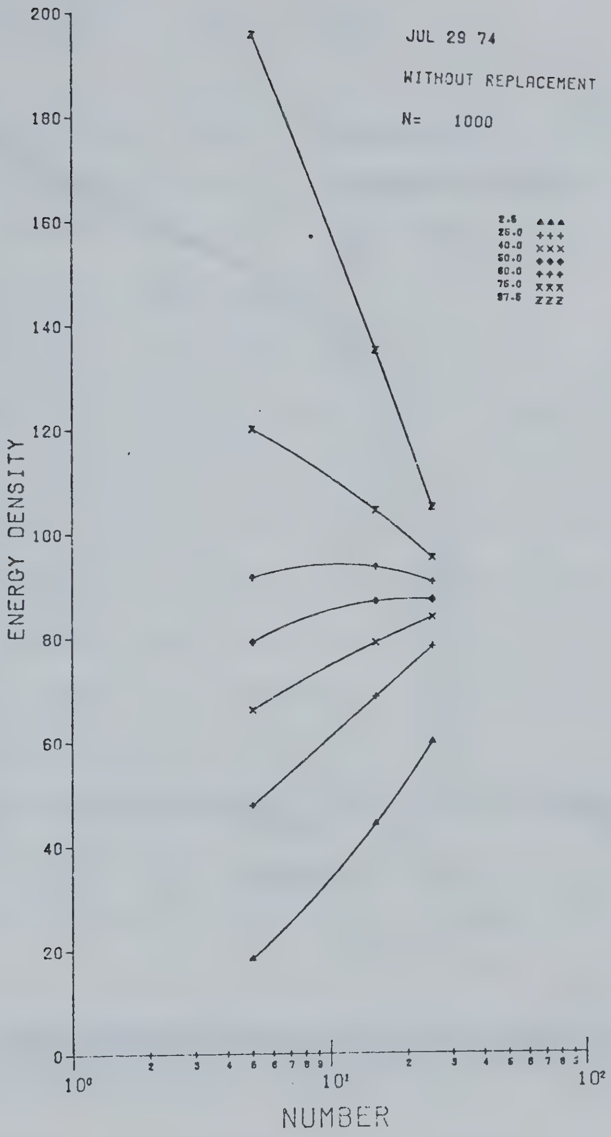

Figure 4.5 Isopleths of the probability distribution function of the sample means for 29 July 1974 hailswath (sampling without replacement)

sample size. The standard deviation decreases approximately as $k^{-.87}$ for increasing values of k from 5 to 25. As the sample size increases towards the population size (k=Z=34), the

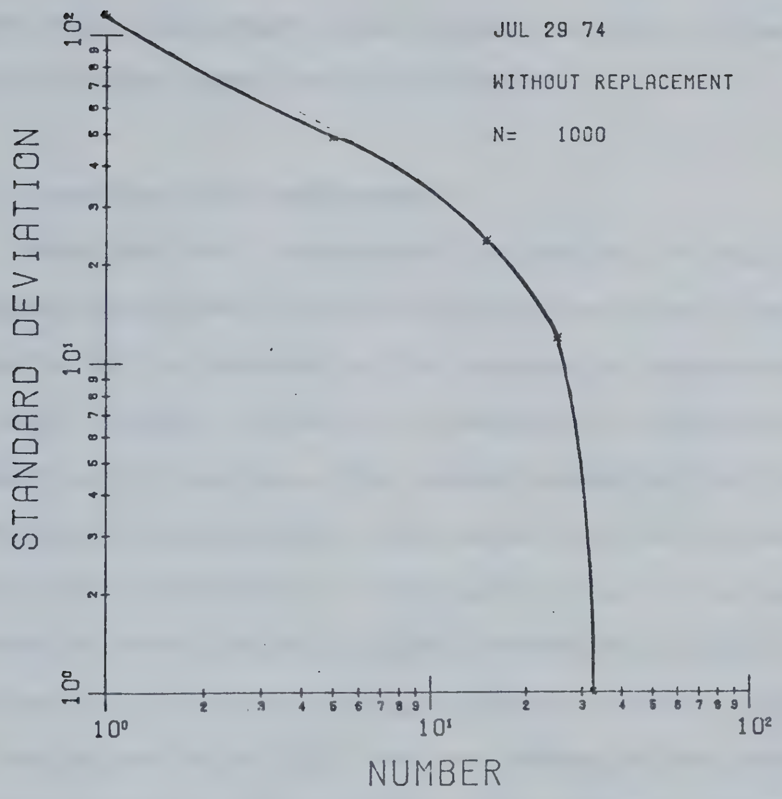

Figure 4.6 The standard deviation of the sample means as a function of the sample size (sampling without replacement)

standard deviation must decrease more rapidly towards zero. The dependency of the standard deviation on k can be calculated by fitting the data points [6] with a power-law equation of the form

---

[6] A least squares fit is applied.

$$\text{standard deviation} = \frac{b}{k^x} \qquad (4.2)$$

where b is a constant. From Figure 4.6 (for k from 5 to 25) this equation gives x=0.87 and b=210.

4.2 Sampling With Replacement

Sampling with replacement is similiar to sampling without replacement except that once an element has been selected it is returned to the population before choosing the next element. Hence it is possible to choose the same element more than once. The random selection and the statistical calculations are carried out in the manner described in Section 4.1. The sample size is no longer limited by the population size (number of hailpads in the hailswath) as is the case for sampling without replacement. For the storm of 29 July 1974 the graph of the probability density function with k equal to 15, 60 and 105 is given in Figure 4.7. The distributions in this figure appear to approach a Gaussian form as k becomes large. This technique is governed by the central-limit theorem, as compared to sampling without replacement (which is not). Figure 4.8 gives the probability distribution function for the 29 July 1974 hailswath. In this figure, a sharp decrease is observed in the 2.5 and 97.5 percent probability isopleths for k=15 to 60, while the 25 to 75 percent probability isopleths show a lesser decrease. The standard deviation of the sample means (Figure 4.9) shows a steady decrease with increasing

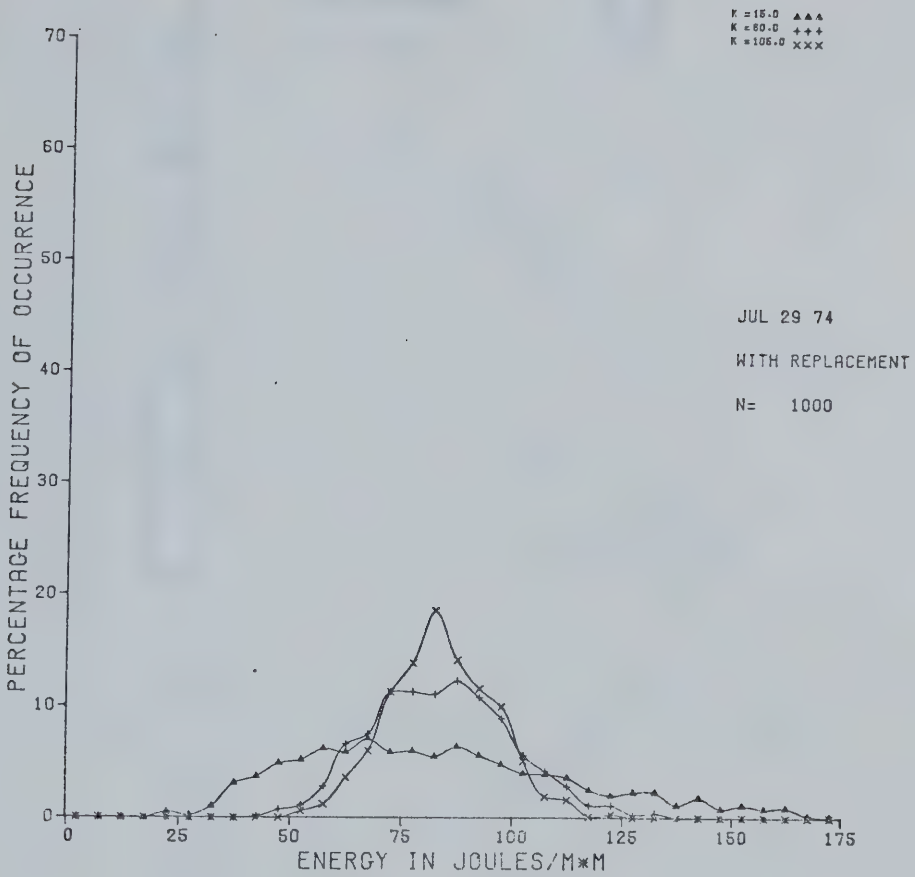

Figure 4.7 The probability density function of the sample means for 29 July 1974 hailswath (sampling with replacement)

sample size (for k=15 to 105, x=.51 and b=125 in Equation 4.2). This is in good agreement with the central-limit theorem, which gives x=.50 and b=120.6. In Figure 4.9 is also shown the variation of the standard deviation of the means as a function of the sample size for k=1 to 15. For

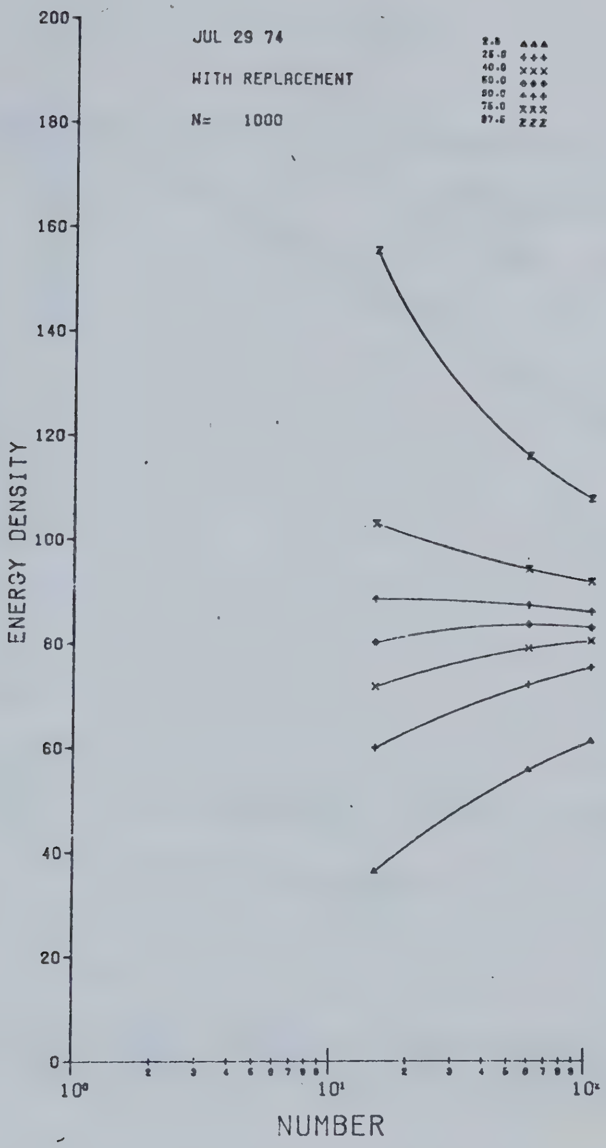

Figure 4.8 Isopleths of the probability distribution function of the sample means for 29 July 1974 hailswath (sampling with replacement)

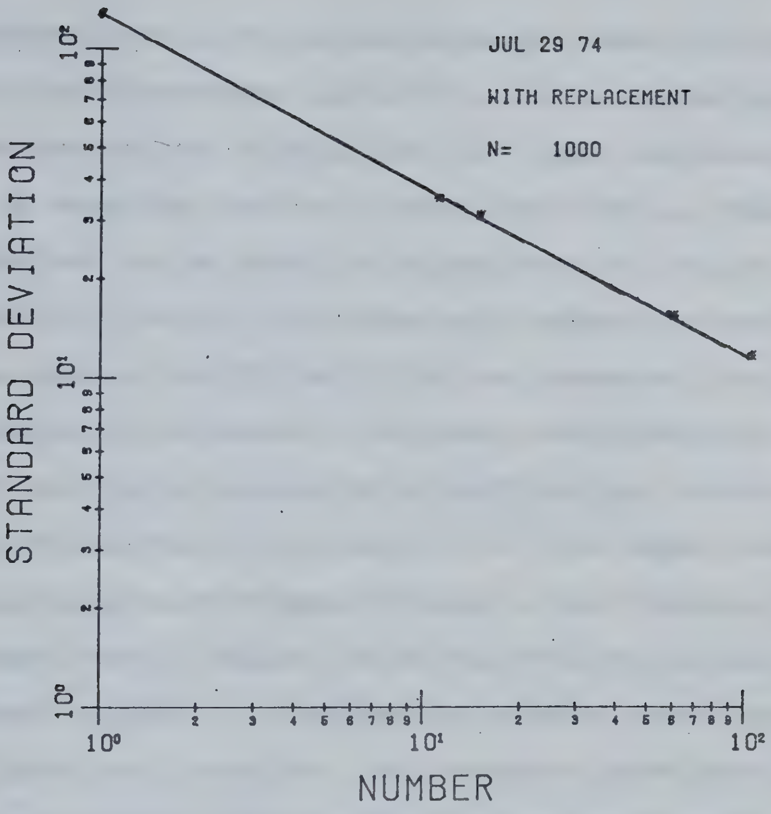

Figure 4.9 The standard deviation of the means as a function of the sample number (sampling with replacement)

k=1, the standard deviation equals 126.5 J m^{-2}, [7] just slightly higher than 125 J m^{-2} the value computed for k=15 to 105 using Equation 4.2, and higher than 120.6 J m^{-2} (the

---

[7] The standard deviation equals 126.5 J m^{-2} because N=1000, as $N \rightarrow \infty$ it is expected that this standard deviation would be equal to the standard deviation of the population mean.

standard deviation of the population).

4.3 Sampling From a Fitted Two-parameter Gamma Distribution

The third procedure is to fit a two-parameter gamma distribution to the original data and apply the Monte Carlo method by sampling from the fitted distribution. Other distributions can be used, if a good data fit can be obtained (e.g. Kappa 2 distribution). Before the results from the data of the 29 July 1974 are presented, the gamma distribution is discussed. The impact energy density values derived from three seasons of hailpad data are positive and range in value from 0.1 to 2332.6 J m^{-2}. Low impact energy densities occur most frequently with a rapid decrease to high impact energy density where the relative frequency of occurrence is small. A distribution of this nature can be fitted quite well using the two-parameter gamma distribution (see Figure 4.10). This distribution has been found useful in fitting and transforming distributions of various meteorological variates which are restricted to positive values such as precipitation, vapor pressure and precipitable water (Panofsky and Brier, 1963).

The two-parameter gamma distribution (Keeping, 1962) is defined by the frequency function:

$$f(x) = \frac{e^{-x/\beta}\, x^{\alpha-1}}{\beta^{\alpha}\Gamma(\alpha)} \quad (\beta > 0, \alpha > 0) \qquad (4.3)$$

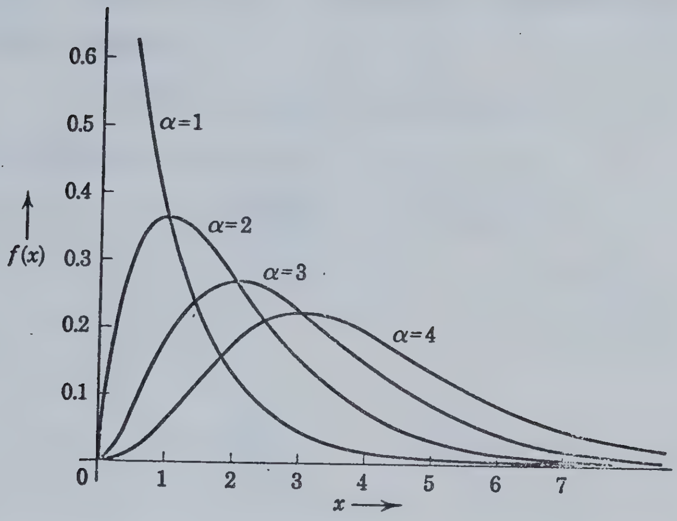

Figure 4.10 Density function for the gamma distribution

where $\Gamma(\alpha)$ is the gamma function defined as:

$$\Gamma(\alpha) = \int_0^{\infty} x^{\alpha-1} e^{-x} dx \quad (\alpha > 0) \qquad (4.4)$$

and

$$\Gamma(\alpha) = (\alpha-1)\Gamma(\alpha-1) = (\alpha-1)! \qquad (4.5)$$

if α is an integer.

The mean of the gamma distribution is $\alpha\beta$ and its standard deviation is $\beta\sqrt{\alpha}$.

The optimal estimates of $\hat{\alpha}$ and $\hat{\beta}$, (Panofsky and Brier, 1963) using:

$$A = \ln \bar{X} - \frac{1}{N}\sum_i \ln x_i \qquad (4.6)$$

are given respectively by:

$$\hat{\alpha} = \frac{1 + \sqrt{1 + \frac{4}{3}A}}{4A} \qquad (4.7)$$

and

$$\hat{\beta} = \frac{\bar{X}}{\hat{\alpha}} \qquad (4.8)$$

Using Equations 4.7 and 4.8, the two parameters ($\hat{\alpha}$ and $\hat{\beta}$) for the population data [8] were calculated and a frequency distribution obtained. In this technique it is possible to select from the distribution an impact energy density value which does not exist in the original data base. In Figure 4.2, the fitted two-parameter gamma distribution is given by the curved line, with triangles in the middle of the class interval. The fit of the two-parameter gamma distribution as a cumulative frequency is demonstrated in Figure 4.3. Figure 4.2 shows that for impact energy values less than about 100 J m^{-2} the gamma distribution slightly underestimates the frequency of

---

[8] For the 29 July 1974 data: $\hat{\alpha}$ =.63, $\hat{\beta}$ =133.5, $\hat{\alpha}\hat{\beta}$ (mean)=84.1 and $\hat{\beta}\sqrt{\hat{\alpha}}$ (standard deviation)=106.0.

occurrence of the original data and why the standard deviation obtained from the gamma distribution is less than that of the population. Grouping the impact energy densities in 25 J m^{-2} classes for the 29 July 1974 hailswath the value of χ^2 was 6.17. With $\chi^2_{.95}$=21.0 (with 12 degrees of freedom) we conclude that the gamma distribution gives a good fit to the original data. The mean of the two-parameter gamma distribution is 84.13 J m^{-2} (same as the population mean) and the standard deviation is 106.0 J m^{-2} (compared with the population mean of 120.6).

The Monte Carlo method is applied using k equal to 15, 60 and 105. Figure 4.11 shows the distribution of the sample means for the various sample sizes. For k greater than 15 the distribution begins to exhibit a Gaussian form as expected according to the central limit theorem. Unlike the technique of sampling without replacement, in this procedure k is no longer restricted by the size of the population. The disadvantage of this procedure is that it requires a good fit to the original data, while for the other two procedures no such requirement is necessary. Comparing the probability of frequency of occurrence of impact energy values for given sample numbers (Figures 4.5, 4.8 and 4.12), it is observed that for the fitted two-parameter gamma distribution the sample means will be within 25 percent of the population mean more frequently than in either of the previous two procedures. The 25 and 75 percent probability isopleths are nearly horizontal between k values of 60 and 150 as was

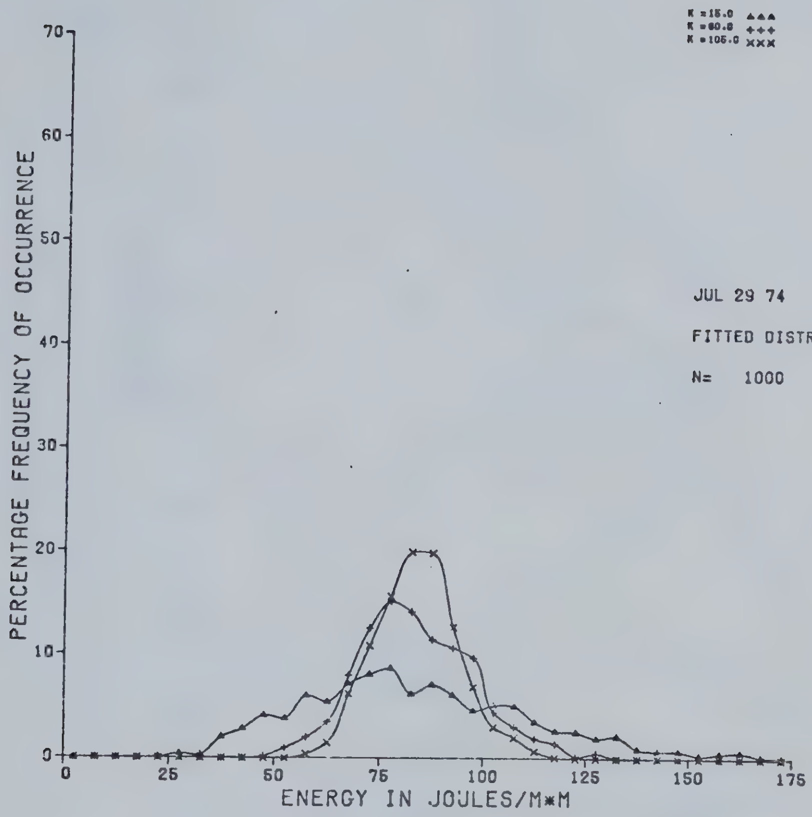

Figure 4.11 The probability density function of the sample means for the 29 July 1974 hailswath (sampling from a two-parameter gamma distribution)

similarly observed for sampling with replacement. Figure 4.13 shows the standard deviation of the sample means as a function of sample size. The standard deviation of the sample means shows a steady decrease with increasing sample size (for k=15 to 105, x=.54 and b=120 in Equation 4.2) and

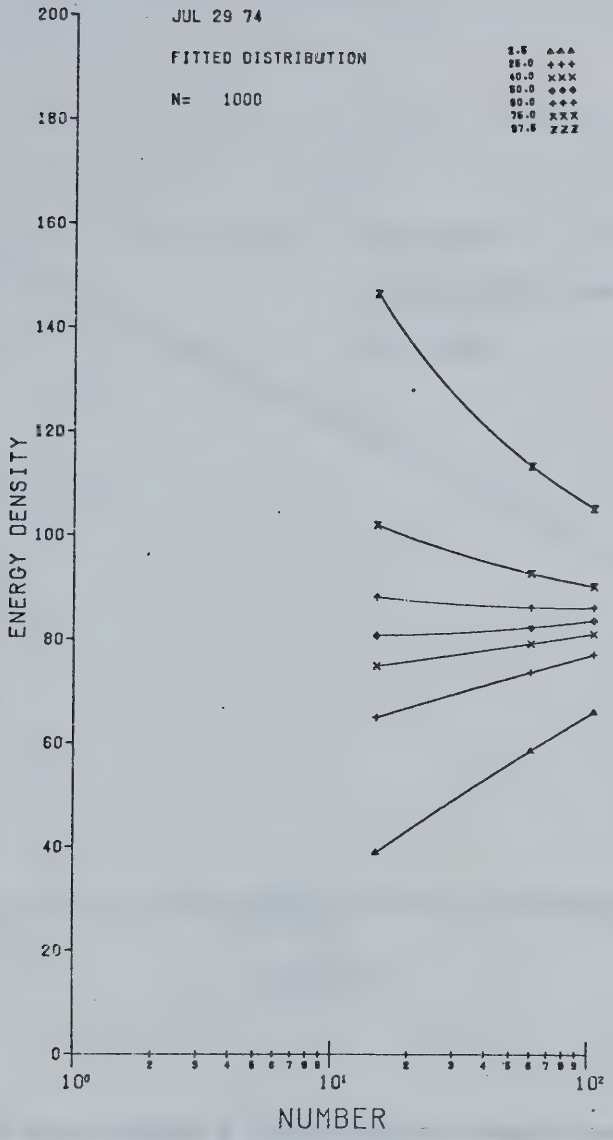

Figure 4.12 Isopleths of the probability distribution function of the sample means for 29 July 1974 hailswath (sampling from a two-parameter gamma distribution)

shows agreement with the central-limit theorem and the work of Strong and Lozowski (1977).

4.4 Stratified Sampling

In stratified sampling, the cumulative distribution of

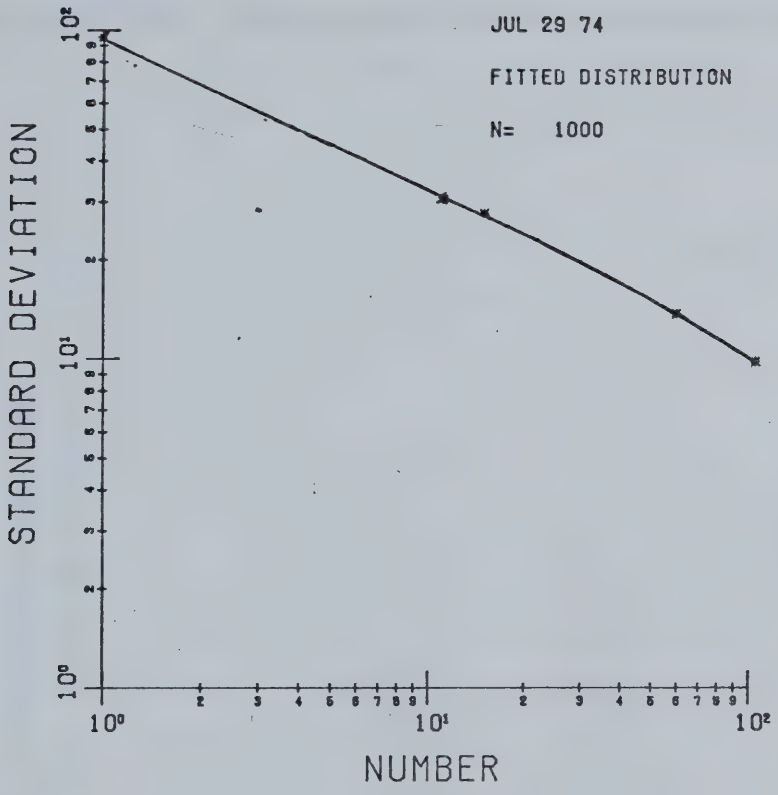

Figure 4.13 The standard deviation of sample means as a function of the sample size (sampling from a two-parameter gamma distribution)

the impact energy density is divided into M equal probability segments. From each segment k/M [9] samples are randomly selected with replacement using subroutine GGU3.

---

[9] k/M should be an integer, to assure that the same number of samples are obtained from each of the M segments.

The total of k samples are used to give the sample mean. The process was repeated 1000 times for the 29 July 1974 hailswath. This technique has the advantage over the

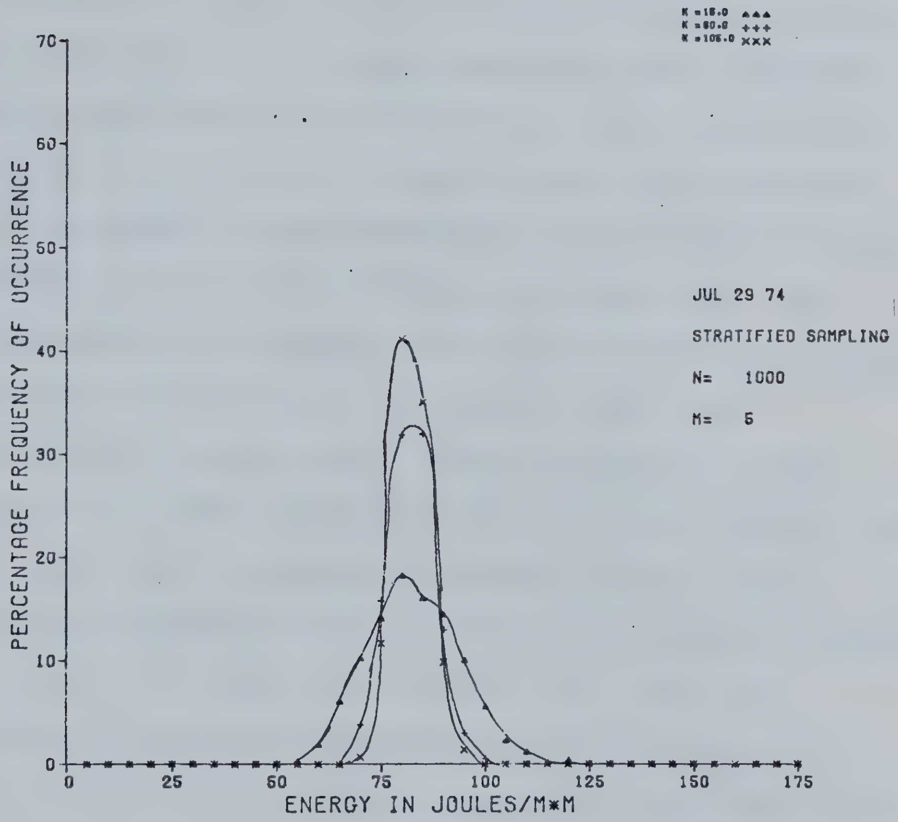

Figure 4.14 The probability density function of the sample means for 29 July 1974 hailswath (stratified sampling)

previous three techniques in that the sampling is made from various impact energy density bands. In the other approaches

it is possible that all k values could come from either a low or high energy region. With stratified sampling this is not possible. It is therefore believed that this type of sampling may better simulate the kind of sampling performed by the hailpad network for those hailswaths where the impact energy distribution is not patchy.

For the example of the 29 July 1974 storm, two cases are presented: (1) M=5 (five segments) with k (the total sample size) being 15, 60 and 105 and (2) M=15 (fifteen segments) with k having the same values as in the first case. The graph of the probability density function for M=5 is Figure 4.14 while for M=15 it is Figure 4.15. The distributions are narrower than for non-stratified sampling, and show a resemblance to the Gaussian form. The distributions for the same k become narrower for M=15 (Figure 4.15) than is observed for M=5 (Figure 4.14). Figure 4.16 shows that 95 percent of the mean impact energy densities lie within a range of 42 J m^{-2} (for M=5) as compared to within 13 J m^{-2} for M=15 (Figure 4.17). The equi-probability lines are clustered in a very narrow impact energy band in Figure 4.17 as compared to that observed in Figures 4.8, 4.12 or 4.16. The standard deviation of the sample means for M=3, 5 and 15 are shown in Figure 4.18. In all three cases, the standard deviation of the sample means decreases as k increase from 15 to 150. The values of x for M=3, 5 and 15 are .50, .49 and .49 (in Equation 4.2), while the values of b are 62.0, 42.0 and 14.7 respectively.

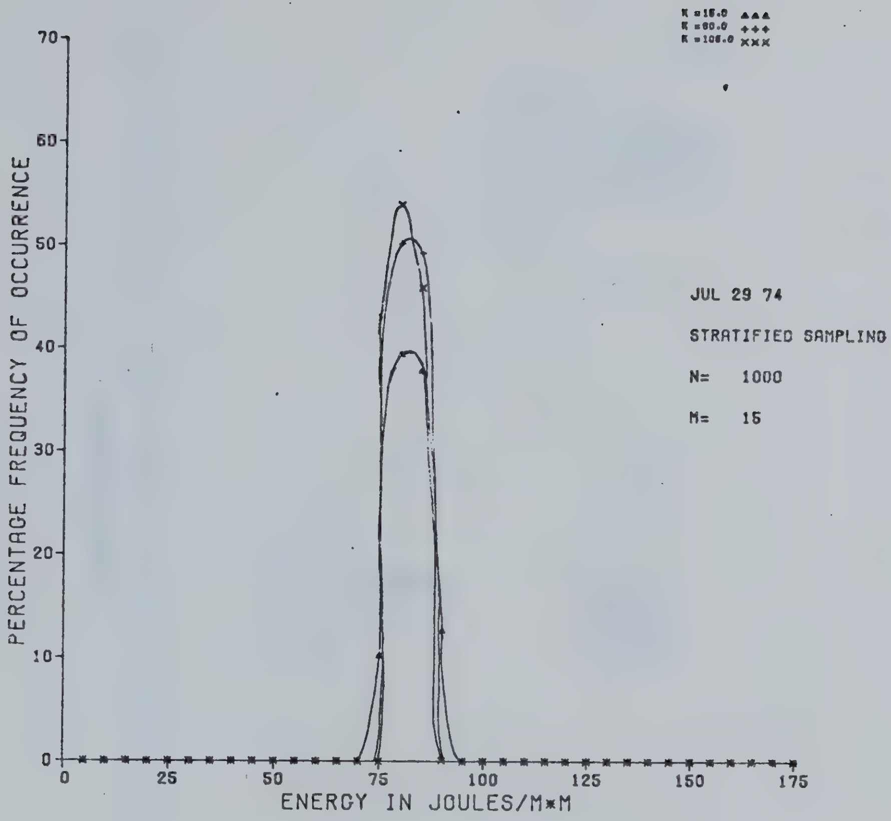

Figure 4.15 The probability density function of the sample means for the 29 July 1974 hailswath (stratified sampling)

4.5 Spatial Sampling

In this section, the attempt is to more closely approach the network sampling by trying to simulate two-dimensional spatial sampling computationally. In this technique a "true" spatial distribution is estimated by a contoured interpolation method. This technique takes into account the fact that the impact energy density values are distributed in two-dimensional space, as is the sampling

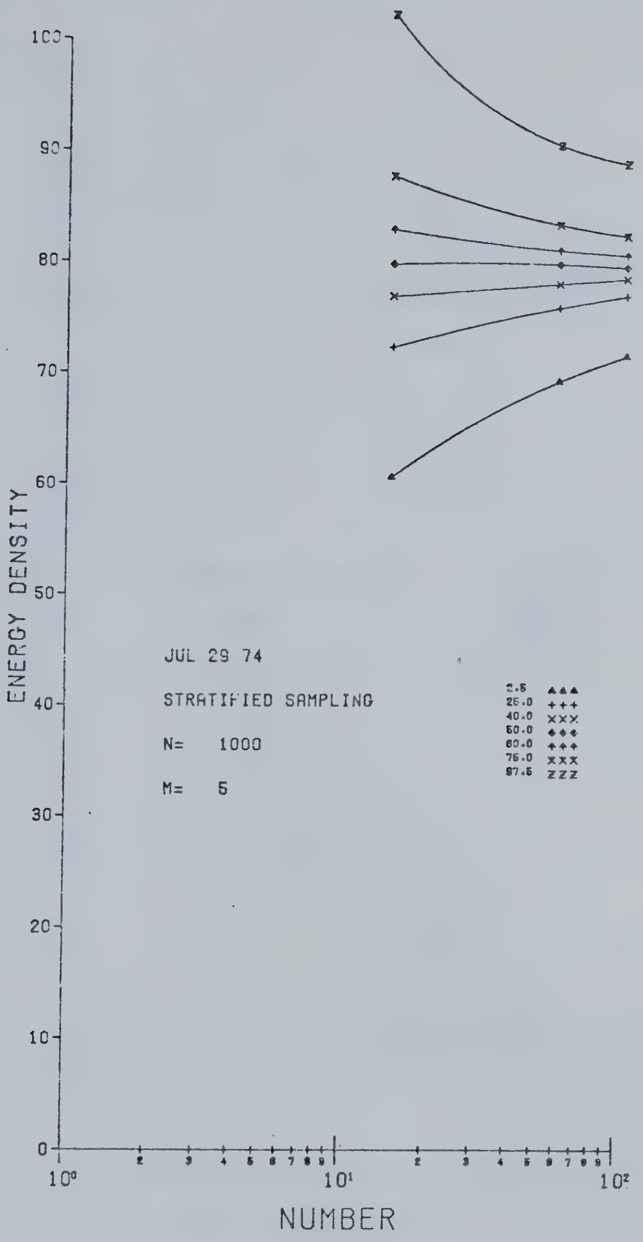

Figure 4.16 The probability distribution function of the sample means for 29 July 1974 hailswath (stratified sampling)

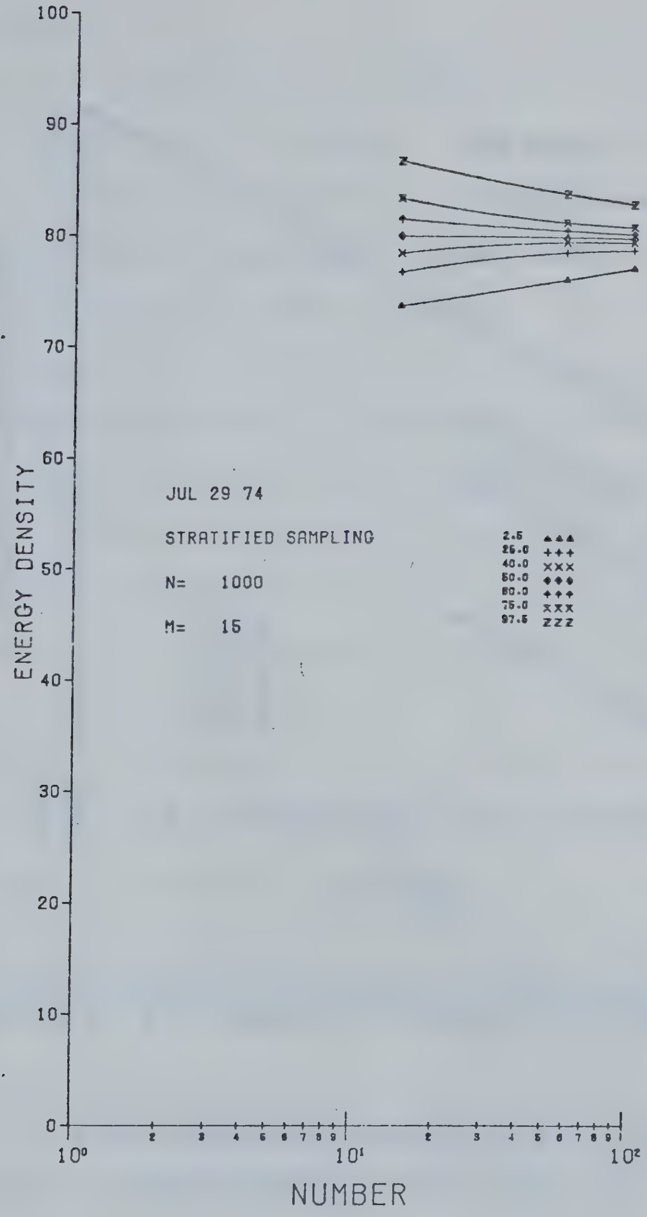

Figure 4.17 The probability distribution function of the sample means for 29 July 1974 hailswath (stratified sampling)

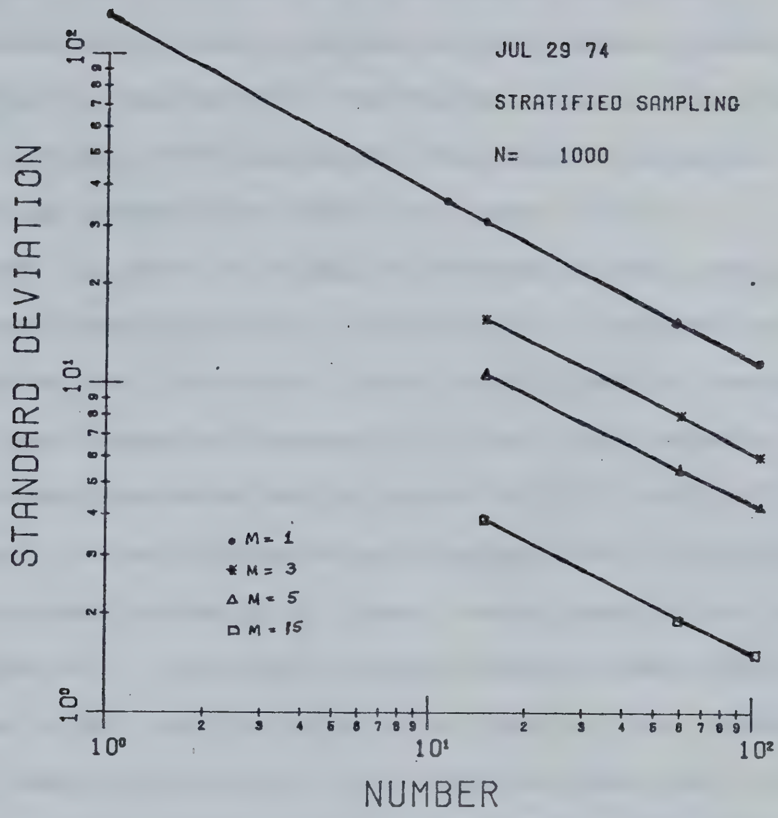

Figure 4.18 The standard deviation of the sample means as a function of the sample size (stratified sampling)

network [10] . The contouring programs used in this dissertation are those developed for a DEC PDP-9 computer by

---

[10] In reality, the hailpad sampling network is distributed in three dimensions, because of a variation in height above sea level from station to station. Here it is assumed that this variation is minimal. This is a valid assumption for central Alberta.

R. Newton(1973) [11] .

The first approach is to estimate the "true" distribution by using a method of statistical prediction [12] presented by Newton(1973) for the 34 impact energy densities of the 29 July 1974 hailswath. The results using the contouring program are shown in Figure 4.19 [13] .

Next in order to simulate two-dimensional spatial sampling computationally a square grid is imposed on the two-dimensional contoured impact energy density analysis and points are chosen at random within each grid square. The first case considered was a square grid of length 11.5 km (132 km^2) [14] and from each grid square (k=77) through which the hailswath crossed, an impact energy density was chosen at random [15] . The impact energy densities were then added for the grids, and the simulation repeated one thousand times. Next, a larger area was selected such that the length of the square grid was 22.9 km (526 km^2). Again from each grid through which the hailswath crossed, an impact energy

---

[11] Unfortunately its conversion to the University of Alberta AMDAHL 470V/6 is still pending. Hence, the examples given in this section are the result of extensive manipulation and data transfers between the two computers.

[12] A technique in which a "probability function" is used to predict the "most probable" value at any point on a map area which has been defined by a number of sampled data values. From a practical point of view this might be considered a system of data averaging.

[13] In Section 4.5, the north direction on the graphs is up, while west is to the left-hand side.

[14] Figure 4.20 shows a square grid of length 11.5 km superimposed on this figure.

[15] An x-value was first chosen at random using GGU3, then a y-value was similarly chosen.

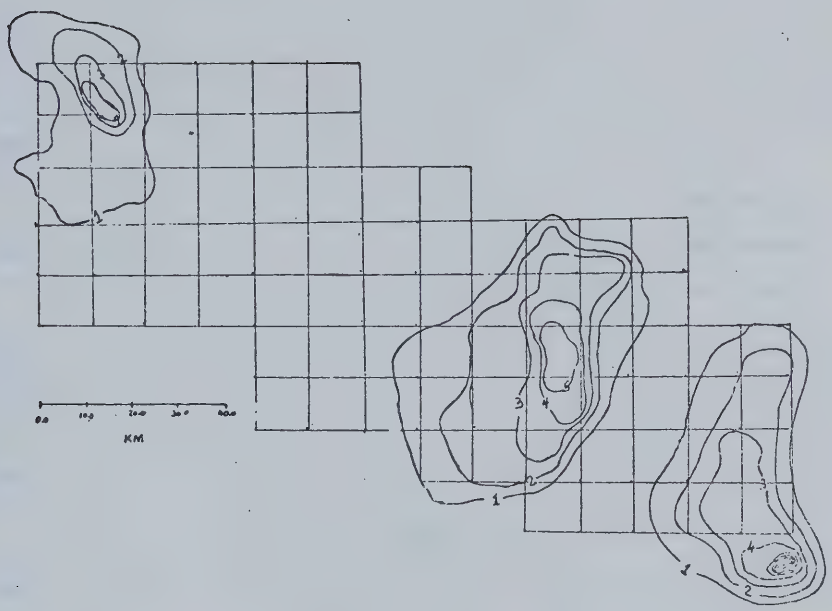

Figure 4.19 The contoured values for the 34 impact energy densities from the 29 July 1974 hailswath. A square grid of length 11.5 km is superimposed on the contoured swath. The contouring is based on actual values at the hailpad sites, however, for the purpose of displaying the impact energy densities in graph form the contoured values for this hailswath were assigned unit values from 1 to 9 with 1 representing the 50.0 J m^{-2} contour ; 2 the 100.0 J m^{-2} contour; and so on.

density was chosen at random. For the 526 km² grids, k was 14, choosing one impact energy density in the grids influenced by the hailswath. Figure 4.20 shows the probability density function obtained using the 132 km² and

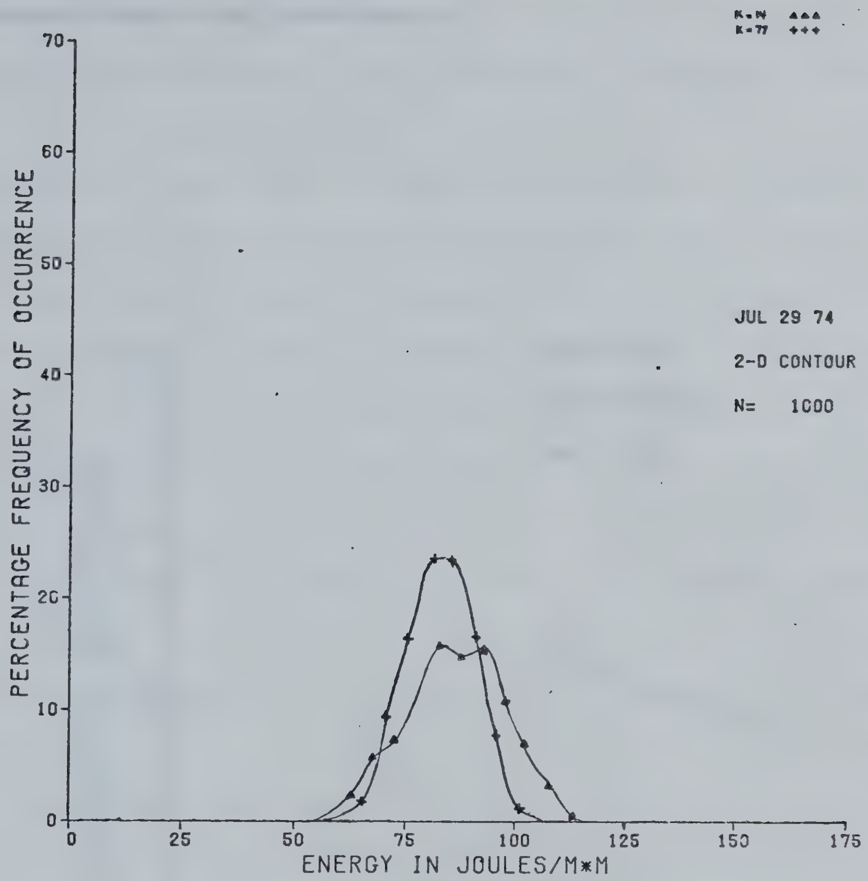

Figure 4.20 The probability density function (spatial sampling)

526 km² square grids. The distribution shows a resemblance to the Gaussian form with an increase in sample size. The standard deviation of the sample means as a function of the sample size (given in Figure 4.21) decreases with increasing sample size ($x=.36$ and $b=32$ in Equation 4.2). The slope of the standard deviation is lower than that obtained for

stratified sampling (for M=3,x=.50) as is also b (the standard deviation intercept).

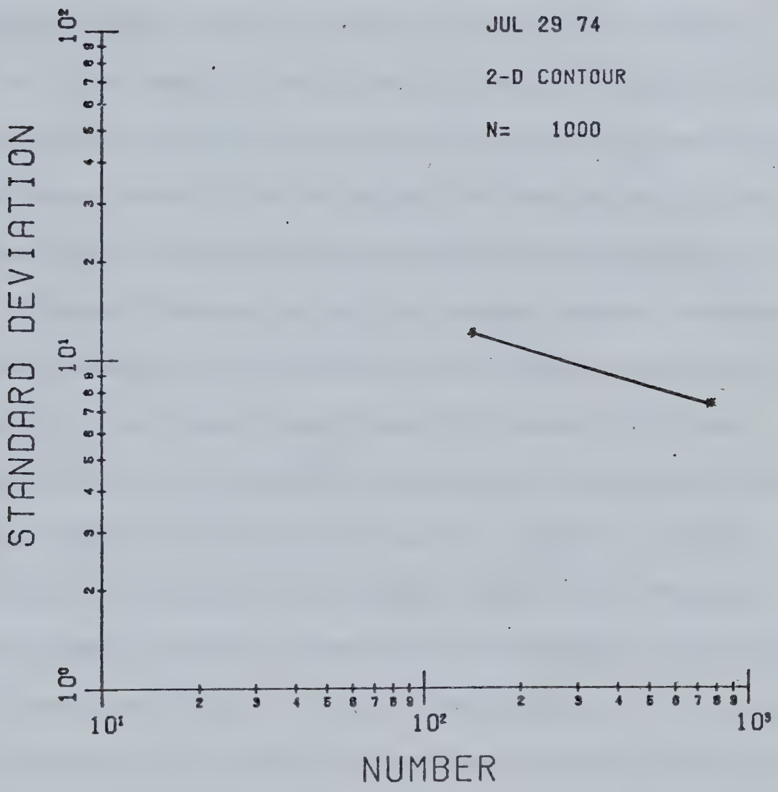

Figure 4.21 The standard deviation of the sample means as function of the sample size (spatial sampling)

In summary, of the five procedures, sampling without

replacement is the only one in which k (the sample size) is restricted to the population size. It is questionable whether the procedure itself represents the sort of sampling that can be expected from a hailpad network due to the restricted sample size. The second technique, sampling with replacement, uses the original data which seems to be satisfactory; however, this method suffers from the disadvantage that the k values may come from either a low or a high band of impact energy densities. If such is the case, a bias can occur in the extremes. In order to overcome this disadvantage, stratified sampling is tested as the fourth procedure. Both techniques show the same decrease in slope in the standard deviation of the sample means, however, for stratified sampling the standard deviation intercept (b in Equation 4.2) is lower than that for non-stratified sampling. Also for stratified sampling, the sample means show less variation in impact energy density (in the probability distribution function) than that observed for non-stratified sampling. The third technique introduced is that of sampling from a fitted distribution. This approach is satisfactory if a good fit to the original data is obtained. The results[16] from this technique are comparable with those obtained for sampling with replacement (non-stratified). The last approach is spatial sampling, and

---

[16] The probability density function, probability distribution function, and standard deviation for a given sample size.

since the areal distribution of impact energy densities is considered in this technique, it is believed that this approach best simulates the type of sampling performed by a hailpad network. In all the techniques examined (except sampling without replacement) the standard deviation of the sample means behaved approximately as $k^{-1/2}$. The relationship for sampling without replacement was $k^{-.87}$ for k from 5 to 25 with the exponent of k increasing rapidly to a large value [17] as k approaches 34 (the population mean).

In this chapter five procedures were discussed using the data from the 29 July 1974 hailswath. Other hailswaths were analyzed in a similiar fashion and the results for these are given in Chapter 5.

---

[17] The slope approaches $-\infty$ as k approaches 34.

CHAPTER 5

RESULTS FOR OTHER STORMS

5.1 Introduction

In this chapter, the results from five hailswaths [1] in the three years 1974(3) [2] and 1975(2) are examined using the first four techniques described in Chapters 3 and 4. At present the fifth technique requires that the DEC PDP-9 computer programs (developed by Newton) be transferred and modified to the University of Alberta AMDAHL 470V/6 computer. Further extensive computer program development is required as support for the modified computer programs before the technique could be used for analysis of hailpad data. This technique, it is believed is the sort of sampling that hailpads do in the network and therefore the technique is suggested as an area of future research. Only impact energy densities within the hailswath are used in the analysis. In most cases other impact energy densities are available for the hail day, but some of these are not associated with the hailswath [3] since they were produced by

---

[1] The hailswath of the 29 July 1974 is included as the fifth hailswath in this dissertation.
[2] The number in parenthesis is the number of hailswaths used for each year.
[3] Precipitation and hailfall reports and radar echo information for the hail day were used to determine which impact energy density values were associated with the hailswath of interest.

other storms occurring on that day. Since hailswaths have different characteristics (for example, motion and direction of the hailswath, maximum hail size they produce, among others) it is not unreasonable that impact energy density distributions also vary among hailswaths. Hence impact energy densities from the other storms which occurred on the same day are not used in the analysis.

The maps of hail and precipitation observations [4] reported by the volunteer observers are found in Appendix II. Six graphs resulting from the application of the various techniques to the analyzed hailswaths are shown in the appendices [5] . The graphs of percentage frequency of occurrence of impact energy densities for each hailswath analyzed are found in Appendix III, while those for the cumulative frequency are in Appendix IV. The other four graphs (probability density function; probability distribution function; standard deviation of the sample means as a function of the sample size and standard deviation of the sample means versus the number of hailpads per 1000 km^2) are found in each of the following four appendices:

a) Appendix V: Graphs for Sampling Without Replacement

---

[4] These maps were plotted on the Calcomp Plotter connected to the University of Alberta computer by a computer program (unpublished) developed by the author in 1968 and modified in 1974 and 1975.

[5] Results for the 29 July 1974 hailswath are not given in the appendices since they appear in Chapter 4.

b) Appendix VI: Graphs for Sampling With Replacement

c) Appendix VII: Graphs for Sampling From a Fitted Two-parameter Gamma Distribution

d) Appendix VIII: Graphs for Stratified Sampling

Before we examine the four procedures, a summary of the hailswaths [6] analyzed is given in Table 5.1. The first column gives the date of the hailswath while the second column indicates the number of dented hailpads used in this study. The third column gives the area (km²) of the hailswath in which the hailpads were collected; this area was determined from hailpad and hailcard observations. The boundary of the hailswath was sketched by hand and the area calculated using a planimeter. The fourth column gives the maximum hail size (in cm) observed by the hailpads, the fifth column the average impact energy density, as

Table 5.1 Summary of Hailswaths Analyzed

Date	No. of Pads	Area (km²)	Max.Size cm	Ave. I Density	S.d.of I Density
24 June 1974	20	3820	3.0	107.8	112.0
5 July 1974	21	1303	1.4	81.6	70.6
29 July 1974	34	3183	2.0	84.1	120.6
3 July 1975	18	886	2.5	131.6	124.0
20 July 1975	32	883	2.5	70.3	101.0

---

[6] The hailswaths considered in this dissertation are moderate to large (in terms of area and impact energy densities) and hence the generality of the results may be limited.

calculated from the hailpads while the last column gives the standard deviation of the calculated impact energy densities. The average impact energy densities given here show the typical values that have been found in the hailpad data of 1974 to 1976 when there were more than 15 hailpads in a hailswath. These results then are representative for the larger, more damaging hailstorms.

5.2 Comparison of the Sampling Techniques

In this section three techniques [7] are examined using the five hailswaths. The technique of sampling without replacement it is believed does not represent the sort of sampling that can be expected from a hailpad network, and hence this technique is discussed briefly. In sampling from a fitted distribution it is desirable that a good fit be obtained to the original data. Consequently we now examine the results of fitting the two-parameter gamma distribution to data from the five hailswaths (see Appendix III for the cumulative frequency graphs). A measure of the discrepancy existing between the observed and expected frequencies is supplied by the statistic χ^2 (Spiegel,1961) given by

$$\chi^2 = \sum_j \frac{(o_j - e_j)^2}{e_j} \qquad (5.1)$$

---

[7] The three techniques are: sampling with replacement (non-stratified, sampling from a fitted distribution and stratified sampling.

where o_j and e_j represent respectively the observed and expected frequencies in the jth class interval. If $\chi^2 = 0$, the observed and the fitted frequencies agree exactly; while the larger the value of χ^2, the greater is the discrepancy between the observed and expected frequencies. Here the expected frequencies are computed on the basis of the hypothesis H_0, that is if χ^2 given by Equation 5.1 is greater than $\chi^2_{.95}$(critical value at the .05 significance level), then we would conclude that the observed frequencies differ significantly from the expected frequencies and would reject H_0 at the 5 percent level of significance. Otherwise the hypothesis would not be rejected. The results for the five hailswaths are given in Table 5.2. The first column

Table 5.2 Summary of the Chi-Square Test for the Hailswaths Analyzed

Date	χ^2	d.f.	$\chi^2_{.95}$	$\chi^2_{.99}$	Description of Fit
24 June 1974	6.5	12	21.0	26.2	Good
5 July 1974	18.8	8	15.5	20.1	Reasonable
29 July 1974	6.2	12	21.0	26.2	Good
3 July 1975	13.3	12	21.0	26.2	Good
20 July 1975	4.7	12	21.0	26.2	Good

gives the date of the hailswath; the second, the statistic χ^2 using Equation 5.1 with the impact energy densities

grouped in 25 J m^{-2} classes[8]; the third, the number of degrees of freedom; the fourth, the .95 level of significance; the fifth, the .99 level of significance; and the last column, a description of the fit[9]. Overall, for the five hailswaths examined in this dissertation, the two-parameter gamma distribution gives a reasonable fit to the hailpad data[10].

5.2.1 Probability Density Function

The probability density functions show resemblance to the Gaussian form with increase in the sample size (i.e. for values greater than 15) for the techniques examined. The resemblance to this form becomes more rapid (and hence more apparent) for stratified sampling than for either non-stratified sampling or sampling from the fitted distribution. It is also for stratified sampling that the probability density function shows the largest percentage of

---

[8] The class intervals are grouped such that the lowest observed frequency is greater than one unit. "In practice, the classes with low expected frequency usually come near the ends of the distribution, and it is common practice to combine or "pool" the end-classes until the e_j (expected frequency in the ith class) reach a satisfactory size. The objection to pooling is that some important differences between o_j and e_j in the end-classes may be hidden by this treatment." (Keeping,1962,p.252)

[9] A fit is described as good if $\chi^2 < \chi^2_{.95}$; reasonable if $\chi^2_{.95} \leq \chi^2 \leq \chi^2_{.99}$; and poor if $\chi^2 > \chi^2_{.99}$.

[10] The two-parameter gamma distribution implies that there is a very small but finite (non-zero) probability of obtaining a very large impact energy density (i.e. there is no maximum impact energy density cut-off). Thus, in a sense, this distribution can be considered as a poor fit to any hailpad impact energy density distribution.

occurrence for a given sample size.

5.2.2 Probability Distribution Function

The graphs of the probability distribution function are another way of displaying the results found in the graphs of the probability density function. For a given hailswath, the spread in range of the 95 percent confidence limits varies from technique to technique. The equi-probability isopleth lines converge towards the population mean with increasing sample size for all the hailswaths examined. The greater the spread between these lines the greater the variability in the impact energy densities. Sampling with replacement and sampling from the fitted distribution show comparable variability in the 95 percent confidence limits of the impact energy density. The improvement in the variability of the 95 percent confidence limits (compared to the above two techniques) shows up in stratified sampling. Here (for k from 15 to 105), the 95 percent confidence limits vary from 20 to 50 percent of the impact energy density obtained for the other two techniques.

5.2.3 Standard Deviation of the Sample Means as a Function of the Sample Size

For the hailswaths analyzed the standard deviation decreases with increasing sample size. It is this rate of decrease which is of interest. Using a least squares fit in Equation 4.2 it is possible to obtain an estimate of how the

standard deviation of the sample means varies with the sample size. The results are shown in Table 5.3. For the hailswaths analyzed, the standard deviation of sample means varies from $k^{-.87}$ to $k^{-1.31}$, for sampling without replacement. For the other three techniques, little variation is found in the exponent of the power law approximation of the standard deviation of the sample means. The variation in the x (in k^{-x}) for k in the range 15 to 105 is from .48 to .54 for the three techniques. This shows good agreement with x=.50 given by the central-limit theorem. Hence for the hailswaths examined the standard deviation varies essentially as $k^{-1/2}$.

Table 5.3 Summary of exponent in a power law approximation to the variation of the standard deviation of the sample means as a function of the sample size for the four techniques

Date	Without	With	Fitted	Stratified
24 June 1974	1.06	.51	.49	.48
5 July 1974	1.02	.51	.51	.48
29 July 1974	.87	.51	.54	.49
3 July 1975	1.31	.49	.49	.50
20 July 1975	.93	.49	.48	.50

In the above discussion, the sample number was not normalized for the area of the hailswaths from which the data was collected. Of the hailswaths considered, some hailswaths are at least three times as big as other hailswaths in area, while the number of hailpad observations is only one and half times as great. To compensate for the area difference, the sample size is expressed in terms of

the number of hailpad observations collected per 1000 km².

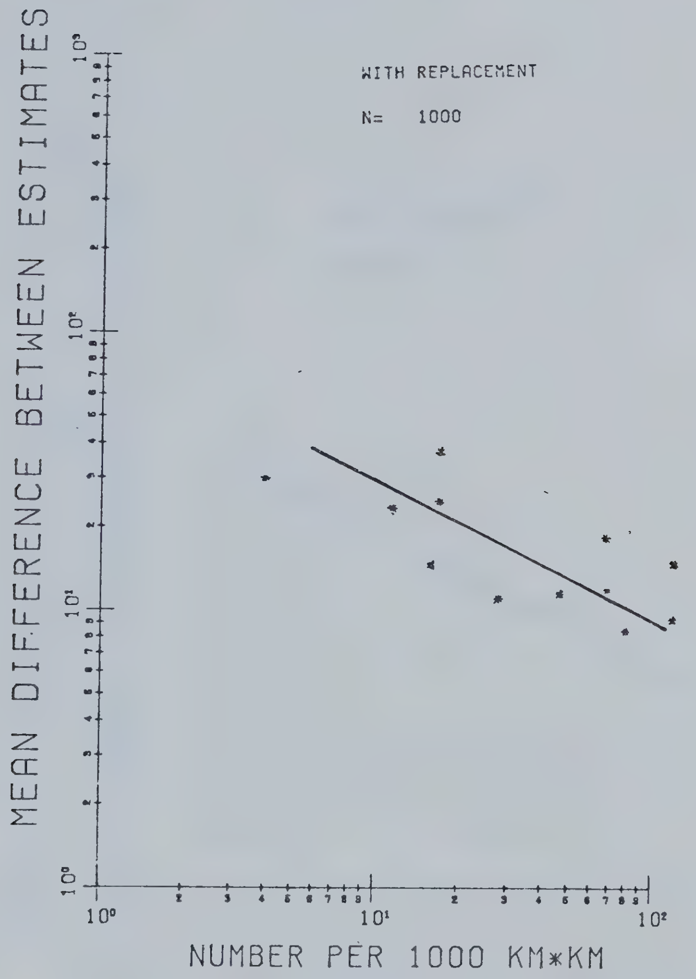

Figure 5.1 The mean difference between estimates (in percent) for sample density in a 1000 km² area. The solid line is the best fit line. (sampling with replacement)

The graphs of the variation of the standard deviation with the normalized sample density are given in the appendices. The slope of the standard deviation for the normalized

sample density is the same as for the non-normalized sample density (values are the same as that given in Table 5.3).

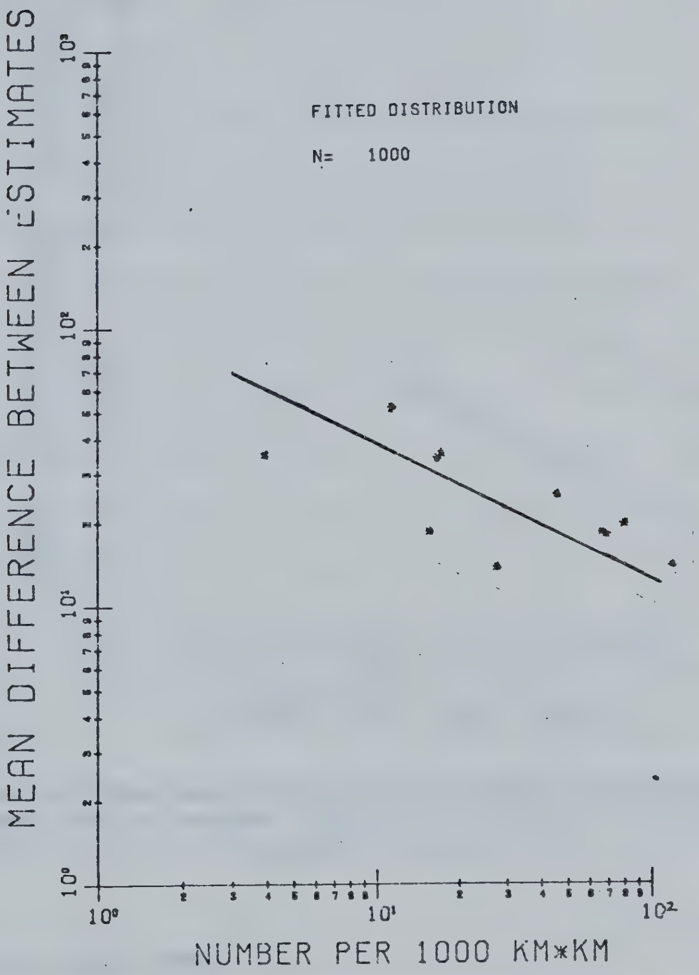

Figure 5.2 The mean difference between estimates (in percent) for a sample density of 1000 km² (sampling from the best fitted two-parameter gamma distribution)

5.2.4 Mean Difference Between Estimates for a Sampling

[illegible]

[illegible]

[illegible]

[illegible]

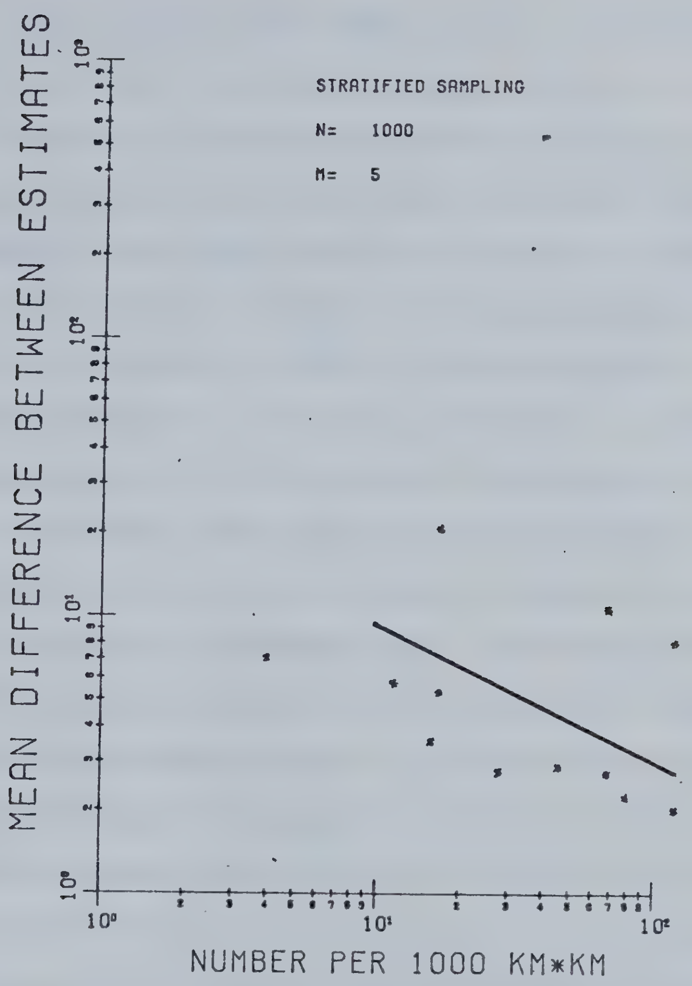

Figure 5.3 The mean difference between estimates (in percent) for a sample density of 1000 km² (stratified sampling) (M=5)

Density per 1000 km²

Figure 5.1 shows the variation of the mean absolute difference between the sample means $\overline{x_i}$ (i=1,N) and the mean of the sample means $\overline{\overline{x_i}}$ (in percent) as a function of a sample size per 1000 km² (for sampling with replacement) for the five hailswaths examined. This graph is the counterpart for

hailfall (for sampling with replacement) to the work of Collier et.al.(1975) on rainfall (see Chapter 1, Figure 1.7). In Figure 5.1 the mean difference decreases with an increasing density of hailpads in the 1000 km² area. The least squares line (solid line in Figure 5.1) gives x equal to .50 (where the mean difference is proportional to K^{-x}) for the five hailswaths. Thus, on the average for the hailswaths analyzed, a factor of 2 decrease in the mean difference requires an increase of 4 fold in the sampling density. Similarly, the graph for sampling from a fitted two-parameter distribution is shown in Figure 5.2. The value of x is .50 for this technique also. For stratified sampling (with M=5) the least squares curve is given in Figure 5.3 for the five hailswaths (with x=.50). The slopes of the least square lines are about the same in all three techniques although the intercept on the vertical axis (mean difference between estimates or value of b in Equation 4.2) is different. Of the three techniques, stratified sampling has the lowest mean difference between estimates, while the other two techniques are about equal.

In summary, to observe the same decrease in the mean difference, all three techniques require the same increase in sampling density. However, for a specific mean difference between estimates, stratified sampling requires a lower sample density than the other two techniques.

CHAPTER 6

CONCLUSIONS

In this dissertation five simulation techniques have been presented and applied using the Monte Carlo method in an attempt to simulate sampling by a hailpad network. The first four techniques have been examined for five hailswaths that occurred in the last three years (1974 to 1976) in central Alberta. Which technique best simulates the sort of sampling that hailpads do in a hailswath, depends on the nature of the hailswath itself. If the impact energy densities are of a continuous nature [1] within the hailswath then the technique of stratified sampling (with replacement) might best simulate the sampling that hailpads would do in that hailswath. If on the other hand, the number of these "pockets" is large compared with the number of hailpad stations then a technique like non-stratified sampling (with replacement) might best describe the procedure. This then brings up the question of when stratified sampling may give a better representation of network sampling and when it may not. The answer to this question may lie in the auto-correlation function for the impact energy densities of the hailswath. An integral scale $\mathcal{L}$ can be defined by

---

[1] By continous nature we mean pockets of impact energy densities decrease continuously from areas of maximum impact energy density to areas of minimum impact energy density and then increase to areas of maximum impact energy density.

$$\mathcal{L}^2 = \frac{1}{\pi}\int_{x=-\infty}^{x=\infty}\int_{y=-\infty}^{\infty} c(x,y)\,dx\,dy \qquad (6.1)$$

where $c(x,y)$ is the normalized correlation coefficient. This coefficient is defined as

$$c(x',y') = \frac{\int_{x=-\infty}^{\infty}\int_{y=-\infty}^{\infty} E(x,y)E(x+x',y+y')\,dx\,dy}{\int_{x=-\infty}^{\infty}\int_{y=-\infty}^{\infty} E^2(x,y)\,dx\,dy} \qquad (6.2)$$

where $E(x,y)$ is the energy density field.

If the mean hailpad separation is much smaller than $\mathcal{L}$, stratified sampling should be a close approximation to the network sampling. If on the other hand, the mean hailpad separation is much greater than $\mathcal{L}$, then random sampling (with replacement) may be as good a representation of network sampling. When the mean hailpad separation is about equal to $\mathcal{L}$, then it is questionable as to which approach (if any) is appropriate for simulating the sampling of the hailpad network.

Sampling with replacement (non-stratified), is probably best applicable to hailswaths where the impact energy density distribution in any small sub-section of the hailswath is essentially the same as that in the entire hailswath. Sampling from a fitted two-parameter gamma distribution is satisfactory (compared to random sampling from the original distribution) if a good fit to the

original data can be obtained [2]. The results from the five hailswaths show that this distribution gives a reasonable fit to the impact energy densities. This technique is probably best applicable to severe hailswaths where a large range [3] of impact energy densities is observed.

The results of this study show that the probability density function of the sample means approximates the Gaussian form [4] in the four techniques (in most cases) for sample sizes greater than 15. The variation of the standard deviation as a function of the sample size is on the average proportional to $k^{-1/2}$ (k in the range 15 to 105) for the three techniques [5]. In all three of these techniques the standard deviation showed agreement with the central-limit theorem, that the sample size is proportional to $k^{-1/2}$.

The graphs of the variation of the mean difference between sample means as a function of the number of hailpads per 1000km² for the five hailswaths are the counter-part to those given by Collier et.al.(1975) for rainfall. This is the first time that results for hailswaths have been given in this type of display. The results show that the mean

---

[2] Stratified sampling can also be performed for the fitted distribution.

[3] Impact energy densities have been observed to vary from .1 to over 2000 J m^{-2}.

[4] A quantitative estimate of how well the probability density function of the sample means approximates the Gaussian form can be obtained by using χ^2.

[5] The three techniques are: sampling with replacement (non-stratified), sampling from a fitted distribution and stratified sampling.

difference between the sample mean and the population mean is on the average proportional to $k^{-.50}$ for the three techniques. Hence for the hailswaths analyzed, a factor of two decrease in the mean difference requires an increase of four-fold in the sampling density.

The results further show that in order to commit a 10 percent error [6] between the sample means and the mean of the sample means, 90 hailpads are required in a 1000 km^2 area (or 1 hailpad per 11.1 km^2) if non-stratified sampling is representative of what the network does. The number of hailpads (again for a 10 percent error in the impact energy density) increases to 200 per 1000 km^2 area (1 hailpad per 5.0 km^2) using the fitted two-parameter gamma distribution. An improvement in the sampling density is observed for stratified sampling (M=5), where for a 10 percent error between the estimates, only 10 hailpads are needed in a 1000 km^2 area (1 hailpad per 100 km^2).

These results show that the dense hailpad network (see Chapter 2) has a sufficient number of hailpads in the network to determine the mean energy density of the hailfall within a 10 percent error [7] . The precipitation network, on the other hand [8] , has an insufficient number of stations in the network to obtain in sampling a 10 percent error in the

---

[6] The difference between seeded and unseeded storms, which one is trying to discover may be as small as 10 percent.

[7] Requiring a 100 percent response from the hailpad network operators in the area.

[8] With 500 stations over an area of 34,467 km^2

impact energy density[9]. The minimum error in determining the total impact energy density for hailswaths of the kind considered here with the present precipitation network would be about 18 percent,[10] assuming a 100 percent response[11] in the hailpad observation network.

---

[9] For sampling with replacement and sampling from a fitted two-parameter distribution.

[10] Using results from the fitted two-parameter gamma distribution.

[11] A conservative estimate of the response on a given hailstorm would be 20 percent. The non-response is due hailpads not having been set out as a result of holidays, lack of time and so on. This is not expected to lead to a bias in the returns.

TABLE OF SYMBOLS

α -alpha (parameter used in the gamma distribution)

A_i -number of hailstones in the ith size category

β -beta (scale parameter used in the gamma distribution)

C -drag coefficient of a hailstone in free-fall

D -diameter of a hailstone

D_D -dent diameter

D_H -hail diameter

D -diameter of hailstones in the ith size category

g -acceleration due to gravity (981.3 cm s^{-2} at 53° N)

I_E -impact energy

I_{ET} -impact energy density (without a wind)

I_{ETH} -impact energy density (with a horizontal wind V_H)

k -sample size

m -mass of a hailstone

M -number of segments

N -number of times a sampling technique is repeated

ρ -density of a hailstone

ρ_a -density of air

s -standard deviation of the sample means

V_H -horizontal wind speed

V_T -terminal velocity of a hailstone

θ -angle to the vertical at which the hailstone strikes

$\bar{x}_i$ -sample means

$\bar{\bar{x}}_i$ -mean of the sample means

Z -total number of hailpads in a hailswath

BIBLIOGRAPHY

Admirat, P., 1972: Structures fines des chutes de grêle naturelles (fine structures of natural hailfalls) in Recherches sur la Prévention de la Grêle. Climatologie Générale et structure fine des Chutes de Grêle Naturelles. Projet "Languedoc" Étee 1972. Rapport Tech. No.14, Décembre, GIEFA.

Beckwith, W.B., 1960: Analysis of hailstorms in the Denver network. J. Meteorology, 23, 348-353.

Burley, M.W., R. Pfleger, and J.Y. Wang, 1964: Hailstorms in Wisconsin. Mo. Wea. Rev., 92, 121-127.

Changnon, S.A., 1961: Annual and seasonal average hail day distributions in Illinois, Missouri, and Iowa. Appendix A, CHIAA Res. Rept. 11, Chicago, 8 pp.

Changnon, S.A., 1962: Areal frequencies of hail and thunderstorm days in Illinois. Mon. Wea. Rev., 90, 519-524.

Changnon, S.A., 1966a: Effects of Lake Michigan on severe weather. Great Lakes Research Division, Pub. 15, 220-234.

Changnon, S.A., 1966b: Climatology of hail in south western South Dakota. Final Report of Project Hailswath, Summary-Conclusions, Rapid City, 16 pp.

Changnon, S.A., 1967: Areal-temporal variations of hail intensity in Illinois. J. of Appl. Meteorology, 6, 536-541.

Changnon, S.A., 1968a: Precipitation Climatology of Lake Michigan Basin. Bull.52, Ill. State Water Survey, Urbana, 46 pp.

Changnon, S.A., 1968b: Effects of sampling density on areal extent of damaging hail. J. of Appl. Meteorology, 7, 518-521.

Changnon, S.A., 1968c: Surface models of hailstorms. Proc. of Int. Conf. on Cloud Physics, AMS, Boston, 478-482.

Changnon, S.A., 1968d: Summary of 1967 hail research in Illinois. CHIAA Res. Rept. 39, Chicago, 50pp.

Changnon, S.A., 1969a: Hail evaluation techniques. Part 1, Final Report NSF GA-482, Urbana, 99 pp.

Changnon, S.A., 1969b: Urban-produced thunderstorms at St. Louis and Chicago. Preprints 6th Conf. on Severe Local Storms,AMS,Boston,95-99.

Changnon, S.A., 1970: Hailstreaks. J. Atmos. Sci., 27, 109-125.

Changnon, S.A., 1971: Hailfall characteristics related to crop damage. J. of Appl. Meteorology, 10, 270-274.

Changnon, S.A., H. Danford, and P.T. Schickedanz, 1967: Hail patterns in Illinois and South Dakota. Proc. 5th Conf. on Severe Local Storms, AMS, Boston, 325-335.

Collier, C.G., T.W.Harrold, and C.A.Nickolass, 1975: A

Comparison of areal rainfall as measured by a rainfall - calibrated radar system and raingauge networks of various densities. Proc. 16th Radar Meteorology Conf., Houston, Texas, 467-471.

Decker, W.L., 1952: Hail damage frequency distributions for Iowa, and a method of evaluating the probability of a specified amount of hail damage. Trans. Am. Geophy. U., 33, 204-210.

Deibert, R.J. and J.H. Renick(Editors), 1975: Alberta hail project field program 1974. Alberta Agriculture, IWMB, Rept. 1, Three Hills, Alberta, 37 pp.

Deibert, R.J.(Editor), 1976: Alberta hail project field program 1975. Alberta Agriculture, AWMB, Rept. 2, Three Hills, Alberta, 67 pp.

Deibert, R.J.(Editor), 1977: Alberta hail project field program 1976. Alberta Agriculture, AWMB, Rept. 4, Three Hills, Alberta. 82 pp.

Douglas, R.H., and W. Hitschfeld, 1959: Patterns of hailstorms in Alberta. Royal Meteorological Soc. Quart. J., 85, 105-119.

Eddy, A., 1976: Optimal raingage densities and accumulation times: a decision-making procedure. J. of Appl. Meteorology, 15, 962-971.

Enger, I., A.L. Bussemy, and R.J. Roth, 1963: Relationship of physical factors to Kansas crop-hail insurance loss costs as developed by multiple regression and multiple discriminant techniques. TRC Service Corp., Hartford, Conn.,6 pp.

Feller, W., 1950: An Introduction to probability theory and its applications. John Wiley and Sons, Inc., New York, 509 pp.

Gray, D.M.(Editor), 1970: Handbook on the Principles of Hydrology.Ottawa. (not paginated)

Harrison, H.T., and W.B. Beckwith, 1951: Studies on the

distribution and forecasting of hail in the western United States. Bull. AMS, 32, 119-131.

Harrold, T.W., and P.G.Kitchingman, 1975: Measurement of surface rainfall using radar when the beam intersects the melting layer. Proc. 16th Radar Meterology Conf., Houston, Texas. 473-478.

Hershfield, D.M., 1965: On the spacing of rain gauges. IASH & WMO Symposium on Design of Hyrdrometeorological Networks,Quebec City, 7 pp.

Huff, F.A., 1960: Relations between summer hailstorms in Illinios and associated synoptic weather. CHIAA Res. Rept. 5, Chicago, 18 pp.

Huff, F.A., 1961: Correlation between summer hail patterns in Illinois and associated climatological events. CHIAA Res. Rept. 10, Chicago, 17 pp.

Huff, F.A., 1970: Sampling errors in measurement of mean precipitation. J. of Appl. Meteorology, 9, 35-44.

Huff, F.A., and S.A. Changnon, 1959: Hail climatology of Illinois. Rept. Inv. 38, Ill. State Water Survey, Urbana, 46 pp.

Keeping, E.S., 1962: Introduction to Statistical Inference. Van Nostrand, New York, 451 pp.

Koscielski, A., 1967: Hail occurrence in Perkins County, South Dakota. Rept. to S. Dak. Wea. Control Comm., Pierre, S.D., 10 pp.

Lemons, H., 1942: Hail as a factor in the regional climatology of the United States. Geographical Rev., 32, 471-175.

Longley, R.W., and C.E. Thompson, 1965: A study of the causes of hail. J. Appl. Meteorology, 4, 69-82.

Lozowski, E.P., and A.G. Beattie, 1975: Field measurements of hailstone aerodynamics. Unpublished paper presented at the 9th Annual Congress Can. Meteor. Soc., May 1975, Vancouver, B.C.

Marshall,J.S.,and W.Hitschfeld,1953: Interpretation of the fluctuating echo from randomly distributed scatterers. Pt.1,Canadian J. of Physics, 31, 962-994.

Metropolis, N., and S. Ulam, 1949: The Monte Carlo Method. J.Amer. Statistical Assoc., 44, No.247, 335-341.

Morgan, G.M. Jr., and N.G. Towery, 1974: Small scale variability of hail and its significance for hail prevention experiments.Preprints 4th Conf. Wea. Mod., AMS,Boston,143-149.

Morgan, G.M. Jr., and N.G. Towery, 1975: On the role of strong winds in damage to crops by hail and its estimation with a simple instrument. Preprints, 9th Conference on Severe Local Storms, Norman, Oklahoma, AMS, Boston, pp. 424-443.

Musil, D., and A. Dennis, 1968: Convective storms of 1966-67 in western Nebraska. Rept. 68-7, Inst. of Atmos. Sciences, S. Dak., Rapid City, 7 pp.

Neff, E.L., 1965: Principles of precipitation network design

for intensive hydrologic investigations. WMO-IASH Symposium on Design of Hydrometeorological Network, Quebec City, 9 pp.

Newton, R., 1973: A Statistical Prediction Technique for Deriving Contour Maps from Geophysical Data. Mathematical Geology, Vol.5, No. 2, pp 179-189.

Nicks, A.D.,1965: Field evaluation of rain gage network design principles. WMO-IASH Symposium on Design of Hydrometeorological Network,Quebec, 18pp.

Panofsky, H.A., and G.W. Brier, 1963: Some application of statistics to meteorology. Pennsylvania State University, University Park Pennsylvania, 224 pp.

Pell, J., 1969: The Alberta hailstorm as observed on the ground and by radar. Ph.D. thesis, Dept. of Meteorology, McGill University, Montreal, 313 pp.

Pell, J., 1971: Variations with time of six Alberta hail parameters. Preprints 7th Conf. Severe Local Storms,

AMS, Boston, 226-233.

Renne, D.S., and P.C. Sinclair, 1968: Stability and synoptic features of high plains hailstorm formation. Proc. 5th Conf. on Severe Local Storms, AMS, Boston, 125-130.

Schickedanz, P.T., and S.A. Changnon, 1970: A study of crop-hail insurance records for northeastern Colorado with respect to the design of the National Hail Experiment. Final Report. NCAR 155-70, Urbana, 86 pp.

Schickedanz, P.T., and S.A. Changnon, 1971: The design and evaluation of the national hail research experiment in northeast Colorado. J. Wea. Mod., 3, 160-176.

Schleusener, R.A., and P.C. Jennings, 1960: An energy method for relative estimates of hail intensity. Bull, AMS, 41, 372-376.

Schleusener, R.A., and T.J. Henderson, 1962: Observational data on the position of hailfall with respect to precipitation cells. AMS Conf. on Severe Storms,

Norman, Okla., 8 pp.

Schleusener, R.A., 1963: Hailstorm characterization and the crystal structure of hail. Meteor. Mono., 5, 173-176.

Schleusener, R.A.,J.D.Marwitz,and W.L.Cox,1965:Hailfall data from fixed network for the evaluation of a hail modification experiment.J. of Appl. Meteorology, 4, 61-68.

Shrieder, Y.A., 1966: The Monte Carlo method. Pergamon Press, 381 pp.

Smith,P.L.Jr.,1964: Interpretation of the fluctuating echo from randomly distributed scatterers.Part 3, McGill University. Stormy Weather Group, MW-39.

Spiegel,M.R.,1961: Schaum's Outline Series. Theory and Problems of Statistics. Schaum Publishing Co, New York,359pp.

Stout, G.E. 1962: Summary of research on hailstorms in Kansas during 1961. CHIAA Res. Rept. 12, Chicago, 58 pp.

Stout, G.E., 1963: Summary of research on hailstorm days 1962. CHIAA Res. Rept. 16, Chicago, 39 pp.

Stout, G.E., 1965: Summary of research on hailstorm days 1964. CHIAA Res. Rept. 24, Chicago, 49 pp.

Stout, G.E., and S.A. Changnon, 1967: Comparison of hail-day patterns in Kansas with surface features and crop-hail insurance patterns. CHIAA. Res. Rept. 34, Chicago, 15 pp.

Stout, G.E., and S.A. Changnon, 1968: Climatography of hail in the central United States. CHIAA Res. Rept. 38, Chicago, 46 pp.

Stromberg, G.,(Chairman), 1972: Interim report of the special committee on crop insurance and weather modification. Legislative Assembly of Alberta, 20 pp.

[illegible]

Smith, G.D., 1969? Summary of research on hailstorm days [illegible]

[illegible] Tech. Atmos. Res. Rept. 24, [illegible]

[illegible] with surface latitudes and [illegible]

Stout, G.E., and S.A. Changnon, 1968. Climatography of hail [illegible]

[illegible]

Strong, G.S., 1974: The objective measurement of Alberta hailfall. M.Sc. thesis, Meteorology Division, Dept. of Geography, University of Alberta, Edmonton, Alberta, 182 pp.

Strong, G.S., and E.P. Lozowski, 1977: An Alberta study to objectively measure hailfall intensity. Atmosphere, 11, 33-53.

Summers, P.W., (Editor), 1968: Alberta hail studies 1967 field program. Res. Council of Alberta, Edmonton, 60 pp.

Summers, P.W., and L. Wojtiw, 1971: The economic impact of hail damage in Alberta, Canada and its dependence on various hailfall parameters. Proc. Seventh Severe Local Storms Conf., Amer. Meteor. Soc., Kansas City, Mo., 158-163.

Swinbank, W.C., 1971: The National Hail Research Experiment. Proc. Inter. Conf. on Weather Mod., Canberra, Australia, AMS, 203-206.

Vento, D., and G.M. Morgan, Jr., 1976: Statistical evaluation of the energy imparted to hail by wind in Europe and United States. Second WMO Scientific Conf. on Weather Modification, WMO-No 443, pp. 281-286.

Wojtiw, L., and J.H. Renick, 1973: Hailfall and crop damage in Alberta. Alberta Research Hail Studies Rept. 73-1, 7-10.

Wojtiw, L., 1975a: Climatic summaries of hailfall in central Alberta (1957-1973). Alberta Research, Atmospheric Sci. Rept. 75-1, Edmonton, 102 pp.

Wojtiw, L., 1975b: Hailfall and crop damage in central Alberta. J. of Weath. Mod., _7_, 28-42.

Wojtiw, L., 1977: Climatology of hailstorms in central Alberta. The Albertan Geographer. _13_, Edmonton, 15-27.

APPENDIX I

FORTRAN IV COMPUTER PROGRAMS

The following pages contain a listing of the FORTRAN IV computer programs used on the University of Alberta AMDAHL 470V/6 computer, in this dissertation. Program PAD1 was used for the first four techniques in the Monte Carlo method. The input values required for initiating the computer program are:

(a) N-number of draws(integer value from 1 to 99,999)

(b) k_{max}-maximum sample size(integer value from 1 to 999)

(c) k_{min}-minimum sample size(integer value from 1 to 999)

(d) Δk-increments of k(integer value from 1 to 998)

(e) A-area of hailswath in km(integer value from 1 to 99,999)

(f) Type of technique:01-Sampling from a fitted two-parameter gamma distribution; 02-Sampling without replacement;03-Sampling with replacement;04-Stratified sampling.

Program PAD2 was modified from PAD1 to accomplish spatial sampling. Input parameters (a) and (e) are required for this program. This computer program requires data which has been contoured in a 2-D space(here computer programs developed by R.Newton were used and applied on the DEC PDP-9 computer).

Program PLOT was used to produce maps of the hailfall and the hailpad locations. Here hailpad and hailfall data

are required for initiation of the computer program.

All three computer programs given here require support of subroutines from various libraries (i.e. *PLOTLIB, *IMSLLIB).

```
$L PAD1
C     APPLICATION OF MONTE CARLO METHOD TO
C     HAILPAD IMPACT ENERGY VALUES
      DIMENSION A(120,3),R(200),AI(120,20),V(250)
      DIMENSION VA(20),BI(120,20),VB(20),CF(9,20)
      DIMENSION VYY(500),VX(60),VY(60),CE(5000)
      DIMENSION AVT(20),AVB(20),VRA(60),VRB(60)
      DIMENSION PX(60),PQ(60),PP(60),QQQ(9)
      DIMENSION PPP(120),PQP(120),IPMM(2)
        DIMENSION VII(120),VJJ(120),VKK(120)
       DIMENSION VXXXX(50),W8(2000),VYYYY(50)
       DIMENSION WWW(5000)
      DIMENSION XZZ(2000)
      COMMON BUF(2048)
      CALL PLOTS(BUF,8192)
      DATA QQ/'*'/
C
C
C
C
C     THIS PROGRAM APPLIES THE MONTE CARLO METHOD USING
C     THREE DIFFERENT SAMPLING TECHNIQUES: IE. 1) CODE 001
C     SAMPLING FROM A FITTED TWO PARAMETER GAMMA DISTRIB'N
C     2) CODE 002 SAMPLING WITHOUT REPLACEMENT.
C     3) CODE 003 SAMPLING WITH REPLACEMENT.
C     THE FOLLOWING INPUT PARAMETERS ARE REQUIRED:
C     NTT(I5) FORMAT)-IS THE NUMBER OF DRAWS (TYPICAL VALUE
C     IS 1000).
C     IWP(I3 FORMAT)-IS THE MAXIUM SAMPLE NUMBER STARTING
C     AT 5 AND INCREASING IN INCREMENTS OF 25
C     KKK (I3 FORMAT) IS ONE OF THREE SAMPLING TECHNIQUES
C     DATA INPUT IS OF THE FORM:A(I,3),AS1,AS2,AS3,(8X,
C     3X,F8.2,A3,A2,A3) ON UNIT 8 WHERE A(I,3) ARE THE
C     IMPACT ENERGY VALUES. AS1,AS2,AS3 IS THE DATE OF THE
C     HAILPAD VALUE.  OUTPUT REQUIRES THREE UNITS:
C     9 UNITS FOR THE PLOTS:
C     6 UNITS SCRATCH FILE
C     7 UNITS, ANOTHER SCRATCH FILE OR TERMINAL
C     THIS PROGRAM WAS DEVELOPED FROM NOV. 1976 TO
C     MARCH 1977 BY L. WOJTIW.
C
C
C
C
      XMAX=10.
      I=1
      INSEED=574657
      QQQ(1)=1.0
      QQQ(2)=2.5
      QQQ(3)=25.0
      QQQ(4)=40.0
      QQQ(5)=50.0
      QQQ(6)=60.
      QQQ(7)=75.0
      QQQ(8)=97.5
      QQQ(9)=100.0
   33 READ(5,30)NTI,IWP,KKK
          READ(5,431)IAREA,IBASE,IINC
431        FORMAT(I5,2I3)
```

```
      GO TO (831,831,831,832),KKK
832       READ(5,833)JJJP
833       FORMAT(I2)
  831 AIINC=IINC
            AREA=IAREA
      BMAX=0.
      XISY=0.
      XNT=NTT
      DO 36 IJ=1,200
36    V(IJ)=QQ
      DO 50 ITT=1,500
      DO 50 IZX=1,20
      BI(ITT,IZX)=0.
50    AI(ITT,IZX)=0.
30    FORMAT(I5,5I3)
      DO 51 ITT=1,20
      VA(ITT)=0.
51    VB(ITT)=0.
      IF(NTT.EQ.1)GO TO 31
2     READ(8,1,END=10)A(I,3),AS1,AS2,AS3
      IF(A(I,3).GE.2500.) GO TO 2
91    FORMAT(1F8.3,2I5)
      XMAX=AMAX1(XMAX,A(I,3))
      I=I+1
      GO TO 2
10    N=I-1
      WRITE(7,30)N
1     FORMAT (8X,4X,F7.2,A3,A2,A3)
        DO 701 I=1,N
701       VII(I)=A(I,3)
C     WRITE(7,37) (VII(I),I=1,N)
       IQI=0
704       ZA=XMAX
         DO 702 I=1,N
           IF(VII(I).LT.ZA) GO TO 703
       GO TO 702
703      IZE=I
       ZA=VII(I)
702      CONTINUE
       IQI=IQI+1
       VJJ(IQI)=VII(IZE)
        VII(IZE)=XMAX
       IF(IQI.GE.(N+1)) GO TO 705
       GO TO 704
705      WRITE(7,37) (VJJ(I),I=1,N)
       DO 708 I=1,N
       ZII=I
708     VKK(I)=ZII*100./N
C      WRITE(7,37) (VKK(I),I=1,N)
      IVM1=N/JJJP
710      FORMAT(1X,2F10.2,3X,2I5)
C      WRITE(7,710)VKK(IVM1),VKK(IVM2),IVM1,IVM2
C
C
C
C     CALCULATION OF ALPHA AND BETA PARAMETERS FOR THE
C     GAMMA DISTRIBUTION.
C
C
C
```

```
      SUM1=0.0
      SUM2=0.0
      DO 150 I=1,N
      SUM2=SUM2+ALOG(A(I,3))
      SUM1=SUM1+A(I,3)
150   CONTINUE
      XM=SUM1/N
      XML=SUM2/N
      AA=ALOG(XM)-XML
      AX=1.0+4.0/3.0*AA
      AQ=(1.0+SQRT(AX))/4.0*AA
      BQ=XM/AQ
      CQQ=BQ*AQ
          WRITE(7,37)AQ,BQ,CQQ,XM
      SUM3=0.
       DO 732 IN=1,N
         YUR=(A(IN,3)-XM)*(A(IN,3)-XM)
3790      FORMAT(1X,10F8.1)
732           SUM3=SUM3+YUR
        YBN=N
      SUM4=SUM3/YBN
       SUM5=SUM4**.5
          WRITE(6,3790)YBN
        WRITE(6,3790)SUM3,SUM4,SUM5
      SY=0.
      DO 4 I=1,N
      IRR=(A(I,3)/5.)+1.
      AI(IRR,1)=AI(IRR,1)+1.
4     SY=SY+A(I,3)
      XN=N
      JXJ=(XMAX/5.)+1.
      DO 500 J=1,JXJ
      JXMP=(J-1)*5
      Q=AI(J,1)*100./XN
      VYY(J)=Q
  504 IZ=Q*3.
      IF(IZ.EQ.0) GO TO 500
500   CONTINUE
      SYM=SY/XN
      IW=2
      IWMP=IBASE
      WRITE (6,40) SYM
  100 IT=1
      TSYM=0.
   17 DO 18 IX=1,N
      XZZ(IX)=0.
18    R(IX)=0.
      SUMX=0.
      GO TO(46,47,48,609),KKK
C
C
C
C     KKK CHOOSES THE SAMPLING TECHNIQUE ACCORDING TO THE
C     ABOVE CODE.
C
C
C
   46 CALL GGTMAJ(INSEED,AQ,BQ,IWMP,WWW,R)
40    FORMAT(1X,2F8.3,3I5)
  731 DO 14 I=1,IWMP
```

```
            SUMX=SUMX+R(I)
             XZZ(I)=R(I)
      14    CONTINUE
            GO TO 49
        609 ISTOP=IWMP/JJJP
             IVM3=N-IVM1*JJJP
              XCIVM1=IVM1
              AP=1.0/XCIVM1
            DO 713 IEND=1,JJJP
            DO 712 I=1,ISTOP
            CALL GGU3(INSEED,1,RX)
             IR=RX/AP
               IR=IR+IVM1*(IEND-1)
              XXIR=RX/AP
                XXIR=XXIR+IVM1*(IEND-1)
             CIR=IR
            YYIR=XXIR-CIR
            ICQ=(IEND-1)*3+I
              IF(YYIR.LE..01) GO TO 729
             TTIR=YYIR/VKK(1)
            UUIR=(VJJ(IR+IVM3+1)-VJJ(IR+IVM3))*TTIR
            SUMX=SUMX+VJJ(IR+IVM3)+UUIR
            XZZ(ICQ)=VJJ(IR+IVM3)+UUIR
              GO TO 712
      729     SUMX=SUMX+VJJ(IR+IVM3)
            XZZ(ICQ)=VJJ(IR+IVM3)
      712      CONTINUE
      713      CONTINUE
            GO TO 49
      47    DO 52 I=1,IWMP
            AP=1.0/XN
      55    CALL GGU3(INSEED,1,RX)
            IR=RX/AP
            IF(R(IR).GT.0.) GO TO 55
            R(IR)=1.
            SUMX=SUMX+A(IR,3)
            XZZ(I)=A(IR,3)
      52    CONTINUE
            GO TO 49
      48    DO 53 I=1,IWMP
            AP=1.0/XN
      54    CALL GGU3(INSEED,1,RX)
            IF(RX.LE.0.0) GO TO 54
            IR=RX/AP
            SUMX=SUMX+A(IR,3)
            XZZ(I)=A(IR,3)
      53    CONTINUE
      C       WRITE(6,37) (XZZ(I),I=1,IWMP)
         49 AMS=IWMP
            ASYM=SUMX/AMS
            W8(IT)=ASYM
            BMAX=AMAX1(BMAX,ASYM)
            TSYM=TSYM+ASYM
            ISYM=(ASYM/5.)+1.
            CE(IT)=ASYM
            AI(ISYM,IW)=AI(ISYM,IW)+1.
        202 IT=II+1
            IF(IT.LE.NTT) GO TO 17
            VB(IW)=TSYM/XNT
            I8=IT-1
```

```
            WRITE(6,37)VB(IW)
         VAR=0.
         DO 650 ICW=1,NTT
 650       VAR=VAR+(W8(ICW)-VB(IW))*(W8(ICW)-VB(IW))
         VA(IW)=((VAR/XNT)**.5)
          WRITE(6,37)VA(IW)
         IWMP=IWMP+IINC
         ICH=1
         ICF=1
 936     QPNT=NTT
         ICG=QPNT*QQQ(ICH)/100.
 934     CA=XMAX
          DO 931 I=1,NTT
          IF(CE(I).LT.CA) GO TO 932
         GO TO 931
 932     ICE=I
         CA=CE(I)
 931     CONTINUE
         IF(ICF.EQ.ICG) GO TO 933
         ICF=ICF+1
         CE(ICE)=XMAX
         GO TO 934
 933     CF(ICH,IW)=CE(ICE)
         ICH=ICH+1
         IF(ICH.GE.10) GO TO 935
         GO TO 936
 935     IW=IW+1
         DO 940 I=1,5000
 940     CE(I)=0.
         WRITE(7,300)IWMP
         IF(IWMP.GT.IWP) GO TO 99
         GO TO 100
      99 WRITE(7,34)NTT
         IZP=IW-1
 34      FORMAT(1X,15HNUMBER OF DRAWS,I8)
         JMP=(BMAX/5.)+1.
         IXPP=IW-1
 102     FORMAT(1X,I4,3X,20F6.0)
         DO 105 IJ=1,IZP
         BI(1,IJ)=AI(1,IJ)*100./XNT
         DO 104 II=2,JMP
         BI(II,IJ)=(AI(II,IJ)*100./XNT)+(BI(II-1,IJ))
 104     CONTINUE
 105     CONTINUE
 300           FORMAT(I5)
 C
 C
 C
 C       PLOTTING THE PERCENTAGE FREQUENCY OF OCCURRENCE
 C       GRAPH FOR IMPACT ENERGY VALUES>
 C
 C
 C
 31      CALL PLOT(0.0,0.,3)
         CALL PLOT(4.0,4.0,-3)
         CALL AXIS2(0.0,0.,'ENERGY DENSITY IN JOULES/M*M',-28,
        *7.0,0.,0.,100.,1.)
         CALL AXIS2(0.,0.,'PERCENTAGE FREQUENCY OF OCCURRENCE',
        *34,7.,90.,0.,10.,-1.)
            CALL PL1A(4.,3.5,5,NTT,AS1,AS2,AS3,JJJP)
```

```
      DO 920 I=1,48
      AX=I*25.
      ABC=AX/BQ
      CALL MDGAM(ABC,AQ,PROB,IER)
      PP(I)=PROB*100.
  920 PQ(I)=AX
      PX(1)=PP(1)
      DO 951 I=2,48
  951 PX(I)=PP(I)-PP(I-1)
      IZA=1
      I=1
  902 SUM=0.
      DO 901 IJ=1,5
      IPP=I+IJ-1
  901 SUM=SUM+VYY(IPP)
      VRA(IZA)=SUM
      I=I+5
      IZA=IZA+1
      IF(IZA.GE.49) GO TO 904
      GO TO 902
  904 WRITE(7,993) (VRA(IK),IK=1,12)
  993 FORMAT(12F8.2)
      CALL PLOT(0.,0.,3)
      DO 905 I=1,28
      WWI=I
      WA=(WWI-1.)/4.
      VRB(I)=VRA(I)/10.
      CALL PLOT(WA,VRB(I),2)
      WB=WWI/4.
      CALL PLOT(WB,VRB(I),2)
  905 CONTINUE
      WA=.125
      UV=PX(1)/10.
      CALL PLOT(WA,UV,3)
      CALL SYMBOL(WA,UV,.06,02,0.0,-1)
      DO 952 I=2,28
      WWI=I
      WA=(WWI/4.)-.125
      UV=PX(I)/10.
      CALL PLOT(WA,UV,2)
  952 CALL SYMBOL(WA,UV,.06,02,0.0,-1)
      CALL PLOT(0.,15.,-3)
C
C
C
C     PLOTTING THE CUMULATIVE FREQUENCY GRAPH FOR
C     IMPACT ENERGY
C
C
C
      CALL AXIS2(0.,0.,'ENERGY DENSITY JOULES/M*M',-25,
     *7.0,0.,0.,100.,1.)
      CALL AXIS2(0.,0.,'CUMULATIVE FREQUENCY',20,
     *5.,90.,0.,20.,-1.)
       CALL PL1A(4.,3.5,5,NTT,AS1,AS2,AS3,JJJF)
      CALL PLOT(0.,0.,3)
      VC=VRB(1)
      DO 906 I=1,28
      WWI=I
      WA=WWI/4.
```

```
      VM=VC/2.
      CALL PLOT(WA,VM,2)
      CALL SYMBOL(WA,VM,.06,011,0.0,-1)
      VC=VC+VRB(I+1)
906   CONTINUE
      CALL PLOT(0.,0.,3)
      DO 978 I=1,28
      WWI=I
      WA=WWI/4.
      UV=PP(I)/20.
      CALL PLOT(WA,UV,2)
978   CALL SYMBOL(WA,UV,.06,02,0.0,-1)
C
C
C
C     PLOTTING THE STANDARD DEVIATION FOR A SAMPLE SIZE.
C
C
C
37          FORMAT(1X,10F8.2)
      CALL PLOT(12.,0.,-3)
      CALL LOGAX(0.,0.,'NUMBER',-6,
     *5.,0.,0.,-2.,0.)
      CALL LOGAX(0.,0.,'STANDARD DEVIATION',18,
     *5.,90.,0.,-2.,0.)
        CALL PL1A(3.,5.,KKK,NTT,AS1,AS2,AS3,JJJP)
      ARA=IBASE
      I=2
908   IF((ARA.LE.0.).OR.(VA(I).LE.0.)) GO TO 981
      AVT(I)=ALOG10(ARA)
      AVB(I)=ALOG10(VA(I))
  981 ARA=ARA+AIINC
        WRITE(6,37)ARA,VA(I),AVT(I),AVB(I)
      I=I+1
      IF(I.GT.IZP) GO TO 907
      GO TO 908
907   NOP=IZP
      CALL PLOT(0.,0.,3)
      AQP=AVT(2)*5./2.
      AQR=AVB(2)*5./2.
      CALL SYMBOL(AQP,AQR,.06,011,0.0,-1)
      CALL SMOOTH(AQP,AQR,0)
      IXZ=NOP-1
      DO 909 I=3,IXZ
      AQP=AVT(I)*5./2.
      AQR=AVB(I)*5./2.
      CALL SMOOTH(AQP,AQR,-2)
909   CONTINUE
      AMM=AVT(NOP)*5./2.
      AMN=AVB(NOP)*5./2.
      CALL SMOOTH(AMM,AMN,-25)
      DO 955 I=3,NOP
      AQP=AVT(I)*5./2.
      AQR=AVB(I)*5./2.
955   CALL SYMBOL(AQP,AQR,.06,011,0.0,-1)
      CALL PLOT(0.,-15.,-3)
C         /
C
C
C     PLOT OF THE IMPACT ENERGY FOR A GIVEN SAMPLE SIZE
```

```
C
C
C
      CALL LOGAX(0.,0.,'NUMBER',-6,5.0,0.,0.,-2.,0.)
      IF(KKK.EQ.4) GO TO 834
      CALL AXIS2(0.,0.,'ENERGY DENSITY',14,10.,90.,0.,20.,-1.)
      GO TO 835
834   CALL AXIS2(0.,0.,'ENERGY DENSITY',14,10.,90.,0.,10.,-1.)
  835 CALL PLOT(0.,0.,3)
         CALL PL1A(7.,4.,KKK,NTT,AS1,AS2,AS3,JJJP)
      IF(KKK.EQ.4) GO TO 836
      DO 911 I=2,8
      AXX=IBASE
      CQ=CF(I,2)/20.
      BXX=(ALOG10(AXX))*2.5
      CALL SYMBOL(BXX,CQ,.06,I,0.0,-1)
      DO 912 J=3,IZP
      AXX=AXX+AIINC
      CQ=CF(I,J)/20.
      BXX=(ALOG10(AXX))*2.5
 912  CALL SYMBOL(BXX,CQ,.06,I,0.0,-1)
911   CONTINUE
      DO 956 I=2,8
      AXX=IBASE
      CQ=CF(I,2)/20.
      BXX=(ALOG10(AXX))*2.5
      CALL SMOOTH(BXX,CQ,0)
      DO 957 J=3,IXZ
      AXX=AXX+AIINC
      CQ=CF(I,J)/20.
       BXX=(ALOG10(AXX))*2.5
957   CALL SMOOTH(BXX,CQ,-2)
      AXX=AXX+AIINC
      CQ=CF(I,NOP)/20.
      BXX=(ALOG10(AXX))*2.5
      CALL SMOOTH(BXX,CQ,-25)
956   CONTINUE
      GO TO 837
836      DO 838 I=2,8
      AXX=IBASE
      CQ=CF(I,2)/10.
      BXX=(ALOG10(AXX))*2.5
       CALL SYMBOL(BXX,CQ,.06,I,0.0,-1)
      DO 839 J=3,IZP
      AXX=AXX+AIINC
      CQ=CF(I,J)/10.
      BXX=(ALOG10(AXX))*2.5
839      CALL SYMBOL(BXX,CQ,.06,I,0.0,-1)
838       CONTINUE
       DO 840 I=2,8
       AXX=IBASE
       CQ=CF(I,2)/10.
       BXX=(ALOG10(AXX))*2.5
       CALL SMOOTH(BXX,CQ,0)
      DO 841 J=3,IXZ
      AXX=AXX+AIINC
      CQ=CF(I,J)/10.
      BXX=(ALOG10(AXX))*2.5
841      CALL SMOOTH(BXX,CQ,-2)
       AXX=AXX+AIINC
```

```
       CQ=CF(I,NOP)/10.
      BXX=(ALOG10(AXX))*2.5
       CALL SMOOTH(BXX,CQ,-25)
840     CONTINUE
  837 CALL PLOT(8.,7.,3)
      DO 991 I=2,8
      UG=I
      UF=7.13-(UG-1)*.125
      URR=UF-.1
      UH=QQQ(I)
      CALL NUMBER(8.1,UF,.06,UH,0.,1)
      CALL SYMBOL(8.5,UF,.06,I,0.,-1)
      CALL SYMBOL(8.6,UF,.06,I,0.,-1)
991   CALL SYMBOL(8.7,UF,.06,I,0.,-1)
      CALL PLOT(15.,0.,-3)
C
C
C
C     PLOT OF THE PROBABILITY OF OCCURENCE FOR AN IMPACT
C     ENERGY VALUE.
C
C
C
      CALL AXIS2(0.,0.,'ENERGY IN JOULES/M*M',
     *-20,7.,0.,0.,25.,1.)
      CALL AXIS2(0.,0.,'PERCENTAGE FREQUENCY OF OCCURRENCE',
     *34,7.,90.,0.,10.,-1.)
        CALL PL1A(6.,4.5,KKK,NTT,AS1,AS2,AS3,JJJP)
      DO 954 J=2,IZP
      CALL PLOT(0.,0.,3)
      XCP=AI(1,J)*10./XNT
      CALL SMOOTH(.1,XCP,0)
      DO 953 I=2,34
      XOP=I
      XOP=(XOP*.2)-.1
      XCP=AI(I,J)*10./XNT
      CALL SMOOTH(XOP,XCP,-2)
953   CONTINUE
      XCP=AI(35,J)*10./XNT
      CALL SMOOTH(6.9,XCP,-25)
  954 CONTINUE
      DO 958 J=2,IZP
      CALL PLOT(0 ,0.,3)
      XCP=AI(1,J)*10./XNT
      CALL SYMBOL(.1,XCP,.06,J,0.,-1)
      DO 959 I=2,35
      XOP=I
      XOP=(XOP*.2)-.1
      XCP=AI(I,J)*10./XNT
      CALL SYMBOL(XOP,XCP,.06,J,0.,-1)
959   CONTINUE
958   CONTINUE
      CALL PLOT(8.,7.,3)
      UH=IBASE
      DO 960 I=2,IZP
      UG=I
      UF=7.13-(UG-3.)*.125
      URR=UF-.1
       CALL SYMBOL(5.9,UF,.06,3HK =,0.,3)
      CALL NUMBER(6.1,UF,.06,UH,0.,1)
```

```
      CALL SYMBOL(6.5,UF,.06,I,0.,-1)
      CALL SYMBOL(6.6,UF,.06,I,0.,-1)
      UH=UH+AIINC
  960 CALL SYMBOL(6.7,UF,.06,I,0.,-1)
      CALL PLOT(0.,15.,-3)
C
C
C
C     PLOT OF THE PROBABILITY OF OCCURENCE FOR AN IMPACT
C     ENERGY VALUE.
C
C
C
      CALL AXIS2(0.,0.,'ENERGY IN JOULES/M*M',
     *-20,7.,0.,0.,25.,1.)
      CALL AXIS2(0.,0.,'PERCENTAGE FREQUENCY OF OCCURRENCE',
     *34,7.,90.,0.,10.,-1.)
      DO 988 J=2,IZP
      CALL PLOT(0.,0.,3)
      CALL PL1A(6.,4.5,KKK,NTT,AS1,AS2,AS3,JJJP)
      XCP=AI(1,J)*10./XNT
      CALL SYMBOL(.2,XCP,.06,J,0.,-1)
      DO 989 I=2,35
      XOP=I
      XOP=XOP*.2
      XCP=AI(I,J)*10./XNT
      CALL SYMBOL(XOP,XCP,.06,J,0.,-1)
  989 CONTINUE
  988 CONTINUE
      CALL PLOT(8.,7.,3)
      UH=IBASE
      DO 980 I=2,IZP
      UG=I
      UF=7.13-(UG-3.)*.125
      URR=UF-.1
      CALL SYMBOL(5.9,UF,.06,3HK =,0.,3)
      CALL NUMBER(6.1,UF,.06,UH,0.,1)
      CALL SYMBOL(6.5,UF,.06,I,0.,-1)
      CALL SYMBOL(6.6,UF,.06,I,0.,-1)
      UH=UH+AIINC
  980 CALL SYMBOL(6.7,UF,.06,I,0.,-1)
      CALL PLOT(12.,0.,-3)
      CALL LOGAX(0.,0.,'NUMBER PER 1000 KM*KM',-21,
     *5.,0.,0.,-2.,0.)
       CALL PL1A(6.,4.5,KKK,NTT,AS1,AS2,AS3,JJJP)
      CALL LOGAX(0.,0.,'STANDARD DEVIATION',18,
     *5.,90.,-1.,-2.,0.)
         XAREA=1000./AREA
           ARA=IBASE
       I=2
  858  AVT(I)=ALOG10(ARA*XAREA)
        ARA=ARA+AIINC
       I=I+1
          IF(I.GT.IZP) GO TO 857
       GO TO 858
  857      NOP=IZP
      CALL PLOT(0.,0.,3)
      AQP=AVT(2)*5./2.
      AQR=(AVB(2)+1.)*5./2.
      CALL SYMBOL(AQP,AQR,.06,011,0.0,-1)
```

```
      CALL SMOOTH(AQP,AQR,0)
      IXZ=NOP-1
      DO 809 I=3,IXZ
      AQP=AVT(I)*5./2.
      AQR=(AVB(I)+1.)*5./2.
      CALL SMOOTH(AQP,AQR,-2)
809   CONTINUE
      AMM=AVT(NOP)*5./2.
      AMN=(AVB(NOP)+1.)*5./2.
      CALL SMOOTH(AMM,AMN,-25)
      DO 855 I=3,NOP
      AQP=AVT(I)*5./2.
      AQR=(AVB(I)+1.)*5./2.
855   CALL SYMBOL(AQP,AQR,.06,011,0.0,-1)
      CALL PLOT(0.,-15.,-3)
      CALL LOGAX(0.,0.,'NUMBER PER 1000 KM*KM',-21,
     *5.,0.,0.,-2.,0.)
      CALL LOGAX(0.,0.,'MEAN DIFFERENCE BETWEEN ESTIMATES',
     *33,7.5,90.,-1.,-3.,0.)
        CALL PL1A(6.,4.5,KKK,NTT,AS1,AS2,AS3,JJJP)
         XAREA=1000./AREA
           ARA=IBASE
       I=2
 256   AVT(I)=ALOG10(ARA*XAREA)
      WRITE(6,37)AVT(I),ARA,VA(I)
        ARA=ARA+AIINC
       I=I+1
          IF(I.GT.IZP) GO TO 257
       GO TO 256
257        NOP=IZP
      CALL PLOT(0.,0.,3)
          WRITE(6,37)XM,(VA(IVMP),IVMP=2,NOP)
      AQP=AVT(2)*2.5
      AQR=(VA(2))*100./VB(2)
  261   CQR=(ALOG10(AQR)+1.)*2.5
        WRITE(6,37)AQR,CQR
      CALL SYMBOL(AQP,CQR,.06,011,0.0,-1)
      CALL SMOOTH(AQP,CQR,0)
      IXZ=NOP-1
      DO 258 I=3,IXZ
      AQP=AVT(I)*2.5
      AQR=(VA(I))*100./VB(I)
  263  CQR=(ALOG10(AQR)+1.)*2.5
         WRITE(6,37) AQR,CQR
      CALL SMOOTH(AQP,CQR,-2)
258   CONTINUE
      AMM=AVT(NOP)*2.5
      AQR=(VA(NOP))*100./VB(NOP)
  265 CQR=(ALOG10(AQR)+1.)*2.5
       WRITE(6,37)AQR,CQR
      CALL SMOOTH(AMM,CQR,-25)
       DO 271 I=3,NOP
        AQP=AVT(I)*2.5
       AQR=(VA(I))*100./VB(I)
 273     CQR=(ALOG10(AQR)+1.)*2.5
271       CALL SYMBOL(AQP,CQR,.06,011,0.0,-1)
      CALL PLOT(10.,0.,999)
      STOP
      END
      SUBROUTINE PL1A(XST,YST,KKK,NTT,AS1,AS2,AS3,JJJP)
```

```
C
C
C
C     SUBROUTINE TO PLACE THE DATE OF STORM ON THE VARIOUS
C     PLOTS.
C
C
C
      CALL SYMBOL(XST,YST,.10,AS1,0.,3)
      CALL SYMBOL(XST+.4,YST,.10,AS2,0.,2)
      CALL SYMBOL(XST+.6,YST,.10,AS3,0.,3)
        UST=YST-.4
        GO TO (251,252,253,254,256),KKK
251        CALL SYMBOL(XST,UST,.10,19HFITTED DISTRIBUTION,0.,19
        GO TO 255
252       CALL SYMBOL(XST,UST,.10,19HWITHOUT REPLACEMENT,0.,19)
      GO TO 255
253       CALL SYMBOL(XST,UST,.10,16HWITH REPLACEMENT,0.,16)
        GO TO 255
254      CALL SYMBOL(XST,UST,.10,19HSTRATIFIED SAMPLING,0.,19)
      CALL SYMBOL(XST,UST-.8,.10,2HM=,0.,2)
       XPJJ=JJJP
      CALL NUMBER(XST+.5,UST-.8,.10,XPJJ,0.,-1)
255         CALL SYMBOL(XST,UST-.4,.10,2HN=,0.,2)
            XNTT=NTT
        CALL NUMBER(XST+.5,UST-.4,.10,XNTT,0.,-1)
  256 RETURN
      END
END OF FILE
```

```
$L PAD2
C     APPLICATION OF MONTE CARLO METHOD TO
C     HAILPAD IMPACT ENERGY VALUES
      DIMENSION A(120,3),R(200),AI(120,20),V(250)
      DIMENSION VA(20),BI(120,20),VB(20),CF(9,20)
      DIMENSION VYY(500),VX(60),VY(60),CE(5000)
      DIMENSION AVT(20),AVB(20),VRA(60),VRB(60)
      DIMENSION PX(60),PQ(60),PP(60),QQQ(9)
      DIMENSION PPP(120),PQP(120),IPMM(2)
        DIMENSION VII(120),VJJ(120),VKK(120)
       DIMENSION VXXXX(50),VYYYY(50),VTT(10)
          COMMON WW(30,30),W8(2000)
      COMMON BUF(2048)
      CALL PLOTS(BUF,8192)
      XMAX=10.
      I=1
      INSEED=123457
   33 READ(5,30)NTT,IWP,KKK
          READ(5,431)IAREA
       READ(5,432)IZK
432      FORMAT(I2)
431        FORMAT(I5,2I3)
            AREA=IAREA
      BMAX=0.
      XISY=0.
      XNT=NTT
      I=1
3     READ(8,1,END=04)A(I,3),AS1,AS2,AS3
1     FORMAT(8X,4X,F7.2,A3,A2,A3)
      I=I+1
      GO TO 3
04    SY=0.
      N=I-1
      DO 23 I=1,N
23    SY=SY+A(I,3)
      XN=N
      SYM=SY/XN
      DO 50 ITT=1,500
      DO 50 IZX=1,20
      BI(ITT,IZX)=0.
50    AI(ITT,IZX)=0.
       ICQ=1
       DMS=0.0
        DO 611 I=1,30
        DO 611 J=1,30
611        WW(I,J)=0.0
614        READ(1,612,END=613)I8,I9,AI8
612      FORMAT(I2,1X,I2,7X,F7.2)
       WW(I8,I9)=AI8
        GO TO 614
30    FORMAT(I5,5I3)
  613 DO 51 ITT=1,20
      VA(ITT)=0.
51    VB(ITT)=0.
710      FORMAT(1X,2F10.2,3X,2I5)
      IW=2
  100 IT=1
      VAR=0.
      TSYM=0.
```

```
   17 DO 18 IX=1,N
18    R(IX)=0.
      SUMX=0.
610      AMS=0.
      DO 644 IDQ=1,ICQ
       CALL GGU3(INSEED,2,R)
      XSUM=0.
      XNN=0.
      I1=1
      J1=1
7          IF((WW(I1,J1).EQ.0.).OR.(WW(I1,J1+IZK).EQ.0.0)) GO T
       IF((WW(I1+IZK,J1).EQ.0.).OR.(WW(I1+IZK,J1+IZK).EQ.0.)) G
        WA1=WW(I1,J1)-WW(I1,J1+IZK)
       IF(WA1.LE.0.0) WA1=-1.*WA1
        V1=WW(I1,J1)+WA1*R(1)
       WA2=WW(I1+IZK,J1)-WW(I1+IZK,J1+IZK)
       IF(WA2.LE.0.0) WA2=-1.*WA2
       V2=WW(I1+IZK,J1)+WA2*R(1)
       VM=(V1+V2)/2.
      WA3=WW(I1,J1)-WW(I1+IZK,J1)
       IF(WA3.LE.0.0) WA3=-1.*WA3
       W1=WW(I1,J1)+WA3*R(2)
       WA4=WW(I1,J1+IZK)-WW(I1+IZK,J1+IZK)
       IF(WA4.LE.0.0) WA4=-1.*WA4
       W2=WW(I1,J1+IZK)+WA4*R(2)
       WM=(W1+W2)/2.
      VAL=(VM+WM)/2.
      XSUM=XSUM+VAL
      XNN=XNN+1.
10    FORMAT(1X,2I3,3F8.2)
6     J1=J1+IZK
      IF(J1.GE.29) GO TO 5
      GO TO 7
5     J1=1
      I1=I1+IZK
      IF(I1.GE.29) GO TO 8
      GO TO 7
   8   SUMX=XSUM+SUMX
644         AMS=XNN+AMS
        ASYM=SUMX/AMS
       W8(IT)=ASYM
      QCI=ICQ
       IWMP=XNN/QCI
623       IINC=XNN/QCI
      TSYM=TSYM+ASYM
      ISYM=(ASYM/5.)+1.
      CE(IT)=ASYM
      AI(ISYM,IW)=AI(ISYM,IW)+1.
  202 IT=IT+1
      IF(IT.LE.NTT) GO TO 17
      VTT(ICQ)=AMS
      VB(IW)=(TSYM/XNT)
       I8=IT-1
         WRITE(6,37)VB(IW),AMS,XNN
       VAR=0.
       DO 650 ICW=1,NTT
650    VAR=VAR+(W8(ICW)-VB(IW))*(W8(ICW)-VB(IW))
       VA(IW)=((VAR/XNT)**.5)
       WRITE(6,37)VA(IW)
        ICQ=ICQ+1
```

```
935   IW=IW+1
37        FORMAT(1X,10F8.2)
      WRITE(7,300)IWMP
      IF(ICQ.GE.4) GO TO 99
      GO TO 100
   99 WRITE(7,34)NTT
      IZP=IW-1
34    FORMAT(1X,15HNUMBER CF DRAWS,I8)
      JMP=(BMAX/5.)+1.
      IXPP=IW-1
102   FORMAT(1X,I4,3X,20F6.0)
300         FORMAT(I5)
31    CALL PLOT(0.0,0.,3)
      CALL PLOT(4.0,4.0,-3)
      CALL LOGAX(0.,0.,'NUMBER',-6,
     *5.,0.,1.,-2.,0.)
      CALL LOGAX(0.,0.,'STANDARD DEVIATION',18,
     *5.,90.,0.,-2.,0.)
        CALL PL1A(3.,5.,KKK,NTT,AS1,AS2,AS3)
      JPP=1
      ARA=VTT(JPP)
      I=2
 908  AVT(I)=ALOG10(ARA)
      AVB(I)=ALOG10(VA(I))
       WRITE(6,37)ARA,VA(I),AVT(I),AVB(I)
      I=I+1
          JPP=JPP+1
      ARA=VTT(JPP)
      IF(I.GT.IZP) GO TO 907
      GO TO 908
907   NOP=IZP
      CALL PLOT(0.,0.,3)
      AQP=AVT(2)*5./2.
      AQR=AVB(2)*5./2.
      CALL SYMBOL(AQP,AQR,.06,011,0.0,-1)
      CALL SMOOTH(AQP,AQR,0)
      IXZ=NOP-1
      DO 909 I=3,IXZ
      AQP=AVT(I)*5./2.
      AQR=AVB(I)*5./2.
      CALL SMOOTH(AQP,AQR,-2)
909   CONTINUE
      AMM=AVT(NOP)*5./2.
      AMN=AVB(NOP)*5./2.
      CALL SMOOTH(AMM,AMN,-25)
      DO 955 I=3,NOP
      AQP=AVT(I)*5./2.
      AQR=AVB(I)*5./2.
955   CALL SYMBOL(AQP,AQR,.06,011,0.0,-1)
      CALL PLOT(0.,15.,-3)
C
C
C
C     PLOT OF THE PROBABILITY OF OCCURENCE FOR AN IMPACT
C     ENERGY VALUE.
C
C
C
      CALL AXIS2(0.,0.,'ENERGY IN JOULES/M*M',
     *-20,7.,0.,0.,25.,1.)
```

```
      CALL AXIS2(0.,0.,'PERCENTAGE FREQUENCY OF OCCURRENCE',
     *34,7.,90.,0.,10.,-1.)
        CALL PL1A(6.,4.5,KKK,NTT,AS1,AS2,AS3)
      DO 954 J=2,IZP
      CALL PLOT(0.,0.,3)
      XCP=AI(1,J)*10./XNT
      CALL SMOOTH(.1,XCP,0)
      DO 953 I=2,34
      XOP=I
      XOP=(XOP*.2)-.1
      XCP=AI(I,J)*10./XNT
      CALL SMOOTH(XOP,XCP,-2)
953   CONTINUE
      XCP=AI(35,J)*10./XNT
      CALL SMOOTH(6.9,XCP,-25)
  954 CONTINUE
      DO 958 J=2,IZP
      CALL PLOT(0.,0.,3)
      XCP=AI(1,J)*10./XNT
      CALL SYMBOL(.1,XCP,.06,J,0.,-1)
      DO 959 I=2,35
      XOP=I
      XOP=XOP*.2
      XCP=AI(I,J)*10./XNT
      CALL SYMBOL(XOP,XCP,.06,J,0.,-1)
959   CONTINUE
958   CONTINUE
      CALL PLOT(8.,7.,3)
      JPP=1
      DO 960 I=2,IZP
       UH=VTT(JPP)
      UG=I
      UF=7.13-(UG-3.)*.125
      URR=UF-.1
      CALL NUMBER(5.9,UF,.06,3HK =,0.,3)
       CALL NUMBER(6.1,UF,.06,UH,0.,1)
      CALL SYMBOL(6.5,UF,.06,I,0.,-1)
      CALL SYMBOL(6.6,UF,.06,I,0.,-1)
       JPP=JPP+1
960   CALL SYMBOL(6.7,UF,.06,I,0.,-1)
      CALL PLOT(15.,0.,-3)
C
C
C
C     PLOT OF THE PROBABILITY OF OCCURENCE FOR AN IMPACT
C     ENERGY VALUE.
C
C
C
      CALL AXIS2(0.,0.,'ENERGY IN JOULES/M*M',
     *-20,7.,0.,0.,25.,1.)
      CALL AXIS2(0.,0.,'PERCENTAGE FREQUENCY OF OCCURRENCE',
     *34,7.,90.,0.,10.,-1.)
      DO 988 J=2,IZP
      CALL PLOT(0.,0.,3)
      CALL PL1A(6.,4.5,KKK,NTT,AS1,AS2,AS3)
      XCP=AI(1,J)*10./XNT
      CALL SYMBOL(.2,XCP,.06,J,0.,-1)
      DO 989 I=2,35
      XOP=I
```

```
          XOP=XOP*.2
          XCP=AI(I,J)*10./XNT
          CALL SYMBCL(XOP,XCP,.06,J,0.,-1)
    989   CONTINUE
    988   CONTINUE
          CALL PLOT(8.,7.,3)
             JPP=1
          DO 980 I=2,IZP
          UH=VTT(JPP)
          UG=I
          UF=7.13-(UG-3.)*.125
          URR=UF-.1
           CALL NUMBER(5.9,UF,.06,3HK =,0.,1)
           CALL NUMBER(6.1,UF,.06,UH,0.,1)
          CALL SYMBOL(6.5,UF,.06,I,0.,-1)
          CALL SYMBOL(6.6,UF,.06,I,0.,-1)
           JPP=JPP+1
    980   CALL SYMBOL(6.7,UF,.06,I,0.,-1)
          CALL PLOT(0.,-15.,-3)
          CALL LOGAX(0.,0.,'NUMBER PER 1000 KM*KM',-21,
         *5.,0.,0.,-2.,0.)
           CALL PL1A(6.,4.5,KKK,NTT,AS1,AS2,AS3)
          CALL LOGAX(0.,0.,'STANDARD DEVIATION',18,
         *5.,90.,-1.,-2.,0.)
             XAREA=1000./AREA
           JPP=1
               ARA=VTT(JPP)
           I=2
     858   AVT(I)=ALOG10(ARA*XAREA)
           I=I+1
              IF(I.GT.IZP) GO TO 857
          JPP=JPP+1
          ARA=VTT(JPP)
           GO TO 858
    857        NOP=IZP
          CALL PLOT(0.,0.,3)
          AQP=AVT(2)*5./2.
          AQR=(AVB(2)+1.)*5./2.
          CALL SYMBOL(AQP,AQR,.06,011,0.0,-1)
          CALL SMOOTH(AQP,AQR,0)
          IXZ=NOP-1
          DO 809 I=3,IXZ
          AQP=AVT(I)*5./2.
          AQR=(AVB(I)+1.)*5./2.
          CALL SMOOTH(AQP,AQR,-2)
    809   CONTINUE
          AMM=AVT(NOP)*5./2.
          AMN=(AVB(NOP)+1.)*5./2.
          CALL SMOOTH(AMM,AMN,-25)
          DO 855 I=3,NOP
          AQP=AVT(I)*5./2.
          AQR=(AVB(I)+1.)*5./2.
    855   CALL SYMBOL(AQP,AQR,.06,011,0.0,-1)
          CALL PLOT(15.,0.,-3)
          CALL LOGAX(0.,0.,'NUMBER PER 1000 KM*KM',-21,
         *5.,0.,0.,-2.,0.)
          CALL LOGAX(0.,0.,'MEAN DIFFERENCE BETWEEN ESTIMATES',
         *33,7.5,90.,-1.,-3.,0.)
            CALL PL1A(6.,4.5,KKK,NTT,AS1,AS2,AS3)
             XAREA=1000./AREA
```

```
         JPP=1
           ARA=VTT(JPP)
       I=2
 256   AVT(I)=ALOG10(ARA*XAREA)
       I=I+1
          IF(I.GT.IZP) GO TO 257
       JPP=JPP+1
      ARA=VTT(JPP)
       GO TO 256
257        NOP=IZP
      CALL PLOT(0.,0.,3)
        XM=SYM
          WRITE(6,37)XM,(VA(IVMP),IVMP=2,NOP)
      AQP=AVT(2)*2.5
      AQR=(VA(2))*100./VB(2)
   261  CQR=(ALOG10(AQR)+1.)*2.5
        WRITE(6,37)AQR,CQR
      CALL SYMBOL(AQP,CQR,.06,011,0.0,-1)
      CALL SMOOTH(AQP,CQR,0)
      IXZ=NOP-1
      DO 258 I=3,IXZ
      AQP=AVT(I)*2.5
      AQR=(VA(I))*100./VB(I)
   263 CQR=(ALOG10(AQR)+1.)*2.5
         WRITE(6,37) AQR,CQR
      CALL SMOOTH(AQP,CQR,-2)
258   CONTINUE
      AMM=AVT(NOP)*2.5
      AQR=(VA(NOP))*100./VB(NOP)
   265 CQR=(ALOG10(AQR)+1.)*2.5
       WRITE(6,37)AQR,CQR
      CALL SMOOTH(AMM,CQR,-25)
       DO 271 I=3,NOP
        AQP=AVT(I)*2.5
       AQR=(VA(I))*100./VB(I)
 273     CQR=(ALOG10(AQR)+1.)*2.5
271       CALL SYMBOL(AQP,CQR,.06,011,0.0,-1)
      CALL PLOT(10.,0.,999)
      STOP
      END
      SUBROUTINE PL1A(XST,YST,KKK,NTT,AS1,AS2,AS3)
C
C
C
C     SUBROUTINE TO PLACE THE DATE OF STORM ON THE VARIOUS
C     PLOTS.
C
C
C
      CALL SYMBOL(XST,YST,.10,AS1,0.,3)
      CALL SYMBOL(XST+.4,YST,.10,AS2,0.,2)
      CALL SYMBOL(XST+.6,YST,.10,AS3,0.,3)
        UST=YST-.4
       IF(KKK.EQ.9)GO TO 256
        GO TO (251,252,253,254,256),KKK
251        CALL SYMBOL(XST,UST,.10,19HFITTED DISTRIBUTION,0.,19)
        GO TO 255
252       CALL SYMBOL(XST,UST,.10,19HWITHOUT REPLACEMENT,0.,19)
      GO TO 255
253       CALL SYMBOL(XST,UST,.10,16HWITH REPLACEMENT,0.,16)
```

```
             GO TO 255
      254      CALL SYMBOL(XST,UST,.10,19HSTRATIFIED SAMPLING,0.,19)
            GO TO 255
      256   CALL SYMBOL(XST,UST,.10,11H2-D CONTOUR,0.,11)
      255         CALL SYMBOL(XST,UST-.4,.10,2HN=,0.,2)
                  XNTT=NTT
              CALL NUMBER(XST+.5,UST-.4,.10,XNTT,0.,-1)
            RETURN
            END
END OF FILE
```

```
$L PLOT
          DIMENSION AA(22,25),X(600),Y(600),Z(600),CVAL(10)
          INTEGER IOP(10)/10*0/
          COMMON A(8),BUF(2048),B(25),VOP(10)
           DATA AQ/'YES'/
          CALL PLOTS(BUF,8192)
          IOP(1)=1
          IOP(2)=1
          IOP(3)=0
          IOP(4)=1
          NC=10
          CMIN=25.0
          CSET=CMIN
          CINT=50.0
 95          FORMAT(1X,13F8.2)
  6         YEAR=1976
           XMAX=-5.0
           XMIN=15.0
          YMAX=0.
          YMIN=22.
          IMM=1
            I=1
 2         READ(8,1,END=10)(A(II),II=2,4),AI3
 1         FORMAT(2X,3F2.0,4X,7F7.2)
          CALL GENER(JR)
          YY=A(2)
          XX=A(1)
            XMAX=AMAX1(XMAX,XX)
           XMIN=AMIN1(XMIN,XX)
          YMAX=AMAX1(YMAX,YY)
          YMIN=AMIN1(YMIN,YY)
          X(IMM)=XX
          Y(IMM)=YY
          Z(IMM)=AI3
            IMM=IMM+1
           I=I+1
           GO TO 2
    10    N=IMM
           XSIZE=XMAX-XMIN
           YSIZE=YMAX-YMIN
          WRITE(6,310)XSIZE,YSIZE
 310         FORMAT(1X,2F10.2)
          DO 20 I=1,NC
          CVAL(I)=CSET
          CSET=CSET+CINT
 20       CONTINUE
           CALL PLOT(0.,0.,3)
          DO 300 I=1,N
          VX=X(I)
          VY=Y(I)
          CALL SYMBOL(VX,VY,.06,3,0.,-1)
          CALL NUMBER(VX+.09,VY,.06,Z(I),0.,1)
 300      CONTINUE
           CALL SCCONT(XSIZE,YSIZE,X,Y,Z,N,CVAL,
         *NC,IOP,VOP,XMIN,XMAX,YMIN,YMAX)
 33       CALL PLOT(0.,0.,999)
          STOP
          END
          SUBROUTINE GENER(KTR)
```

```
      COMMON A(8),ZZ(9),BUF(2048)
         A(1)=1.
         A(2)=21.
        IF(A(4).EQ.29) A(2)=23.
      M=(A(2)-1)/6.
      N=(A(1)-1)/2.
      YM=M
      YN=N
      R=A(4)
      T=A(3)
      Y=(6.*(T-19.)+YM+YN/2.+.25)*1.0084
      IS=A(2)
      K=M+1
      GO TO (27,28,27,28,27,28),K
27    P=IS-(1+6*(K-1))
      GO TO 29
28    P=K*6-IS
29    IF(A(1).LE.2) GO TO 30
      N=(A(1)-2.)/2.
      GO TO 31
30    N=A(1)/2.
31    XN=N
      L=(A(3)-15.)/4.
      Z=1.3
      C=5.2
      IF(L.LE.4.) GO TO 32
      Z=1.2
      C=-.2
      L=L-4
32    IF(R.LE.10) GO TO 33
      X=(6.*(29.-R)+C-Z*(L-1.)-P-XN/2.-.25)*1.0125
      GO TO 34
33    X=-(6.*(R-1.)+P+XN/2.+.25)*1.0125
34    Y=Y+.00014*X*X
      A(1) = X/8.
      A(2) =(Y-.25)/8.
      RETURN
      END
      SUBROUTINE OUTLIN(YEAR)
      COMMON A(8),ZZ(9),BUF(2048)
      CALL PLOT(0.,0.,3)
      CALL PLOT(30.5,14.5,-3)
      CALL PLOT(0.,0.,3)
      CALL PLOT(-24.2,0.,2)
      CALL PLOT(-5.35,-4.46,3)
      CALL PLOT(-5.35,5.75,2)
       CALL PLOT(-21.91,-5.25,3)
       CALL PLOT(-21.91,6.6,2)
      CALL CIRCLE(-3.91,.61,360.,0.,10.0,10.0,0.0)
       CALL PLOT(-15.2,-9.25,3)
      CALL PLOT(-15.2,10.5,2)
       CALL PLOT(-13.7,-9.3,3)
       CALL PLOT(-13.7,10.55,2)
      CALL SYMBOL(-21.,-.1,.08,14HFIFTH MERIDIAN,0.,14)
      CALL SYMBOL( -23.72,2.13,.10,004,90.,-1)
      CALL SYMBOL(-23.72,2.18,.125,'EG',90.,2)
      CALL SYMBOL( -21.20,6.13,.08,003,90.,-1)
      CALL SYMBOL(-21.20,6.18,.08,'CAMROSE',90.,7)
      CALL SYMBOL(-15.2,6.82,.08,003,90.,-1)
      CALL SYMBOL(-15.2,6.87,.08,'STETTLER',90.,8)
```

```
      CALL SYMBOL(-18.2,2.23,.08,003,90.,-1)
      CALL SYMBOL(-18.2,2.28,.08,'PONOKA',90.,6)
      CALL SYMBOL(-17.9,-1.25,.08,003,90.,-1)
      CALL SYMBOL(-17.9,-1.20,.08,'RIMBEY',90.,6)
      CALL SYMBOL(-15.63,-4.86,.10,004,90.,-1)
      CALL SYMBOL(-15.63,-4.81,.125,'RM',90.,2)
      CALL SYMBOL(  -13.91,.61,.10,011,90.,-1)
      CALL SYMBOL(-13.91,.66,.125,'QF',90.,2)
      CALL SYMBOL(-10.61,-3.34,.08,003,90.,-1)
      CALL SYMBOL(-10.61,-3.29,.08,'SUNDRE',90.,6)
      CALL SYMBOL(-10.58,-.57,.08,003,90.,-1)
      CALL SYMBOL( -9.84,3.90,.08,003,90.,-1)
      CALL SYMBOL(-9.84,3.95,.08,'THREE HILLS',90.,11)
      CALL SYMBOL( -7.7,7.0,.08,003,90.,-1)
      CALL SYMBOL(-7.7,7.05,.08,'DRUMHELLER',90.,10)
      CALL NUMBER (-3.5,11.65,.16,YEAR ,90.,-1)
        CALL SYMBOL(-4.69,-.12,.10,004,90.,-1)
          CALL SYMBOL(-4.69,-.07,.125,'YC',90.,2)
   53 RETURN
      END
END OF FILE
```

Appendix II

HAILSWATHS USED IN THE ANALYSIS

The four hailswaths used in this dissertation are given by date in this appendix. The numbers denote the largest size of hail observed by the farmers. The numbers are associated with familiar objects and are denoted by:

Number	Hailsize Name	Assumed Size Range (cm) [1]
1	Shot	.1 - .3
2	Pea	.4 - 1.2
3	Grape	1.3 - 2.0
4	Walnut	2.1 - 3.2
5	Golfball	3.3 - 5.2
6	Larger than Golfball	>5.2

0=is hail of unknown size

R=rain only

X=no rain or hail

*Denotes the hailpad locations

The vertical line on the figure is the 5th meridian.

The impact energy densities used in this dissertation for each hailswath are:

---

[1] (Wojtiw, 1975a)

24 June 1974

2.20	7.29	9.64	10.03	10.06	11.49	15.13
25.47	38.51	52.39	70.91	83.89	133.20	159.33
168.55	199.24	212.45	250.64	300.21	395.72	

5 July 1974

6.50	9.19	10.58	21.11	21.66	22.84	33.02
38.68	42.17	62.21	74.00	74.48	75.90	82.68
96.01	98.34	113.59	169.30	181.29	203.19	276.34

29 July 1974

0.48	0.55	3.10	4.60	6.50	7.59	9.62
11.51	14.36	15.11	15.57	17.20	20.38	20.88
23.41	25.20	25.33	41.20	42.19	50.78	51.97
57.19	64.38	76.51	78.25	98.06	106.83	129.97
146.90	213.43	259.76	294.02	380.82	546.78	

3 July 1975

0.47	3.19	4.95	14.01	41.37	59.69	60.09
70.05	70.09	85.65	117.28	125.31	216.66	222.06
248.29	254.26	319.16	456.68			

20 July 1975

1.16 3.14 3.52 4.18 6.33 10.35 10.38

12.42 12.56 13.17 14.60 15.96 16.49 27.08

29.12 31.14 33.09 38.94 48.89 57.89 65.05

71.53 72.90 86.81 88.56 92.20 100.06 108.18

129.50 203.71 419.44 421.44

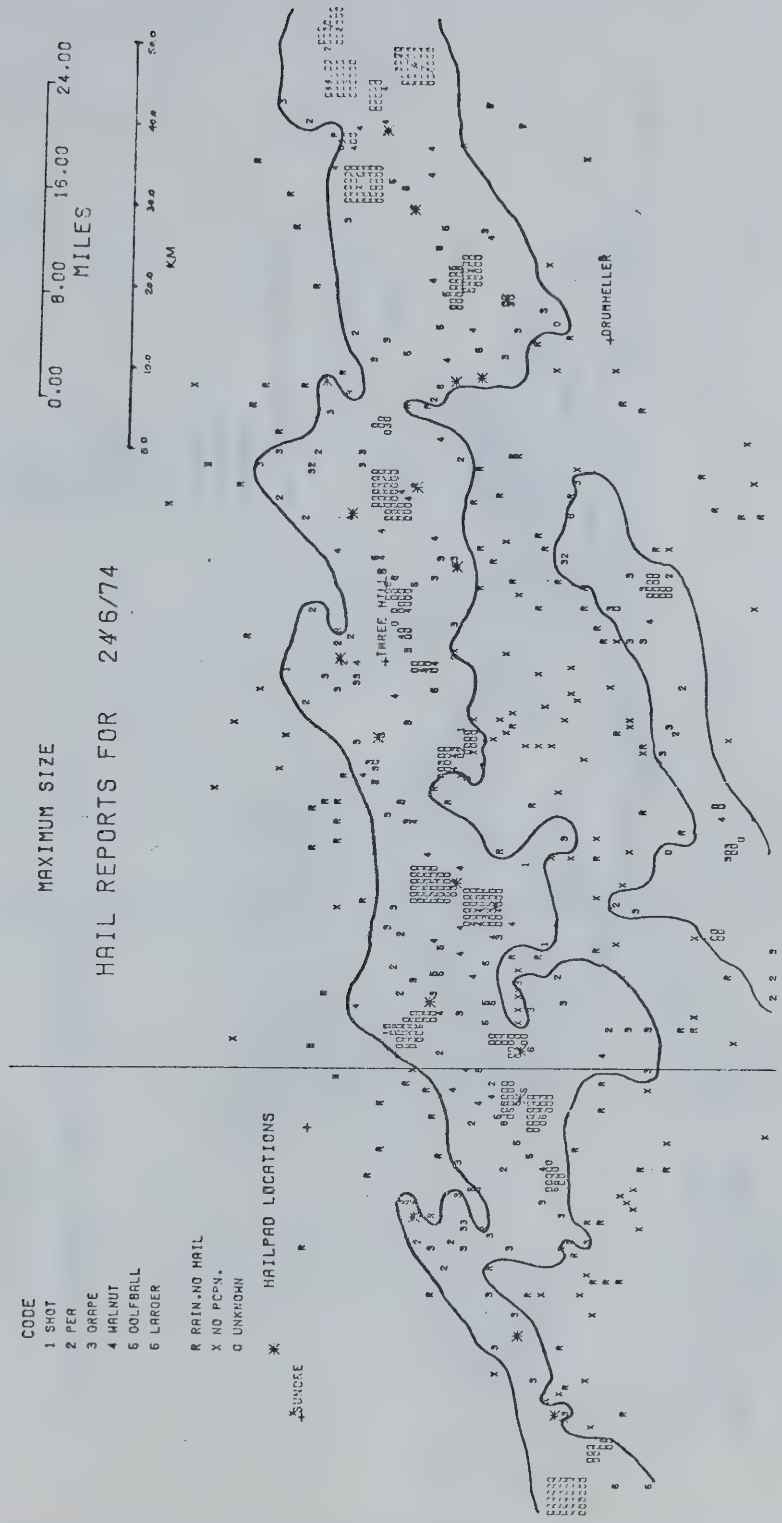

Figure II.1 The hailfall and hailpad locations for the 24 June 1974 hailswath

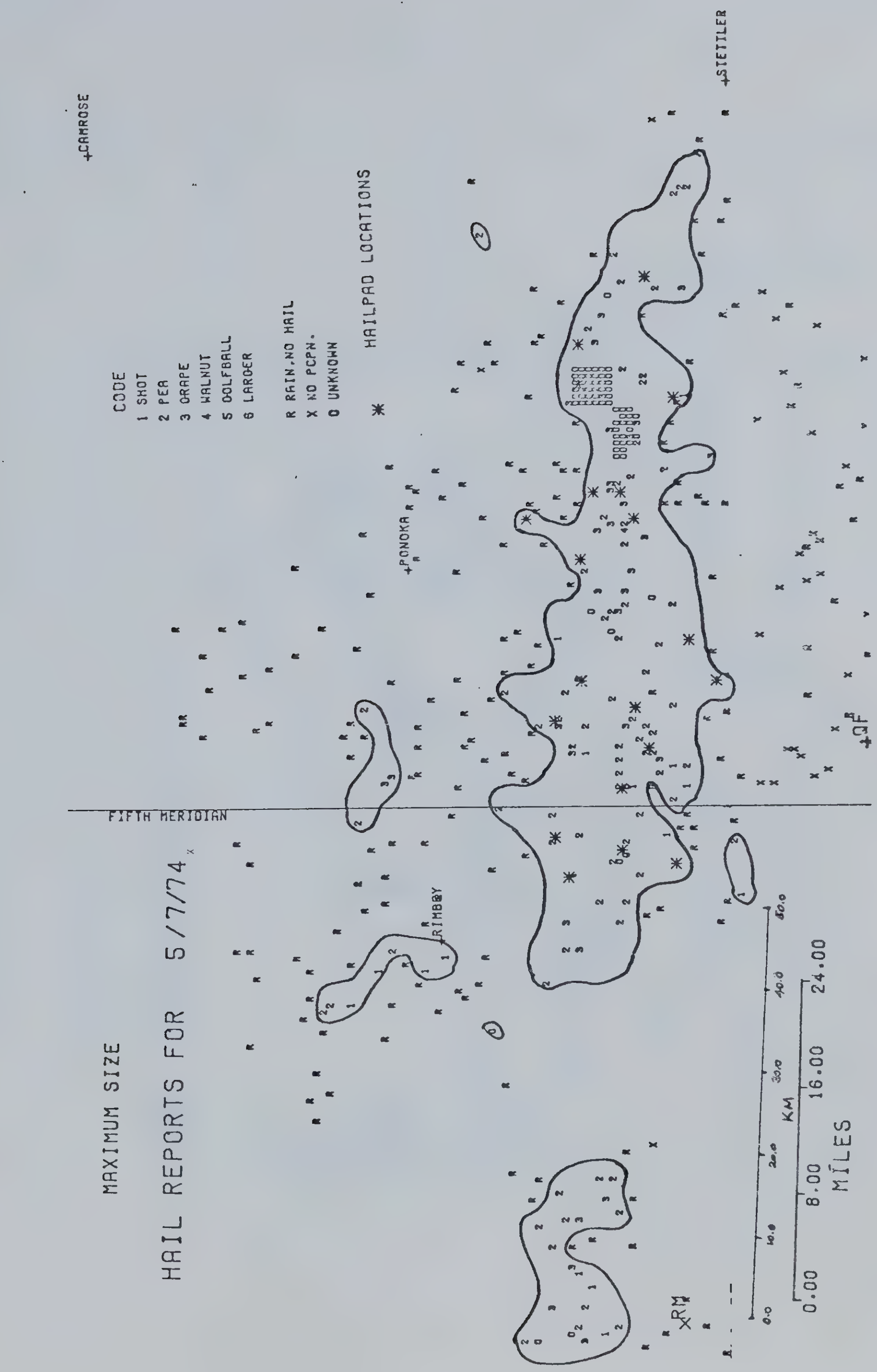

Figure II.2 The hailfall and hailpad locations for the 5 July 1974 hailswath

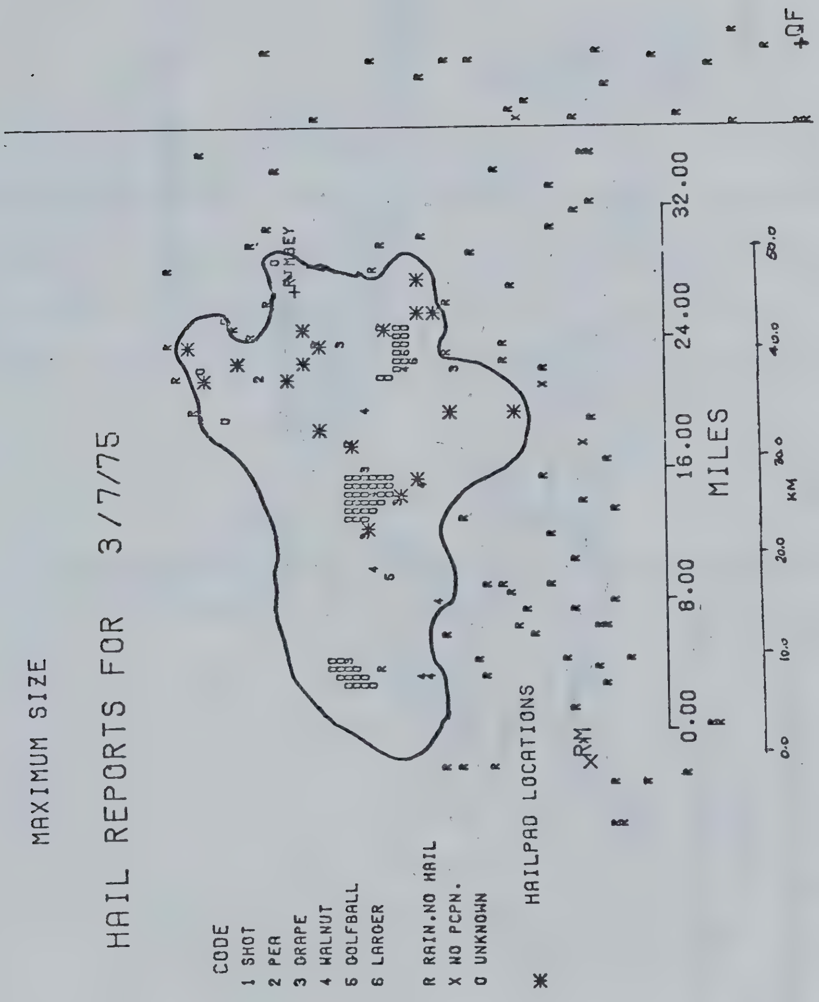

Figure II.3 The hailfall and hailpad locations for the 3 July 1975 hailswath

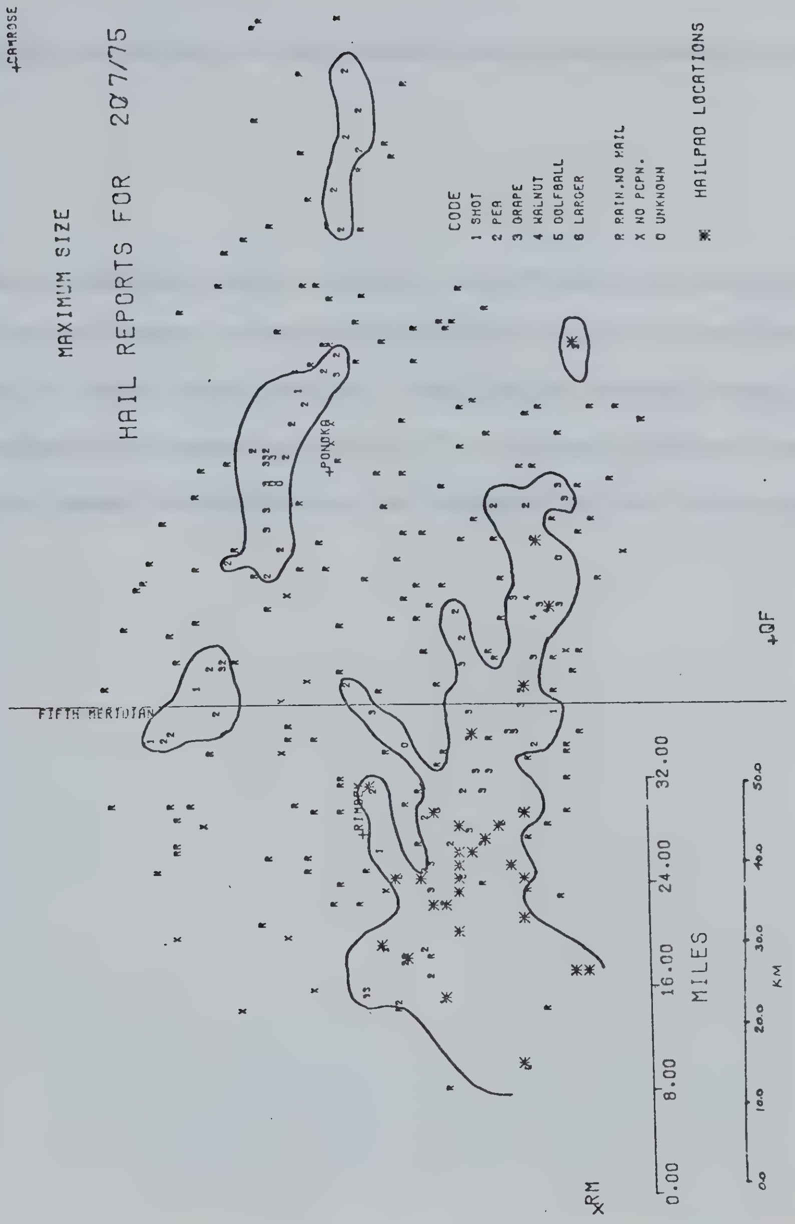

Figure II.4 The hailfall and hailpad locations for the 20 July 1975 hailswath

[illegible]

Appendix III

PERCENTAGE FREQUENCY OF OCCURRENCE OF IMPACT ENERGY DENSITY

The following pages contain the percentage frequency of occurence of impact energy density for the four hailswaths examined in this dissertation. The impact energy densities are grouped in classes of 25 J m^{-2}. The best fitted two-parameter gamma distribution is denoted by the "triangles".

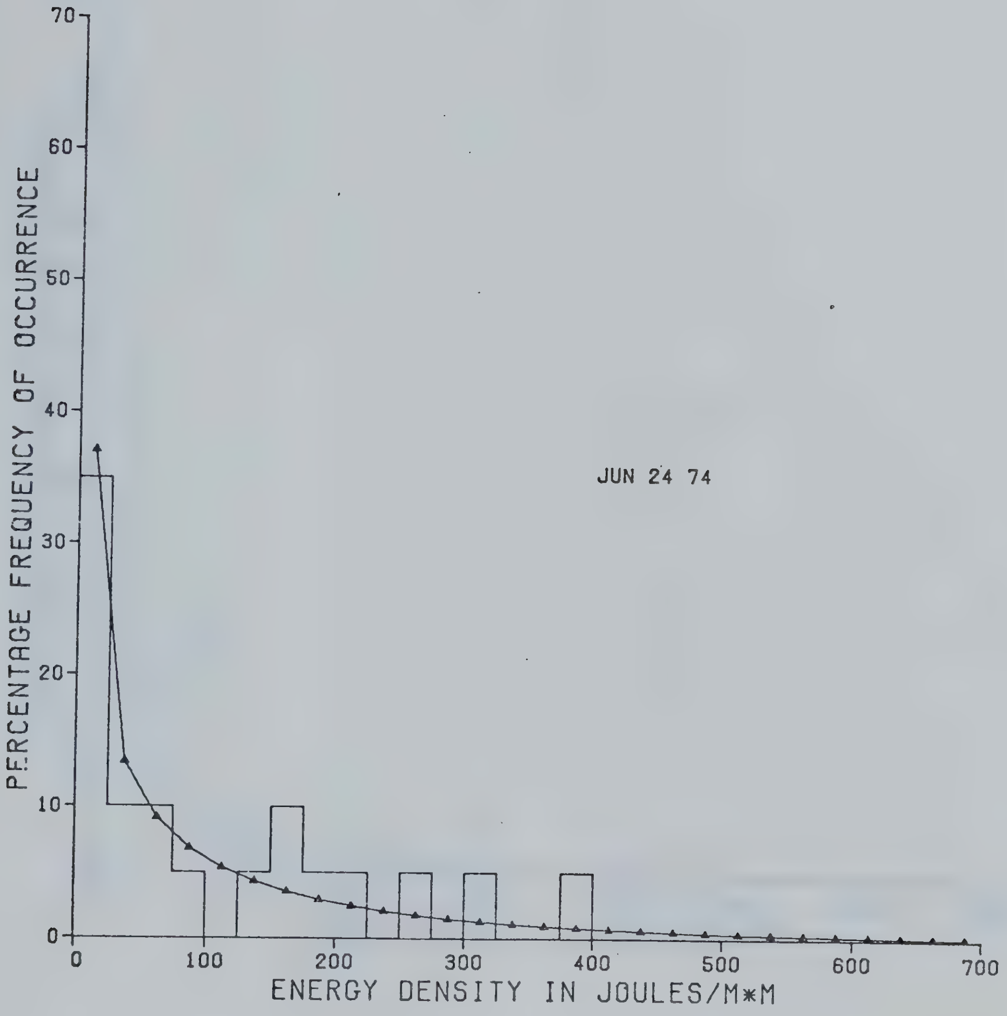

Figure III.1 The percentage frequency of occurrence of impact energy densities for 24 June 1974 hailswath

[illegible]

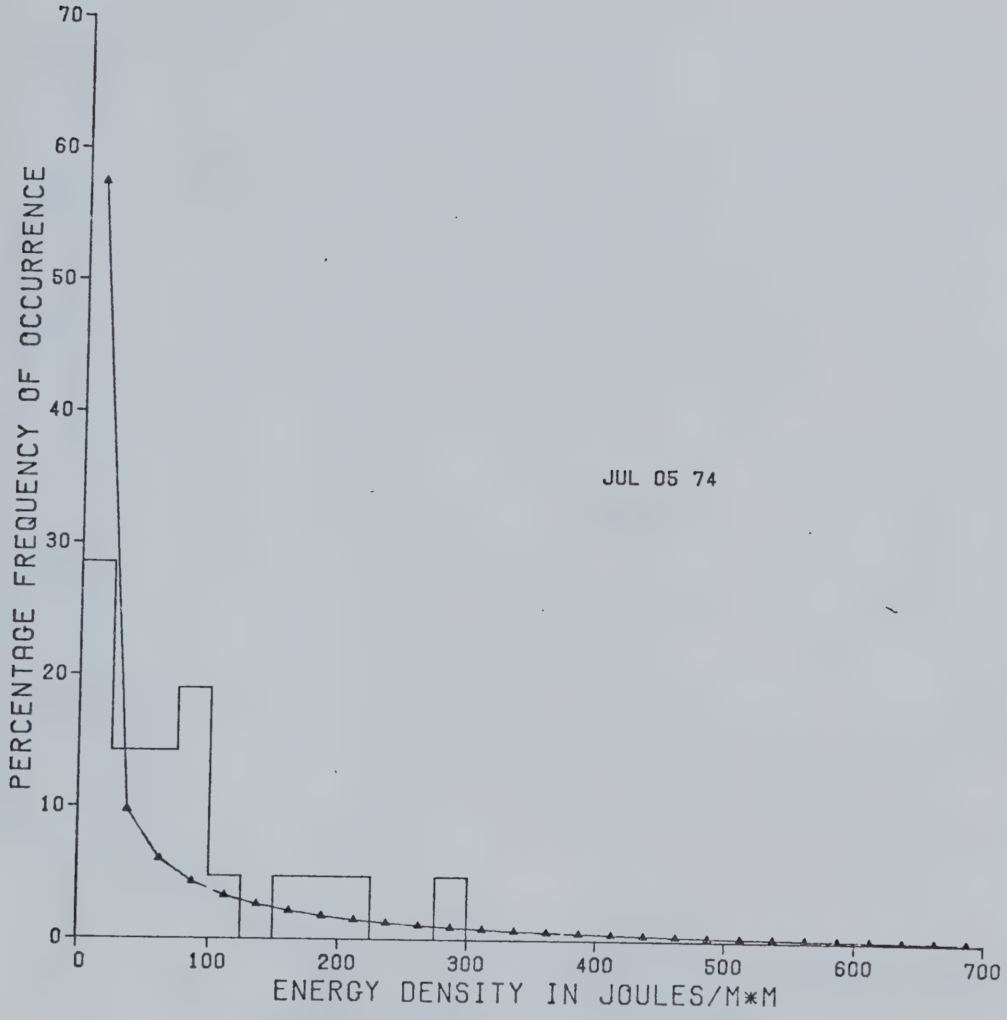

Figure III.2 The percentage frequency of occurrence of impact energy densities for 5 July 1974 hailswath

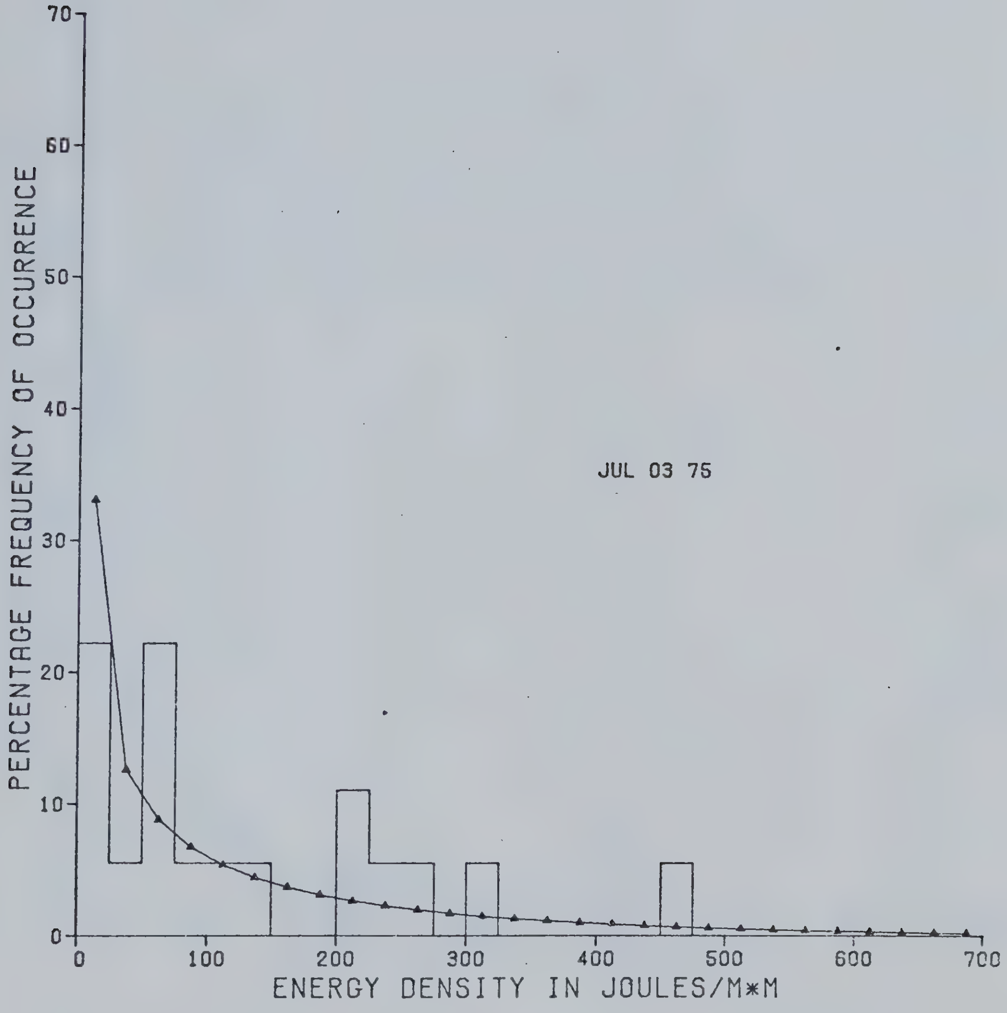

Figure III.3 The percentage frequency of occurrence of impact energy densities for 3 July 1975 hailswath

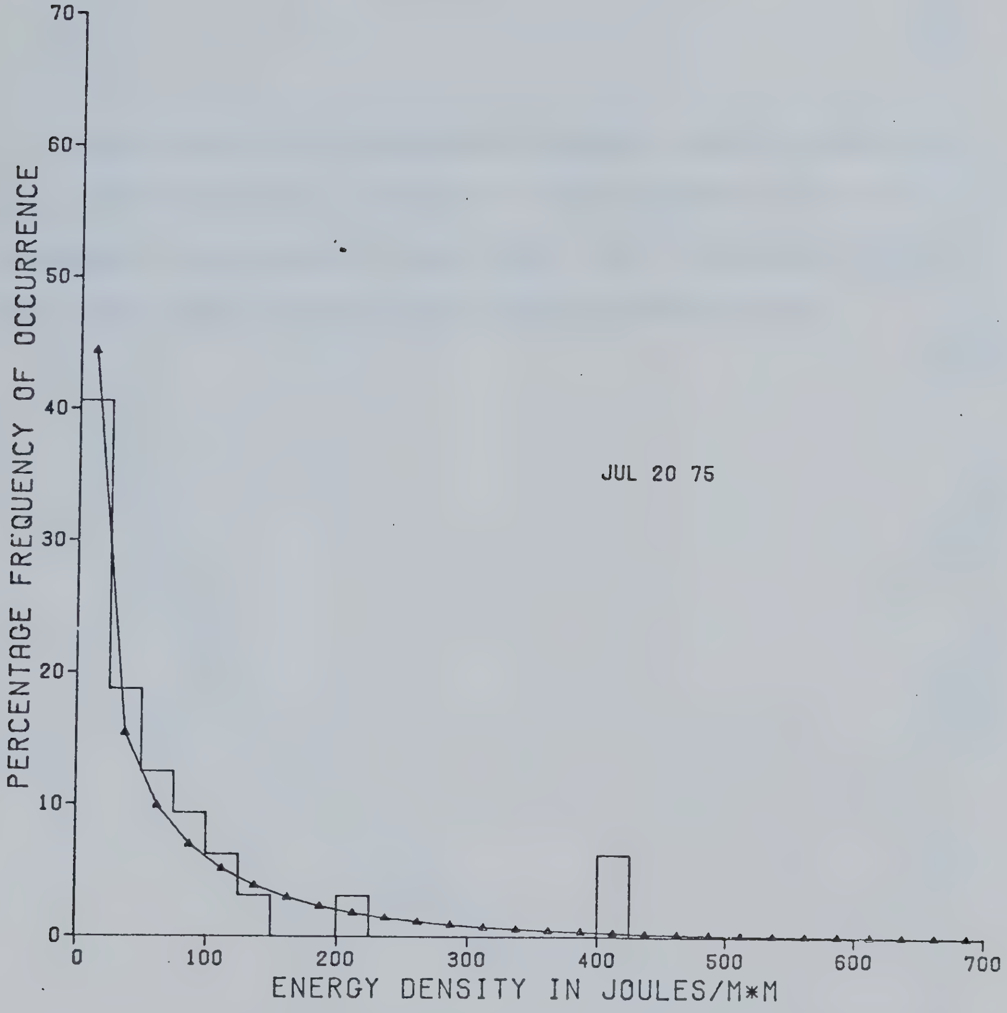

Figure III.4 The percentage frequency of occurrence of impact energy densities for 20 July 1975 hailswath

Appendix IV

CUMMULATIVE FREQUENCY OF IMPACT ENERGY DENSITY

The cumulative frequency of impact energy density for the four hailswaths is given in this appendix. The "X" represent the original data, while the "triangles" denote the best fitted two-parameter gamma distribution.

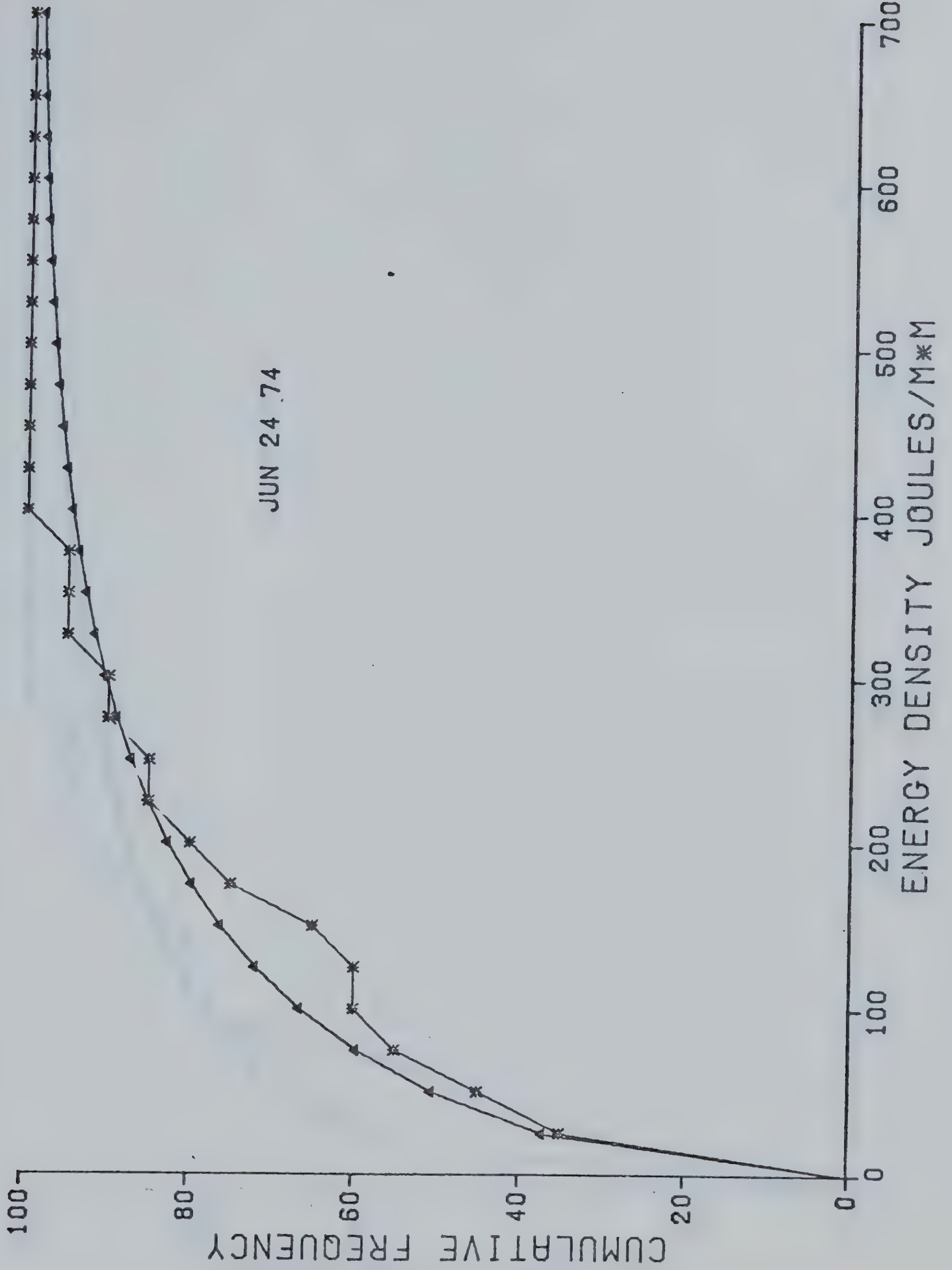

Figure IV.1 The cumulative frequency of impact energy density for 24 June 1974 hailswath

[illegible]

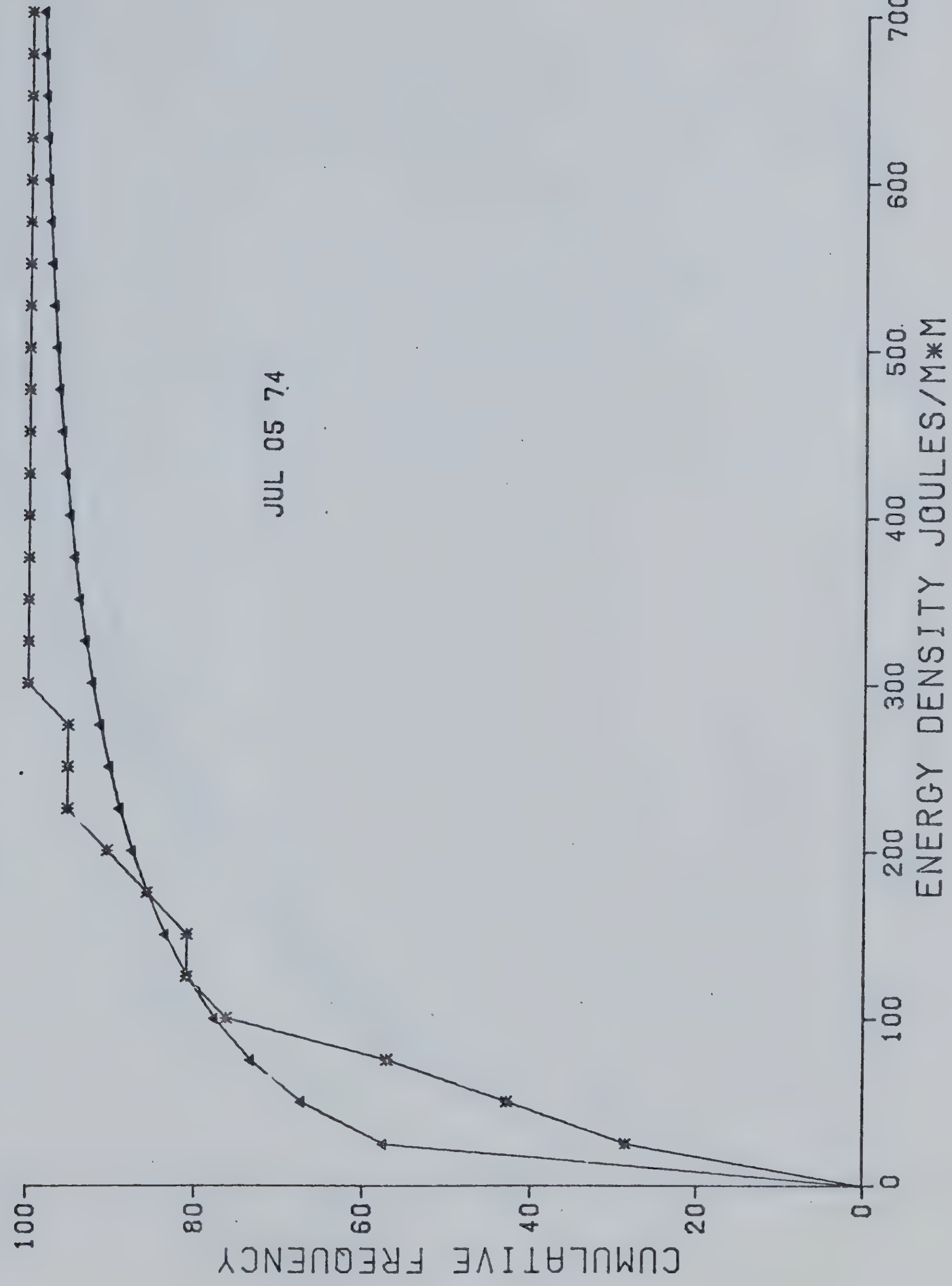

Figure IV.2 The cumulative frequency of impact energy density for 5 July 1974 hailswath

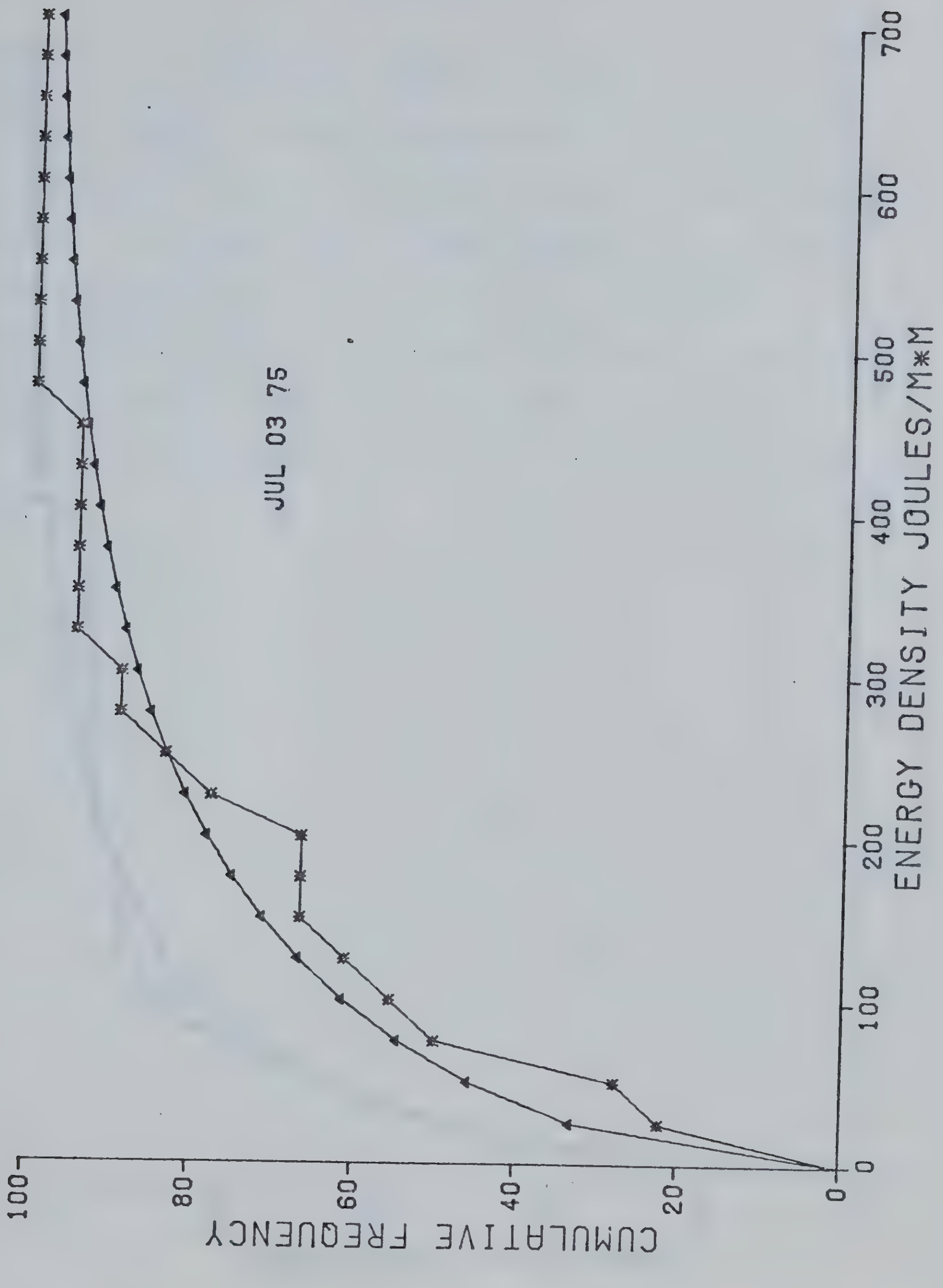

Figure IV.3 The cumulative frequency of impact energy density for 3 July 1975 hailswath

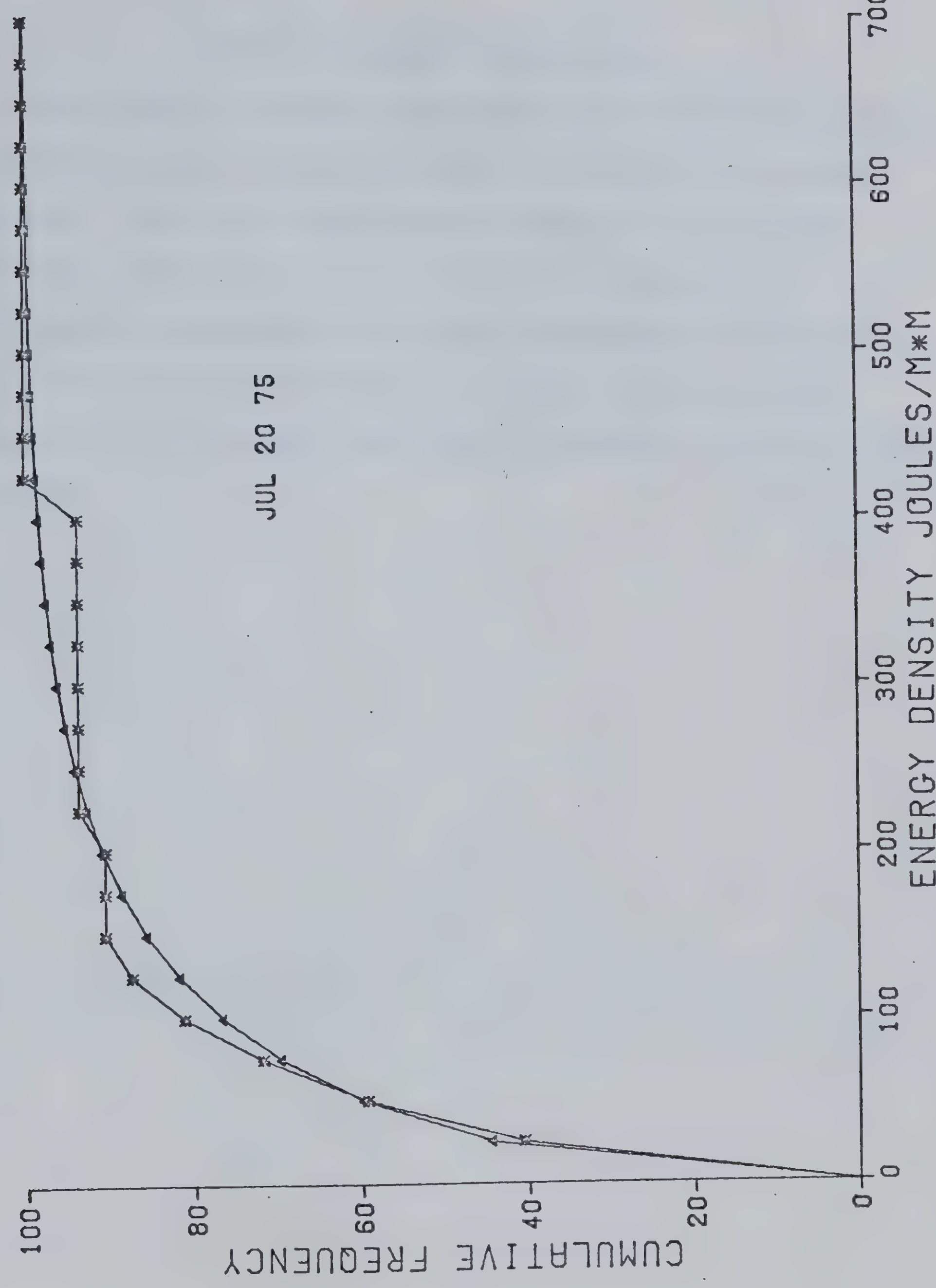

Figure IV.4 The cumulative frequency of impact energy density for 20 July 1975 hailswath

Appendix V

SAMPLING WITHOUT REPLACEMENT

For sampling without replacement, the following figures are given for the four hailswaths: a) Probability density function - here the impact energy density of the sample means are grouped in 5 Jm^{-2} classes; b) Probability distribution function; c) Standard deviation of the sample means as a function of the sample size; and d) Standard deviation of the sample means for the number of hailpads per 1000 km^2.

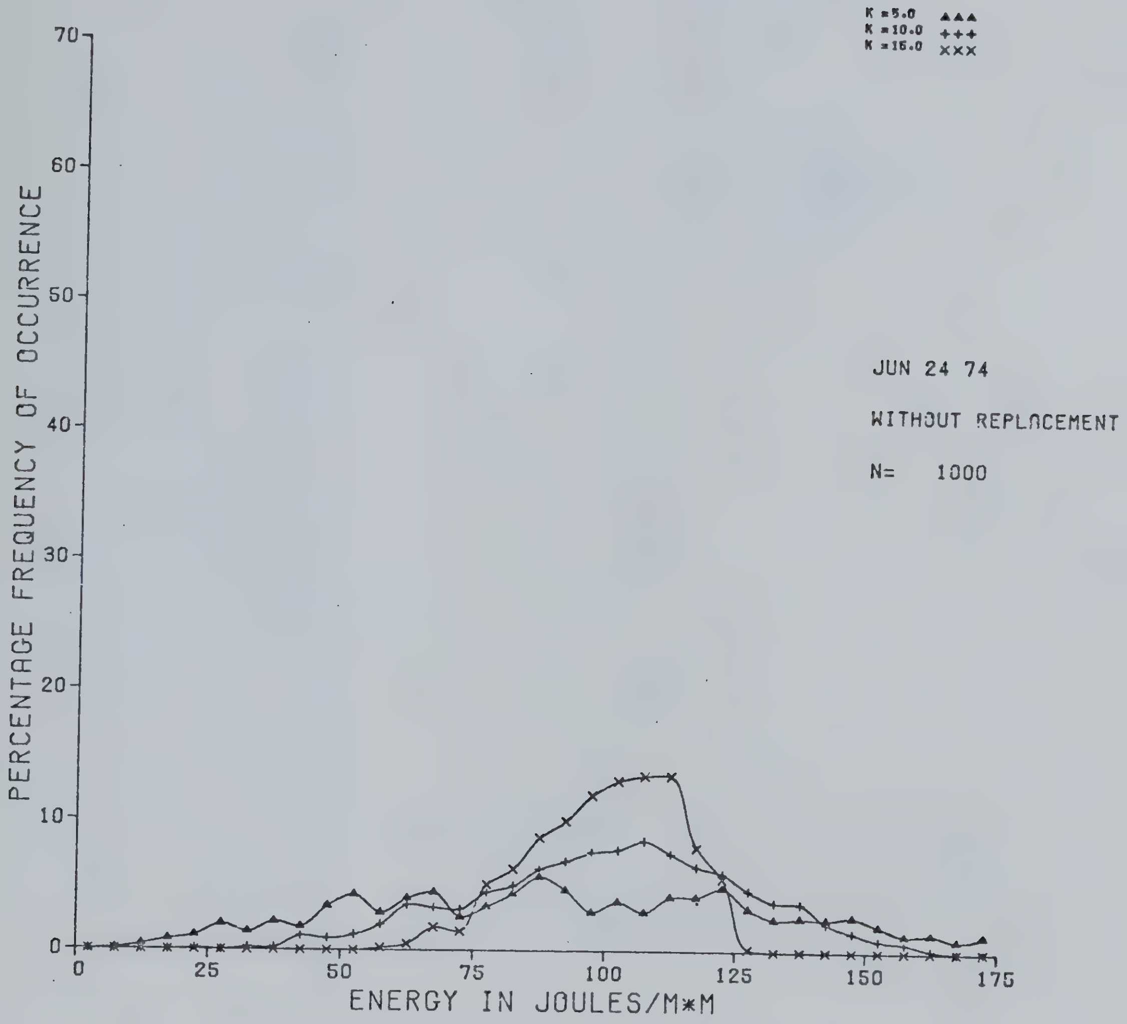

Figure V.1 The probability density function of sample means for 24 June 1974 hailswath

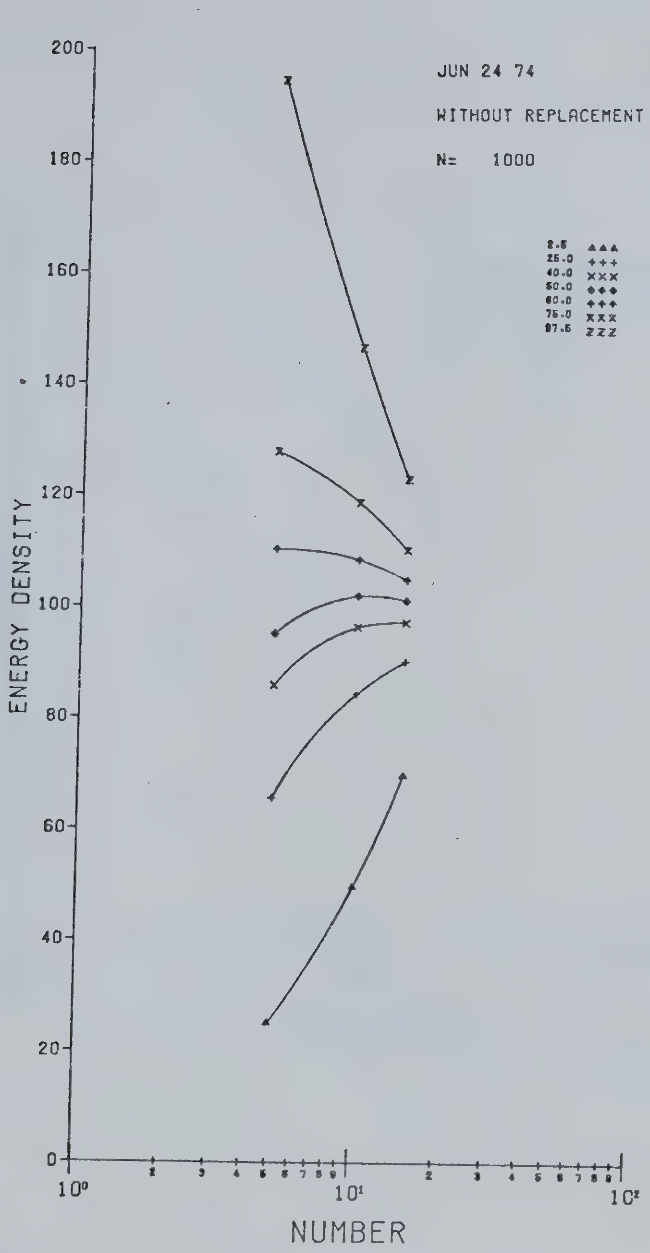

Figure V.2 The probability distribution function for 24 June 1974 hailswath

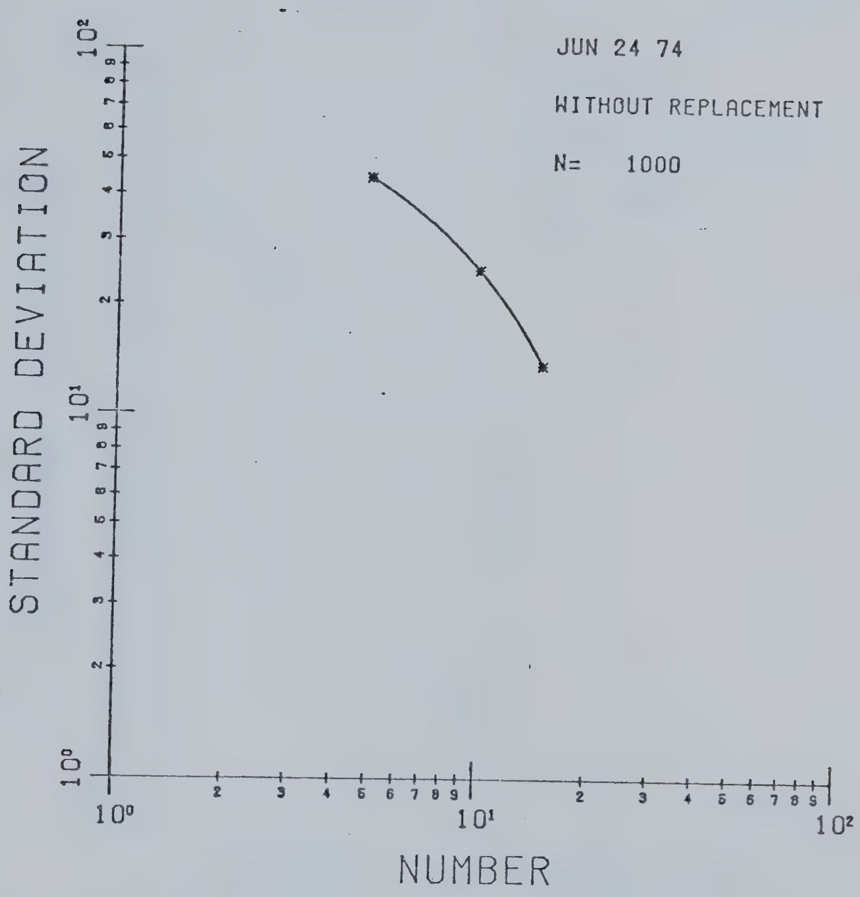

Figure V.3 The standard deviation of the sample means as a function of the sample size for the 24 June 1974 hailswath

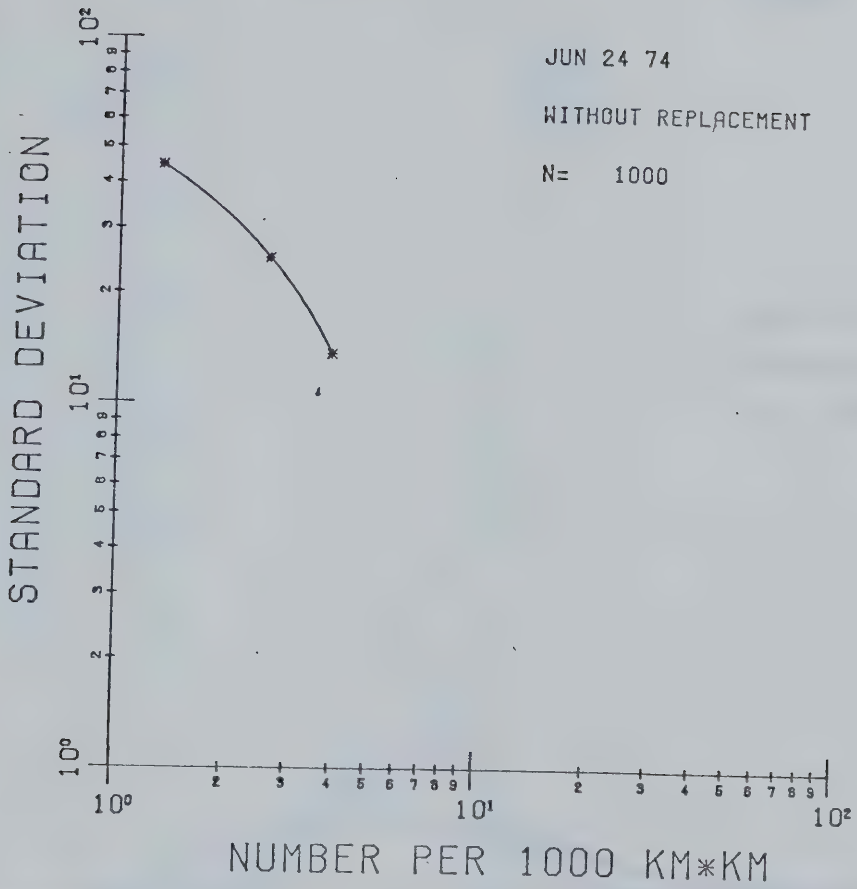

Figure V.4 The standard deviation of the sample means for a sample density in 1000 km² (24 June 1974 hailswath)

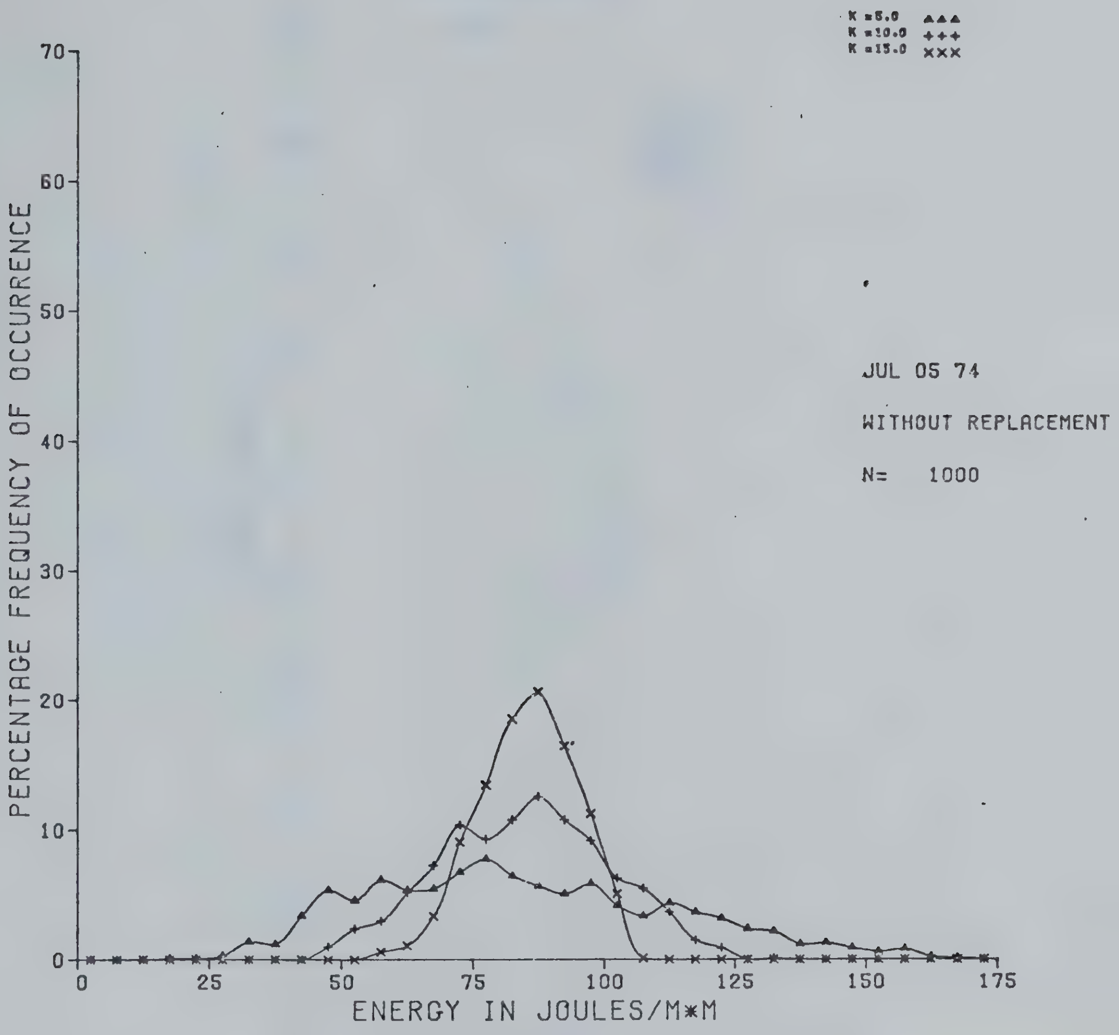

Figure V.5 The probability density function of sample means for 5 July 1974 hailswath

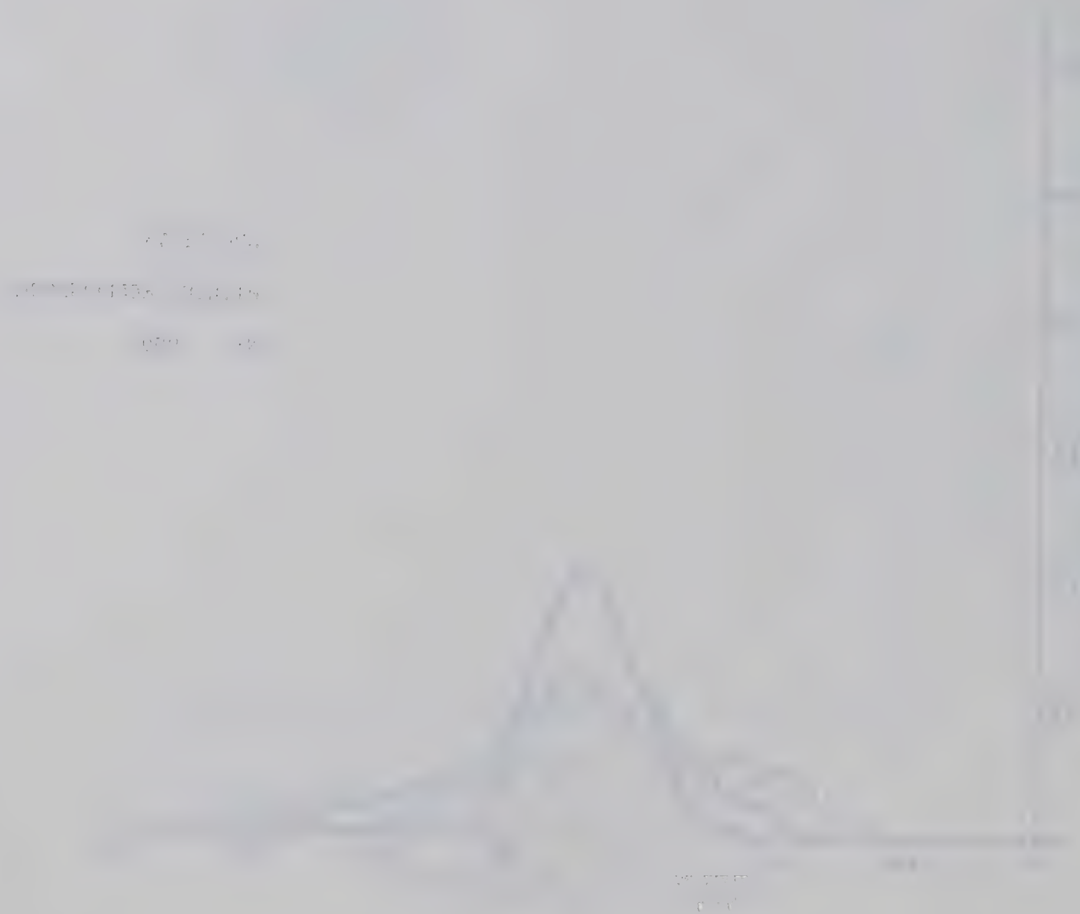

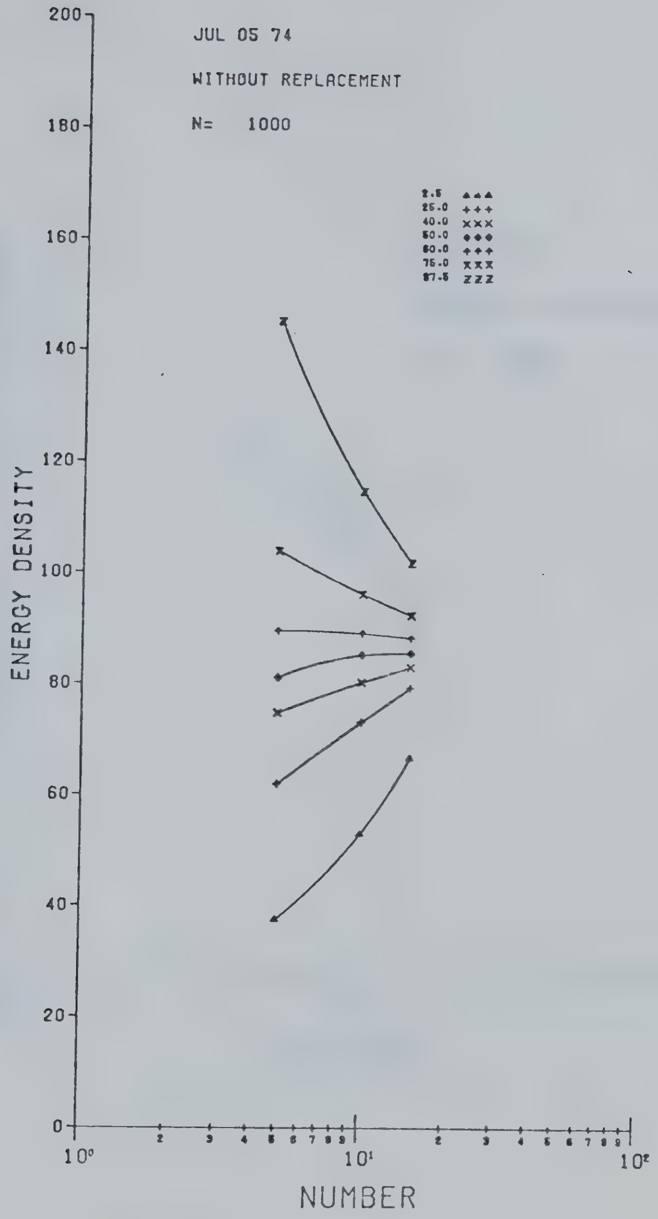

Figure V.6 The probability distribution function for 5 July 1974 hailswath

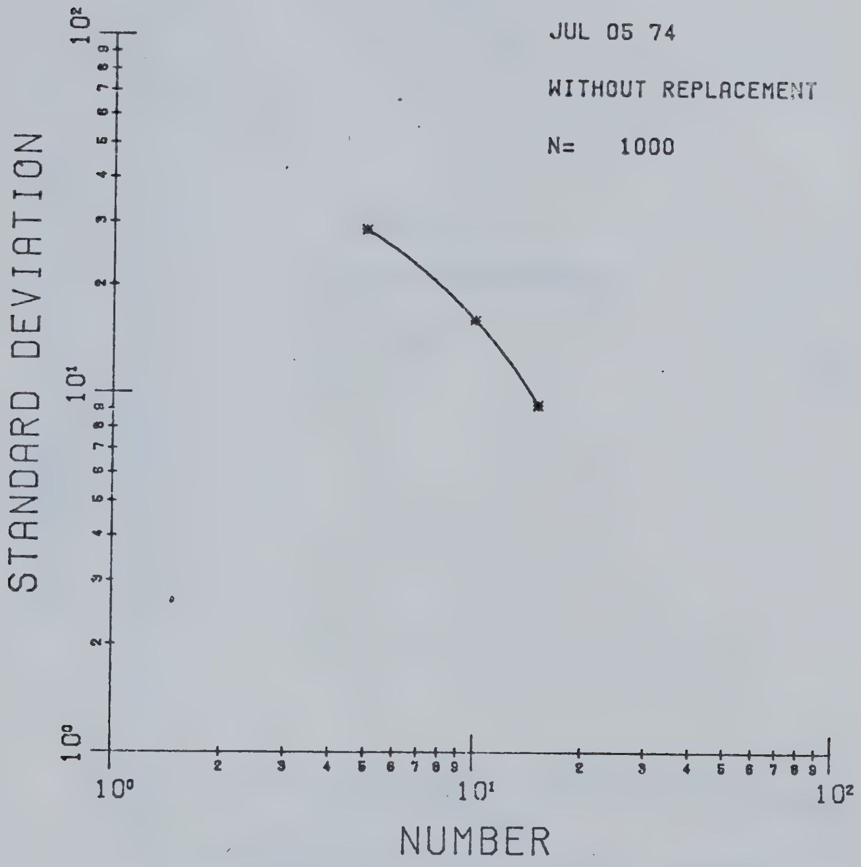

Figure V.7 The standard deviation of the sample means as a function of the sample size for the 5 July 1974 hailswath

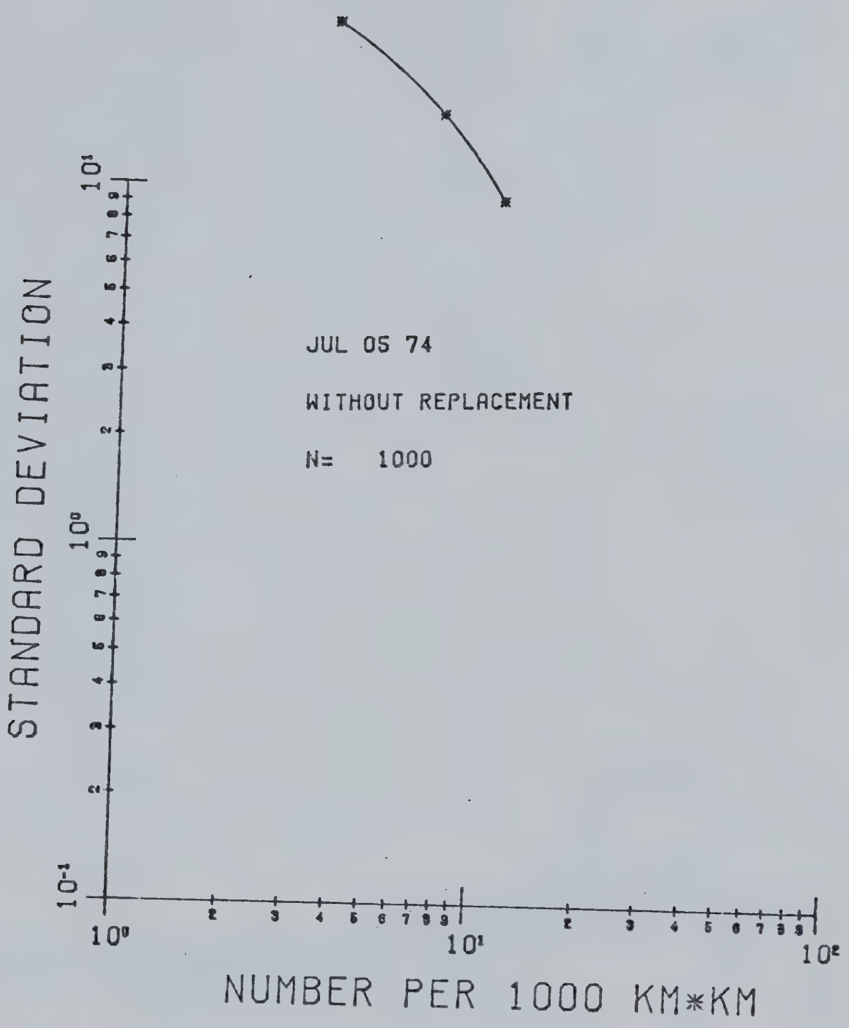

Figure V.8 The standard deviation of the sample means for a sample density in 1000 km² (5 July 1974 hailswath)

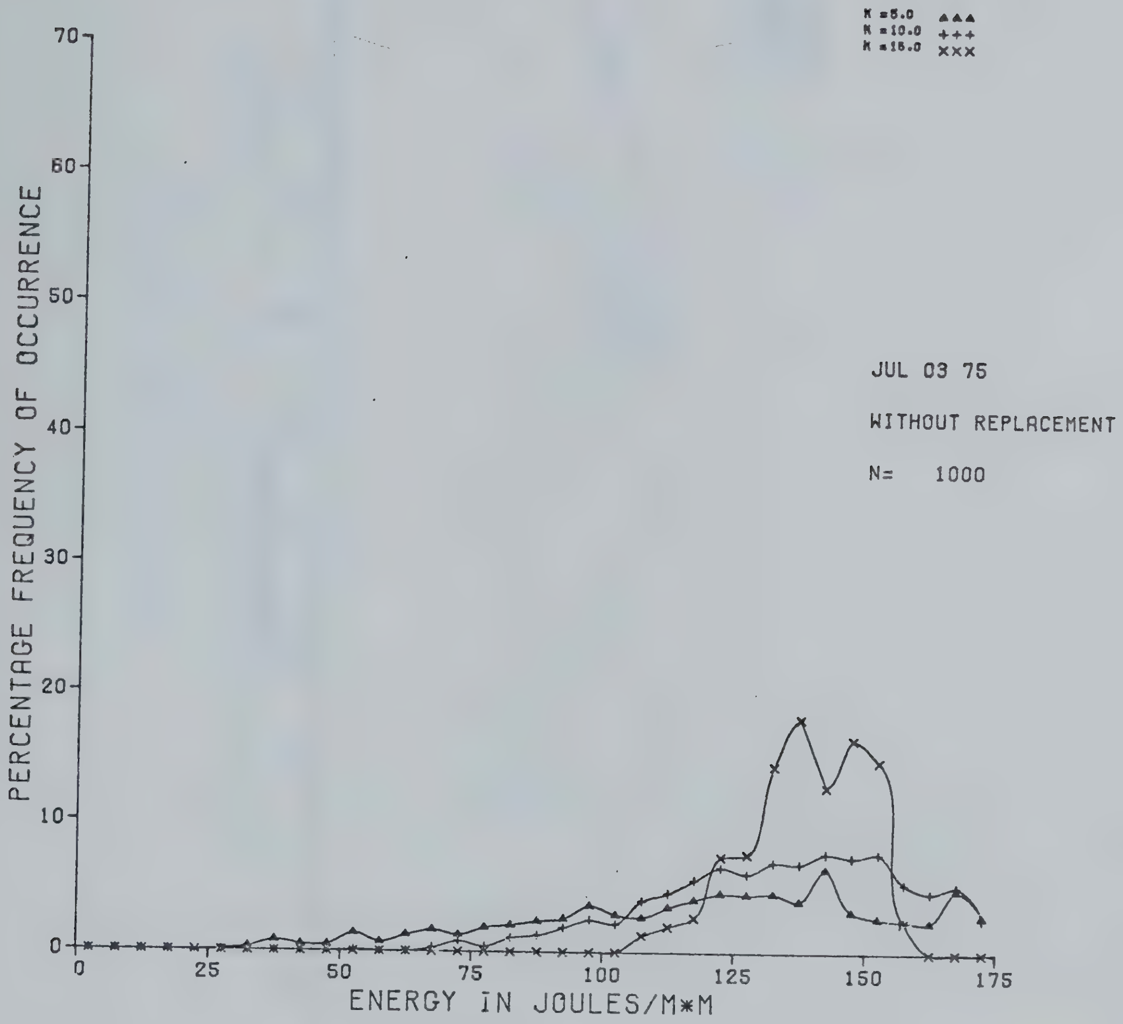

Figure V.9 The probability density function of sample means for 3 July 1975 hailswath

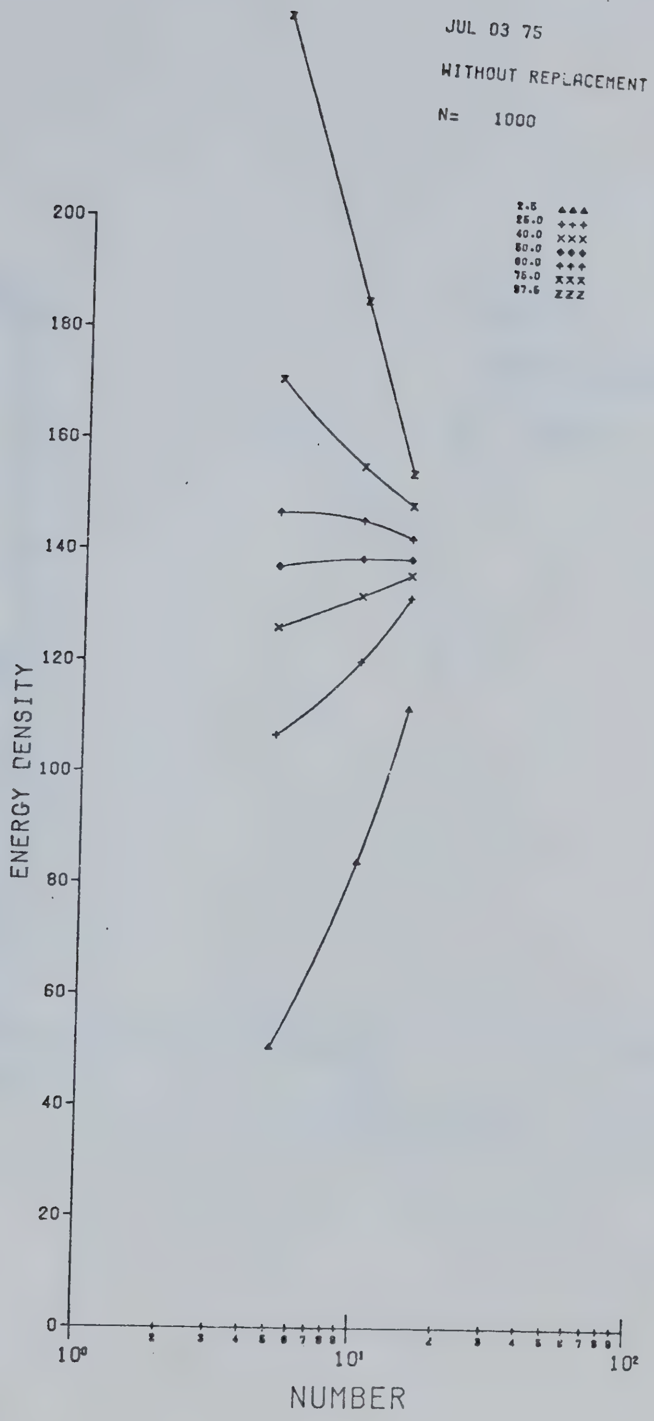

Figure V.10 The probability distribution function for 3 July 1975 hailswath

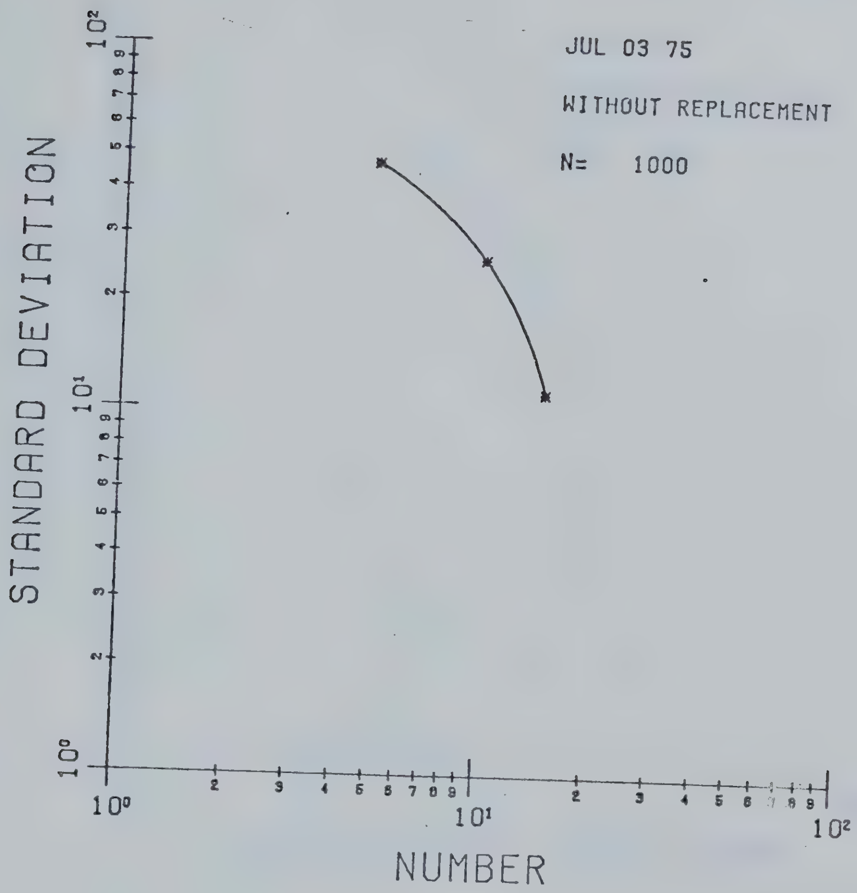

Figure V.11 The standard deviation of the sample means as a function of the sample size for the 3 July 1975 hailswath

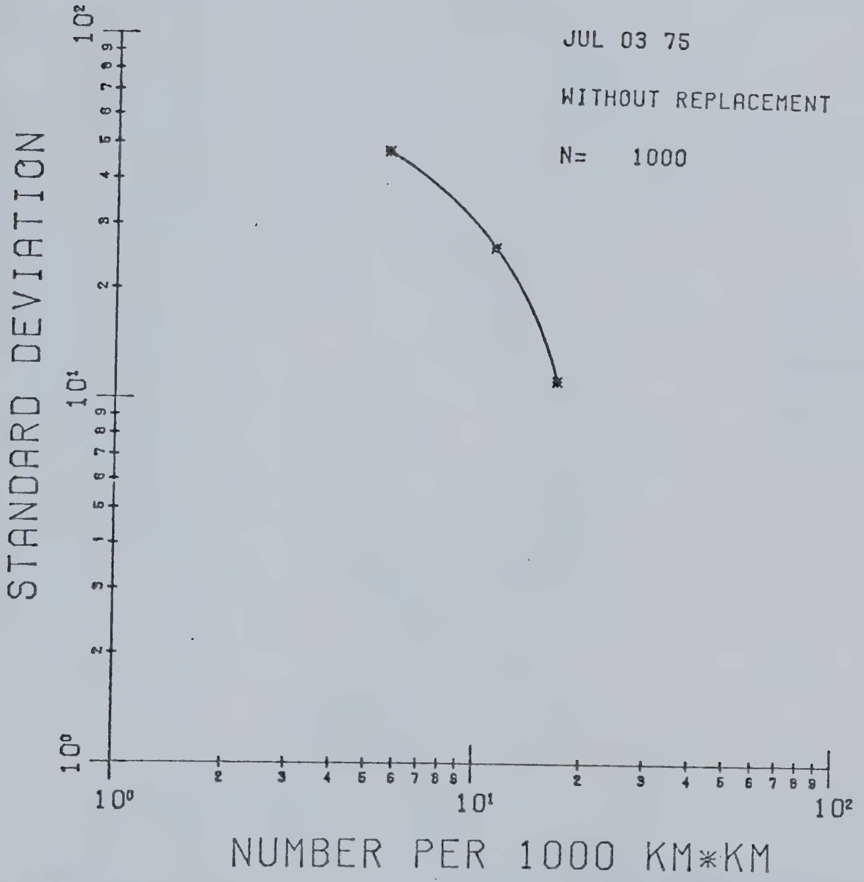

Figure V.12 The standard deviation of the sample means for a sample density in 1000 km² (3 July 1975 hailswath)

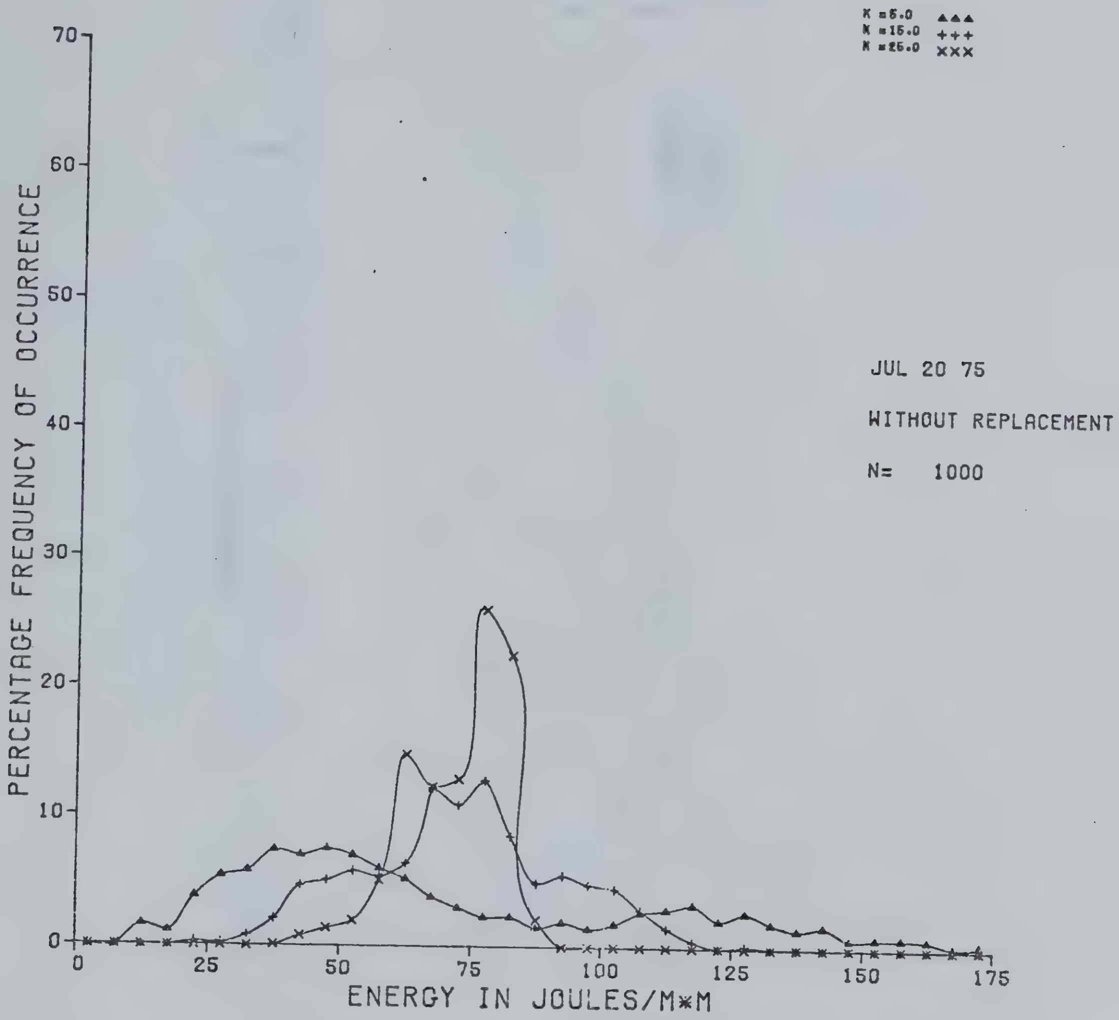

Figure V.13 The probability density function of sample means for 20 July 1975 hailswath

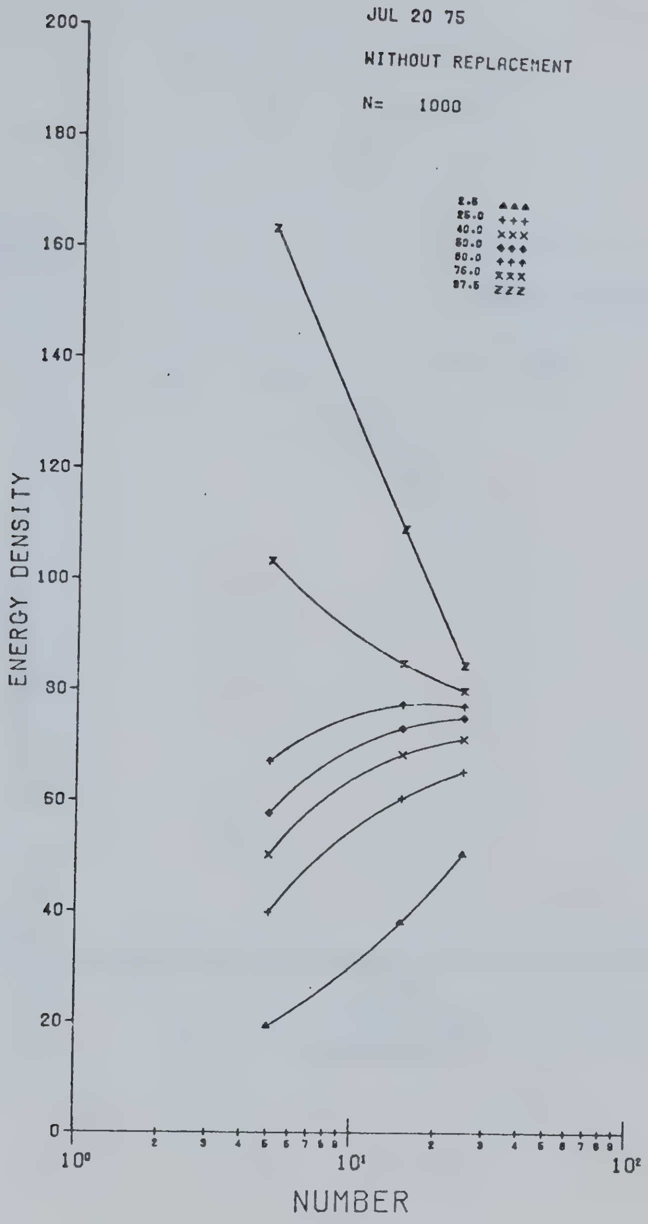

Figure V.14 The probability distribution function for 20 July 1975 hailswath

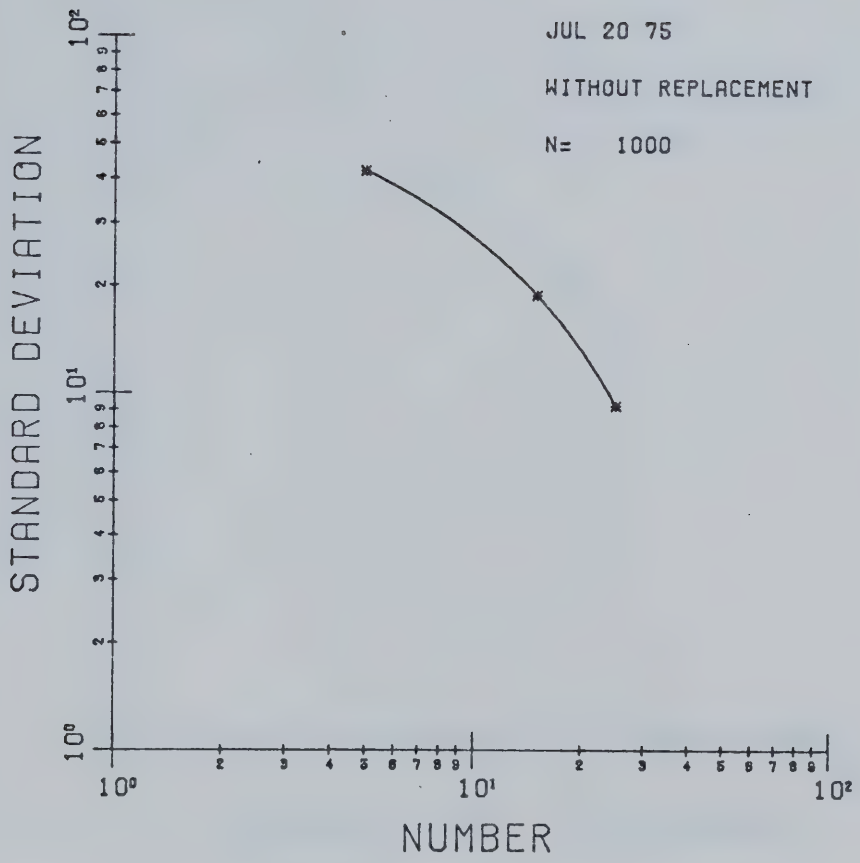

Figure V.15 The standard deviation of the sample means as a function of the sample size (20 July 1975 hailswath)

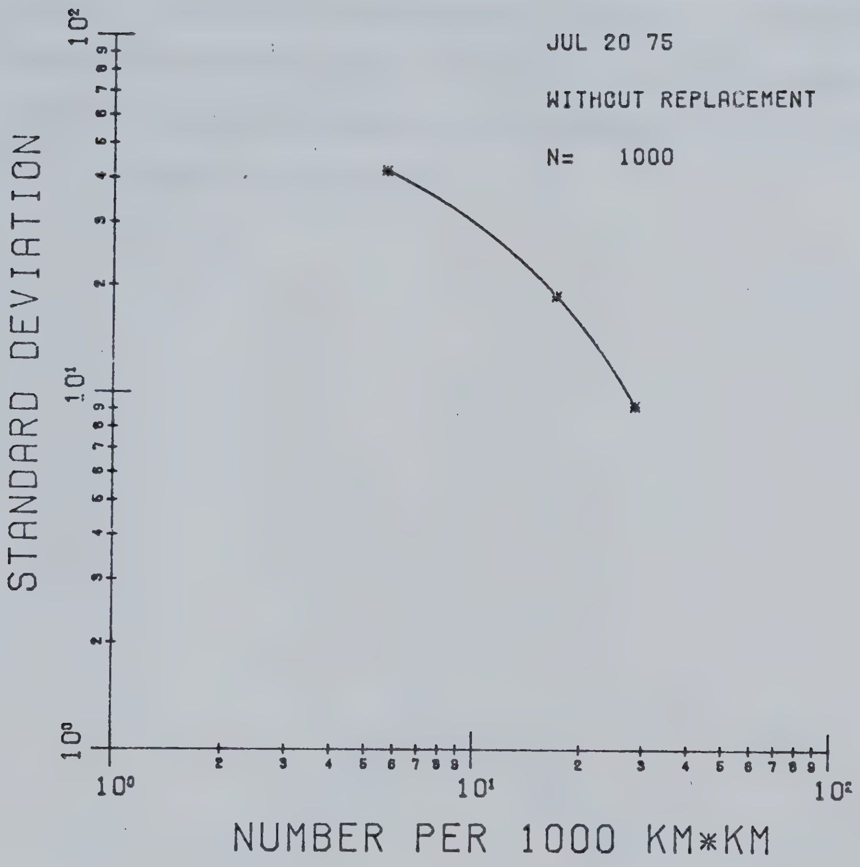

Figure V.16 The standard deviation of the sample means for a sample density in 1000 km² (20 July 1975 hailswath)

Appendix VI

SAMPLING WITH REPLACEMENT

For sampling with replacement, the following figures are given for the four hailswaths: a) Probability density function; b) Probability distribution function; c) Standard deviation of the sample means as a function of the sample size; and d) Standard deviation of the sample means for the number of hailpads per 1000 km^2.

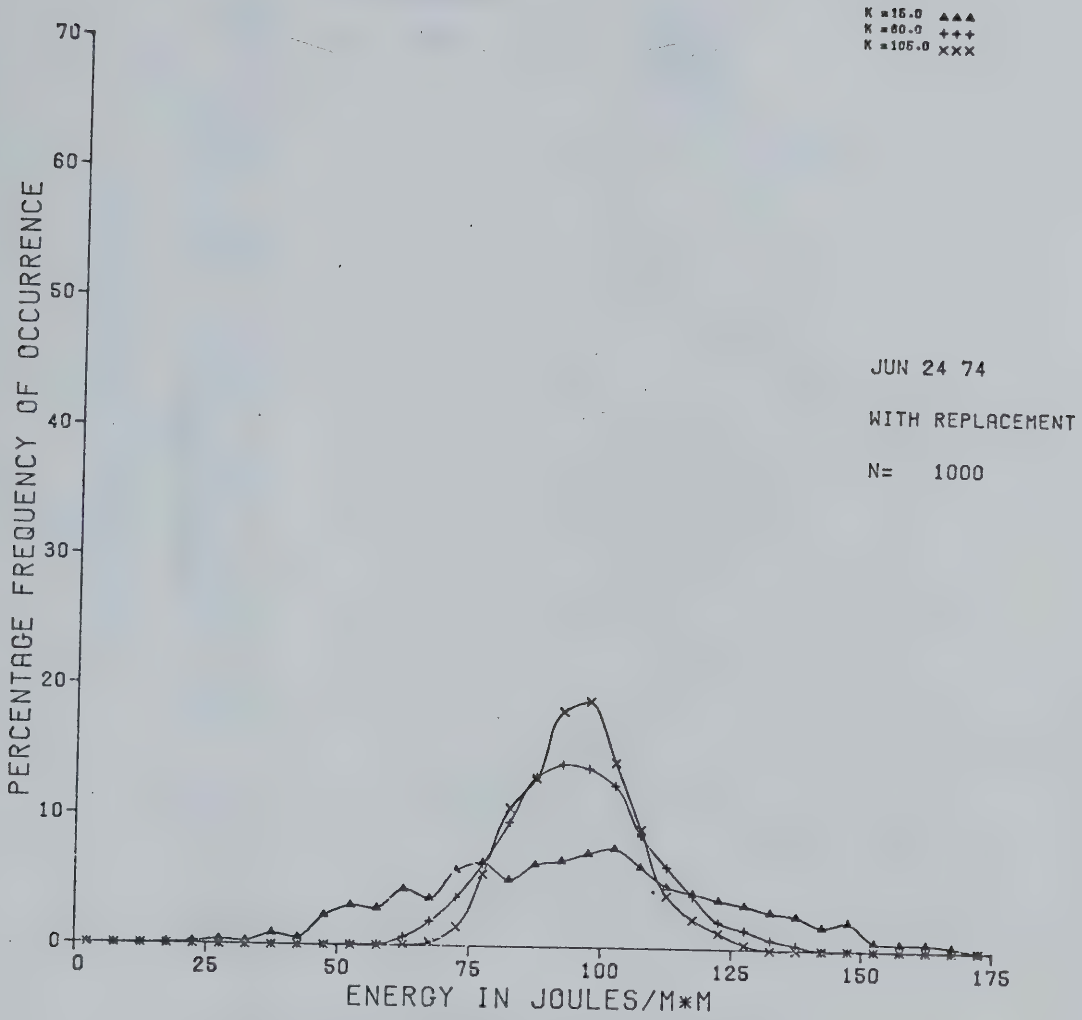

Figure VI.1 The probability density function of sample means for 24 June 1974 hailswath

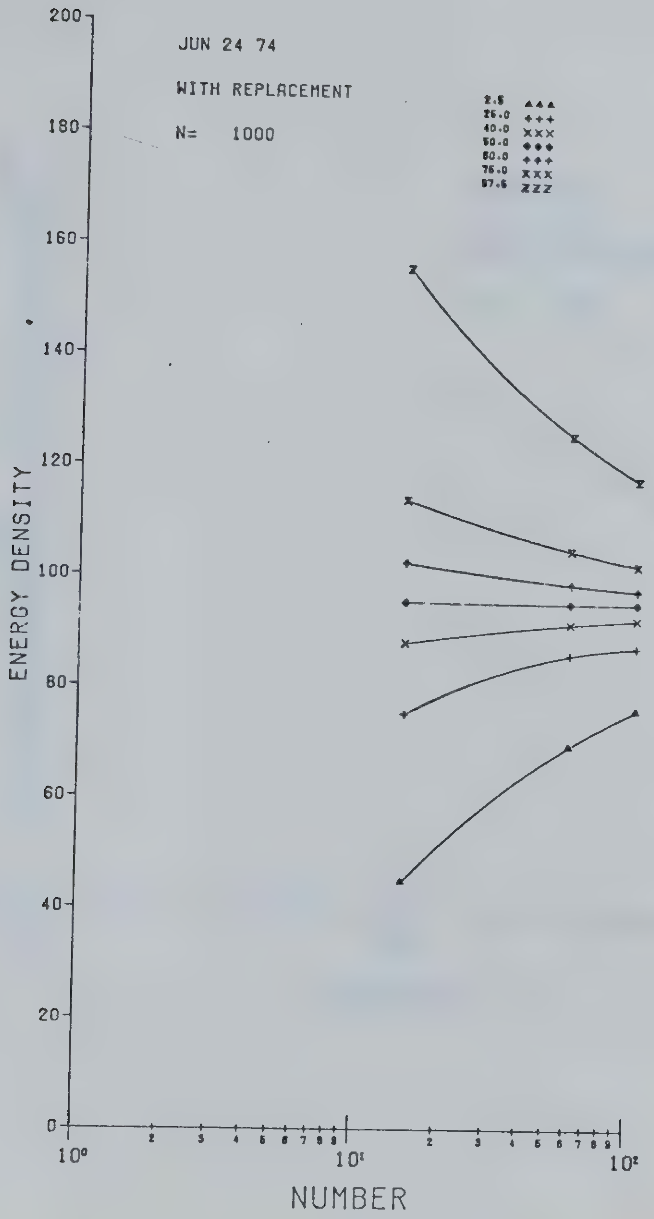

Figure VI.2 The probability distribution function for 24 June 1974 hailswath

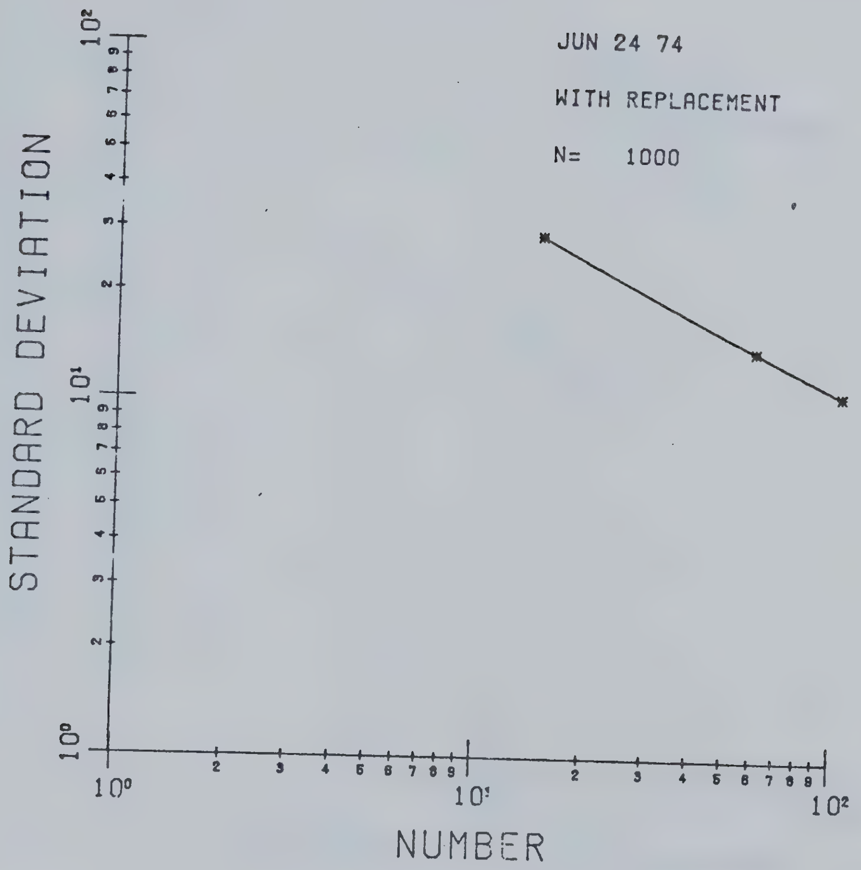

Figure VI.3 The standard deviation of the sample means as a function of the sample size (24 June 1974 hailswath)

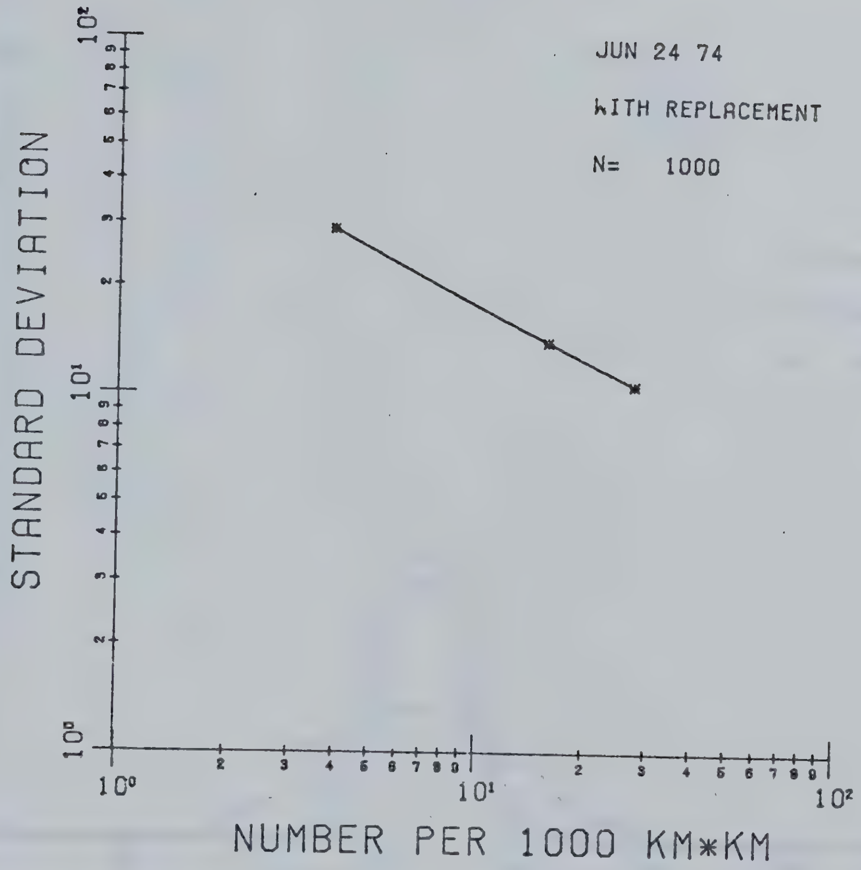

Figure VI.4 The standard deviation of the sample means for a sample density in 1000 km² (24 June 1974 hailswath)

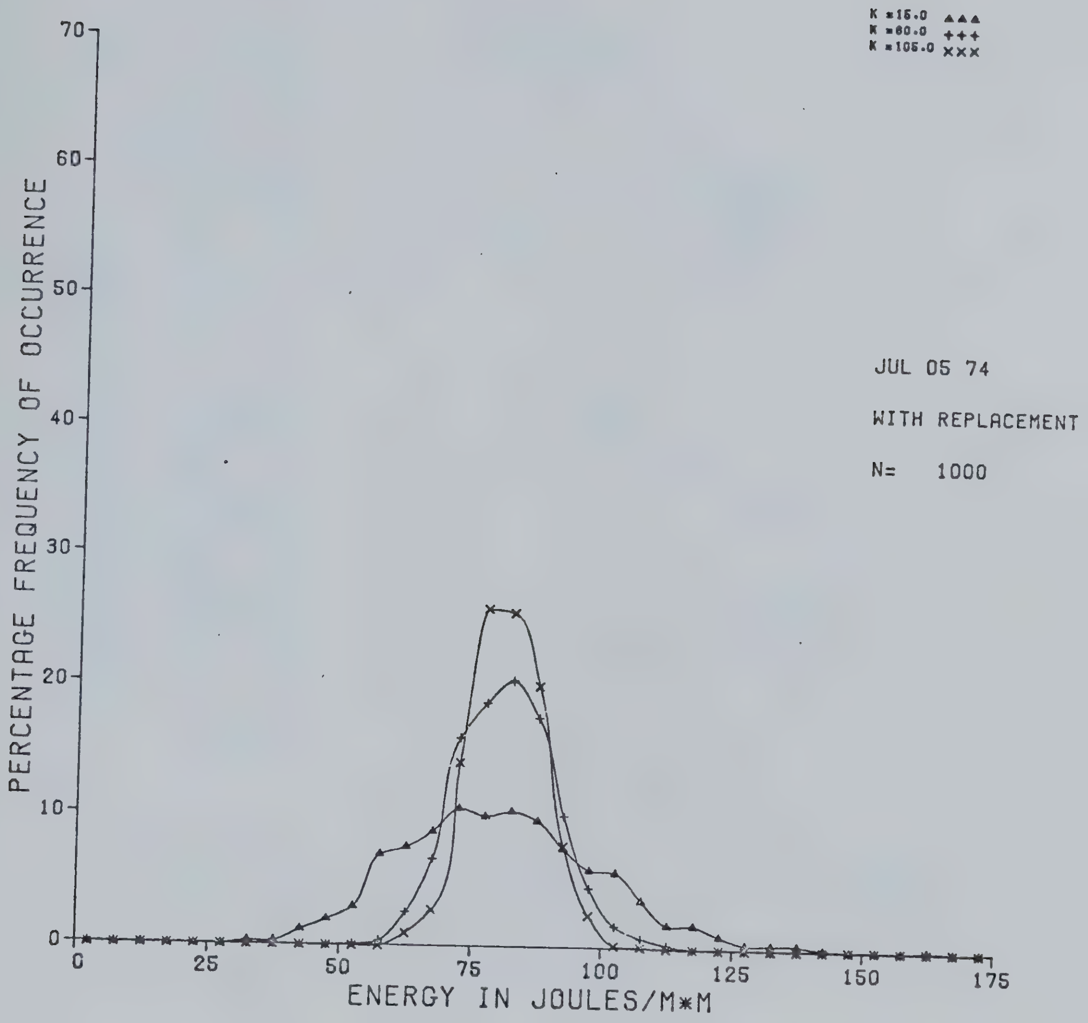

Figure VI.5 The probability density function of sample means for 5 July 1974 hailswath

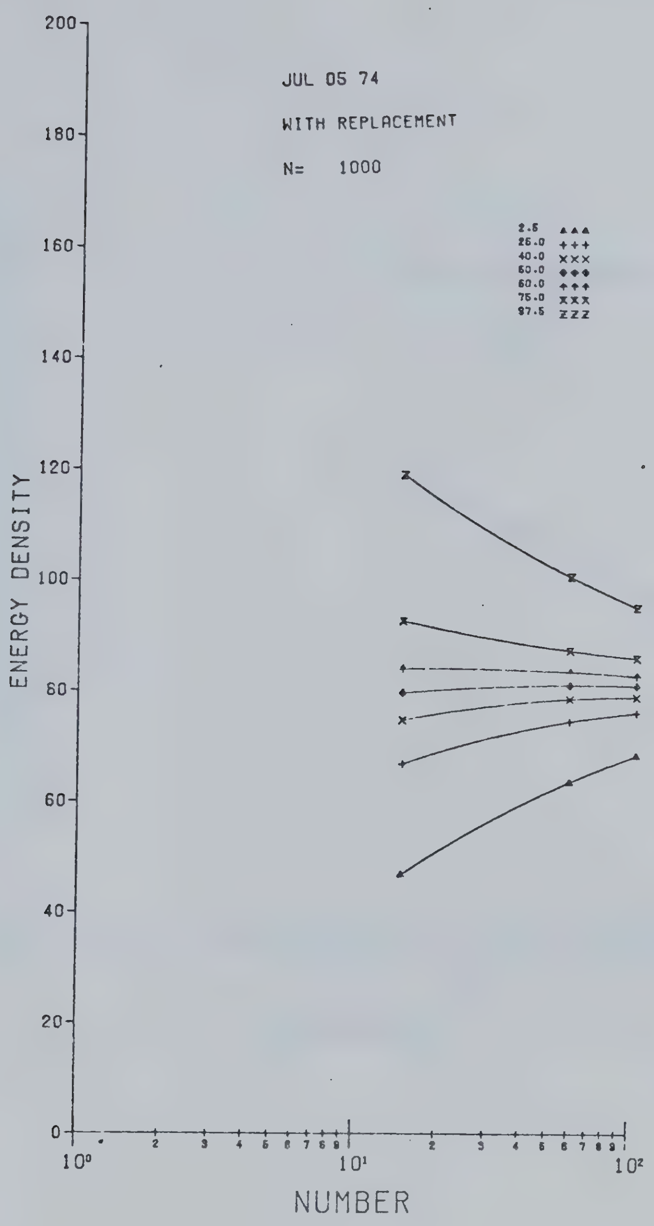

Figure VI.6 The probability distribution function for 5 July 1974 hailswath

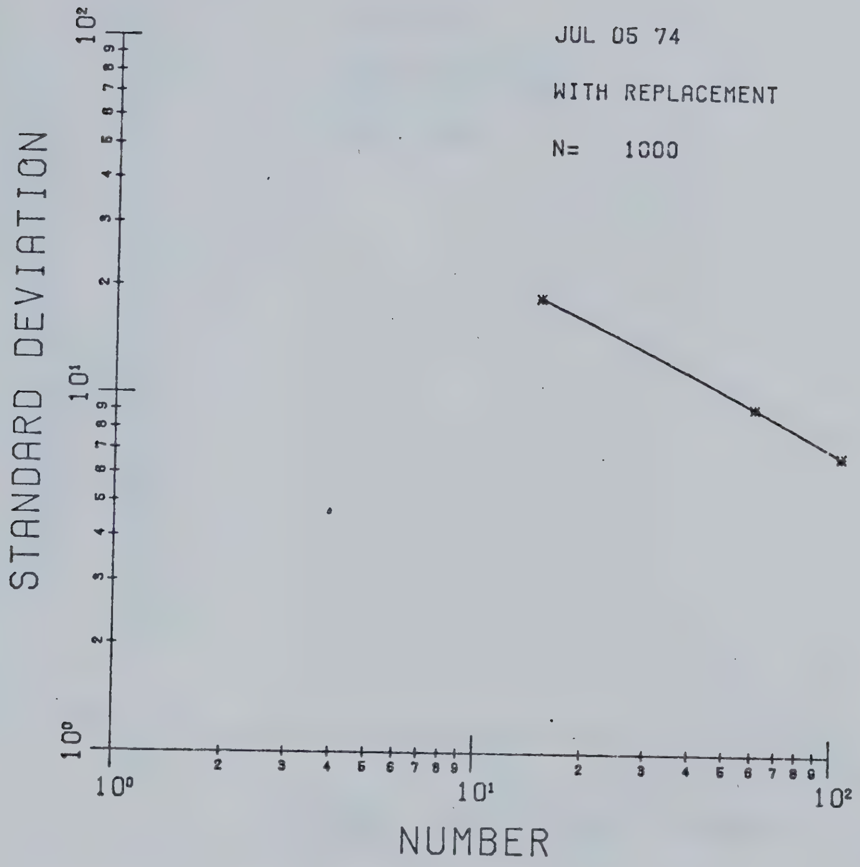

Figure VI.7 The standard deviation of the sample means as a function of the sample size (5 July 1974 hailswath)

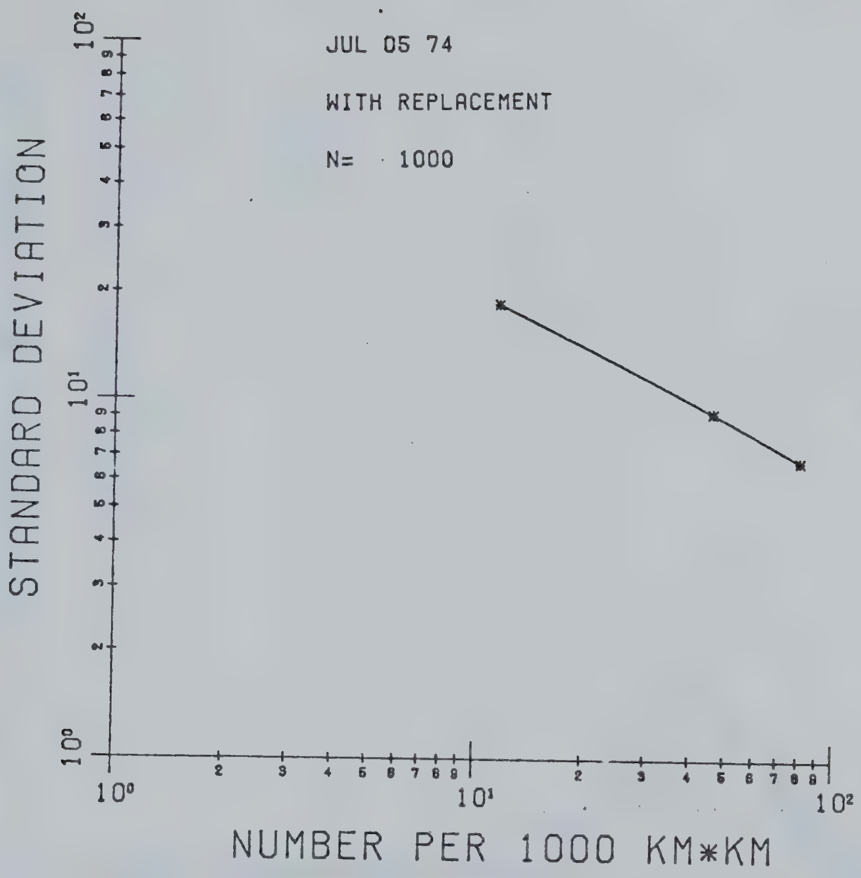

Figure VI.8 The standard deviation of the sample means for a sample density in 1000 km² (5 July 1974 hailswath)

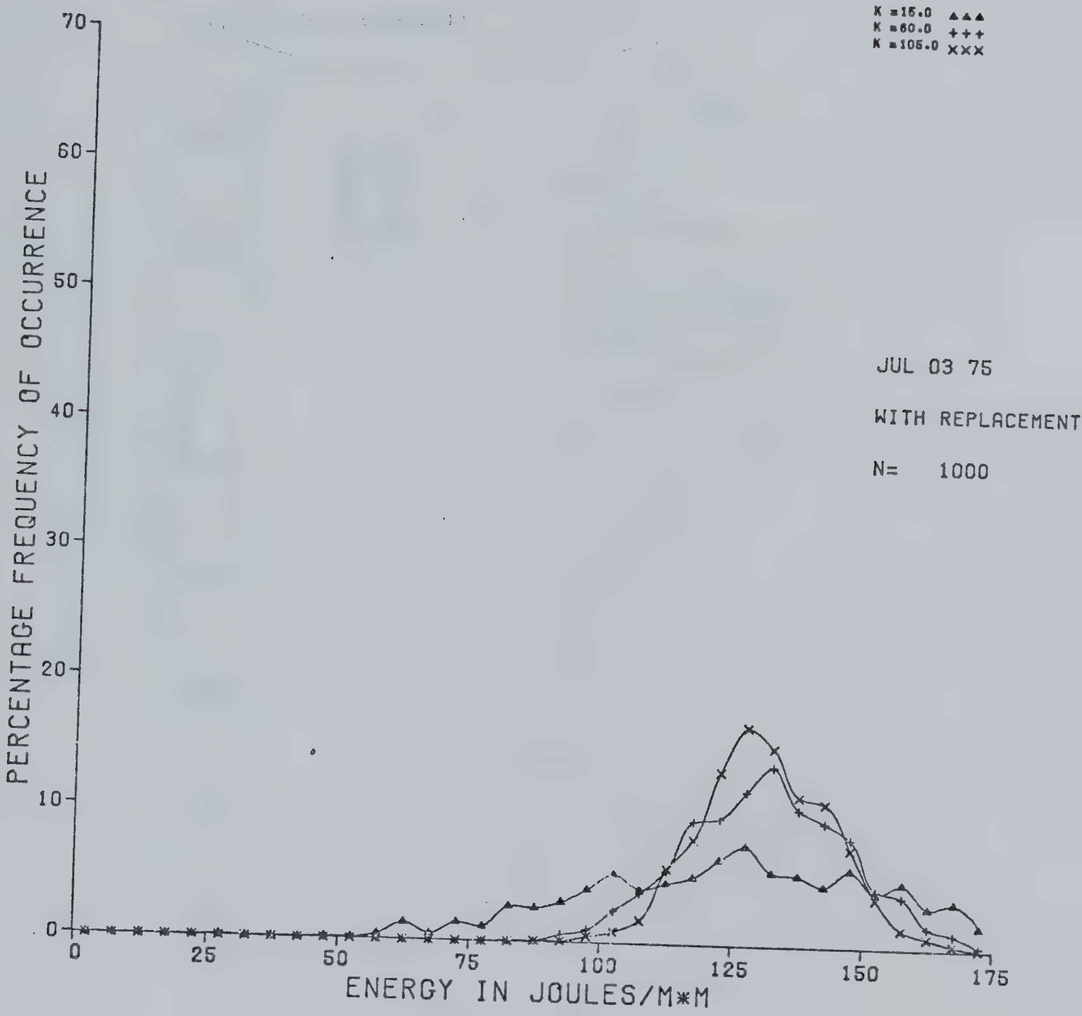

Figure VI.9 The probability density function of sample means for 3 July 1975 hailswath

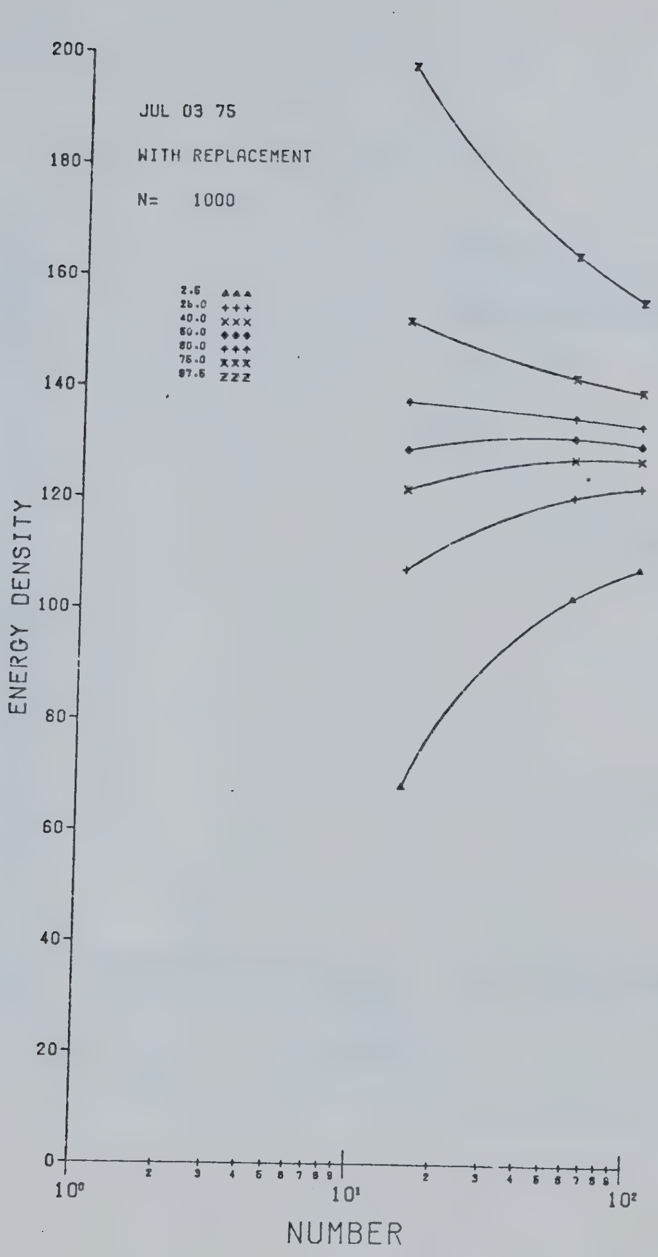

Figure VI.10 The probability distribution function for 3 July 1975 hailswath

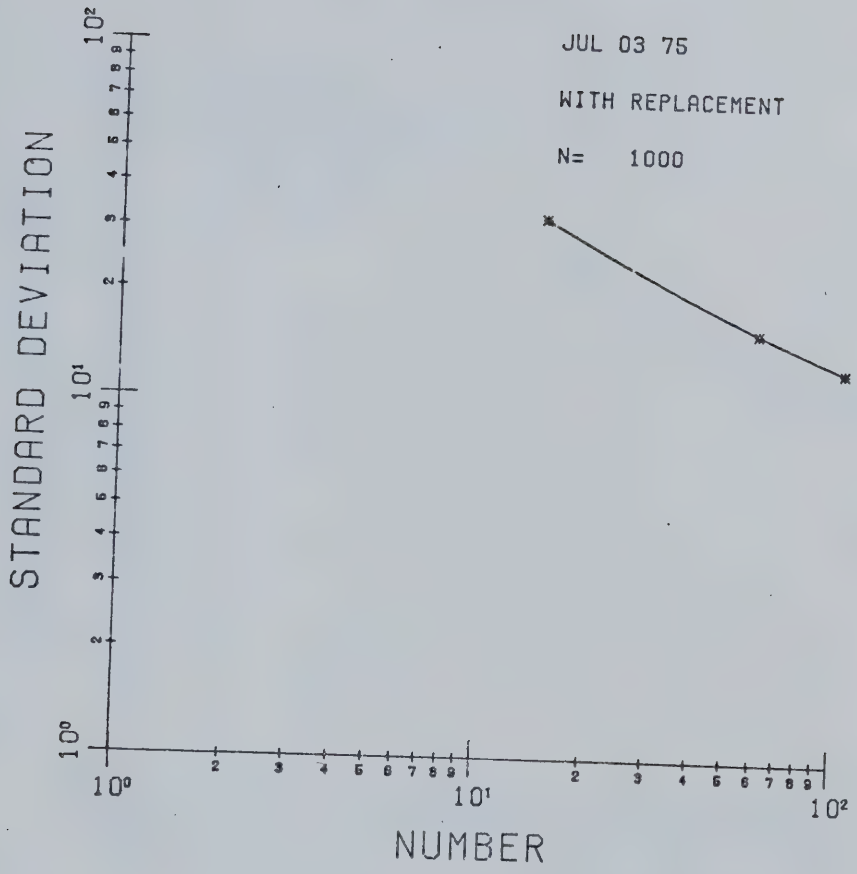

Figure VI.11 The standard deviation of the sample means as a function of the sample size (3 July 1975 hailswath)

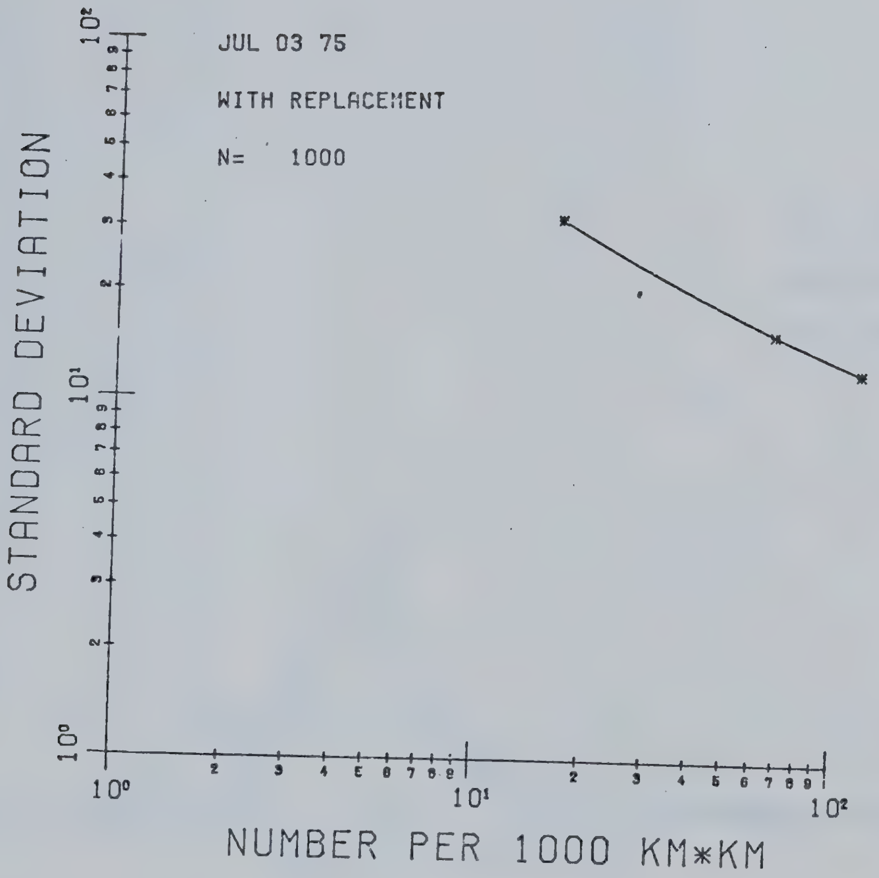

Figure VI.12 The standard deviation of the sample means for a sample density in 1000 km² (3 July 1975 hailswath)

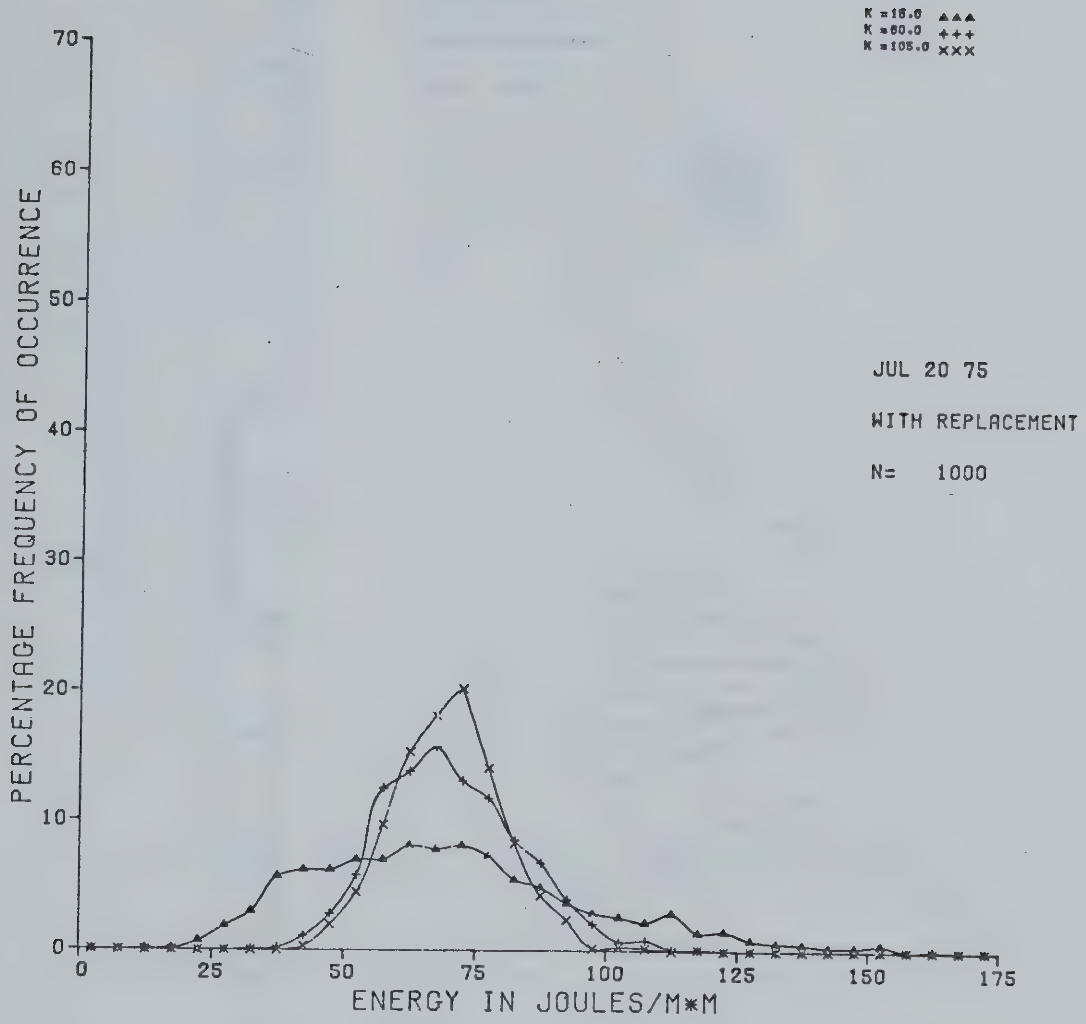

Figure VI.13 The probability density function of sample means for 20 July 1975 hailswath

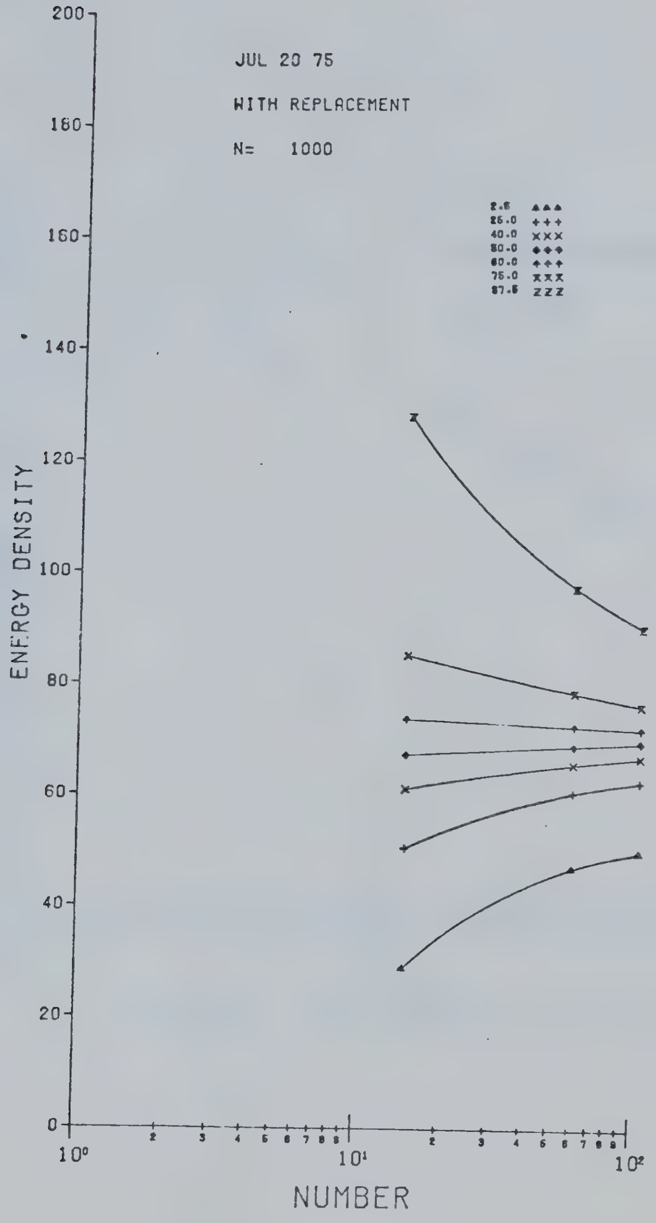

Figure VI.14 The probability distribution function for 20 July 1975 hailswath

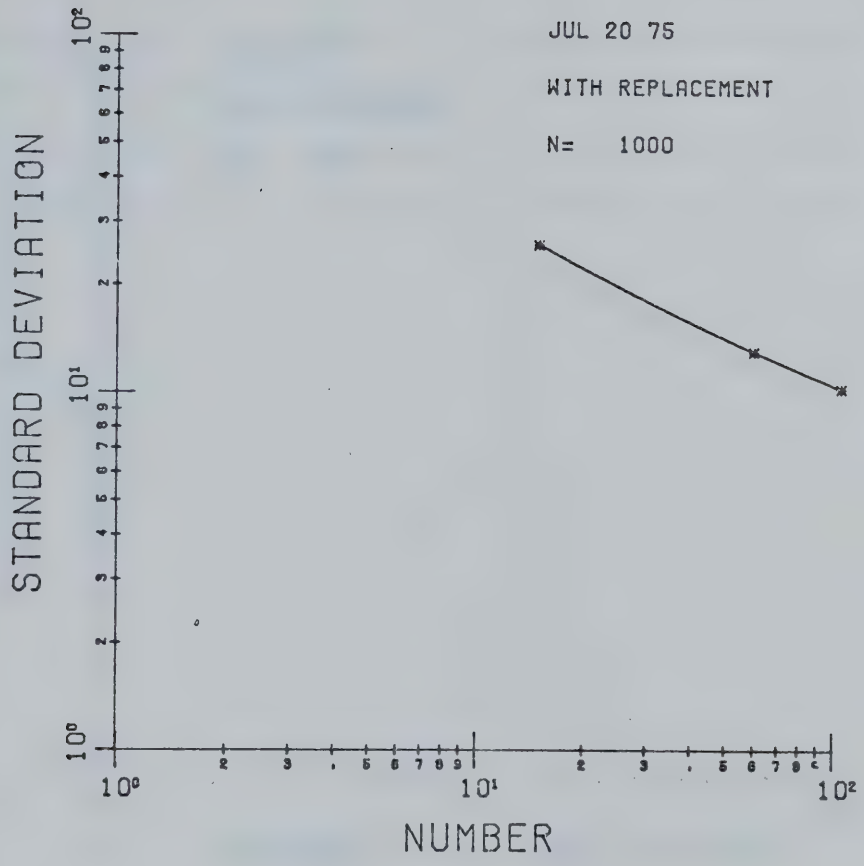

Figure VI.15 The standard deviation of the sample means as a function of the sample size (20 July 1975 hailswath)

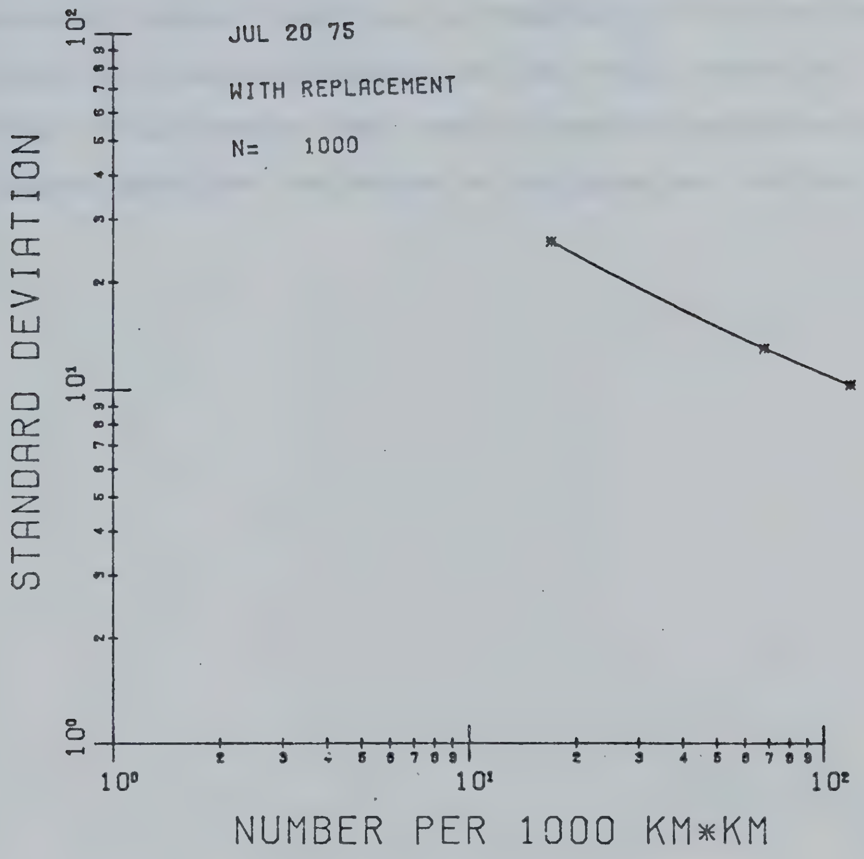

Figure VI.16 The standard deviation of the sample means for a sample density in 1000 km² (20 July 1975 hailswath)

Appendix VII

SAMPLING FROM A FITTED DISTRIBUTION

For sampling for a fitted two-parameter gamma, the following figures are given for the four hailswaths: a) Probability density function; b) Probability distribution function; c) Standard deviation of the sample means as a function of the sample size; and d) Standard deviation of the sample means for the number of hailpads per 1000 km^2.

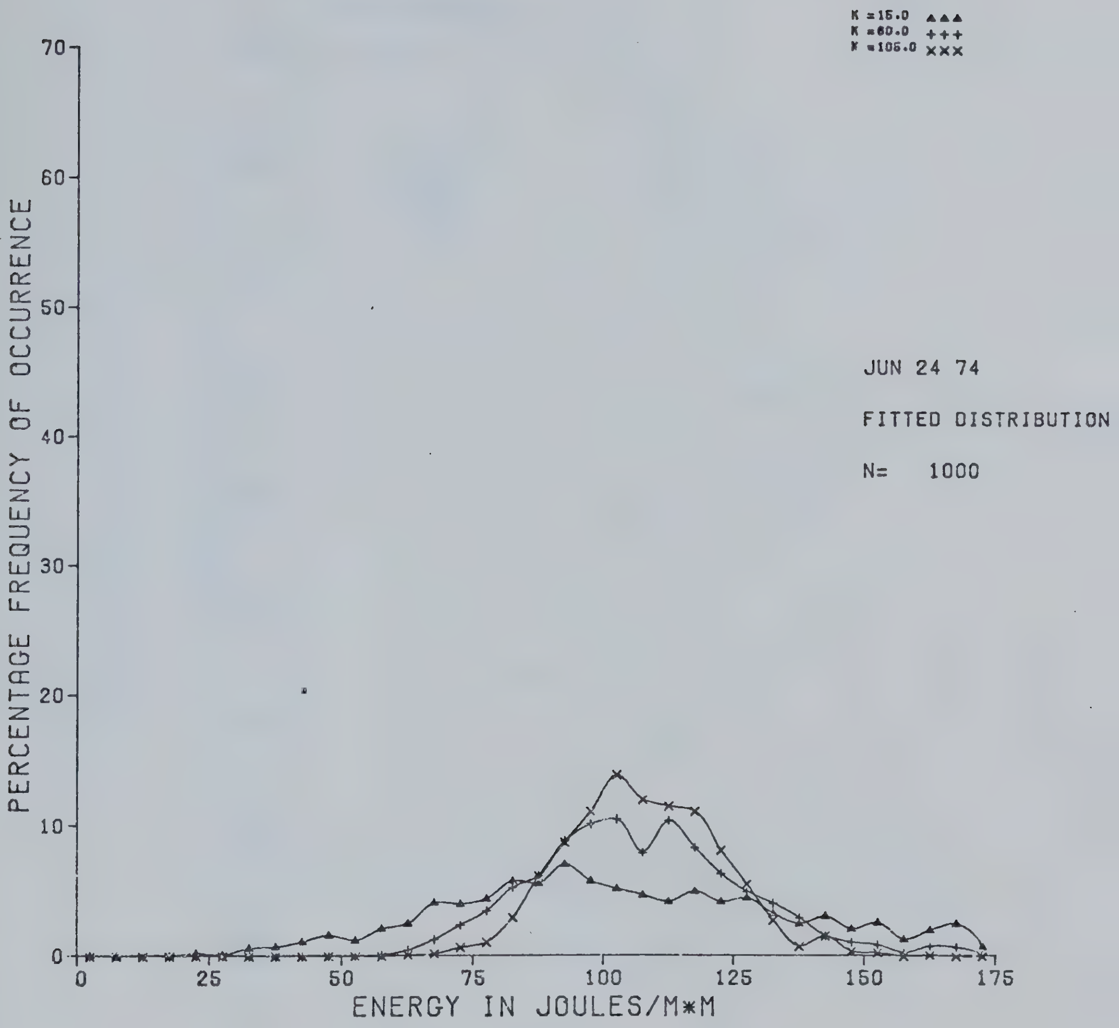

Figure VII.1 The probability density function of sample means for 24 June 1974 hailswath

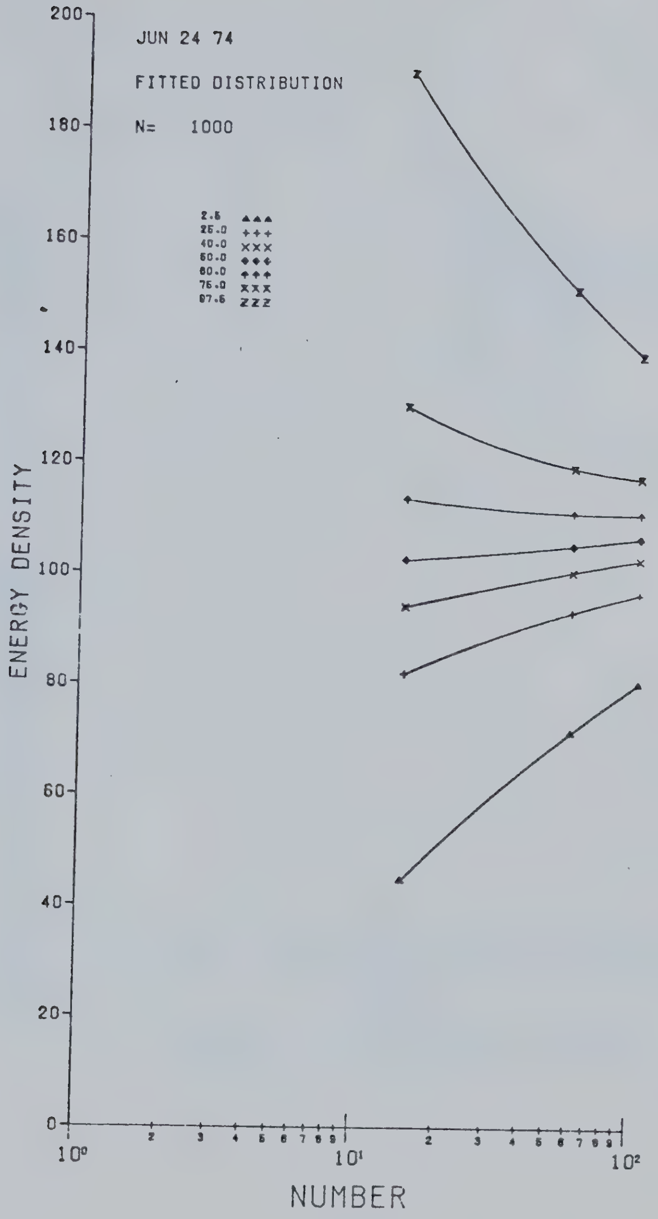

Figure VII.2 The probability distribution function for 24 June 1974 hailswath

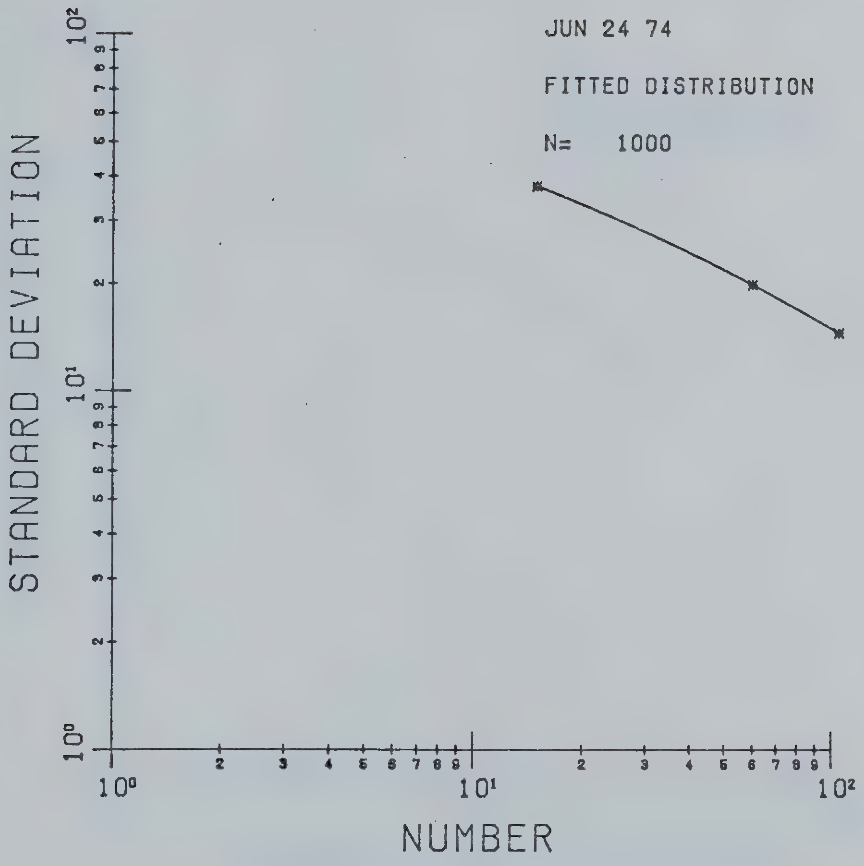

Figure VII.3 The standard deviation of the sample means as a function of the sample size (24 June 1974 hailswath)

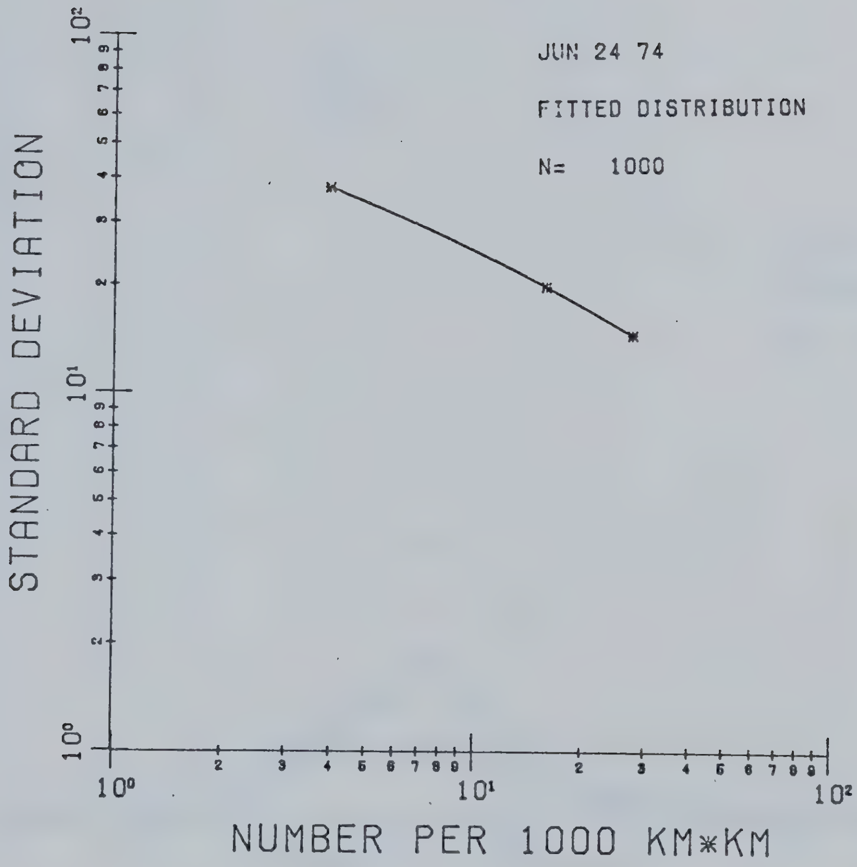

Figure VII.4 The standard deviation of the sample means for a sample density in 1000 km² (24 June 1974 hailswath)

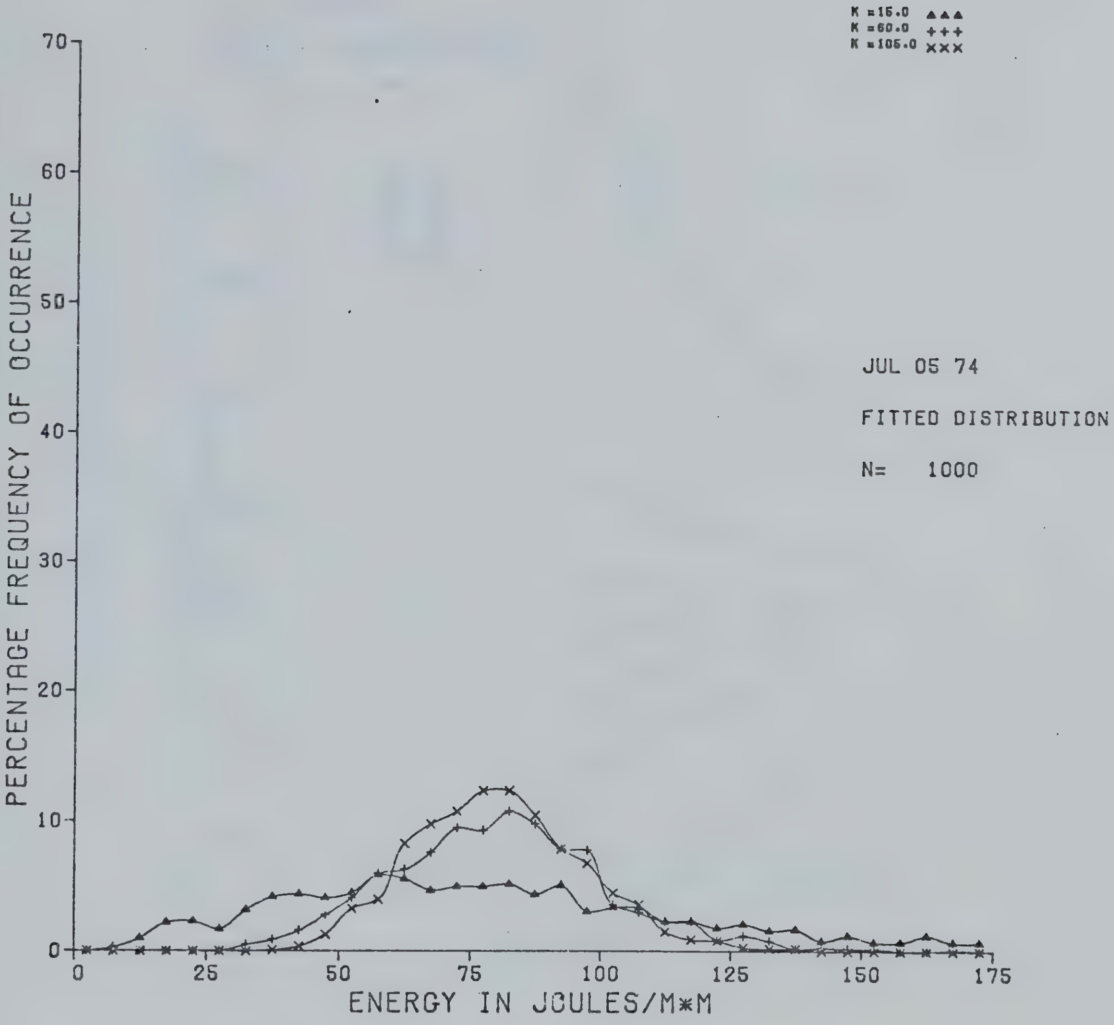

Figure VII.5 The probability density function of sample means for 5 July 1974 hailswath (Impact energy density values are grouped in 5 J m^{-2} classes)

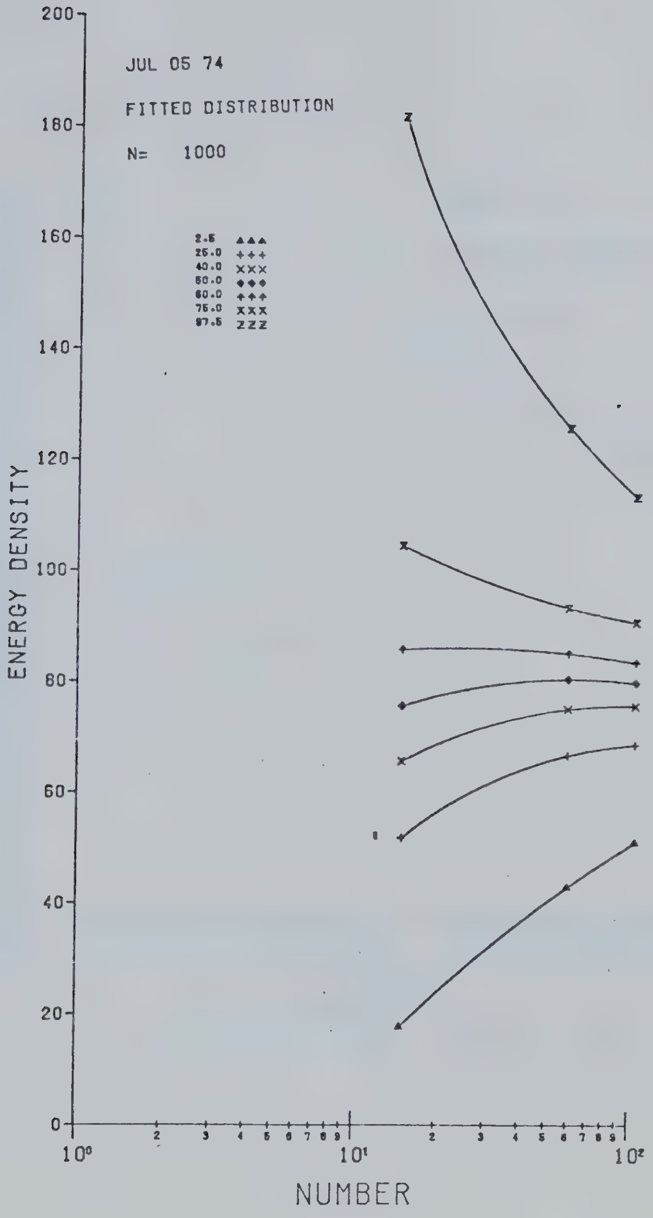

Figure VII.6 The probability distribution function for 5 July 1974 hailswath

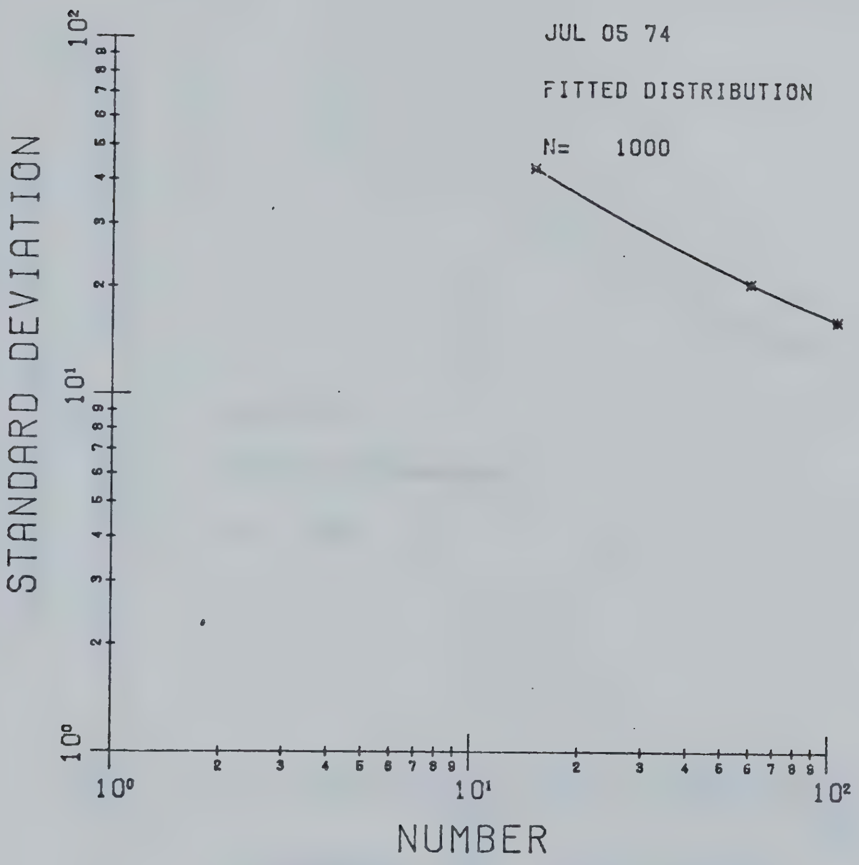

Figure VII.7 The standard deviation of the sample means as a function of the sample size (5 July 1974 hailswath)

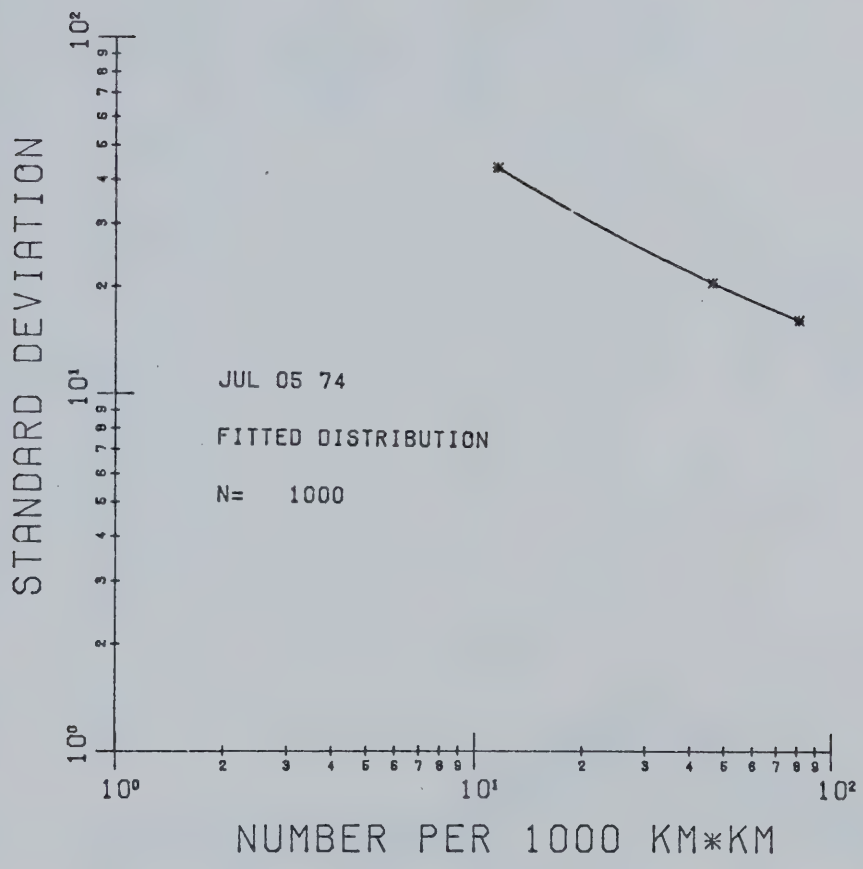

Figure VII.8 The standard deviation of the sample means for a sample density in 1000 km² (5 July 1974 hailswath)

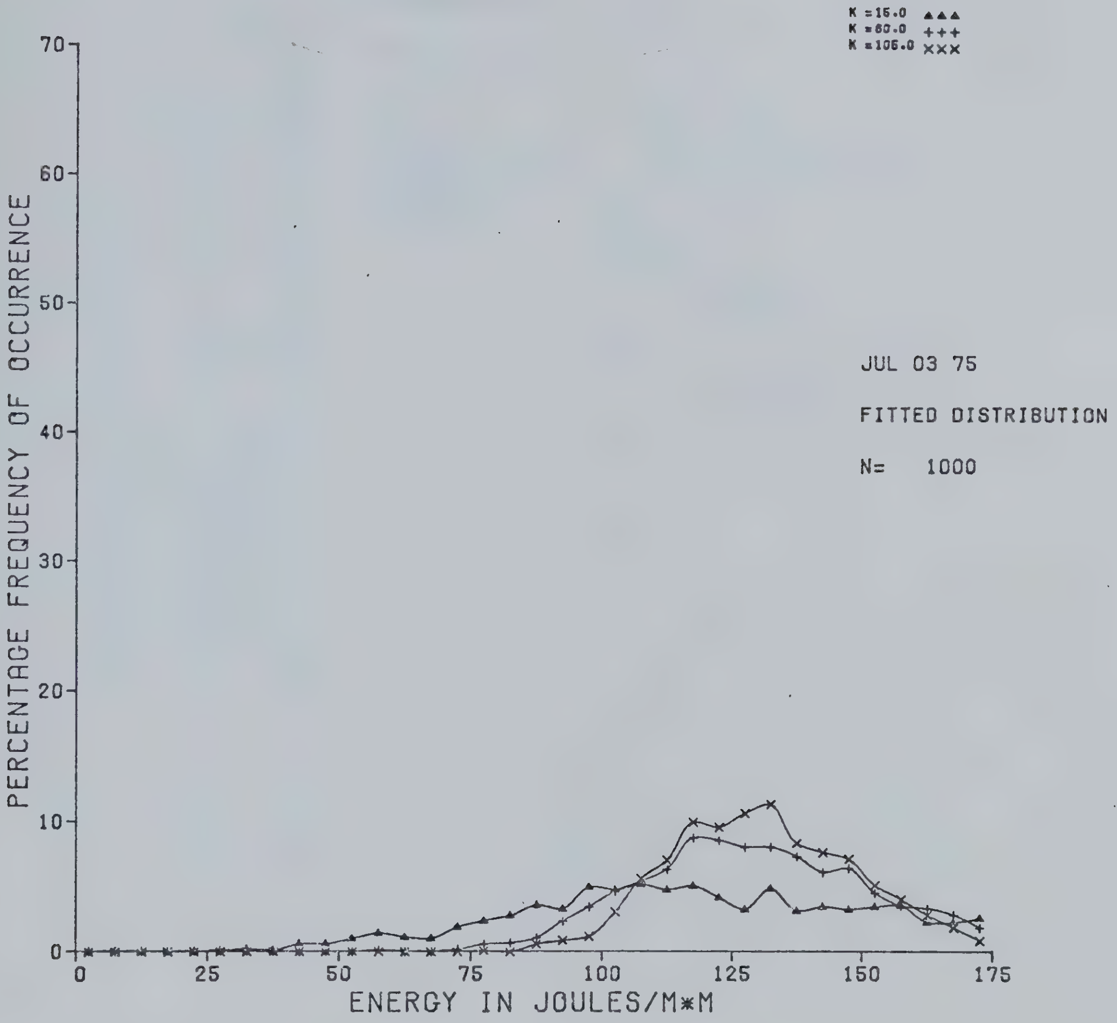

Figure VII.9 The probability density function of sample means for 3 July 1975 hailswath (Impact energy density values are grouped in 5 J m^{-2} classes)

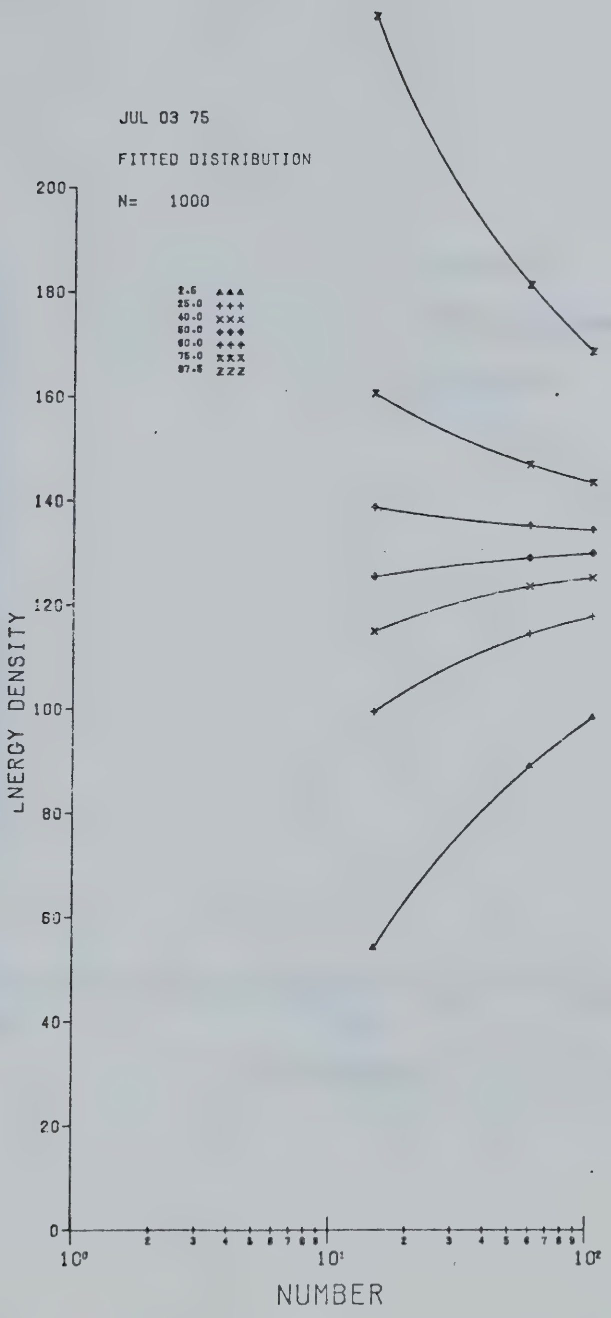

Figure VII.10 The probability distribution function for 3 July 1975 hailswath

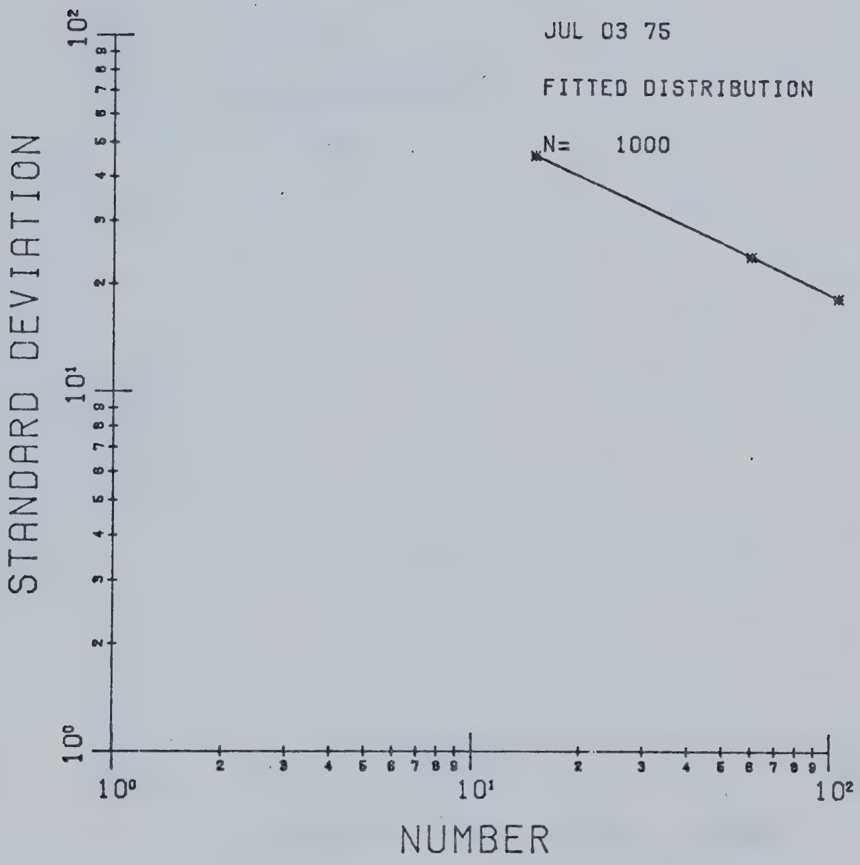

Figure VII.11 The standard deviation of the sample means as a function of the sample size (3 July 1975 hailswath)

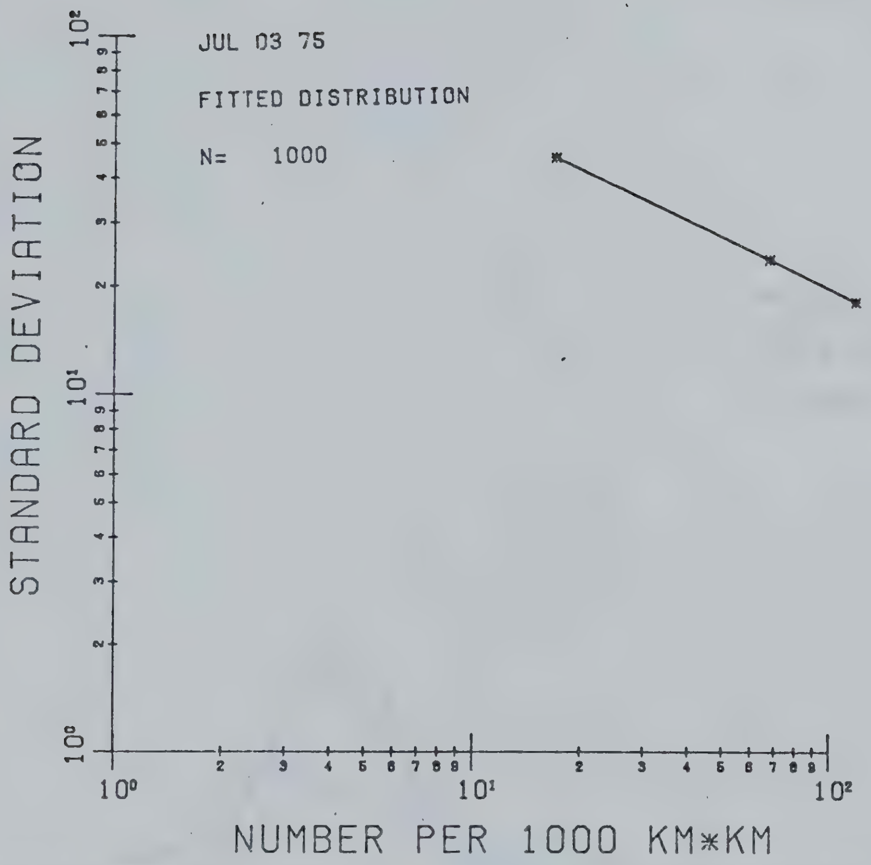

Figure VII.12 The standard deviation of the sample means for a sample density in 1000 km² (3 July 1975 hailswath)

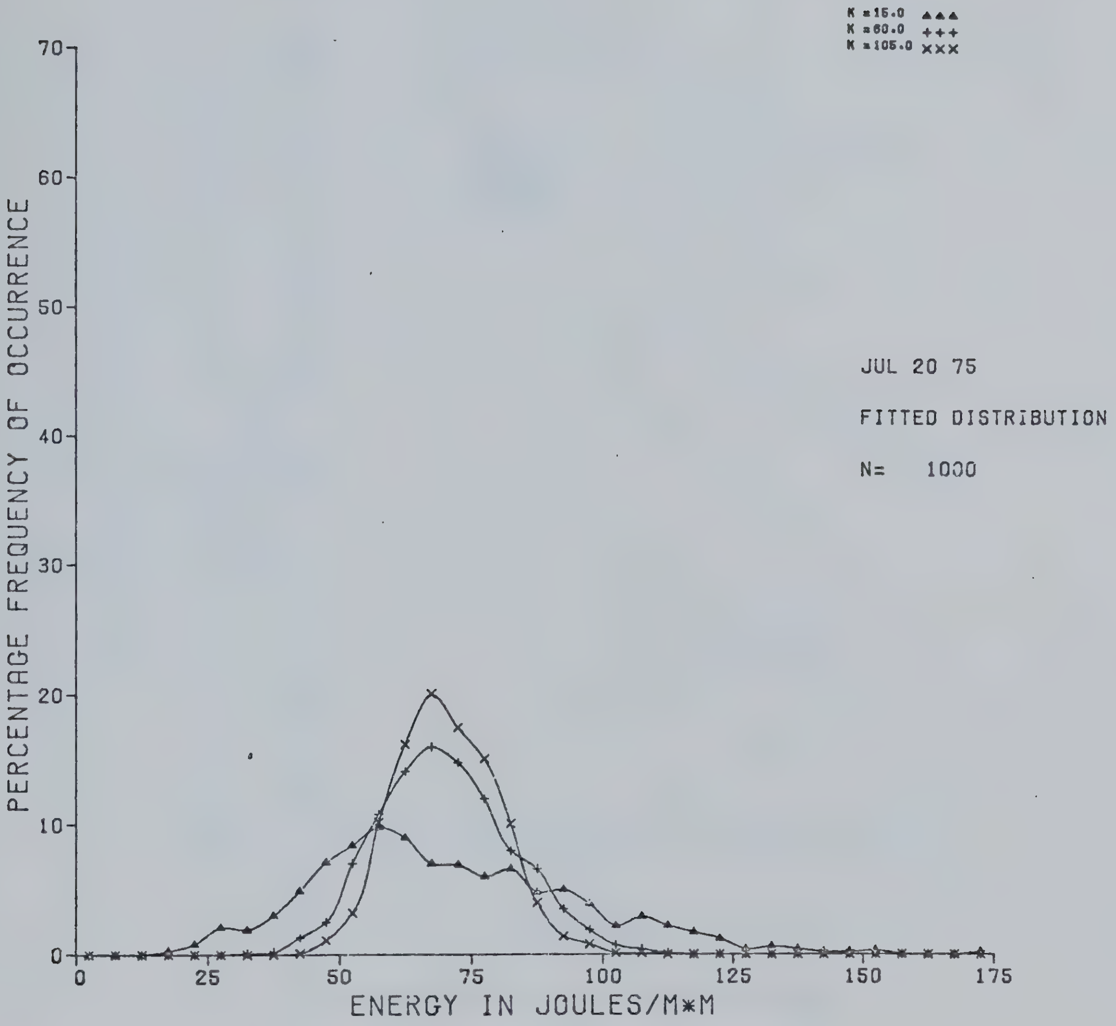

Figure VII.13 The probability density function of sample means for 20 July 1975 hailswath (Impact energy density values are grouped in 5 J m^{-2} classes)

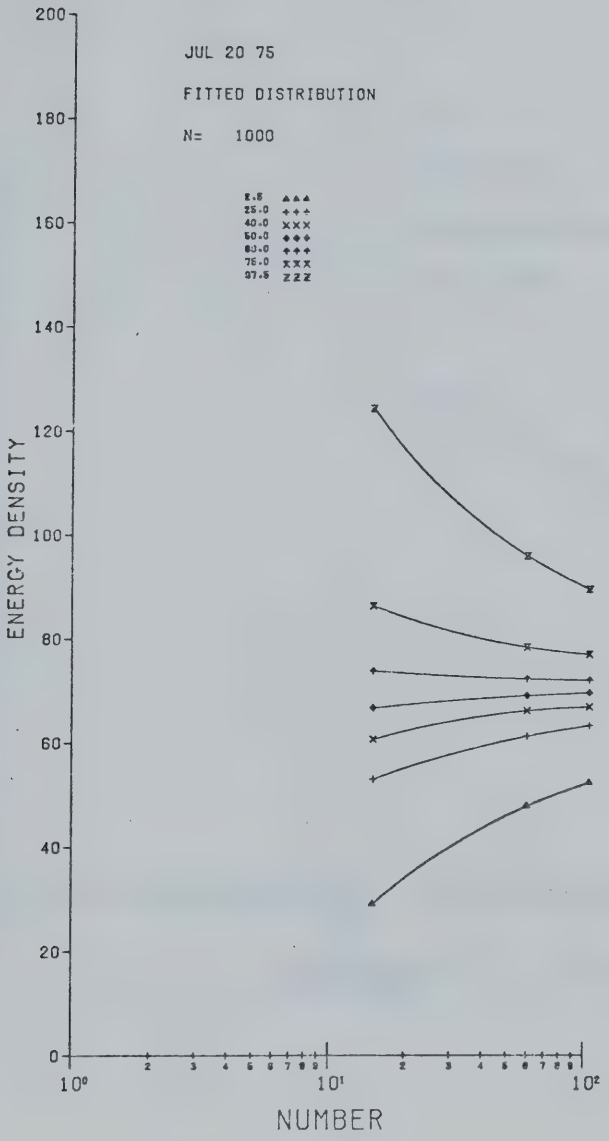

Figure VII.14 The probability distribution function for 20 July 1975 hailswath

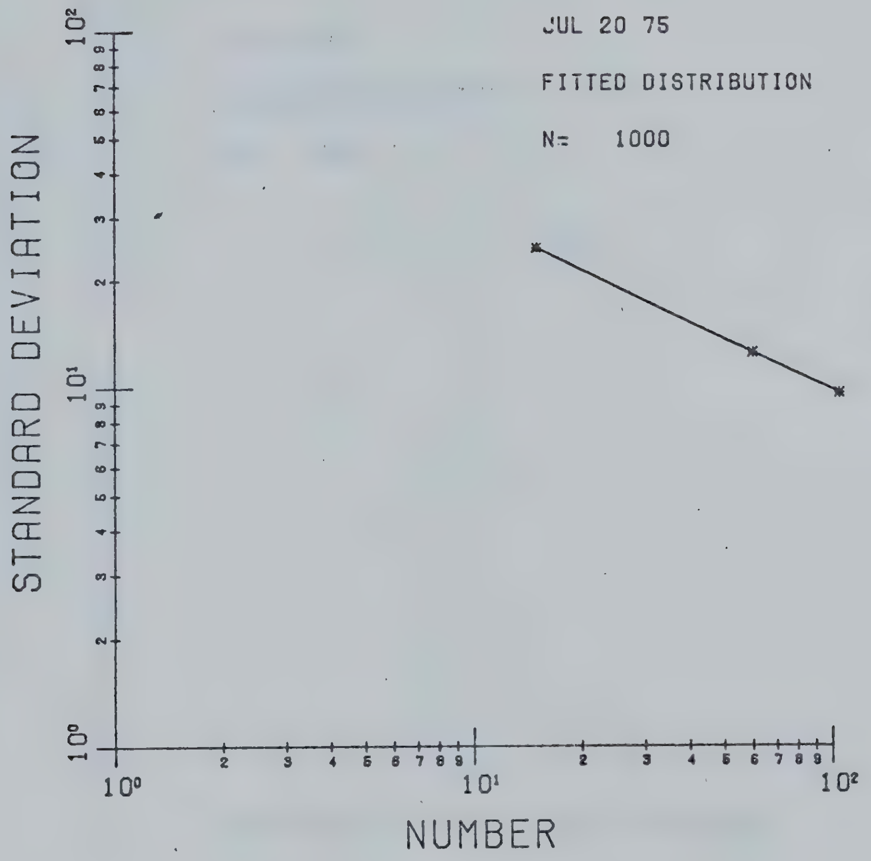

Figure VII.15 The standard deviation of the sample means as a function of the sample size (20 July 1975 hailswath)

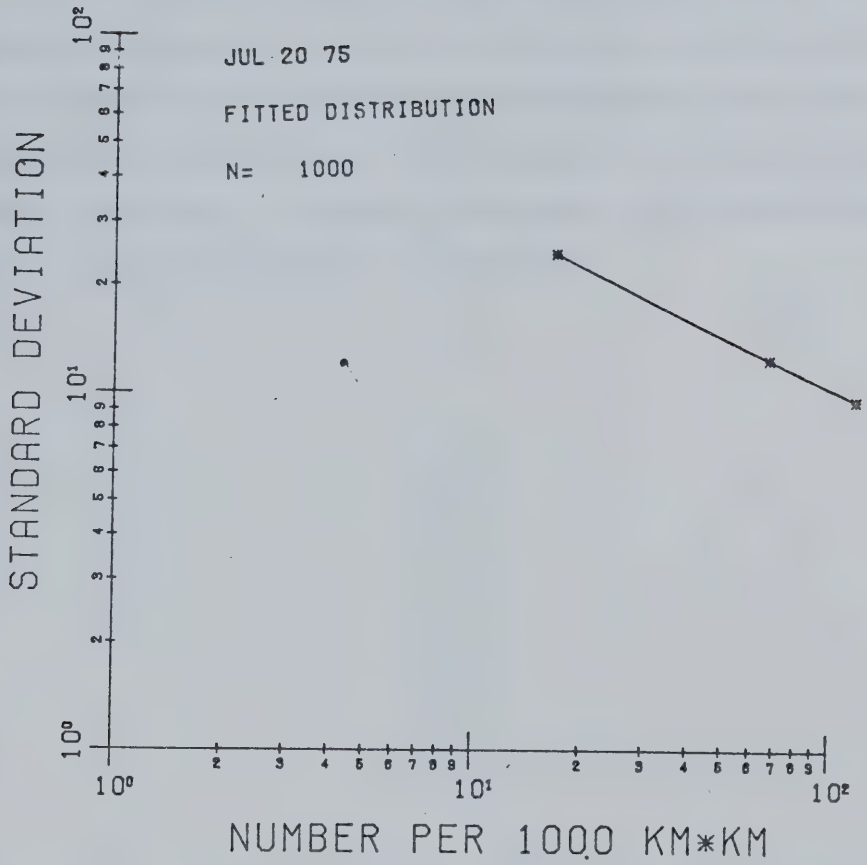

Figure VII.16 The standard deviation of the sample means for a sample density in 1000 km² (20 July 1975 hailswath)

Appendix VIII

STRATIFIED SAMPLING WITH REPLACEMENT

For stratified sampling with replacement, the following figures are given for the four hailswaths: a) Probability density function; b) Probability distribution function; c) Standard deviation of the sample means as a function of the sample size; and d) Standard deviation of the sample means for the number of hailpads per 1000 km².

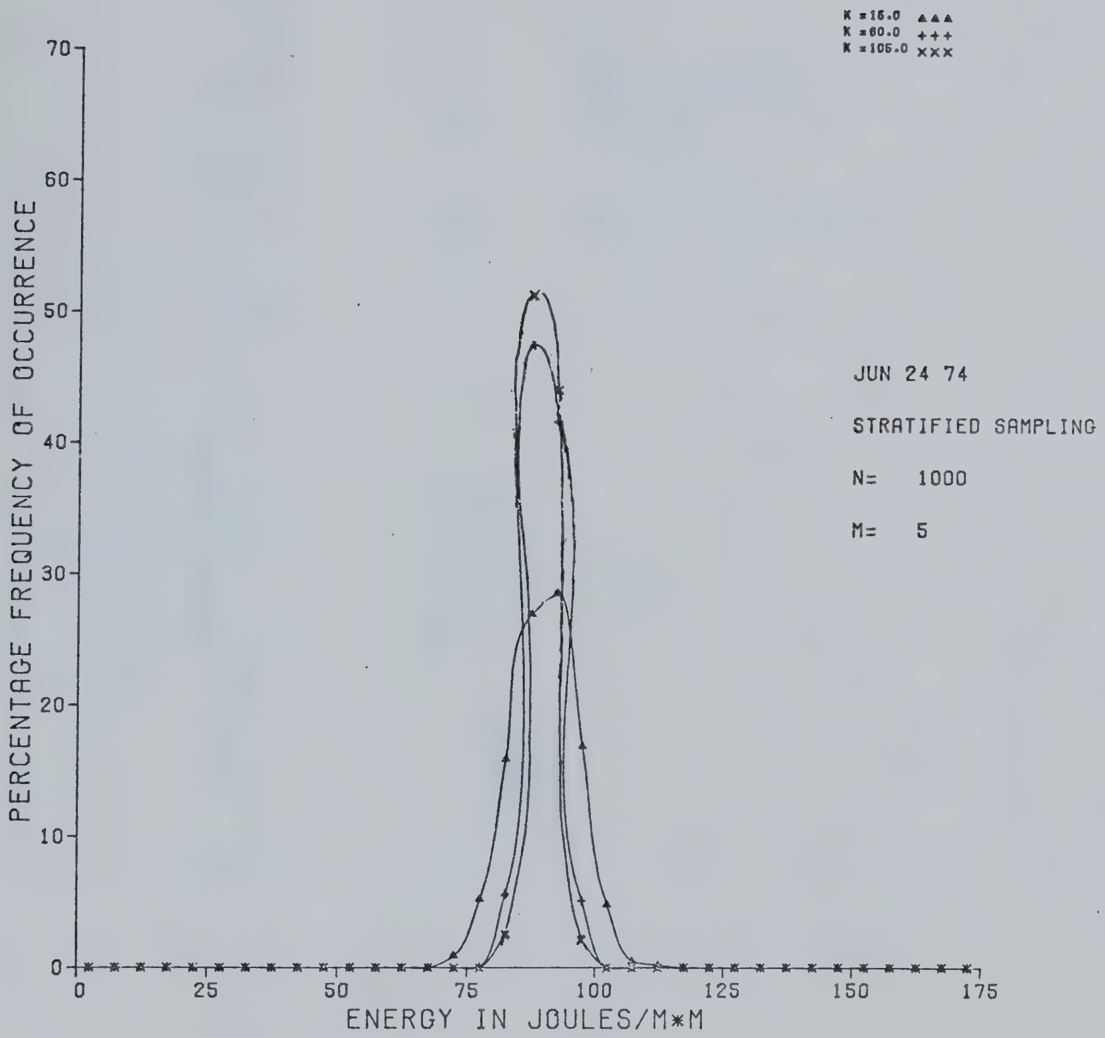

Figure VIII.1 The probability density function of sample means for 24 June 1974 hailswath (Impact energy density values are grouped in 5 J m^{-2} classes)

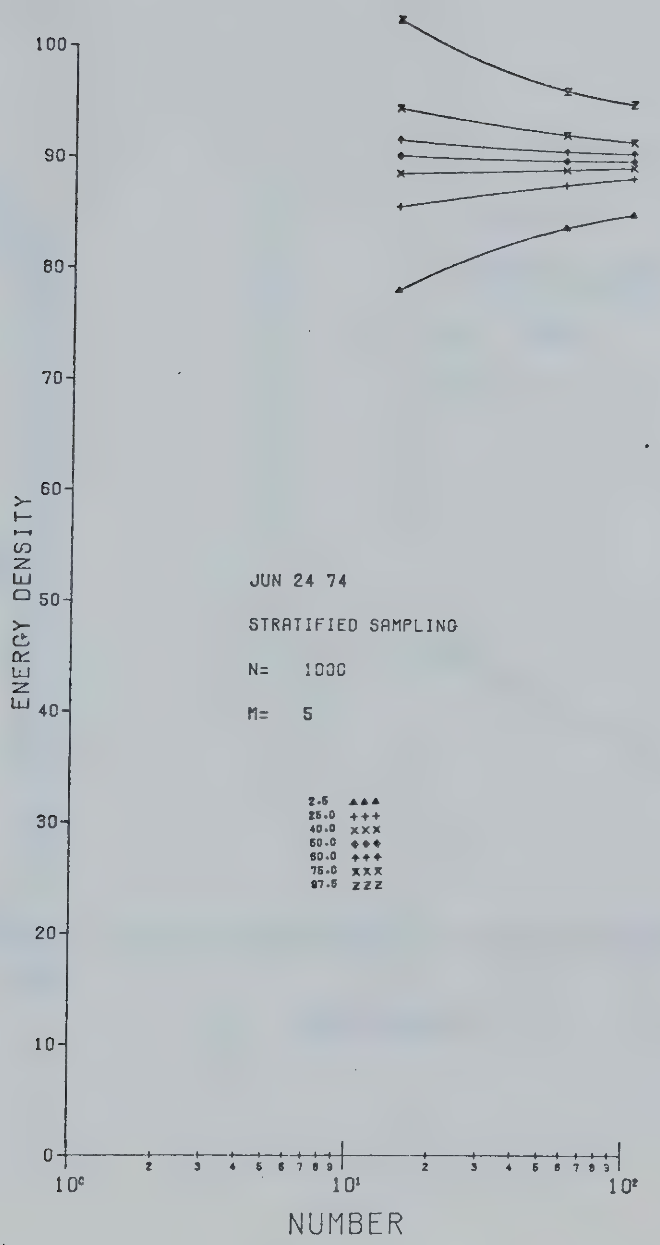

Figure VIII.2 The probability distribution function for 24 June 1974 hailswath

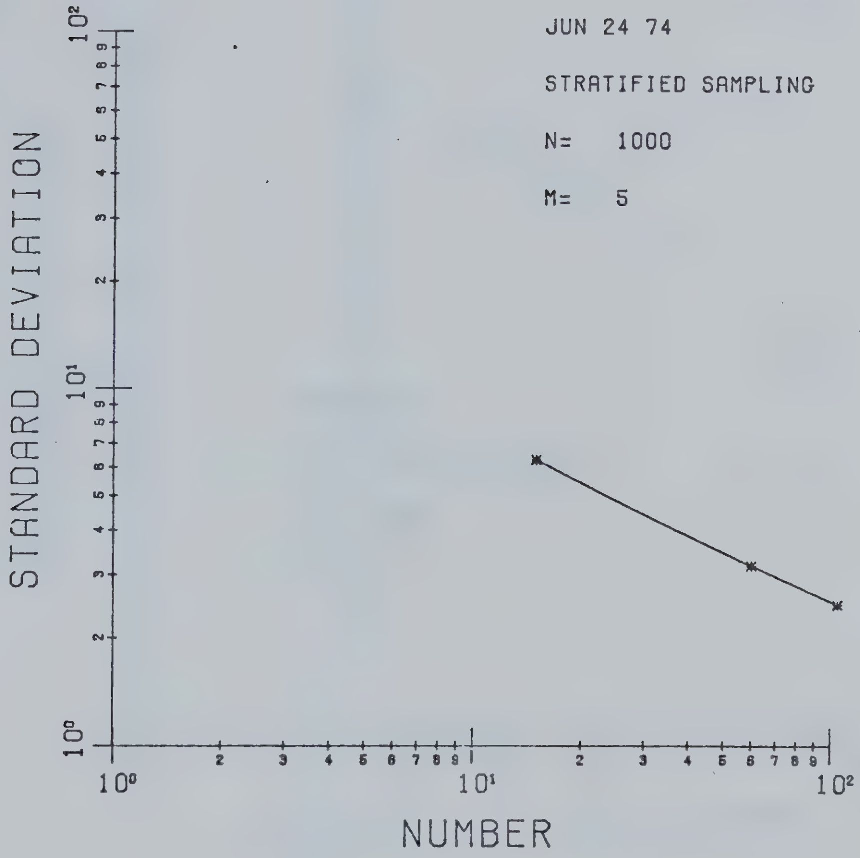

Figure VIII.3 The standard deviation of the sample means as a function of the sample size (24 June 1974 hailswath)

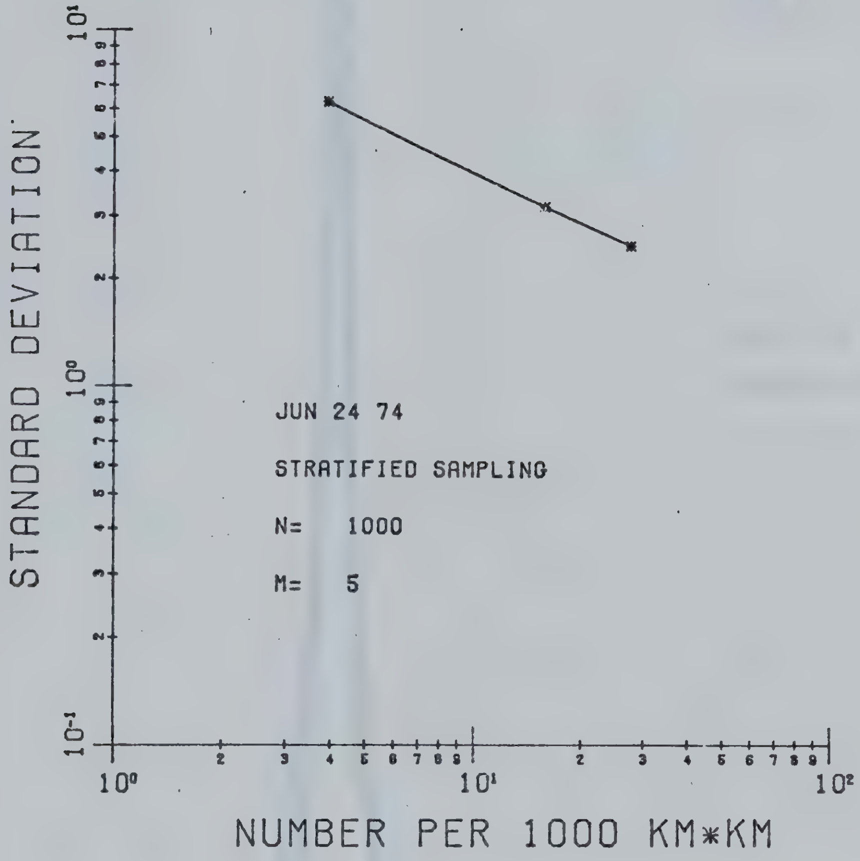

Figure VIII.4 The standard deviation of the sample means for a sample density in 1000 km² (24 June 1974 hailswath)

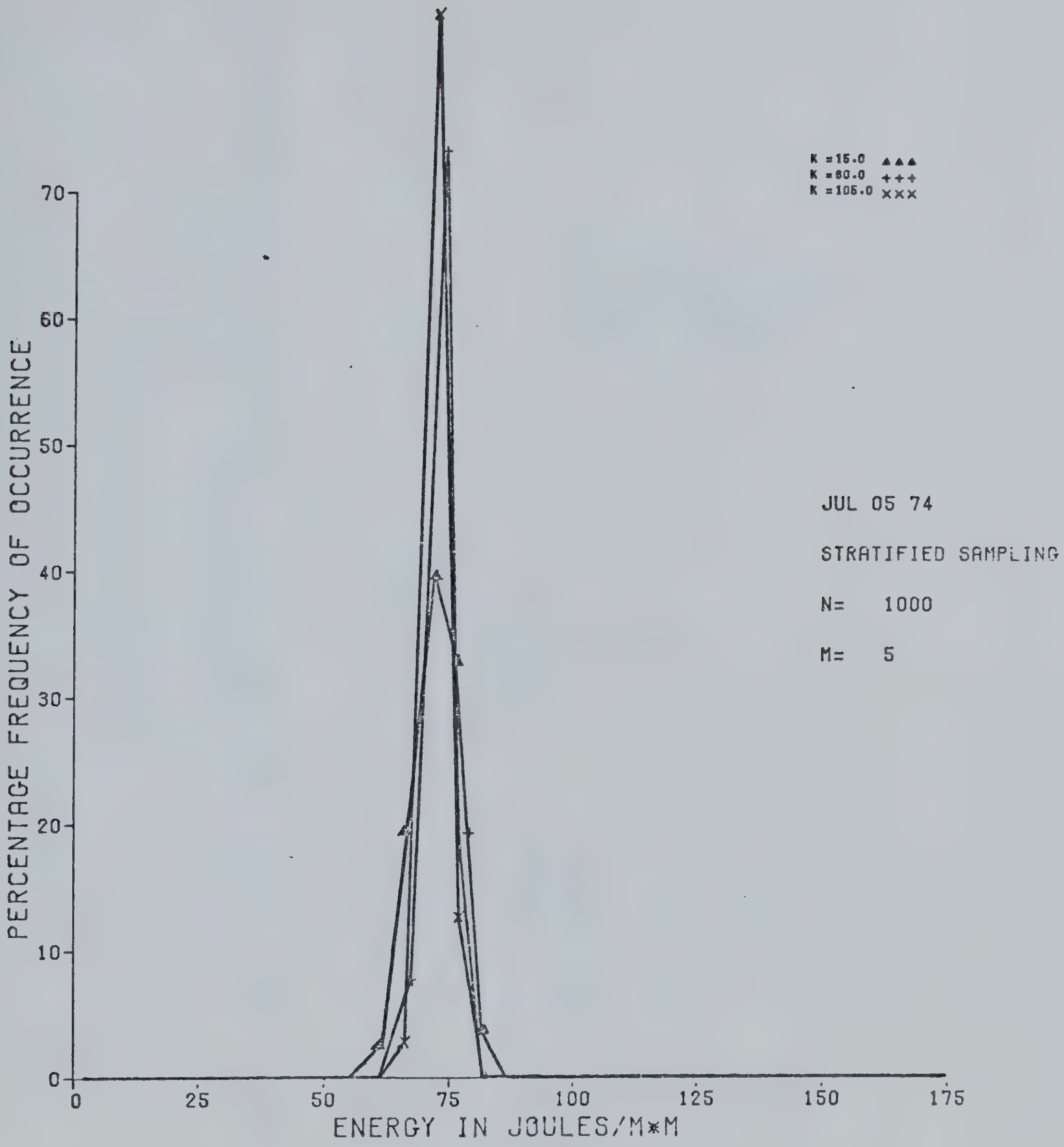

Figure VIII.5 The probability density function of sample means for 5 July 1974 hailswath (Impact energy density values are grouped in 5 J m^{-2} classes)

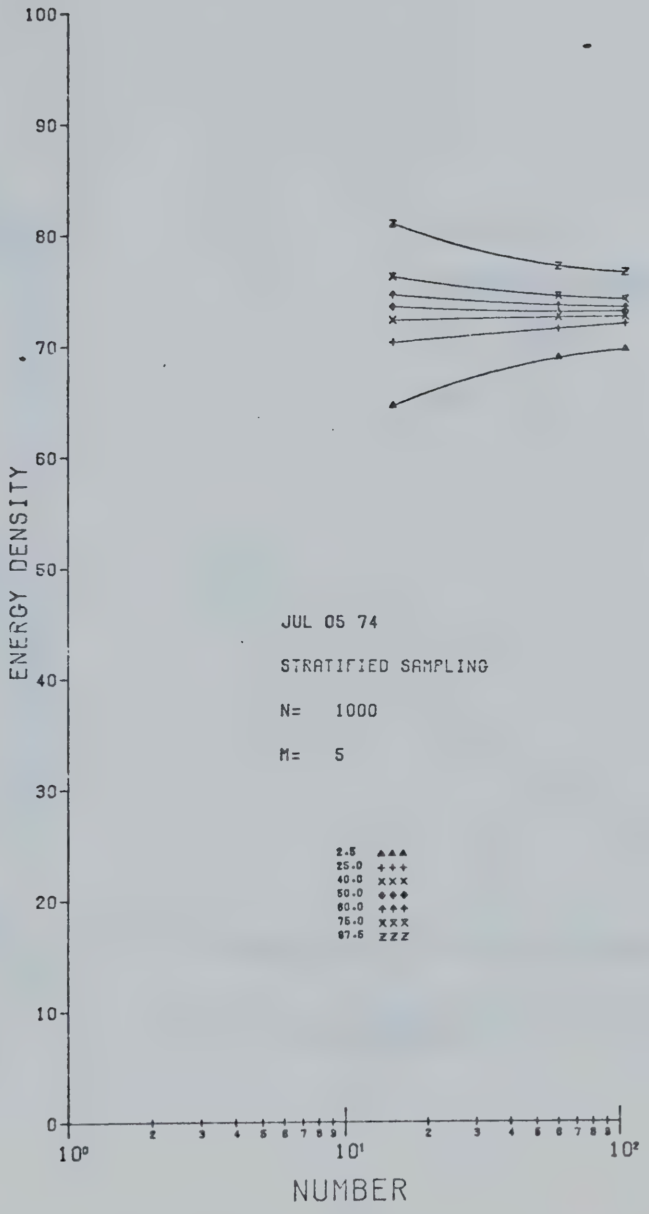

Figure VIII.6 The probability distribution function for 5 July 1974 hailswath

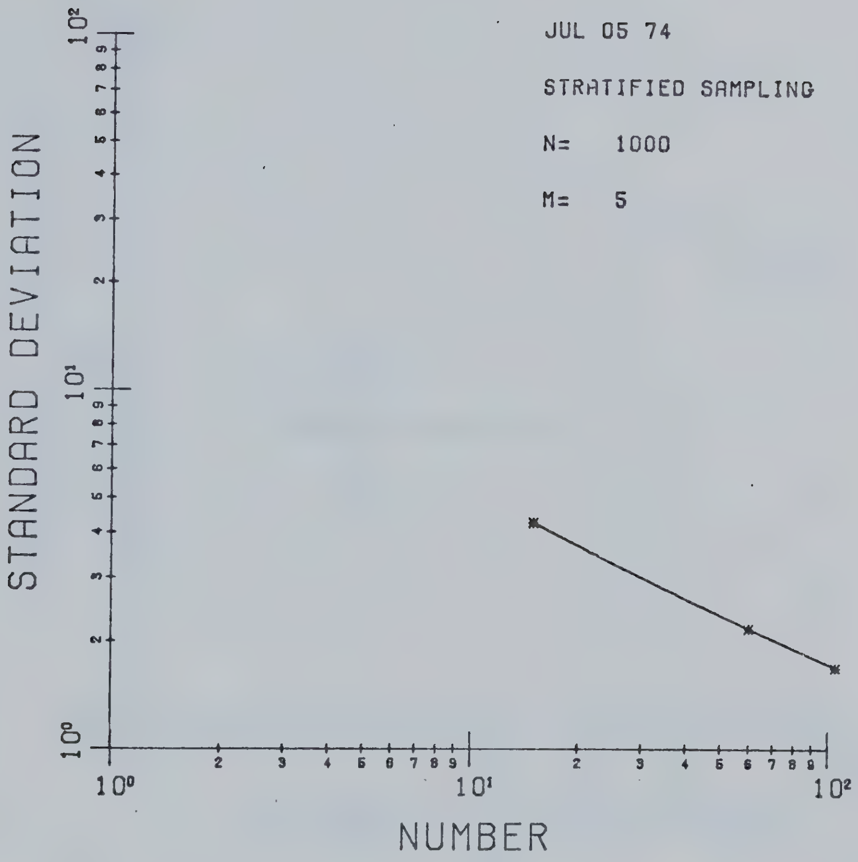

Figure VIII.7 The standard deviation of the sample means as a function of the sample size (5 July 1974 hailswath)

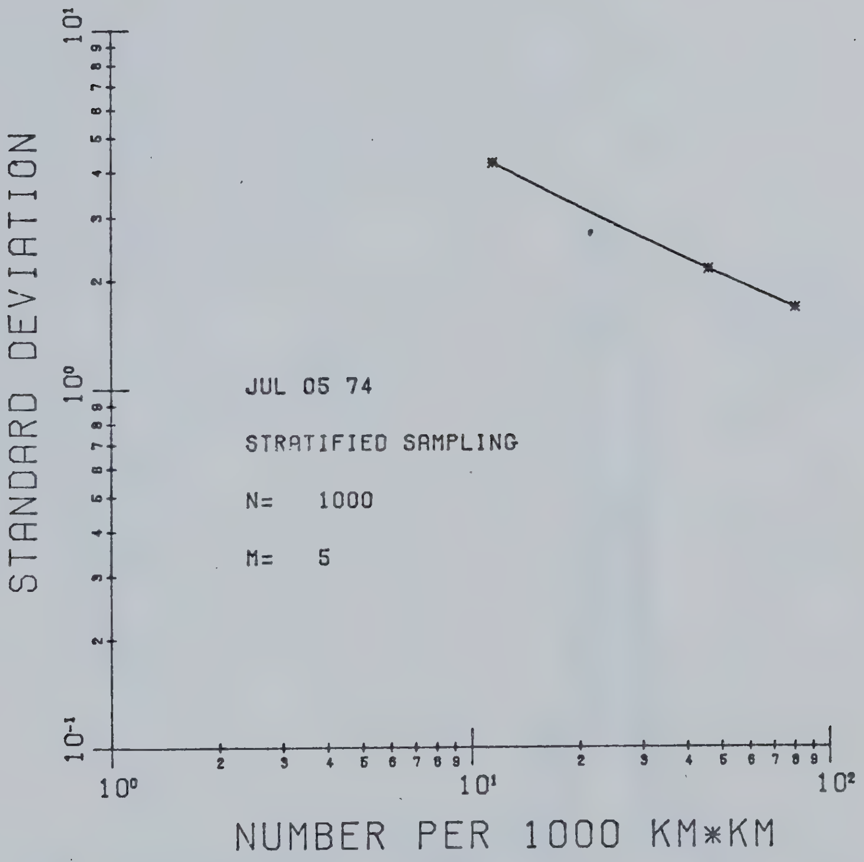

Figure VIII.8 The standard deviation of the sample means for a sample density in 1000 km^2 (5 July 1974 hailswath)

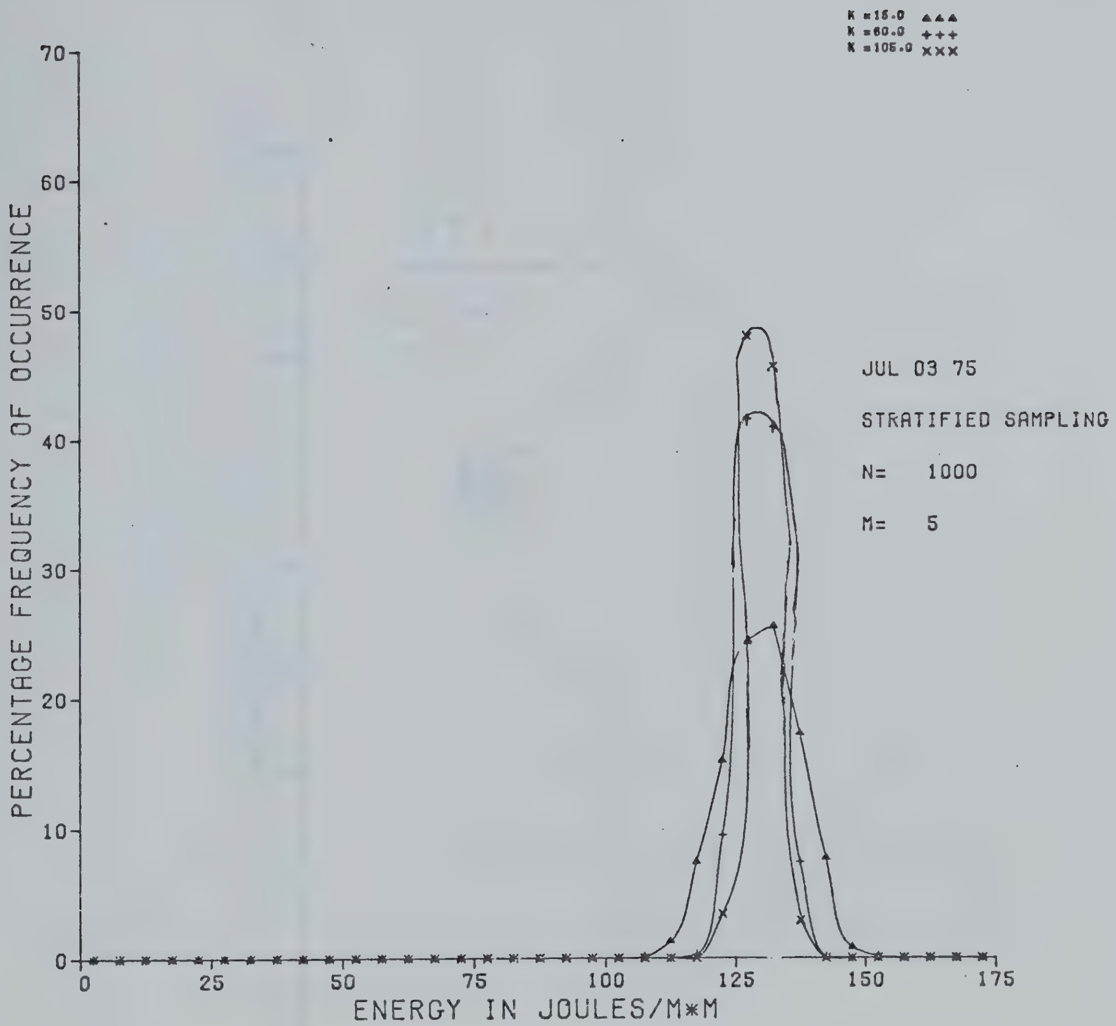

Figure VIII.9 The probability density function of sample means for 3 July 1975 hailswath (Impact energy density values are grouped in 5 J m^{-2} classes)

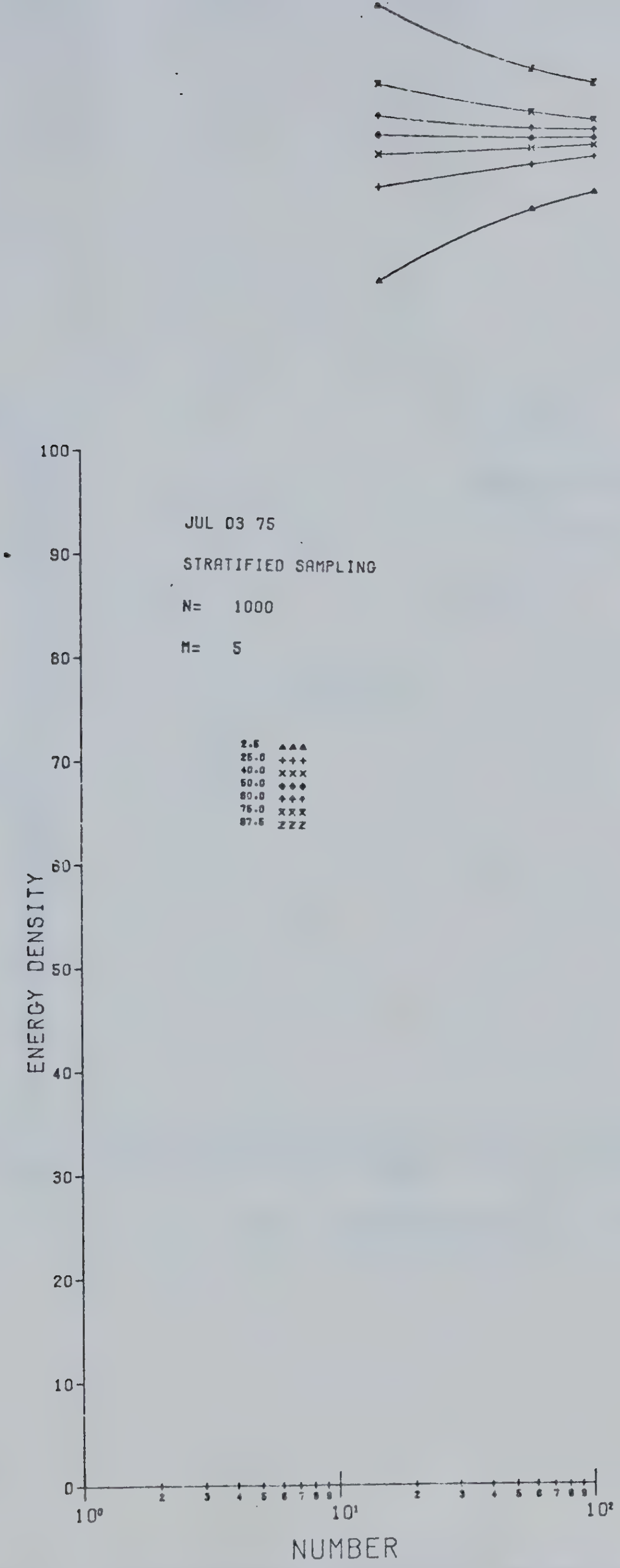

Figure VIII.10 The probability distribution function for 3 July 1975 hailswath

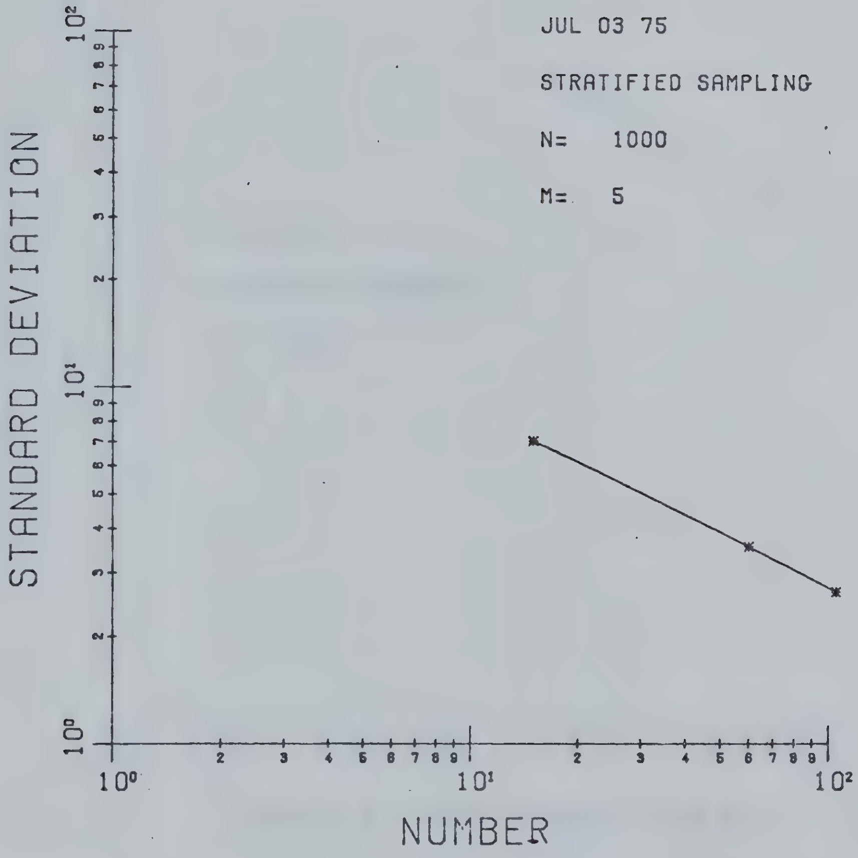

Figure VIII.11 The standard deviation of the sample means as a function of the sample size (3 July 1975 hailswath)

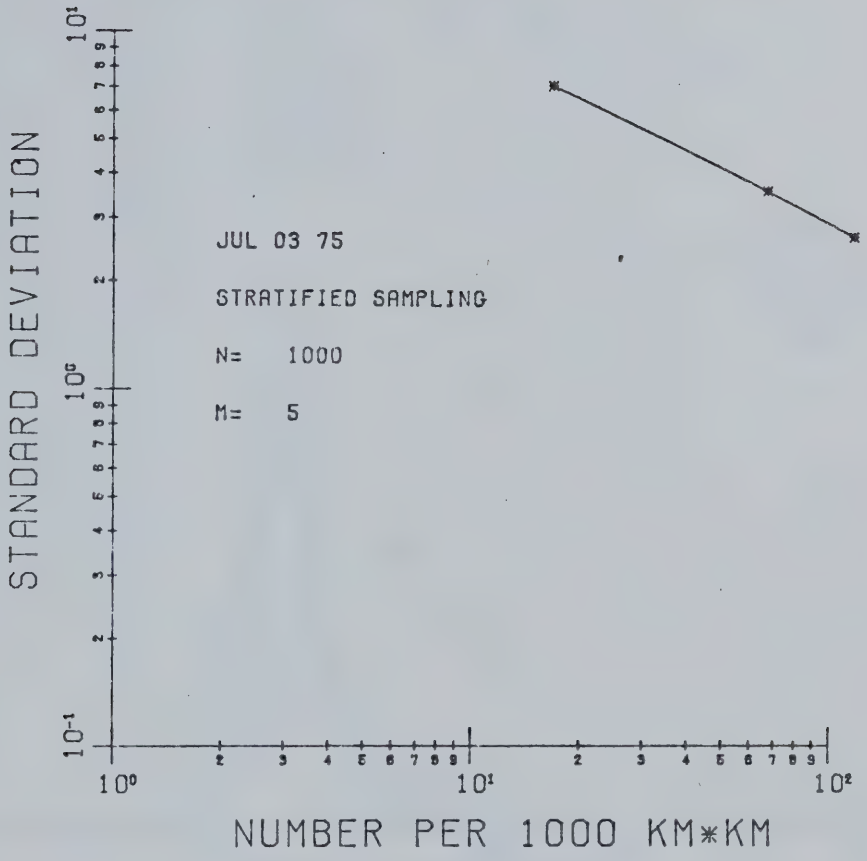

Figure VIII.12 The standard deviation of the sample means for a sample density in 1000 km² (3 July 1975 hailswath)

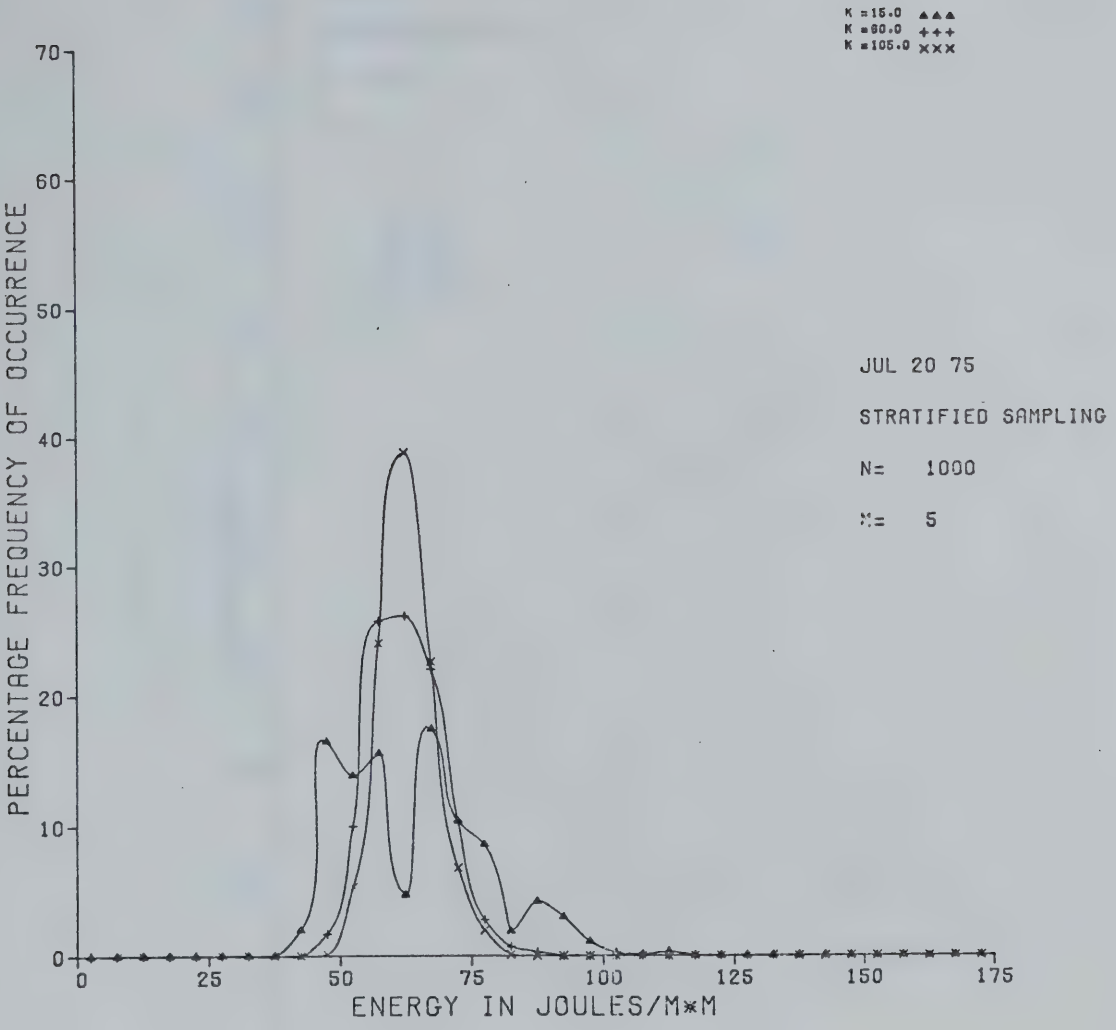

Figure VIII.13 The probability density function of sample means for 20 July 1975 hailswath (Impact energy density values are grouped in 5 J m^{-2} classes)

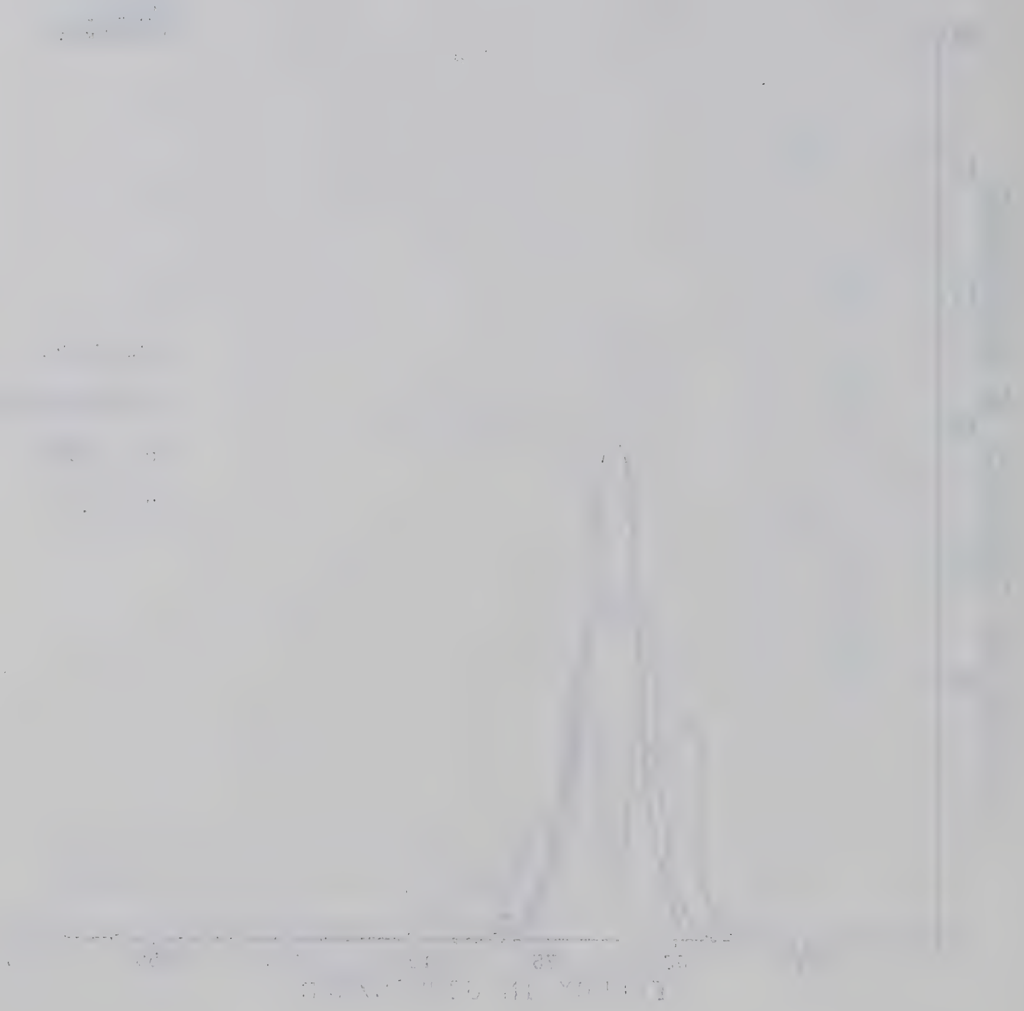

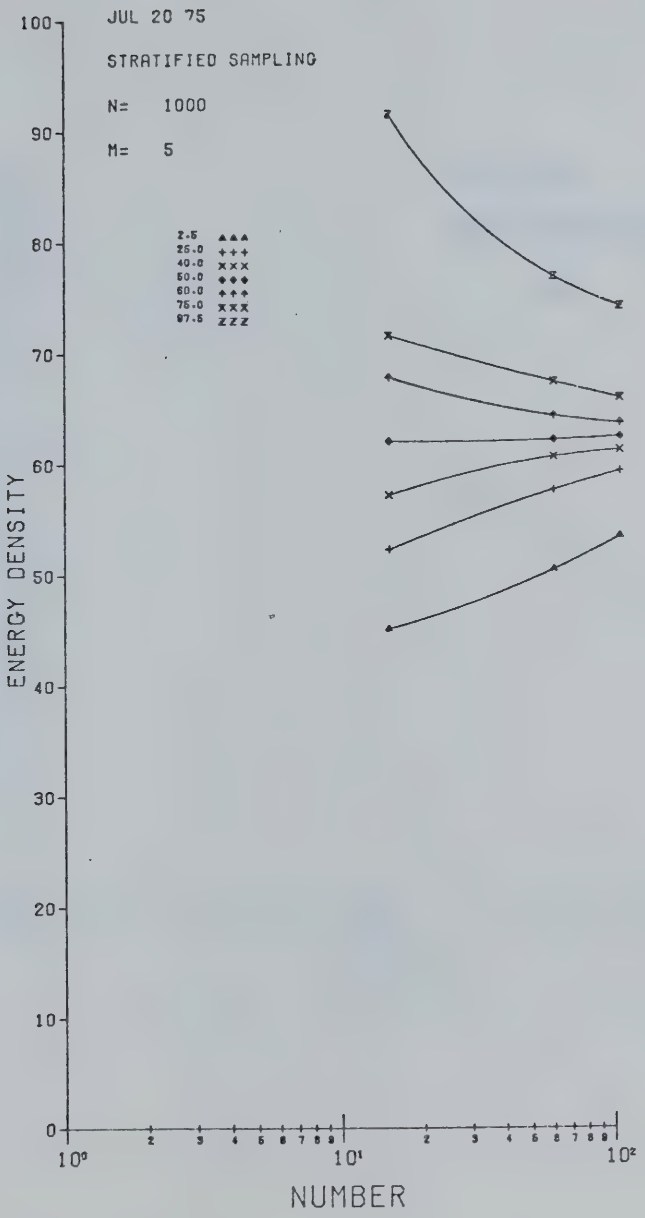

Figure VIII.14 The probability distribution function for 20 July 1975 hailswath

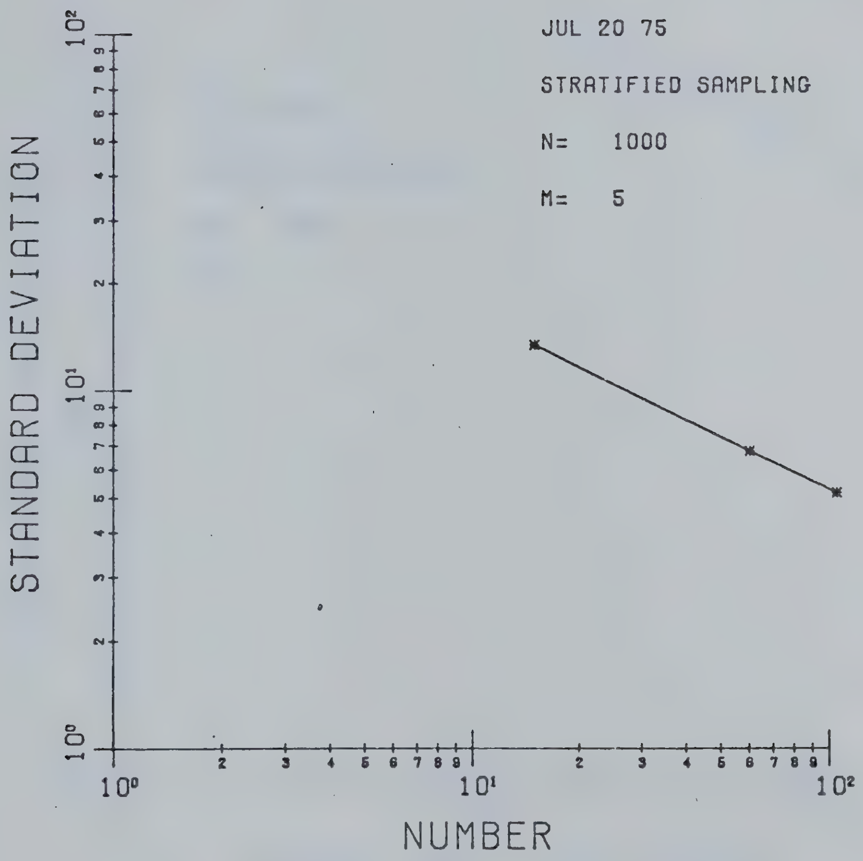

Figure VIII.15 The standard deviation of the sample means as a function of the sample size (20 July 1975 hailswath)

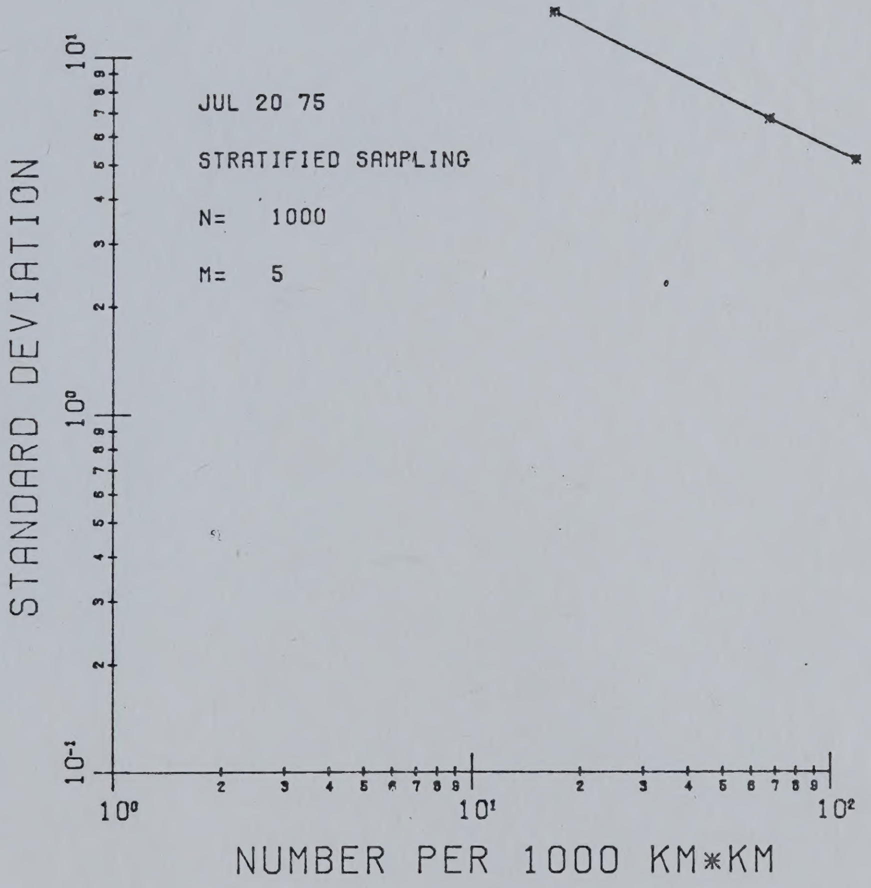

Figure VIII.16 The standard deviation of the sample means for a sample density in 1000 km² (20 July 1975 hailswath)

B30190